Longevity of the adaptive immune cell compartment in the human small intestine

Raquel Bartolomé Casado

Department of Pathology

Centre for Immune Regulation

Institute of Clinical Medicine

Faculty of Medicine

University of Oslo

2020

<<Sólo envejecemos de verdad, por dentro,

cuando dejamos de amar y de sentir curiosidad.>>

[We only really age, inside,

when we stop loving and being curious.]

-Elsa Punset, Spanish writer

"Memory is the scribe of the soul"

— Aristotle

Table of Contents

Acknowledgements

My sincere thanks also go to the present and past members at LIIPAT/ Department of Pathology. Thank you for generating a positive and stimulating environment, for all our scientific discussions during our project meetings, and also the non-scientific ones during lunches and coffee breaks. I will forever be thankful to Fridtjof Lund-Johansen, whose contagious enthusiasm at the lab reinforced my conviction of becoming a scientist. I wish also to extend my thanks to all my officemates during these PhD years and to the administrative staff at the Department of Pathology, Hege Eliassen and Marte Rabo Carlsen, for their valuable help.

A very special thank you goes to my friends in Oslo, in particular to Brana Stanković, Graciela López Soop and Ibon Eguiluz-Gracia, for reminding me that there is life outside of the lab. Many thanks also to my supportive friends in Salamanca, Burgos (my hometown in Spain) and those scattered around the world.

I would like to express my immense gratitude to my family for continued support and encouragement throughout this long process. A warm and heartfelt thank you goes to my grandmother, my aunts Ana and Yoli and my sister Lara; you all have always been an inspiration to me. Special thanks to my grandfather for encouraging me to find my own way in life. A big thank you to my father, for teaching me the value of the hard work and for giving me the "wings", even when it means to be far from home. Thanks to my mother, because I owe you all that I am.

Finally, a special and important thanks goes to Andrés Espinosa Cabellos, for your optimism, love and support in the good and bad times. For being my travel partner in this wonderful journey that is life. Thank you for being there.

Oslo, January 2020

Raquel Bartolomé Casado

Abbreviations

AhR, aryl hydrocarbon receptor

ANOVA, analysis of variance

APC, antigen-presenting cell

BCR, B-cell receptor

BM, bone marrow

CAR, chimeric antigen receptor

CCR, chemokine receptor

CD, cluster of differentiation

CTL, cytotoxic lymphocyte

DC, dendritic cell

FACS, fluorescence-activated cell sorting

FAE, follicle –associated epithelium

FC, flow cytometry

FcRn, neonatal Fc receptor

Foxp3, Forkhead box P3

GALT, gut-associated lymphoid tissue

GC, germinal Center

GVHD, graft versus host disease

HLA, human leukocyte antigen

IBD, inflammatory bowel disease

IE, intra-epithelial

IF, immunofluorescence

IFN, interferon

Ig, immunoglobulin

IHC, immunohistochemistry

IL, interleukin

ILC, innate lymphoid cell

ILF, isolated lymph follicles

iNKT, invariant natural killer T cells

KLF2, Kruppel-like factor 2

LP, lamina propria

LTi, lymphoid tissue inducer cells

LT-α, lymphotoxin-alpha

MAIT, mucosal-associated invariant T cells

M-cell, microfold cell

MHC, major histocompatibility complex

MLN, mesenteric lymph nodes

NK, natural killer

PBMCs, peripheral blood mononuclear cells

PCR, polymerase chain reaction

PP, peyer's patches

SI, small intestine

SIgA, secretory IgA

SMART, switching mechanism at 5' end of RNA template

STAT, signal transducer ad activator of transcription

T_{CM}, central memory T cell

TCR, T-cell receptor

T_{EM}, effector memory T cell

T_{FH}, follicular T helper cell

T_H, T helper cell

TGF, transforming growth factor

TNF, tumor necrosis factor

T_{reg}, regulatory T cell

T_{RM}, resident memory T cell

TSLP, thymic stromal lymphopoietin

List of Publications

This thesis is based on the following papers:

Paper I. Resident memory CD8 T cells persist for years in human small intestine.

Bartolomé-Casado R, Landsverk OJB, Chauhan SK, Richter L, Phung D, Greiff V, Risnes LF, Yao Y, Neumann RS, Yaqub S, Øyen O, Horneland R, Aandahl EM, Paulsen V, Sollid LM, Qiao SW, Baekkevold ES, Jahnsen FL.

J Exp Med. 2019 Jul 23.

Paper II. CD4^{+} T cells persists for years in the human small intestine and mediate robust Th1 immunity

Bartolomé-Casado R, Landsverk OJB, Chauhan SK, Sætre F, Yaqub S, Hagen Thorvaldsen K, Yaqub S, Øyen O, Horneland R, Aandahl EM, Aabakken L, Baekkevold ES, Jahnsen FL.

BioRxiv 10.1101/863407 December 3 2019.

Paper III. The human small intestine contains two distinct subsets of Foxp3+ regulatory CD4+ T cells with very different lifespan and functional properties.

Chauhan SK, **Bartolomé-Casado R**, Landsverk OJB, Jahnsen J, Horneland R, Yaqub S, Aandahl EM, Lundin K, Bækkevold ES, Jahnsen FL

Manuscript.

Paper IV. Antibody-secreting plasma cells persist for decades in human intestine

Landsverk OJ, Snir O, **Casado RB***, Richter L*, Mold JE, Réu P, Horneland R, Paulsen V, Yaqub S, Aandahl EM, Øyen OM, Thorarensen HS, Salehpour M, Possnert G, Frisén J, Sollid LM, Baekkevold ES, Jahnsen FL.
(* These authors contributed equally to this work).

J Exp Med. 2017 Feb; 214(2):309-317

1. INTRODUCTION

1.1 General considerations about the immune system

The immune system is a complex network of organs, tissues, and cells that have evolved to defend the body against pathogens as well as damaged cells and cancer cells. In order to prevent tissue injury, the immune system has learnt to distinguish self from non-self and its response is tightly regulated (Janeway, 1992). In mammals, the immune system is broadly divided into two main arms: innate and adaptive immunity.

The *innate immune system* constitutes the first line of defense and protects the host immediately after infection. It comprises physical barriers (such as the skin, mucus membranes, and saliva) together with different cell types including granulocytes, monocytes, macrophages, dendritic cells, mast cells, natural killer (NK) cells, and innate lymphoid cells as well as soluble proteins, like the complement system. This first innate response is important to restrain the infection but also to communicate and coordinate the response of the adaptive immune system. This communication is mediated by direct cell contact and through a broad variety of small molecules called cytokines. The *adaptive immune system* constitutes a more delayed line of defense (takes days to develop), but it is able to provide an enhanced and highly specific response against the pathogen. Components of the adaptive immune system are the T and B lymphocytes (including antibody-producing plasma cells), which recognize the pathogen through highly specialized antigen receptors.

Immunological memory, defined as the capacity to recall and combat previous encounters with the antigen, is one of the key attributes of the adaptive immune system. This concept has been long recognized since the ancient Greek times, based on Thucydides's observations of plague survivors being "immune" to subsequent waves of the plague epidemic (Crotty and Ahmed, 2004). The immunological memory presents three main characteristics: 1) it is specific for certain structures of the antigen, 2) after re-encounter with the antigen the memory cell provides a more rapid and effective response that is tailored to the nature of the pathogen 3) this evolutionary advantage last for many years once the antigen is cleared, forming a pool of persisting memory cells that are either long-lived cells or maintained through homeostatic turn-over (Crotty and Ahmed, 2004; Farber et al., 2016). T cells and B cells completely fulfill these characteristics, however, a broader definition of immunological memory may also include some

innate cells, such as NK cells and macrophages, which present memory-like features (Netea and Joosten, 2018; Sun and Lanier, 2018).

The focus of this thesis is to study the long-term memory reservoirs in the human small intestine. Specifically, it aims to characterize the persistence, phenotype, and function of different populations of memory T cells, including CD8+ and CD4+ resident memory T cells (T_{RM}), regulatory T cells (T_{reg}) as well as plasma cells (PCs) from human intestinal samples.

1.2 The intestinal immune system

The gut constitutes the largest compartment of the entire immune system (MacDonald, 2008). The huge surface area of the intestinal tract (around 200m^2 in humans) is the major site of entry of many pathogens and is continuously exposed to dietary antigens and toxins (Hooper and Macpherson, 2010). Moreover, the intestine is extensively colonized by trillions of microorganisms (more than 1000 different species of bacteria, but also fungi and viruses) - collectively named the intestinal microbiota - that establish symbiotic relations with the host (Almeida et al., 2019). The main function of the intestinal microbiota is to enhance the host digestion through the degradation of dietary polysaccharides but also plays a crucial role in protecting the host. Intestinal microbiota educates the immune system from early in life (Robertson et al., 2019) and occupies a niche that competes in space and resources with invasive pathogens. The microbiota is more densely distributed in the ileum and the colon, whereas food antigens are more dominant in the duodenum and the jejunum, where the absorption of nutrients takes place (Mowat and Agace, 2014). Therefore, the intestinal immune system has the enormous challenge of protecting the host against pathogens without damaging the intestinal tissue as well as maintaining the tolerance against commensals and dietary antigens. To accomplish this task, the gut contains the greatest number of immune cells in the body, and these intestinal immune cells present unique adaptations to their local environment.

1.2.1   Anatomy of the small intestine

The intestine comprises several anatomically and physiologically different regions. The small intestine is divided into three segments: the duodenum (closest to the stomach), followed by the jejunum and then the ileum. The main function of the small intestine is the digestion and

absorption of nutrients. In order to increase the surface area to optimize this task, the small intestine presents finger-like projections known as *villi*. These villi are covered by a single layer of enterocytes of which the apical layer contains a brush border or microvilli, to facilitate the digestion and absorption. Between the villi, surface invaginations called *crypts* provide a continuous source of stem cells that give rise to different types of mature epithelial cells (Moor et al., 2018). A layer of mucus, derived from by mucins that are secreted by the Goblet cells, helps to limit the contact between the luminal microbiota and the epithelial cell surface (Mowat and Agace, 2014). In addition, the action of the antimicrobial proteins secreted by Paneth cells together with the secretory IgA (SIgA) produced by intestinal plasma cells, contribute to prevent microbial invasion (Hooper and Macpherson, 2010).

The small intestine (SI) is composed of four layers, starting from the lumen: the mucosa (which is subdivided in lamina propria and epithelium), the submucosa, the muscularis propria and the serosa. The intestinal immune system also comprises a complex network of lymphoid structures and highly specialized cells; and functionally, it can be classified as inductive and effector sites.
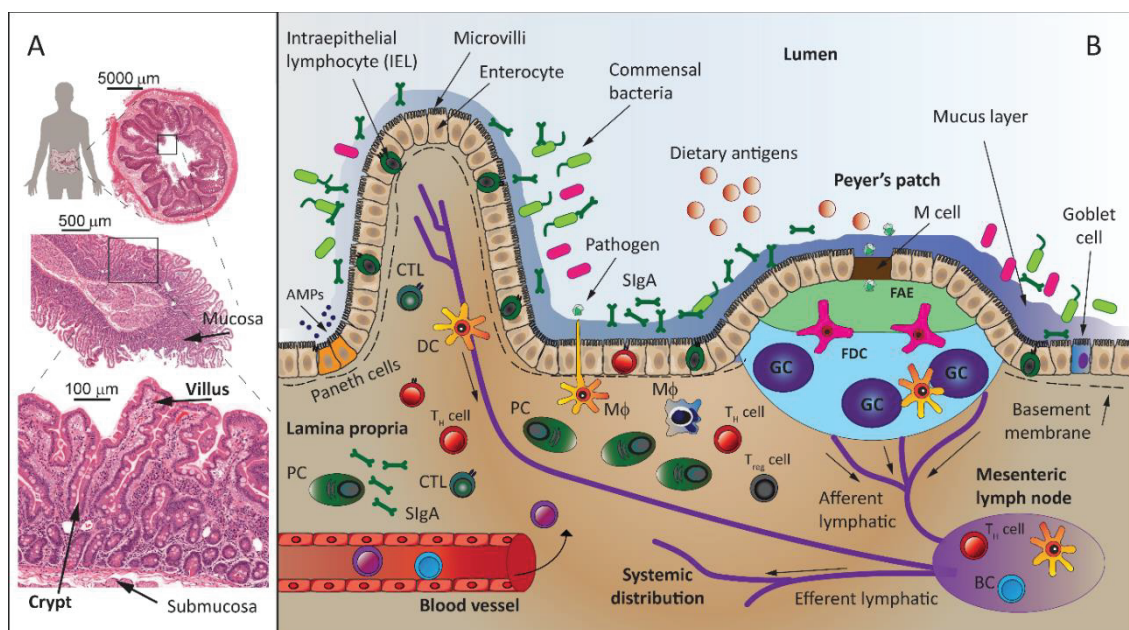
Figure 1. Anatomy of the intestinal immune system. **(A)** Section of human small intestine stained with hematoxylin/eosin. **(B)** The small intestine is exposed to constant antigen stimulation and harbors large numbers of highly specialized immune cells. PC, plasma cell; SIgA, secretory IgA; CTL, cytotoxic lymphocyte; IEL, intraepithelial lymphocyte; AMP, anti-microbial peptides; TH cell, T helper cell; Treg cell, regulatory T cell; BC, B cell; MΦ, macrophage; DC, dendritic cell; FAE, follicle-associated epithelium; FDC, follicular dendritic cell; GC, germinal center. Adapted from (Faria et al., 2017), (Mowat, 2003) and (Mowat and Agace, 2014).

The *inductive sites* are the main places for antigen sampling and priming of naïve lymphocytes. In the small intestine, the inductive sites are comprised by the draining lymph nodes (such as the duodenopancreatic and the mesenteric lymph nodes, MLNs), and the gut-associated lymphoid tissue (GALT), which includes the Peyer's Patches (PP) and the isolated lymph follicles (ILFs). Differing from the systemic lymph nodes, PPs and ILFs lack afferent lymphatics, thus receiving antigen directly from the epithelial surface. The *effector sites* of the intestinal immune system are the lamina propria (LP) and the overlying epithelium, which together accommodate large numbers of end-differentiated antibody-producing B cells (termed plasma cells, PCs) and T cells (Brandtzaeg and Pabst, 2004; Mowat and Agace, 2014).

The epithelium and the LP are separated by a thin collagen layer called basement membrane. These two compartments are highly interconnected; however, they present differences in their immune cell composition: while the LP is densely packed with PCs, T cells and diverse innate cells (macrophages, dendritic cells, mast cells, and eosinophils), the epithelium is dominated by T cells (**Figure 1**).

1.2.2 Intestinal antigen-presenting cells (APCs)

The intestine contains a highly diverse population of mononuclear phagocytes, which includes conventional dendritic cells (cDC) and monocyte-derived tissue-resident macrophages (Mφ). Both populations are professional antigen-presenting cells, thus specialized in sampling and processing of antigens to be presented to T cells on the surface of MHC-class I and II molecules. MHC class I molecules (HLA class I in humans) are constitutively expressed on all the nucleated cells and display endogenous intracellular peptides (Blum et al., 2013; Vyas et al., 2008). In contrast, MHC class II molecules (HLA class II in humans) are only expressed on immune cells (DCs, Mφs, B cells, and T cells), thymic cortical epithelial cells and certain epithelial cells. MHC-II present extracellular antigens that have been degraded in the endosomal/lysosomal pathway (Roche and Furuta, 2015). In addition, APCs can present engulfed antigens through the MHC class I pathway to activate CD8+ T cells in a mechanism known as "cross-presentation" (Ackerman et al., 2006).

Intestinal DCs and Mφs play different but complementary roles in regulating the balance between tolerance and inflammatory responses as well as maintaining tissue homeostasis. They both express a diverse array of pattern-recognition receptors (PRRs), which allow them to recognize highly conserved molecules found in harmful or commensal microbes (pathogen-

associated molecular patterns, PAMPs) (Medzhitov and Janeway, 2002),as well as molecules released by damaged cells (danger-associated molecular patterns, DAMPs) (Matzinger, 2002). Furthermore, they are able to secrete many different cytokines and chemokines to regulate and tailor immune responses.

Different subsets of DCs and Mɸs share common phenotypic markers (such as HLA-DR, CD11c, CD11b, CX$_3$CR1), which complicates their correct discrimination. Because of this, to characterize these cells, it is necessary to distinguish both cell types based on their unique functional features.

1.2.2.1 Macrophages.

Intestinal Mɸs are scattered in the LP, where they constitute the major population of APCs, and some of them can be found in the muscularis region (Faria et al., 2017). All the Mɸs residing in the adult intestine are derived from continuous replacement by monocytes, which are recruited from blood and gradually differentiate in response to the local environment (Joeris et al., 2017). In human SI, all Mɸs express HLA-DR and CD14, and during their differentiation through different intermediary stages, they reduce the expression of monocyte-related markers (such as CCR2 and calprotectin), while they gradually acquire typical markers of mature macrophages (CD163, DC-SIGN, etc.) (Bujko et al., 2018). Mɸs present relatively long-half lives, ranging from several weeks to several months in human small intestine (Bujko et al., 2018).

Intestinal Mɸs are particularly efficient at the uptake of soluble and particulate antigens as well as the elimination of microbes and dead cells by phagocytosis. At the steady-state, they perform this scavenger function while maintaining an anti-inflammatory microenvironment and without releasing pro-inflammatory factors (Bujko et al., 2018; Richter et al., 2018). Intestinal Mɸs produce the anti-inflammatory cytokine IL-10, which contributes to the local maintenance of regulatory T cells (Treg cells), especially in the colon (Cerovic et al., 2014; Joeris et al., 2017). Moreover, Mɸs actively contribute to tissue remodeling and epithelial cell renewal (Cerovic et al., 2014).

1.2.2.2 Dendritic cells.

Intestinal DCs present a short lifespan in the tissue (days), and therefore they need to be continuously replenished by bone marrow (BM) derived committed precursors (pre-DC cells) (Richter et al., 2018). DCs are classified in two major subsets: plasmacytoid DCs (pDCs) and myeloid or conventional DCs (cDCs). pDCs are important mediators of anti-viral responses through the production of high amounts of type-I IFNs (Collin and Bigley, 2018). pDCs are abundant in blood, but very scarce in the intestinal mucosa (Raki et al., 2013). cDCs are efficient

at antigen-presentation and, unlike Mɸs, have the unique capacity to migrate to the draining lymph nodes, where they can prime naïve T cells. cDCs can be further classified into cDC1 and cDC2 subsets (Collin and Bigley, 2018). cDC1 cells promote T_H1 responses and present higher capacity to activate CD8+ T cells through cross-presentation. In contrast, cDC2 cells promote T_H2 and T_H17 responses (these concepts will be further explained in the T-cell chapter).

1.2.2.2.1   *Routes of antigen uptake in the small intestine.*

In the organized-lymphoid structures of the small intestine (PPs and ILFs), luminal microbes are sampled by transcytosis via microfold (M) cells in the follicle –associated epithelium (FAE). The antigens are then transferred to DCs that are located below the FAE, in the subepithelial dome (Schulz and Pabst, 2013). Diverse populations of DCs that reside in the LP can also sample luminal antigens, which are transported across the villous epithelium through different mechanisms. Several mechanisms have been proposed: endocytosis of infected or apoptotic epithelial cells, extension of trans-epithelial dendrites of the DC to the lumen, direct transfer from neighboring tissue-resident Mɸs (Mazzini et al., 2014), and transcytosis through goblet cell conduits (Cerovic et al., 2014). In addition, enterocytes express on their surface the neonatal Fc receptor (FcRn), which binds antibody-antigen complexes and facilitates their transport across the epithelium by transcytosis (Mowat, 2018).

1.2.2.2.2   *Functions of intestinal dendritic cells*

After antigen uptake and activation, DCs upregulate CCR7, allowing them to migrate to the MLNs via afferent lymphatics. DCs arrive at the lymph node as fully mature non-phagocytic cells expressing co-stimulatory molecules (CD80/CD86). DCs are then well-equipped to provide the signals to activate naïve T cells and drive their proliferation and differentiation.

DCs located at the PPs and those migrating to MLNs express enzymes to metabolize retinoic acid (RA), which is the acidic form of vitamin A. RA has an important role on the intestinal immune system, acting in different processes. First, it promotes the imprinting of gut homing receptors on T cells and B cells. Second, it contributes to the local generation of Foxp3+ T_{Reg} cells together with TGF-β. Last, RA mediates class-switching to IgA in B cells in both PPs and MLNs (Bekiaris et al., 2014). Intestinal DCs also express the integrin $\alpha_V\beta_8$, which has the capacity to cleave the latent TGFβ into its active form (Fenton et al., 2017). Active TGF-β is essential for the regulation of different T-cell subsets, promoting the differentiation of Foxp3 T regulatory cells (T_{Reg}), Th17 cells and intraepithelial lymphocytes (IELs).

The functional properties of intestinal DCs can be altered by elements in the intestinal microenvironment, such as epithelial cell-derived factors (i.e. thymic stromal lymphopoietin, TSLP), and several dietary and bacterial metabolites in a process known as local conditioning (Coombes and Powrie, 2008). The consequences of this local conditioning on T cell polarization will be explained further in the text.

1.2.2.2.3 Human dendritic cell subsets

The human SI contains three main DC subsets, all of them can be also found in MLNs even at the steady-state. Human intestinal DCs are HLA-DR+ CD11c+ CD14-, but can be distinguished based on the differential expression of CD103 and SIRPα. The predominant subset, CD103+ SIRPα+ DCs, also express CD1c and IRF4, thus belonging to the cDC2 lineage. This population produces the highest amounts of the enzyme responsible to metabolize RA and the highest expression of $\alpha_V\beta_8$ (Fenton et al., 2017). In line with this, CD103+ SIRPα+ DCs exhibit enhanced capacity of *in vitro* gut-imprinting of T cells and Foxp3 induction compared to the other DC subsets (Joeris et al., 2017). In contrast, CD103+SIRPα- DCs express markers specific for cDC1 lineage (e.g. DNGR-1, XCR1, CD141, and TLR3) and are dependent on BATF3, ID2 and IRF8 expression for their development. In mice, XCR1+ DCs have been shown to play a key role in cross-presenting antigens to CD8+ T cells (Cerovic et al., 2015). The third subset, CD103- SIRPα+ DCs, present heterogeneous expression of monocyte-related markers (like CCR2 and calprotectin) and are transcriptionally and functionally very similar to intestinal Mϕs (Richter et al., 2018), suggesting that this subset comprise a mixed population of *bona fide* DCs and monocyte-derived cells.

1.2.3 Intestinal plasma cells and IgA production

The main function of B cells is to produce antigen-specific antibodies (also termed immunoglobulins, Ig). Each B-cell clone produces immunoglobulins with a unique specificity. Immunoglobulins can be synthesized as soluble proteins or membraned-bound, forming the B-cell receptor (BCR). Immunoglobulins are composed of two identical heavy chains and two light chains, which are joined by disulfide bonds. Immunoglobulins can be also separated into two fragments with different functions, termed the Fab (antigen-binding fragment) and the Fc (crystallizable fragment). The Fab fragment contains the variable regions of the antibody that recognize the antigen, whereas the Fc includes the constant region responsible for specific effector functions, such as binding to Fc receptors on macrophages and phagocytes or activation of complement. There are five isotypes of immunoglobulins (IgG, IgD, IgM, IgA, and IgE), each

one presenting different Fc fragments involved in different effector mechanisms (Schroeder and Cavacini, 2010).

B cells develop in the BM from common lymphoid progenitors that give rise to pro-B cells. During their differentiation, each B-cell precursor undergoes individual rearrangement and assembly of the immunoglobulin genes in several consecutive steps. The first step involves the recombination of the V (variable), J (junction) and D (diversity) gene segments encoding the heavy chains, followed by similar V-J recombination of the light chains during the pre-B cell stage (Herzog et al., 2009; Schlissel, 2003). This maturation process gives rise to immature B cells, which express a surface IgM receptor and undergo negative selection. Self-reactive B-cell clones are eliminated during the negative selection, and the surviving immature B cells leave from the BM to the periphery and differentiate into mature IgM+ IgD+ B cells (Nemazee, 2017). Mature naïve B cells migrate to peripheral lymphoid organs, where they can encounter their specific antigen and differentiate into memory B cells and antibody-secreting PCs. Further maturation of the antibody repertoire enhances the binding to the antigens and the effector functions. Class-switch recombination (CSR) and somatic hypermutation (SHM) are the crucial events for antibody maturation, and both require activation-induced cytidine deaminase (AID). CSR exchanges the gene encoding the heavy chain constant region with a new set of constant genes downstream through a deletion/recombination process. SHM involves the insertion of point mutations in the variable region of the antibody to modify the affinity for the antigen (Xu et al., 2012).

The gastrointestinal tract contains the largest population of PCs in the body (Pabst et al., 2008). Small intestinal PCs are located in the LP where they produce massive amounts of secretory antibodies, predominantly IgA (79%), but also IgM (18%) and IgG (3%) (Brandtzaeg et al., 1999). Intestinal secreted IgA (SIgA) is produced as a dimer and is actively transported across the epithelial barrier by the action of the epithelial polymeric Ig receptor (pIgR) (Brandtzaeg, 2013). The transcytosed SIgA binds to luminal bacteria, preventing their contact with the epithelium and their access across the epithelial barrier (Pabst and Slack, 2019). As part of its immune-exclusion function (see **Figure 2**), SIgA targets both commensal bacteria and pathogenic bacteria and toxins. SIgA-coated bacteria may agglutinate forming clumps, which promotes their clearance through peristalsis (Bunker and Bendelac, 2018).
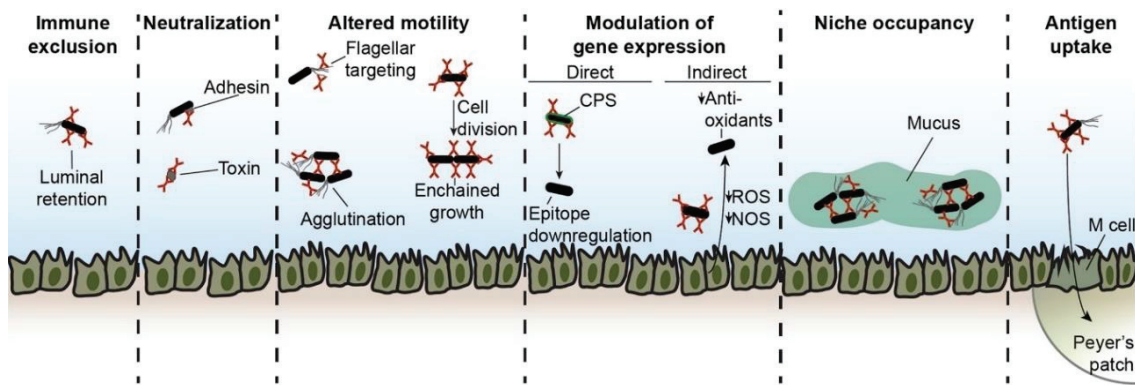
Figure 2. Functions of intestinal SIgA. Reprinted from Immunity 2018, 49/ 2, Jeffrey J. Bunker and Albert Bendelac, IgA Responses to Microbiota, 211-224, © 2018, with permission from Elsevier.

Intestinal PCs can be produced through T cell-dependent and T cell-independent responses, though it is still controversial whether this last mechanism occurs in humans (Spencer and Sollid, 2016). Intestinal PC are mostly generated in PPs and MLNs through a T cell-dependent pathway. This process involves interactions between B cells and CXCR5+ T follicular helper (T$_{FH}$) cells in the follicles of the germinal centers (GC). The stimulation and cytokines provided by the T$_{FH}$ cells (through CD40-L, ICOS, IL-21, and IL-4) and follicular dendritic cells (through TGF-β, BAFF, and IL-6) promote B cells to undergo extensive proliferation, somatic hypermutation (SHC) and class-switch to IgA (Brandtzaeg, 2013; Gutzeit et al., 2014). Activated B cells emerging from the GC-reaction upregulate α$_4$β$_7$ and CCR9 gut homing receptors in response to the RA produced by DCs in the PPs, and migrate to the LP via blood. Once in the LP, B cells differentiate to antibody-secreting PCs (Spencer and Sollid, 2016). The observation that mice genetically lacking T cells retained substantial production of SIgA suggested that T-cell independent pathways may contribute to the generation of IgA-producing PCs. T cell-independent responses might also take place in LP and ILFs, because mice lacking GALT retain some IgA production (Fagarasan et al., 2001; Suzuki and Fagarasan, 2009). In the LP, DCs can capture luminal antigens through transepithelial projections and receive conditioning signals from epithelial cells. DCs can then present their cargo to B cells in the LP or ILFs and secrete BAFF and APRIL. IL-6 produced by LP stromal cells together with BAFF and APRIL from DCs induce class-switch recombination in activated B cells and promote their survival as PCs (Bunker and Bendelac, 2018; Suzuki et al., 2007).

An early study in mice showed that intestinal PCs present a half-life of 4.7 days (Mattioli and Tomasi, 1973), suggesting that the PC pool is highly dynamic. More recent studies found that constant antigenic attrition induces extensive remodeling of the PC repertoire in the intestine (Hapfelmeier et al., 2010). This led to the prevailing notion that a rapid PC turnover

assures the generation of protective responses against a highly diverse and changing array of microbial and dietary antigens. In this scenario, pre-existing PC populations in the LP are constantly displaced by newly generated PCs with renovated antigen specificities that reflect the current luminal content. However, PCs generated in mice during oral infection with cholera toxin were found to persist in the LP for up to 9 months after immunization (Lemke et al., 2016). Despite that human intestinal PCs and BM long-lived PCs present some common phenotypic and transcriptional features (Nair et al., 2016), direct evidence of long-lived PCs in the human intestine is lacking. Further studies are needed to determine whether the intestinal PC pool contains cells with different durability and how long-lived PCs can persist in the human gut.

1.2.4 Intestinal T cells

1.2.4.1 T-cell development

T cells originate from lymphoid precursors in the BM that migrate to the thymus, where their maturation takes place. In humans, thymic T cell development starts *in utero* as early as 9 weeks of gestation, peaks during the first decade of life and declines after puberty, due to progressive thymus involution (Kumar et al., 2018a). During their maturation, the developing T cell progenitors within the thymus (named thymocytes) undergo several differentiation and selection steps that involve interactions with thymic stromal cells and APCs (Anderson and Jenkinson, 2001). As a result, the majority of the T cells generated in the thymus express a functional αβ-T cell receptor (TCR), and 5% bear a γδ-TCR.

Initially, thymocytes lacking CD4 and CD8 co-receptor expression (double-negative, DN) rearrange the TCR-β chain locus. Thymocytes that successfully complete TCR-β rearrangements receive survival signals and upregulate the expression of the CD4 and CD8 co-receptors, becoming double positive (DP) cells. DP thymocytes then rearrange the TCR-α chain and undergo positive selection in the cortex (Spits, 2002). During the positive selection, only cells with a productive αβ-TCR able to recognize self-peptide – MHC complexes with enough affinity survive and continue their differentiation. Thymocytes recognizing peptides presented on MHC II molecules during the positive selection gave rise to mature CD4+ T cells, whereas cells belonging to the CD8+ T-lineage recognize peptides bound to MHC I molecules (Spits, 2002). The subsequent negative selection takes place in the medulla, where thymocytes that bind too strongly to self-antigens presented on MHC molecules are eliminated (Kurd and Robey, 2016). The majority of the thymocytes (around 98%) fail this selection process and die by apoptosis,

but those surviving can then exit the thymus as CD4+ or CD8+ single-positive (SP) mature naïve T cells. Natural regulatory T cells (nT$_{reg}$) express the transcription factor Forkhead box P3 (Foxp3) and represent around 10% of human SP CD4+ T cells (Kumar et al., 2018a). Mature naïve cells leaving the thymus express CD45-RA and the chemokine receptor CCR7, which allows them to migrate to secondary lymphoid organs (SLOs), including lymph nodes (LN) and the white pulp of the spleen (Sallusto et al., 1999; von Andrian and Mackay, 2000).

1.2.4.2 T-cell receptor repertoire

The TCR is a heterodimer of α- and β-chains (or γ- δ-chains) that recognizes peptides presented in either MHC class-I and class-II molecules (MHC restriction). In this section I will focus on TCRαβ+ T cells. On the T cell surface, the TCR is associated with a complex of four signaling subunits (one γ-, one δ-, and two ε) known as CD3, and a cytosolic homodimer of ζ subunits. The cytosolic regions of the TCR complex contain immunoreceptor tyrosine-based activation motifs (ITAMs) to transmit intracellular signals after TCR ligation, ultimately leading to T-cell activation (Call et al., 2002). The additional binding of the co-receptor to the MHC molecule stabilizes the interactions between the TCR and the peptide-MHC complex, facilitating TCR signaling (Konig et al., 1992).

The organization of the TCR gene segments is similar to that of immunoglobulin gene segments. The TCR chains consist of a variable region, important for antigen recognition, and a constant region. The TCRα locus contains variable (V) and joining (J) gene segments, whereas the TCRβ locus contains additional diversity (D) gene segments (**Figure 3**). During VDJ recombination, one random allele of each gene segment is progressively rearranged to the others and random nucleotides are added and/or deleted at the junctional sites between the gene segments (Davis, 1990; Davis and Bjorkman, 1988).

In humans, the pool of mature naïve T cells is highly diverse, consisting of more than 100 million different specificities (termed T-cell clonotypes) that are maintained over decades of life (den Braber et al., 2012; Qi et al., 2014). This extraordinary diversity is generated during T cell development by random combinations of germline segments (combinatorial diversity) and by random additions or deletions at the junction sites (junctional diversity) (Schatz and Ji, 2011).

The sequence encoded by the V(D)J junction is called complementary determining region 3 or CDR3. The CDR3 is the region of the TCR in direct contact with the peptide antigen,

and present the highest variability in both alpha and beta chains. For this reason, populations of T cells carrying identical CDR3 sequence are often defined as a *clonotype*.
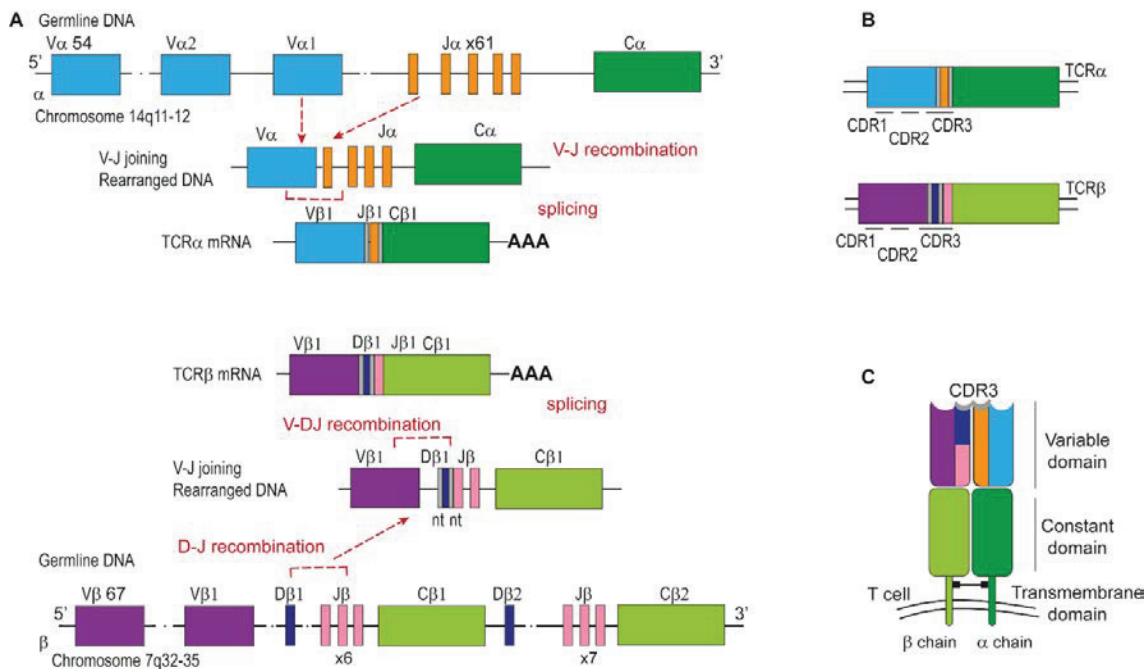
Figure 3. TCR gene arrangement. (A) Genomic organization of TRB and TRA loci. The human TRA locus is located at the chromosome 14 and contains 54 TRAV genes (belonging to 41 subgroups), 61 TRAJ gene segments and a unique TRAC gene. The TRB locus is at the chromosome 7 and consist of 64 to 67 TRBV genes (belonging to 32 subgroups), 13 TRBJ and 2 TRBC genes (Lefranc, 2001). Repertoire diversity is generated by V(D)J recombination of TCR gene segments, additional insertions and deletions at the junctional sites and pairing of TCRα and TCRβ chains. **(B)** Productive arrangements of TCRα and TCRβ transcripts. (C) TCRαβ heterodimer on the T cell surface. Each chain is organized in a constant region and a variable region, the last one responsible for antigen recognition. Adapted from (De Simone et al., 2018).

Additional diversity is achieved by the pairing of TCRα and TCRβ chains, and the total number of combinations in the TCRαβ repertoire is estimated at 10^{18} in humans (Arstila et al., 1999; Sewell, 2012). However, positive and negative selection in the thymus purges most of the specificities, creating a naïve repertoire that is substantially less diverse. Furthermore, antigen exposure in the periphery shapes the repertoire over time, leading to clonal expansion of antigen-specific populations. (Qi et al., 2014; Rudd et al., 2011).

1.2.4.3 T-cell priming

T-cell responses are initiated when a naïve T cell encounters an APC (usually a DC) in organized lymphoid tissues. The activation of the naïve T cell requires the integration of multiple signals through sustained interaction with the DC, leading to the formation of an immune synapse

(Dustin, 2014). In the first event of the T-cell priming, naïve T cells must recognize their specific antigen processed and presented in the groove of MHC molecules and ligate its co-receptor (signal 1). Then, to get fully activated naïve T cells need to receive the appropriate co-stimulatory signals (signal 2) provided though CD28 ligation by CD80/86 molecules on the DC (Baxter and Hodgkin, 2002). In addition, cytokines produced by the DC (signal 3) promote the proliferation and polarization into different effector cells.

Only activated DC present high levels of co-stimulatory molecules. The co-stimulatory signals are first delivered by CD80/86, but later other co-stimulatory receptors, such as CD40, 4-IBBL, CD70 and OX-40L engaging their corresponding ligands on the T cell (CD40L, 4-IBB, CD27, and OX40 respectively) are also involved to modulate the threshold for T cell activation (Chen and Flies, 2013). Both signal 2 and 3 depend on interactions of the DC with the pathogen (for example, through TLR activation) and the surrounding microenvironment (through inflammatory cytokines, danger signals, conditioning signals from the tissue, etc.) (Curtsinger and Mescher, 2010; Kapsenberg, 2003). As a result, activated pathogen-specific T cells undergo extensive clonal expansion, driven by IL-2 expression, and migrate to the site of infection to execute their effector functions. Once the pathogen is cleared, the majority of the effectors die by apoptosis during the contraction phase, and only a small fraction survives as long-lived memory T cells (Kaech et al., 2002; Williams and Bevan, 2007).

1.2.4.4 Effector T- cell subsets

In order to fight against a broad variety of pathogens (viruses, bacteria, parasites) the host must mount specialized immune responses tailored to the insult encountered. The cytokine milieu during the activation of naïve T cells (signal 3) induces a specific gene expression program, which is regulated by modifications in the chromatin structure and activation of certain transcription factors in the differentiating cells (Weng et al., 2012). The resulting effector T cells can be broadly segregated into CD8+ "cytotoxic T lymphocytes, CTLs" and several subsets of CD4+ "T helper, T_H cells".

1.2.4.4.1 Cytotoxic T lymphocytes

CD8+ T cells are essential in the defense against viruses, intracellular bacteria and cancer due to their capacity to directly kill infected or malignant cells. CTLs recognize intracellular peptides bound to ubiquitously expressed MHC class I molecules, and after TCR engagement they release

and direct their cytotoxic granules towards the target cell, inducing its death. Target cell killing is mediated with great precision, avoiding tissue damage (Zhang and Bevan, 2011). To accomplish that, CTL activation is tightly controlled by different mechanisms, for example through the expression of several co-inhibitory and co-stimulatory receptors that bind their ligands on the surface of the DC (Chen and Flies, 2013). Moreover, CD4+ T cell help is needed to support robust CTL responses through the "licensing" of DCs, with both the CD4+ T cell and the CTL recognizing antigens presented on the same DC (Laidlaw et al., 2016; Williams and Bevan, 2007).

CTLs can kill several consecutive target cells rapidly because they store preformed cytotoxic granules, which contain perforin, granulysin and serin proteases named granzymes (Halle et al., 2017). Perforin first acts forming pores in the membrane of the target cell and guiding the delivery of granzyme. In humans, there are 5 types of granzymes (A, B, H, K, and M). All the granzymes are secreted as inactive proenzymes that mediate proteolysis once inside the target cell, inducing cell-death by different mechanisms (Chowdhury and Lieberman, 2008; Lieberman, 2003). Granzyme B, the best-studied, mediates cleavage and activation of caspase-dependent apoptosis. CTLs express FASL and can also kill through the FAS pathway, by activating the apoptosis in target cells expressing FAS. This mechanism is important for lymphocyte homeostasis, regulating the lymphocyte number during the contraction phase (Barry and Bleackley, 2002).

Apart from their cytolytic activity, most CTLs also produce cytokines, including interferon-gamma (IFN-γ), interleukin 2 (IL-2), and tumor necrosis factor alpha (TNF-α) (van Aalderen et al., 2014). IFN-γ inhibits viral replication, and induces MHC class-I and II expression and Mϕ activation, whereas TNF-α increases the antimicrobial action of the Mϕs and induces the recruitment of other immune cells (Kopf et al., 2010). Some degree of heterogeneity exists among effector CD8+ T cells regarding their cytotoxic capacity and the ability to produce individual or multiple cytokines. The responses characterized by CTLs producing two or more cytokines simultaneously (IFN-γ, IL-2, and TNF-α) correlate with enhanced protection against infections (Seder et al., 2008) and superior anti-tumor immunity (Ott et al., 2017).

The generation of IFN-γ and IL-12 cytokines in response to intracellular pathogens promotes CD8+ T cells to differentiate into CTLs (Cox et al., 2013). The T-box transcription factors T-bet and Eomesodermin (Eomes) have crucial roles controlling the cytotoxic differentiation program, for example by inducing the expression of IFN-γ, granzyme B and perforin (Kaech and Cui, 2012) (**Figure 4**).

1.2.4.4.2 T helper subsets

Effector CD4+ T cells (also termed T helper cells) support immune responses by producing cytokines, which induce neighboring cells (such as APCs, CD8+ T cells and B cells) to perform specific functions, or chemokines that recruit other immune cells. The T_H responses comprise diverse subsets, including T_H1, T_H2, T_H17, T_H9, T_H22, T_{FH}, and T_{reg} cells (**Figure 4**).

T_H1 cells promote cell-mediated responses against viruses and intracellular bacteria (such as *Listeria* or mycobacteria) (Mosmann and Coffman, 1989). In response to these pathogens, innate cells (mainly DCs) produce IFN-γ and IL-12 that drive T_H1 differentiation through the activation of Signal Transducer ad Activator of Transcription (STAT)4 and the transcription factor T-bet (Zhu and Paul, 2008; Zhu et al., 2010). T_H1 cells express the signature cytokine IFN-γ, which induces Mφ activation. Additionally, they also produce IL-2, lymphotoxin-alpha (LT-α), and TNF-α that promote Mφ, NK cells and CD8+ T cells to mediate pathogen clearance (Commins et al., 2010). However, a dysregulated T_H1 function can lead to inflammatory conditions and tissue destruction (Kopf et al., 2010).

T_H2-*cell* polarization occurs when the naïve T cell is activated in the presence of IL-4, produced in response to extracellular parasites. IL-4 activates STAT6 and induces the expression of GATA3, the master transcription factor of T_H2 cells (Murphy and Reiner, 2002). GATA3 blocks the expression of IFN-γ, thus suppressing the differentiation into the T_H1 lineage, and promotes the expression of IL-4, IL-5, and IL-13 (Li et al., 2014; Mucida and Cheroutre, 2010). These signature cytokines activate eosinophils, mast cells, basophils, and mediate IgE production by B cells in order to clear the parasite. T_H2 responses are also involved in the development of allergy and asthma (Paul and Zhu, 2010).

TGF-β contributes to reprogram T_H2 cells into a new subset of T_H cells, named *T_H9 cells*. Like T_H2 cells, T_H9 cells are involved in the defense against parasites but they are characterized by the secretion of IL-9. T_H9 cells are potent activators of mast cells, and stimulate mucus production (Koch et al., 2017).
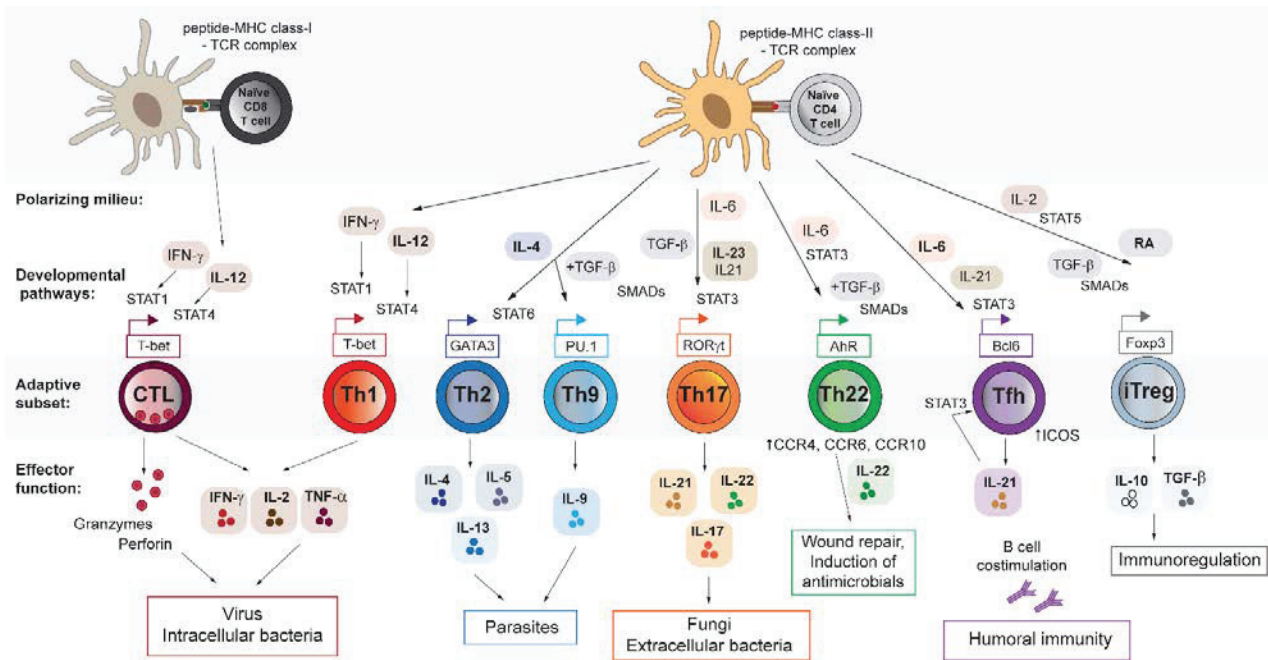
Figure 4. Transcriptional regulation of CD8+ and CD4+ T cell effector subsets. The environmental conditions, such as the exposure to a diverse array of pathogens, determine which cytokines (signal 3) the APC will produce. Naïve CD8 T cells differentiate into CTLs in response to IFN-γ and IL-12. When a naïve CD4 T cell gets activated by an APC, it can develop into several functional Th subsets. The cytokines in the microenvironment polarize the Th differentiation by activating signal transducers and activators of transcription (STAT) proteins that induce the expression of master transcription factors. The resulting Th subset will promote an immune response tailored to the pathogen encounter. When pathogens are absent, the environment favor the development of T regulatory cells (Tregs). iTreg: induced Treg cell. RA: Retinoid acid; SMADs: SMAD proteins, are the signaling transducers for receptors of the TGF-β superfamily. Th: T helper subsets; Tfh: T follicular helper.

T$_H$17 cells are produced in response to extracellular bacteria (e.g. *Staphylococcus aureus*) and fungi, such as *Candida albicans* (Zhu et al., 2010). Moreover, pathogenic T$_H$17 cells have been characterized in the context of a variety of autoimmune diseases, such as multiple sclerosis, rheumatoid arthritis or inflammatory bowel disease (IBD) (Yang et al., 2014). T$_H$17 differentiation is initiated when the naïve T cells is activated in the presence of IL-6 and TGF-β and receives a sustained stimulation with IL-23 and IL-21 (Basso et al., 2009). Together, this cytokine milieu promotes the activation of STAT3 and the expression of the transcription factor ROR-γt, which induces IL-17 production (Li et al., 2014). IL-17, together with IL-6 and IL-8, mediates the activation and recruitment of neutrophils to the site of infection (Commins et al., 2010). The importance of IL-17 is highlighted in patients with genetic diseases causing low levels of IL-17 (i.e. hyper-IgE syndrome), whom suffer from severe fungal and bacterial recurrent infections (Ma et al., 2008).

T$_H$22 cell development depends on the expression of the aryl hydrocarbon receptor (AhR) that induces the production of high levels of IL-22 without IFN-γ, IL-4 or IL-17 expression

(Eyerich et al., 2009). IL-22 acts on epithelial cells promoting the secretion of anti-microbial peptides. T_H22 cells express the skin-homing receptors CCR4, CCR6 and CCR10, and have been involved in wound healing, but also in the pathogenesis of some skin diseases (Fujita, 2013).

Follicular helper T cells (T_{FH}*,)* constitute a CD4+ T_H cell subset specialized in providing help to B cells in the germinal centers. Therefore, T_{FH} cells are characterized by the expression of CXCR5, the chemokine receptor required for homing to B cell follicles. T_{FH} differentiation requires the expression of the transcription factor Bcl6, induced by the cytokines IL-21 and IL-27. T_{FH} cells express a variety of cytokines and costimulatory molecules (such as ICOS) to promote class-switching and production of high-affinity antibodies during the germinal center reactions (Breitfeld et al., 2000; Mucida and Cheroutre, 2010; Zhu et al., 2010).

In addition to the effector subsets described above, which are involved in activating target cells to promote pathogen clearance, another group of CD4+ T cells has a regulatory function. These regulatory T cells (T_{reg}) play a crucial role in limiting the immune responses to prevent immunopathology and promoting tolerance to self- and innocuous antigens. The master transcription factor controlling the development, maintenance, and function of T_{reg} cells is Forkhead box P3 (Foxp3). Patients with IPEX syndrome (immune dysregulation, polyendocrinopathy, enteropathy, X-linked) have mutations in *FOXP3* that cause broad multiorgan autoimmunity (Sakaguchi et al., 2008). Based on their origin, T_{reg} cells can be divided into natural T_{reg} (nT_{reg}) cells and induced T_{reg} (iT_{reg}) cells. nT_{reg} cells are produced directly in the thymus following recognition of self-antigens by the TCR. In contrast, iT_{reg} cells recognize exogenous antigens in the peripheral tissues and are generated under the influence of environmental factors, such as TGF- β and retinoid acid (RA), in the absence of inflammatory cytokines (Whibley et al., 2019). Both populations of T_{reg} cells present high CD25 (IL-2 receptor α-chain) surface expression and low levels of the IL-7 receptor (CD127). It is been suggested that the expression of the transcription factors Helios and neuropilin-1 (Nrp-1) can be used to distinguish between nT_{reg} and iT_{reg} cells, based on the higher expression of these two markers on nT_{reg} cells (Singh et al., 2015; Thornton et al., 2010). Helios seems to be a more specific marker for nT_{reg} cells than Nrp1 given that TGF-β can induce Nrp1 expression *in vivo* and *in vitro.* However, other studies also question the role of Helios as nT_{reg} cell-marker, because Helios expression can be induced during T-cell activation and proliferation (Akimova et al., 2011). Regardless of their origin, T_{reg} cells exert their suppressor functions by different mechanisms. This mechanisms include the production of anti-inflammatory cytokines (such as IL-10 and TGF-β), as well as direct cell-contact mechanisms to promote the suppression of effector T cells (by

cytolysis of target cells) or the disruption of the APC functionality (via receptors such as CTLA-4 and LAG-3 expressed on T$_{reg}$ cells) (Georgiev et al., 2019; Vignali et al., 2008).

Type 1 regulatory T cells (T$_R$1 cells) also perform their suppressive activity releasing large amounts of IL-10 and TGF-β, but unlike T$_{reg}$ cells, T$_R$1 cells lack Foxp3 expression (Roncarolo and Gregori, 2008). T$_R$1 cells are generated after activation of naïve CD4+ T cells with antigen in the presence of IL-10 (Roncarolo et al., 2006), and can be distinguished from other CD4+ T$_H$ and regulatory cell subsets by the co-expression of CD49b and lymphocyte activation gene 3 (LAG-3) (Gagliani et al., 2013).

1.2.4.4.3 Effector T cell plasticity and heterogeneity

Early studies into T$_H$ differentiation using simple and fixed *in vitro* polarization conditions suggested that T$_H$ subsets were distinct and stable lineages. However, recent *in vivo* reports have revealed that T$_H$ subsets display a certain degree of plasticity and heterogeneity, showing that functionally mixed phenotypes exist. This plasticity can be explained by the action of the immunological context and the cytokine milieu influencing the fate of committed effector T cells, which leads to the co-expression of master transcription factors or signature cytokines from another T$_H$ lineages. There is evidence showing that the route of infection may dictate the T$_H$ subset differentiation *in vivo*. For example, intravenous or intranasal infection with *Listeria monocytogenes* has reported to induce T$_H$1 or T$_H$17 cells, respectively (Pepper et al., 2010). In the mucosal tissues, the properties of the DC cells are influenced by the conditioning signals received from epithelial cells (Lambrecht and Hammad, 2003; Rescigno, 2014). Besides the DCs, other types of innate cells (such as neutrophils, γδ-TCR T cells, NK cells, basophils) provide cytokines that contribute to T$_H$ differentiation (Murphy and Stockinger, 2010).

It is still unclear whether some new T$_H$ subsets represent distinct lineages or just alternative pathways of cellular activation in response to changes in the microenvironment during infection. In this regard, T$_H$9 cells may just represent an adaptation of T$_H$2 cells (Murphy and Stockinger, 2010). Similarly, T$_{FH}$ present high degree of plasticity and are able to produce IFN-γ, IL-4, and IL-17. For this reason, it is still debated whether T$_{FH}$ cells represent a committed lineage or just different T$_H$ effectors that acquire CXCR5 expression and migrate to the B follicles (Sallusto, 2016). Moreover, several studies have shown that T$_{reg}$ cells may co-express Foxp3 with other signature transcription factors (T-bet, IRF4, STAT3), making them able to exert selective suppression of certain effector subsets (Sungnak et al., 2019). Some reports also suggest that Foxp3 expression is quite unstable and under certain conditions T$_{reg}$ cells can downregulate Foxp3 and acquire inflammatory T$_H$ or T$_{FH}$ features (Mucida and Cheroutre, 2010; Zhang et al.,

2017). On the other hand, transient Foxp3 expression can be found on activated non- T$_{reg}$ CD4+ T cells (Wang et al., 2007), indicating that Foxp3 expression alone may not be enough to induce regulatory T cell activity.

Despite that cytotoxic function seems to be the common feature of CD8+ T cells, the cytokine milieu can also influence their cytokine profile in a similar way than CD4+ T cells, giving rise to Tc2 cells (T$_H$2 analogue) and Tc17 (T$_H$17 analogue) subsets (Annunziato et al., 2015; Yen et al., 2009). Similarly, cytotoxic CD4+ T cells have been described. These cells display direct cytolytic activity mediated both by perforin/granzymes and FAS, in an MHC-class II fashion (Swain et al., 2012).

1.2.4.5 Intestinal T-cell subsets

The gut contains large numbers of T cells localized in the GALT or scattered in the lamina propria (LP) and the epithelium. CD4+ and CD8+ T cells populate the LP at an approximate ratio of 2:1 at the steady state, like the ratio of the peripheral blood T cells. The epithelium harbors a heterogeneous population of lymphocytes, termed intraepithelial lymphocytes (IELs), most of them being CD8+ T cells.

1.2.4.5.1 Intraepithelial T cells

In the human small intestine, IELs are located at the basal membrane between the enterocytes at a frequency of 10-15 IELs per 100 enterocytes (Ferguson, 1977; Mowat and Agace, 2014). The integrin CD103 (αE), which binds epithelial cadherin (E-cadherin) on the surface of the enterocytes (Schon et al., 1999), is abundantly expressed by IELs, allowing them to accumulate in the intestinal epithelium.

In mice, IE T cells comprise a variety of subsets with different lineages that can be divided into conventional (induced) and unconventional (natural) IELs. *Conventional IELs* express TCR-αβ together with the CD8αβ heterodimer or CD4 co-receptors (**Figure 5**). Conventional IELs originate from naïve T cells that have recognized antigens in the secondary lymph nodes and are MHC class I- or class II- restricted (Hayday et al., 2001). In contrast, *unconventional IELs* express either TCR-αβ or TCR-γδ, and most lack CD8β or CD4 expression but express CD8αα homodimers. The CD8αα strongly binds the thymic leukemia antigen (TL), a non-classical MHC class I molecule expressed in the thymus and on small intestinal epithelium. In contrast to conventional CD4 and CD8αβ co-receptors, CD8αα functions as a repressor of the TCR activation (Cheroutre and Lambolez, 2008). Unconventional IELs arise from DP thymic precursors that recognize self-ligands with very high affinity and escape clonal deletion undergoing an

alternative maturation process termed agonist selection. Unconventional IELs acquire their effector program in the thymus and then migrate directly to the intestinal epithelium. During gestation and at birth, unconventional IELs populate the intestines, decreasing with the age; whereas, conventional IELs are scarce at birth but increase after exposure to antigens with age (Cheroutre et al., 2011; McDonald et al., 2018).

In humans, the intraepithelial T cell compartment is composed of antigen-experienced TCR-αβ CD8αβ+ cells (70-80%), TCR-αβ CD4+ cells (10-15%) and TCR-γδ+ cells (5-20%) (Abadie et al., 2012) (**Figure 5).** Unconventional TCR-αβ CD8αα+ cells are apparently absent in humans. However, TCR-γδ+ IELs can express CD8αα (Mayassi and Jabri, 2018), and the existence of a TCR-αβ CD8αα+ human counterpart is still unclear (Mayassi and Jabri, 2018; Schattgen et al., 2019).
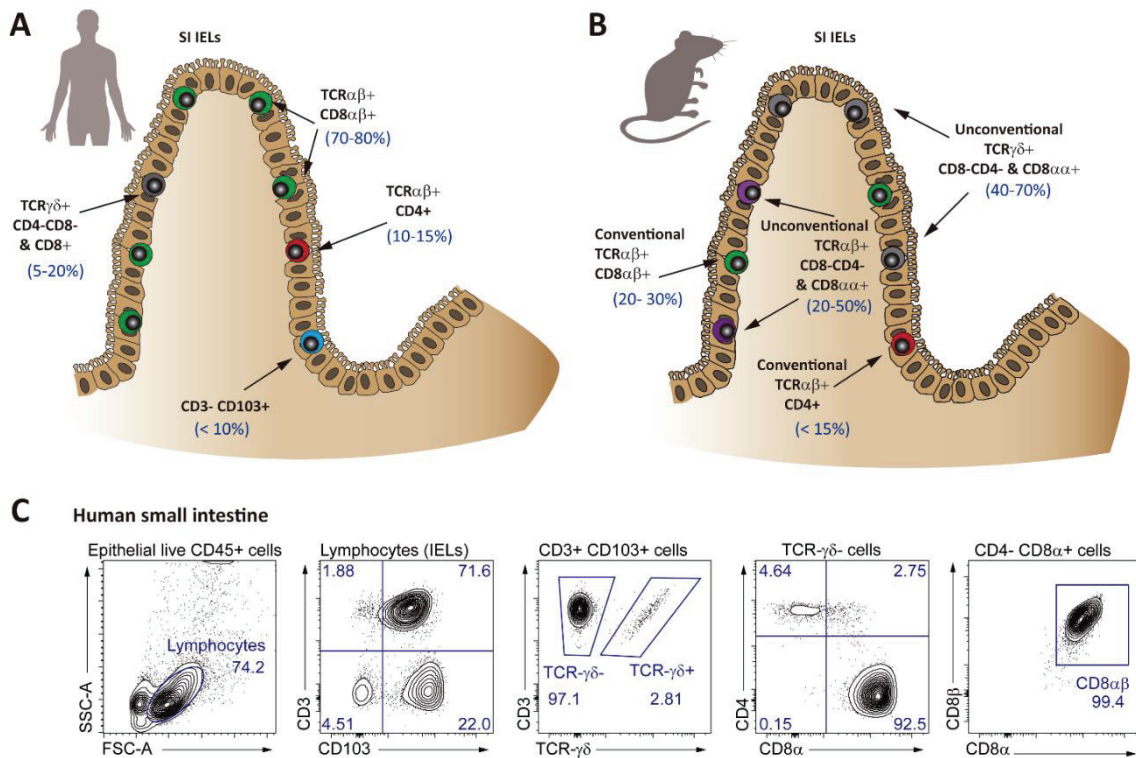
Figure 5. Distribution of the major intraepithelial lymphocyte subsets in SI of humans and mice
(A) Human intraepithelial lymphocyte subsets. **(B)** Murine intraepithelial lymphocyte subsets. Percentages are taken from (Abadie et al., 2012) **(C)** Flow- cytometric analysis of the intraepithelial cell compartment in human small intestine.

IELs are not static, they are constantly patrolling between the intestinal epithelial cells, and they display potent cytolytic activity and a T$_H$1 cytokine profile. These functions are enhanced by exposure to IL-12, IL-15, and IL-18 cytokines produced by intestinal epithelial cells and LP APCs or by engaging of co-stimulatory NK cell receptors (such as CD161, NKG2D, 2B4), which are broadly expressed on all the IEL subsets (Jabri and Ebert, 2007; McDonald et al., 2018).

IELs also express a broad array of co-inhibitory NK cell receptors (such as CD94/NKG2A) that suppress cytotoxicity and cytokine secretion, which ensures they maintain an "activated yet quiescent" state. Through these activating /inhibitory NK receptors IELs sense the inflammatory and stress signals from the tissue microenvironment, which modulates their TCR activation threshold (Jabri and Ebert, 2007). Studies in germ-free mice and mice on an "antigen-free" diet showed that these animals presented reduced numbers of IELs compared to conventional mice, highlighting that IEL differentiation is strongly influenced by the intestinal microenvironment (Cheroutre et al., 2011).

In addition to T cells, both human and murine IELs contain a subset of CD3- CD103+ IELs, which includes group 1 innate lymphoid cells (ILC1) and CD3- CD7+ ILC1-like cells (Ettersperger et al., 2016; McDonald et al., 2018). These two minor populations present a pro-inflammatory cytokine profile and NK cell activity, although their origin and precise identity are still not well described (León et al., 2003; Lutter et al., 2018a).

1.2.4.5.2 Lamina propria T cells

The intestinal LP includes both effector and regulatory antigen-experienced T cells. Despite that CD4+ T cells constitute the most abundant T-cell subset, conventional CD8αβ+ T cells and few TCR-γδ T cells can be also found in the LP. Several reports showed a very low overlap in the TCR repertoires of LP and IE CD8+ T cells, which suggested that there is little to no mixing between these two compartments at the steady-state (Cauley and Lefrancois, 2013).

During homeostasis, the LP CD4+ T-cell population includes T_H1 and T_H17 cells as well as IL-10 producing Foxp3+ T_{reg} cells and Foxp3- T_R1 cells. In contrast, T_H2 cells are virtually absent in healthy humans and animals that are not infected with intestinal parasites (Ai et al., 2014). T_H1 cells can be generated in the LP in response to infections with pathogenic viruses or intracellular bacteria, such as *Listeria monocytogenes* (Romagnoli et al., 2017). Microbiota plays a crucial role in shaping the phenotype and plasticity of the intestinal T cells. T_H1 and T_H17 cells are present at lower numbers in germ-free mice compared to conventional mice (Gensollen et al., 2016). Moreover, some bacterial species, for example, *Bacteroides* have been involved with T_H1-cell induction through the production of polysaccharide A, whereas Segmented Filamentous Bacteria (SFB) promotes the differentiation of T_H17 cells in the LP of mice (Hooper and Macpherson, 2010; Sorini et al., 2018). IL-17 is important for intestinal homeostasis by mediating repair and reinforcement of the epithelial barrier (Maloy and Kullberg, 2008). T_H17 cells also produce IL-22, which stimulates the production of antimicrobial peptides by epithelial cells (Hooper and Macpherson, 2010). However, pro-inflammatory T_H17 cells have been associated

with the pathogenesis of IBD (Shale et al., 2013), and elevated numbers of IL-17+ IFN-γ+ double-producing cells have been found in the intestinal mucosa of IBD patients (Rovedatti et al., 2009).

The relatively low rate of intestinal inflammation among healthy individuals despite the enormous microbial and antigenic load demonstrates that the regulatory mechanisms dominate in the intestine at the steady-state. T_{reg} cells exhibit a high level of adaptation to the intestinal microenvironment. Colonic T_{reg} cells appear to develop in response to the microbiota whereas the majority of the T_{reg} cells in the small intestine appear to develop in response to dietary antigens (Agace and McCoy, 2017). However, our current knowledge about intestinal T_{reg} cells is mainly derived from mouse models, and little is known about the phenotype, origin and functions of the T_{reg} cells in the human gut, especially in the small intestine.

The different mechanisms of antigen uptake by intestinal APCs may influence the T-cell subset differentiation. For example, CD103+ DCs produce TFG-β and RA, both required for the upregulation of Foxp3 and the formation of iT_{reg} cells. In contrast, CD11b+ DCs seem to promote differentiation into T_H1 or T_H17 subsets (Ai et al., 2014). The influence of inflammation, microbiota or dietary products may induce plasticity between the intestinal T_H and regulatory T cell subsets. Apart from the T_H17 to T_H1 conversion, dual expressing Foxp3+ ROR-γt+ cells have been found in human intestinal samples, especially in inflammation settings (Shale et al., 2013). Furthermore, T_H17 to T_{FH} and T_{reg} to T_{FH} plasticity have been also observed in the intestine (Brucklacher-Waldert et al., 2014).

1.2.4.5.3 Intestinal T-cell homing

To perform their immunosurveillance function, circulating T cells have to exit the blood through interactions with the vascular endothelium and enter the peripheral tissues. Leukocyte extravasation is a highly regulated process that comprises several sequential steps: selectin-mediated rolling, chemokine signaling (to induce integrin activation), firm arrest mediated by integrins and transmigration across the endothelial layer (von Andrian and Mackay, 2000). T-cell homing is a tightly controlled process that involves the induction of specific integrins and chemokines on the surface of the T cells. These homing molecules are used to guide T cells to specific regions of the body.

In the intestinal MLNs and PPs, migratory DCs carrying antigens from the PPs or the LP encounter naïve T cells. Upon antigen recognition, DCs imprint gut-tropism on activated T cells. This property depends on the capacity of gut DCs to produce RA, which induces the gut homing receptors $\alpha_4\beta_7$ and CCR9 on T cells. The integrin $\alpha_4\beta_7$ binds MadCAM-1 (mucosal vascular

addressin cell adhesion molecule -1) which is constitutively expressed on intestinal LP vascular endothelium. The chemokine receptor CCR9 interacts with CCL25, which is constitutively and specifically produced by small intestinal epithelial cells (Agace, 2008; Marsal and Agace, 2012). Activated $\alpha_4\beta_7$+ T cells arriving at the intestinal mucosa are exposed to TGF-β, which is abundantly produced by intestinal epithelial cells and DCs. TGF-β mediates the downregulation of α_4 and upregulation of α_E integrin (CD103), which forms a heterodimer with the β_7 chain on T cells and allows them to accumulate in the epithelium (McDonald et al., 2018).

1.2.4.6 Intestinal innate-like lymphocytes

The small intestine contains minor populations of T cells with restricted TCRs and innate immune functions. These subsets include mucosal-associated invariant T cells (MAIT cells) and invariant natural killer T cells (iNKT cells) (Mowat and Agace, 2014). MAIT cells represent a 2-3% of the LP and IE T cells in human jejunum and express a Vα7.2 Jα33 invariant TCR-α chain but restricted TCR-β. MAIT cells recognize metabolites of vitamin B presented by the highly conserved MHC-class I related protein (MR1) (Bennett et al., 2015). MAIT cells are activated by cells infected with bacteria and rapidly release pro-inflammatory cytokines and exert cytotoxic activity, mediated by granzyme-B and perforin (Napier et al., 2015).

iNKT cells represent a T-cell subset expressing NK cell markers, such as CD161 in humans, and displaying an invariant TCR. iNKT cells comprise 0.5 – 1% of the LP and IE T cells and recognize lipids and glycolipids presented by CD1d molecules. CD1d is a nonpolymorphic MCH protein expressed on intestinal epithelial cells (Crosby and Kronenberg, 2018). iNKT cells mediate their effector functions through a rapid release of T_H1 (IFN-γ, TNF-α), T_H2 (IL-4) and T_H17 (IL-17) cytokines (Bennett et al., 2015).

Innate lymphoid cells (ILCs) are non-T non-B lymphocytes lacking myeloid-specific phenotypic markers (Lin-). ILCs do not express antigen-specific receptors; instead, they respond to changes in the environment (such as cytokines) and play a central role in early innate responses in the intestinal mucosa (Sedda et al., 2014). ILCs are currently classified into three distinct groups based on their expression of transcription factors and their effector cytokine profile. ILC1, ILC2 and ILC3 mirror the functions of the T_H1, T_H2 and T_H17 subsets, respectively. Natural killer (NK) cells represent the innate counterpart of the CD8+ T cells and belong to the ILC1 group. In addition, the ILC3 group includes lymphoid tissue inducers (LTi) that are involved in the formation of secondary lymphoid structures (Cherrier et al., 2018).

1.3 T cell memory heterogeneity and migratory patterns

Naïve T-cell immunosurveillance is based on continuous recirculation through the secondary lymph organs (SLOs, including the LNs and the white pulp of the spleen) that drain and collect antigens from the peripheral tissues. The entry to the SLOs requires CD62-L (L-Selectin) expression, which binds the peripheral lymph node addressin (PNAd), and CCR7 expression, which binds the chemokine CCL21 on high endothelial venules. Egress from SLOs is mediated by sphingosine-1-phosphate (S1P) gradient, requiring the expression of the S1P receptor 1 (S1PR1) on T cells (Mueller et al., 2013).

During infection, naïve T cells undergo an extraordinary expansion, increasing as much as 10^5- fold the number of antigen-experienced cells. Following pathogen clearance and the resolution of inflammation, the majority (90-95%) of the effector T cells die, and the ones that survive become part of a heterogeneous pool of memory cells (Kaech et al., 2002). Despite this dramatic contraction, the frequency of antigen-specific memory T cells that survive is still much higher ($\approx$ 1000 fold) than the frequency of the precursor naïve T cells before pathogen encounter, thus reinforcing the immunosurveillance of the host (Blattman et al., 2002; Masopust et al., 2007). Memory T cells display several enhanced functional characteristics compared to naïve T cells. First, memory cells have less stringent requirements for subsequent activation, responding to lower concentrations of antigen and showing less dependency on co-stimulation. Second, memory T cells show increased proliferative potential and more rapid effector response. Third, memory T cells acquire the ability to traffic to peripheral tissues (Berard and Tough, 2002).

Based on their distinct migratory patterns and functional capacities, in 1999 Sallusto et al. classified human circulating memory T cells in peripheral blood into two different subsets: central memory T cells (T_{CM}) and effector memory T cells (T_{EM}) (Sallusto et al., 1999). Like naïve T cells, T_{CM} cells express CD62-L and CCR7, allowing them to enter the SLOs. In contrast, T_{EM} cells are CCR7- CD62-L- and migrate between blood and the peripheral tissues. T_{CM} cells present extensive proliferation and IL-2 production, whereas T_{EM} cells are less proliferative and display a higher capacity to produce effector cytokines, such as IFN-γ or IL-4. In humans, a population of terminally differentiated effector cells re-expressing CD45-RA (T_{EMRA} cells) is found frequently within the CD8+ T cell lineage. T_{EMRA} cells present low proliferative and functional capacity and accumulate with age and persistent infections, such as CMV (Kumar et al., 2018a). Recently, stem cell memory T (T_{SCM}) cells have been identified, comprising memory cells with high self-renewal capacity but no effector function (Gattinoni et al., 2011). The comparative analysis of

telomere length, differentiation potential, proliferative capacity, and effector functions among different T-cell subsets led to the postulation of a linear model of differentiation from naïve to memory T cells to differentiated effectors (**Figure 6**) (Mahnke et al., 2013; Restifo and Gattinoni, 2013). This model has been confirmed by recent studies using epigenetic and transcription factor analysis (Dogra et al., 2016; Moskowitz et al., 2017).

These lineage studies using blood lymphocytes helped to establish the concept of systemic memory, which implies that memory T cell surveillance is mediated through efficient recirculation between blood, lymphoid tissues (T_{CM} cells) and non-lymphoid tissues (T_{EM} cells) (**Figure 6**). However, this paradigm changed when seminal studies showed that substantial numbers of CD8+ and CD4+ T_{EM} cells were maintained long after pathogen clearance (Masopust et al., 2001; Reinhardt et al., 2001). After this finding, the main unsolved question was whether T_{EM} cells continuously recirculate through the tissues or in contrast they permanently reside within the peripheral tissues. Subsequent studies using parabiotic mice provided early evidence that memory CD8+ T cells in the brain and the intestines do not completely equilibrate with their circulating counterparts (Klonowski et al., 2004). In the last decade, several studies have demonstrated that a population of T_{EM} cells is permanently lodged in peripheral tissues (such as the gut, lungs, skin…) without exchanging with the circulation (Gebhardt et al., 2009; Jiang et al., 2012; Masopust et al., 2010; Wakim et al., 2010). This new population of memory T cells was termed tissue-resident memory T cells (T_{RM} cells).
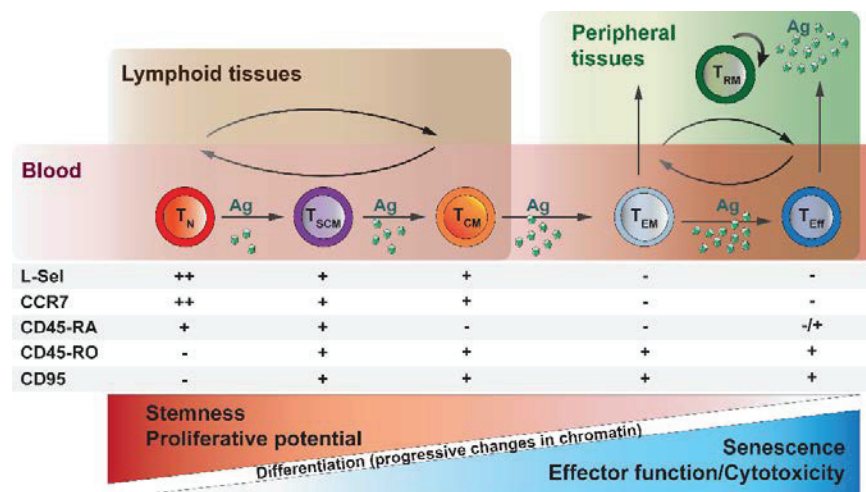
Figure 6. Model for the differentiation of memory T-cell subsets and migratory patterns.
Memory T-cell differentiation is largely a unidirectional process, driven by modifications in the chromatin structure upon successive encounters with the antigen. During this differentiation, the memory T cell progressively loses proliferative capacity and "stemness" (capacity to be multipotent and self-renewing), while acquiring different effector properties and migratory patterns. TCM cells, similarly than TN and TSCM cells, recirculate between blood and lymphoid tissues, whereas TEM cells and TEff cells are responsible for patrolling the peripheral tissues. TRM cells are permanently located in the tissues, where they exert protective functions without re-entering the circulation. TN, Naïve T cell, TSCM, stem cell memory T cell, TCM, central memory T cell; TEM, effector memory T cell; TEff, effector cell; TRM, resident memory T cell. Adapted from (Restifo and Gattinoni, 2013) and (Farber et al., 2014).

1.4 Resident memory T (T_{RM}) cells

1.4.1 Identification of T_{RM} cells

The existence of T$_{RM}$ cells implies that the analysis of T-cell subsets from blood may not correlate with the ongoing immune responses in the peripheral tissues, making essential to sample the tissues directly. Because T$_{RM}$ cells were defined according to their stationary properties, the main challenge for the study of the T$_{RM}$ biology is to distinguish circulating from truly resident T cells. Several experimental methods have been used to evaluate the ability of T cells to recirculate, including parabiotic surgery, *in vivo* antibody labeling, antibody-mediated T cell depletion, transplantation and phenotypic profiling (reviewed in (Masopust and Soerens, 2019; Szabo et al., 2019)). Parabiosis is a surgical technique that joins the vasculature of two congenically distinct mice, sharing the blood supply. After approximately a week, recirculating T cells equilibrate between each parabiont whereas resident T cells fail to equilibrate and remain confined in specific tissues of one mouse (Kamran et al., 2013). These experiments have been essential to define T$_{RM}$ cells as a distinct population, however, they present some caveats. For instance, not all the circulating cells equilibrate equally between the parabionts. In addition, the inflammation caused during the procedure may lead to overestimations of the fraction of circulating cells (Masopust and Soerens, 2019; Szabo et al., 2019).

In humans, early evidence of T cell residency came from studies on skin pathology. In fixed drug eruption it was demonstrated that pathogenic autoreactive T$_{RM}$ cells mediate the development of the recurrent skin lesions (Clark, 2015). Further insights of skin T$_{RM}$ cells arose from the study of T cell lymphoma patients treated with alemtuzumab (anti-CD52 antibody). In these patients, circulating T cells are depleted through antibody-mediated cellular cytotoxicity while non-recirculating T cells are spared, indicating that these cells are truly T$_{RM}$ cells (Watanabe et al., 2015).

Studies using migratory assays in mice revealed that, unlike circulating T cells, most T$_{RM}$ cells express CD69 and CD103 (Mueller and Mackay, 2016). T$_{RM}$ cells are less characterized in humans compared to mice, mostly due to the difficulties in sampling human tissues. However, several studies have analyzed the phenotype of human memory T cell subsets by examining different tissues from organ donors and surgical resections (Cheuk et al., 2017; Oja et al., 2018; Piet et al., 2011; Sathaliyawala et al., 2013; Smolders et al., 2018; Thome et al., 2014; Watanabe et al., 2015). These studies showed that a large fraction of memory T cells expressed CD69 in the spleen, lymph nodes, intestines, lung, skin, and brain whereas CD103 was mainly expressed on

CD8+ T cells within the barrier tissues. Accumulated knowledge during the last decade suggests that T_{RM} cells constitute the predominant memory subset in numerous tissues and organs, both in mice and humans (reviewed in (Mueller and Mackay, 2016; Takamura, 2018)). However, the relative fractions of circulating and resident T cells in human tissues remain unclear. T_{RM} populations lacking CD69 and/or CD103 have been identified (Bergsbaken et al., 2017; Steinert et al., 2015), and CD69 can be transiently expressed by recirculating T cells after TCR engagement or cytokine stimulation (Sancho et al., 2005; Shiow et al., 2006). In conclusion, migratory assays are still the best method to identify T_{RM} cells until more reliable and specific T_{RM} markers are discovered.

1.4.2 Development and maintenance of T_{RM} cells

Activated T cells enter the non-lymphoid tissues during the early phase of the effector response, and once the pathogen is cleared they can stablish permanent residency within the tissue (Masopust et al., 2010). During acute infection, heterogeneous populations of effectors are generated, with diverse transcription factor expression and memory potential (Chang et al., 2014). Mouse models of CD8+ T-cell memory differentiation showed that increased TCR signal strength, co-stimulation, and inflammatory cytokines favor the development of KLRG1^{hi} CD127^{lo} short-lived effector cells (SLECs). SLECs are terminally differentiated cells that present high levels of T-bet expression, low memory potential and decline over time. In contrast, effector cells exposed to lower levels of inflammation may become memory precursor effector cells (MPECs) being KLRG1^{lo} CD127^{hi} and presenting low expression levels of T-bet but high levels of Eomes (Chang et al., 2014; Joshi et al., 2007). Both KLRG1^{hi} and KLRG1^{lo} cells seed the tissues, however, several mouse studies have demonstrated that only KLRG1^{lo} committed precursors have the potential to give rise to T_{RM} cells in the skin and the intestine (Mackay et al., 2013; Sheridan et al., 2014).

After tissue arrival, T_{RM} precursors develop *in situ* in response to environmental signals. T_{RM} differentiation involves the acquisition of a program for long-term persistence and repression of the mechanisms mediating tissue egress (Schenkel and Masopust, 2014). Transcriptomic analysis of murine circulating and resident subsets revealed that T_{RM} cells share a common core signature among different tissues. This core transcriptional profile is progressively engaged during differentiation and it is markedly different from the expression patterns of naïve, T_{CM} and T_{EM} cells (Mackay et al., 2013). Within this common profile, T_{RM} cells exhibited low expression levels of CCR7 and sphingosine-1 phosphate receptor 1 (S1PR1), both

required for leaving the tissues via the lymphatics (Mackay et al., 2013; Masopust and Soerens, 2019). Kruppel-like factor 2 (KLF2), a transcription factor that controls S1PR1 expression, was found downregulated in T$_{RM}$ cells (Mackay and Kallies, 2017). Moreover, the T$_{RM}$ cell marker CD69 has been involved in tissue retention by antagonizing with S1PR1 function (Mackay et al., 2015a). Local production of TGF-β induces both CD69 and CD103 (integrin α$_E$) on intestinal T cells (Casey et al., 2012; Zhang and Bevan, 2013). CD103 forms the α$_E$β$_7$ heterodimer that promotes the adhesion to the epithelium layer via interactions with E-cadherin (Cepek et al., 1994). However, CD103 expression is not required for tissue retention (Casey et al., 2012), and CD103 independent mechanisms of tissue maintenance have been described (Bergsbaken and Bevan, 2015). Similarly, the homeostatic cytokine IL-15 is essential for the persistence of T$_{RM}$ cells in certain tissues, such as the skin (Mackay et al., 2013), but is not required in the pancreas, reproductive tract or the small intestine (Schenkel et al., 2016). Therefore, the requirements for tissue maintenance are not ubiquitous, but rather depend on the particular location and specific adaptations to the environment.

1.4.3 Immunosurveillance and protection by T$_{RM}$ cells

The mucosal surfaces constitute the main portals of entry for infectious agents. At the steady-state, large numbers of pathogen-specific T$_{RM}$ cells are strategically located at these barrier sites, patrolling the epithelial surfaces to detect recurrent pathogens (Dijkgraaf et al., 2019; Thompson et al., 2019). Unlike circulating T$_{CM}$ cells, which require the activation and migration of DCs in order to encounter their cognate antigen in the LNs, T$_{RM}$ cells are poised to provide an immediate response at the sites of pathogen entry. Furthermore, CD8+ T$_{RM}$ cells maintain constitutive expression of granzyme-B and are able to exert direct cytotoxic killing of infected cells to restrain pathogen invasion (Masopust et al., 2006).

Besides their cytotoxic capacity, T$_{RM}$ cells present high levels of transcripts encoding pro-inflammatory cytokines, which can be rapidly produced after T$_{RM}$ activation. T$_{RM}$ pro-inflammatory cytokines, such as IFN-γ, IL-2 and TNF-α, mediate direct anti-pathogen activity and alert neighboring cells to promote a state of broad immune protection in the tissue (referred as "sensing-and-alarm" function) (Ariotti et al., 2014; Iijima and Iwasaki, 2014; Schenkel et al., 2014). In addition, several studies have demonstrated that T$_{RM}$ cells have the capacity to proliferate *in situ* within the first days after antigen re-encounter (Beura et al., 2018; Park et al., 2018c).

1.4.4 Roles of T$_{RM}$ cells in protective immunity, homeostasis, and immunopathology

Numerous studies using different mouse models of infection have shown that CD8+ and CD4+ T$_{RM}$ cells provide protective immune responses to a broad array of tissue-tropic pathogens, including viruses, bacteria, fungi, and parasites (**Table 1**). Given their strategic situation and enhanced protection, T$_{RM}$ cells have emerged as promising targets for vaccines to elicit cellular immunity in the peripheral tissues. In the last years, several studies using novel immunization approaches have demonstrated that protective T$_{RM}$ cells can be established through vaccination (Fernandez-Ruiz et al., 2016; Shin and Iwasaki, 2012; Stary et al., 2015). One of these strategies is called "pull-an prime" and involves parenteral vaccination to induce systemic T-cell responses (prime), followed by local administration of adjuvants or chemokines to recruit activated T cells to the target tissues (pull) (Shin and Iwasaki, 2012).

Apart from their function in the context of infection, T$_{RM}$ cells may play an important role in the control of tissue homeostasis. T$_{RM}$ cells with reactivity against commensals, such as *Candida albicans,* have been identified in human normal skin (Park et al., 2018a). This evidence highlights the importance of T$_{RM}$ cells maintaining the integrity of the barrier surfaces. Similarly, T$_{RM}$ cells may display a homeostatic function controlling cancer cells in the epithelial tissues. In agreement with this assumption, CD8+ CD103+ T$_{RM}$ cells are abundant within human tumors, and high frequencies of tumor-infiltrating T$_{RM}$ cells correlate with prolonged patient survival in different types of cancer (reviewed in (Park et al., 2019)).

The long persistence and robust pro-inflammatory responses of T$_{RM}$ cells can be detrimental when pathological T$_{RM}$ cells recognize self or innocuous antigens (Park and Kupper, 2015). Increasing evidence has shown that T$_{RM}$ cells are involved in tissue-specific autoimmune and inflammatory diseases, including asthma (Hondowicz et al., 2016), psoriasis (Cheuk et al., 2017; Clark, 2011) and inflammatory bowel disease (Noble et al., 2019; Zundler et al., 2019). Moreover, in transplantation settings, passenger donor T$_{RM}$ cells persisting in the graft may trigger inflammation and graft rejection (Lian et al., 2014).

Our current knowledge about the generation, maintenance, phenotype and function of T$_{RM}$ cells is mainly derived from studies in mouse models of infection. Given the central role of T$_{RM}$ cells in tissue immunosurveillance, protective immunity and immunopathology, there is an increasing interest in translating these data into humans. However, it is still not clear whether mouse models can fully recapitulate the generation of T cell memory in humans, which occurs after exposure to a broad variety of pathogens and commensals over many decades in life. To

solve this problem, several studies have used "dirty" mice (mice co-housed with pet-store mice) instead of conventional specific pathogen-free mice (Beura et al., 2016; Reese et al., 2016). However, some T-cell memory populations in peripheral tissues may present intrinsic differences in mice and humans, as was mentioned before for the case of the IELs. Due to sampling problems, most of the studies on T_{RM} cells in humans are limited to phenotypic or *in vitro* functional analysis of tissue resections, and direct evidence of tissue-residency is lacking. A better understanding of the T_{RM} phenotype, ontogeny, and longevity in humans is needed in order to develop future vaccines or immunotherapies targeting these cells.

Table 1. Role of T_{RM} cells in protective immunity in mice.

Tissue	CD8+ T_{RM} cells	CD4+ T_{RM} cells	Refs.
Lung	Influenza		(Teijaro et al., 2011; Wu et al., 2014)
	Respiratory syncytial virus (RSV)		(Kinnear et al., 2018; Morabito et al., 2017)
		Mycobacterium tuberculosis	(Sakai et al., 2014)
		Bordetella pertussis	(Wilk et al., 2017)
		Streptococcus pneumoniae	(Smith et al., 2018)
Female reproductive tract		Herpes Simplex virus (HSV)	(Shin and Iwasaki, 2012)
		Lymphocytic choriomeningitis virus (LCMV)	(Schenkel et al., 2014; Schenkel et al., 2013)
		Chlamydia trachomatis	(Stary et al., 2015)
Skin	Herpes Simplex virus (HSV)		(Gebhardt et al., 2009)
	Vaccinia virus (VV)		(Jiang et al., 2012)
		Leishmania major	(Glennie et al., 2015)
		Candida albicans	(Park et al., 2018a)
Intestine	*Listeria monocytogenes*		(Romagnoli et al., 2017; Sheridan et al., 2014)
		Salmonella	(Benoun et al., 2018)
Liver	Malaria (*Plasmodium berghei*)		(Fernandez-Ruiz et al., 2016)
Salivary gland	Cytomegalovirus (CMV)		(Thom et al., 2015)
Brain	Lymphocytic choriomeningitis virus (LCMV)		(Steinbach et al., 2016)

2. AIMS OF STUDY

The **main objective** of this thesis is to determine the long-term persistence of the cells that constitute the adaptive immune cell compartment in the human small intestine.

Specific aims:

1. To characterize the different populations of tissue-resident and circulating memory CD8+ and CD4+ T cells in human small intestine, examining their phenotype, turnover, and functional capabilities.

2. To characterize the phenotype, lifespan, and function of Foxp3+ regulatory T cells in healthy and inflamed small intestine in humans.

3. To study the heterogeneity within the intestinal PC pool and determine the longevity of the different PC populations in the human small intestine.

3. SUMMARY OF RESULTS

Paper I. Resident memory CD8+ T cells persist for years in human small intestine.

In this study, we examined the turnover of CD8+ T cell subsets in transplanted small intestine (SI) by flow-cytometric analysis of HLA-I mismatched donors. We found that 60% (median, n=15) of both intraepithelial (IE) and lamina propria (LP) CD103+ CD8+ T cells were of donor origin one year after transplantation, suggesting that they constitute CD8+ T_{RM} cells. In contrast, LP CD103- CD8+ T cells were rapidly exchanged (15% median, n=15) after one year. TCR single-cell sequencing of donor CD103+ CD8+ T cells from transplanted SI showed that a significant fraction of expanded TCR clonotypes were maintained during the one-year follow-up period, suggesting that the TCR repertoire of SI CD8+ T_{RM} cells is stably conserved. CD8+ T_{RM} cells presented a distinct phenotype compared to CD103- CD8+ T cells, being CD69$^+$ KLRG1$^-$ CD127^{hi} CD28^{lo} PD1^{lo}. This distinctive phenotype was progressively acquired by the incoming recipient CD8+ T cells in intestinal biopsies over time, suggesting that T_{RM} differentiation may occur *in situ*.
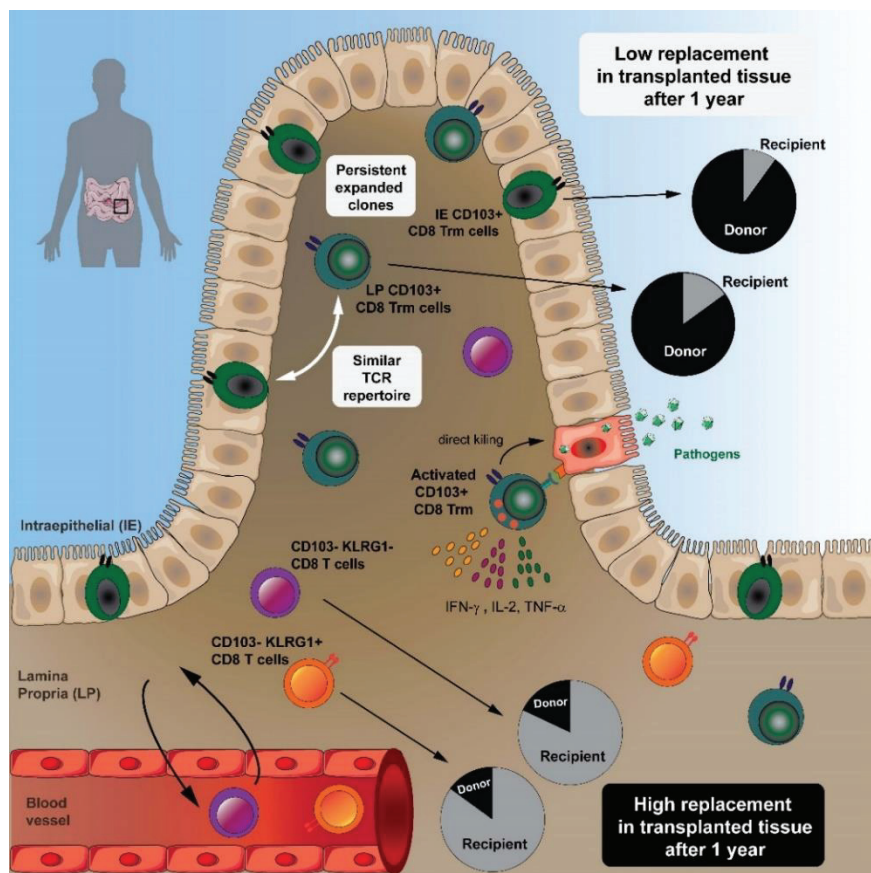
Figure 7. Graphical Abstract, Paper I.

High throughput bulk TCR repertoire analysis of different intestinal CD8+ T cell subsets revealed a high clonotype overlap between the CD8+ T_{RM} cells in LP and IE, in agreement with their similar replacement kinetics, suggesting that these two populations are closely related. In addition, CD103+ and CD103-KLRG1- CD8+ subsets in LP presented substantial clonal overlap, suggesting that CD103+ CD8+ T_{RM} cells might derive from CD103- KLRG1- precursors. CD8+ T_{RM} cells presented a higher percentage of polyfunctional (IFN-γ+, IL-2+, and TNF-α+) cells compared to their CD103$^-$ counterpart, but similar cytotoxic capacity after stimulation. In conclusion, we demonstrated that the majority of the human intestinal CD103+ CD8+ T cells are very persistent and show phenotypic and functional characteristics very similar to the ones described in murine CD8+ T_{RM} cells.

Paper II. CD4$^+$ T cells persist for years in the human small intestine and mediate robust T_H1 immunity

Most of the studies on T_{RM} cell biology have focused on CD8+ T cells and it is still debated whether CD4+ T cells may establish long-term residency in peripheral tissues. In this study, we examined the turnover of CD4+ T cells in transplanted duodenum in humans and we demonstrated that the majority of CD4+ T cells were still donor-derived one year after transplantation. Unlike memory CD4+ T cells in peripheral blood, intestinal CD4+ T cells express CD69 and CD161, but only a minor fraction express CD103. CD103- and CD103+ CD4+ T cells presented similar replacement kinetics in transplanted duodenum, suggesting that both constitute T_{RM} cell populations. On the other hand, recipient CD4+ T cells recruited to the graft progressively acquired a T_{RM} phenotype over time. Functionally, intestinal CD4+ T_{RM} cell were very potent cytokine producers; the vast majority being polyfunctional T_H1 cells, whereas a minor fraction produced IL-17. Moreover, a fraction of intestinal CD4+ T cells produced granzyme-B and perforin after activation. In conclusion, we showed that the intestinal CD4+ T-cell compartment is dominated by resident populations that survive for more than 1 year (probably years) and provide a polyfunctional T_H1 response.

Paper III. The human small intestine contains two distinct subsets of Foxp3+ regulatory CD4+ T cells with very different lifespan and functional properties.

In this study, we found that in human small intestine the population of Foxp3+ T_{Reg} cells constitutes only a 2% (median) of the total CD4+ T cells. This subset comprises CD45-RA- CTLA4+ CD127- cells with the ability to suppress the proliferation of autologous T cells *in vitro*. The

transcription factor Helios, expressed in around 60% of the SI T_{Reg} cells, clearly defines two functionally distinct populations: Helios- T_{Reg} cells persisted for at least 1 year in transplanted duodenum and produced IL-17, IFN-γ and IL-10 after stimulation whereas Helios+ T_{Reg} cells were rapidly exchanged with the circulation and exhibited low production of cytokines. During inflammation, such as active celiac disease, T_{Reg} cells were increased around 5-10-fold compared to normal small intestine. Interestingly, both subsets were found equally expanded in active celiac lesion and their cytokine profiles mirrored the ones at the steady state. In conclusion, we characterized two distinct populations of T_{Reg} cells in the human small intestine: a dynamic population of Helios+ T_{Reg} cells that may resemble the cells described to play an important role in tolerance to food antigens and a tissue-resident population of Helios- Treg cells that may resemble the population of T_{Reg} cells found to be involved in immune tolerance to the intestinal microbiota in mice.

Paper IV. Antibody-secreting plasma cells persist for decades in human intestine

In this study we identified three phenotypically and functionally different PC subsets in human small intestine: CD19+CD45+PCs were dynamically exchanged, whereas CD19-CD45+PCs are mostly, and CD19-CD45-PCs are almost completely of donor origin after one year in intestinal transplants. The distribution of these subsets varies with the age, from CD19+CD45+PCs dominating in young donors to CD19-CD45-PCs being the predominant subset in old individuals. This CD19+CD45+PC population constitutes the most active subset, producing higher amounts of IgA, which might provide a less durable but highly adaptable response to new antigenic challenges. The repertoire overlap analysis supported this differentiation from CD19+CD45+PCs to CD19-CD45-PCs through a CD19-CD45+ intermediate PC subset. Remarkably, by analyzing the C-14 incorporated in the DNA of isolated PC populations we reported that CD19-CD45-PCs cells have a lifespan of about 20 years in human small intestine. Moreover, within this long-lived population we found rotavirus-specific cells, a gut tropic pathogen that most often causes disease in infants and young children. In conclusion, we demonstrated that long-lived PCs exist in human small intestine and that these cells may provide long-lasting protection against recurring infections in the gut.

4. METHODOLOGICAL CONSIDERATIONS

This section discusses the advantages and limitations of the main methods that have been used in this thesis. A detailed description of the material and methods can be found in the methods sections of the individual manuscripts.

4.1 Patient material

All the studies included in this thesis analyzed specimens from human small intestine. Non-pathological resections from duodenum or proximal jejunum were obtained from pancreatic cancer, distal bile duct cancer, or periampullary carcinoma patients undergoing Whipple surgical procedure (pancreaticoduodenectomy). To avoid additional variability, samples from patients receiving neoadjuvant chemotherapy were excluded from the study. Duodenal resections from deceased organ donors as well as biopsies from recipient (native) duodenum and peripheral blood samples from the recipient were obtained at the time of pancreas transplantation of type I diabetes mellitus patients, as explained in (Horneland et al., 2015). Endoscopic biopsies from the transplanted pancreas, transplanted duodenum, and native duodenum are taken at 3 weeks, 6 weeks and 52 weeks post-transplantation as part of the routine rejection surveillance program. For the four studies included in this thesis, we collected endoscopic biopsies (5-10 biopsies) from the donor and native duodenum together with peripheral blood from the patients at the three indicated follow-up time points. All transplanted patients receive a standard immunosuppressive regimen including anti-thymocyte globulin (ATG), tacrolimus, mycophenolate mofetil and corticosteroids. The administration of ATG was controlled by daily T cell counts, aiming at depleting the T cells (< 0.05×10^9 T cells /mL) for 10 days after transplantation (Horneland et al., 2015). Transplanted patients showing clinical or histological signs of rejection or other complications related to the surgical procedure were excluded from the study.

For the **paper III**, endoscopic biopsies were obtained from the duodenum of untreated celiac disease patients. In addition, colonic biopsies were obtained by colonoscopy of individuals with unexplained pain but with normal histology. All the tissue samples (intestinal resections and biopsies) were evaluated blindly by experienced pathologists and only material with normal histology (according to (Ruiz et al., 2010)) was included. Buffy-coats were obtained from healthy

blood donors at the Oslo University Hospital, Oslo, Norway. All patients provided informed written consent and all the studies included in this thesis were approved by the Norwegian Regional Committee for Medical and Health Research Ethics (2010/2720/REK sør-øst and 2012/2278/REK sør-øst).

4.2 Sample processing

Peripheral blood mononuclear cells (PBMCs) from patients or healthy buffy-coats were isolated by density gradient centrifugation (Lymphoprep; Axis-Shield, Oslo, Norway), according to standard protocols. Single-cell suspensions from intestinal resections (5-10 cm) and biopsies were prepared immediately after tissue collection, following the protocol described in (Richter et al., 2018). In brief, intestinal mucosa was incubated with shaking in PBS containing 2mM EDTA during three consecutive washes to remove epithelial cells and intraepithelial lymphocytes. The remaining de-epithelialized LP was digested with 1mg/mL of Liberase TL (Roche) in complete RPMI medium with 20U/mL of DNAse (Roche) for 1h at 37°C. The complete removal of the epithelial layer was confirmed by histology, with the basal membrane remaining intact. The cross-contamination between the epithelial fraction and the enzyme-digested LP was very low, as evaluated also by flow cytometry (**Figure 8**). This assessment was especially important when we analyzed the repertoire overlap of the different CD8+ T cell populations in LP and in the epithelium.

Tissue dissociation protocols using enzymes present the drawback that some epitopes can be cleaved during the enzymatic digestion. To identify these issues, identically treated PBMCs and walk-out lymphocytes were used as controls to test the sensitivity of epitopes toward liberase digestion. CD62-L and CD25 epitopes were found to be cleaved during enzymatic digestion of the tissue with either liberase or collagenase. Therefore, the expression of these two molecules was analyzed after overnight culture of tissue-derived single-cells in complete medium at 37°C.

In all the studies we could use fresh cells as starting material, thanks to our constant supply of samples. This way, we avoided the problems related to the processing of frozen/thawed cells: lower viability, changes in some epitopes sensitive to cryopreservation (such as CD62-L) and changes in cell functionality. However, we aimed to study the TCR repertoire overlap in donor cells from transplanted duodenum of the same patient during the 1 year of follow-up period, which entailed some challenges. Due to clinical complications, graft-rejection (mainly in the pancreas), patient dropouts, etc. only 1 out of 3 samples at the latest time-point (1 year after transplantation) could be included in the study. For this reason, to

prepare single-cell TCR libraries we had to sort cells from biopsies collected at one-year after transplantation together with frozen/thawed single-cell suspensions from LP that were processed and stored the day of the transplantation surgery. Inevitably, the recovery of the frozen/thawed cells was lower than the fresh cells, even after resting the thawed cells in culture
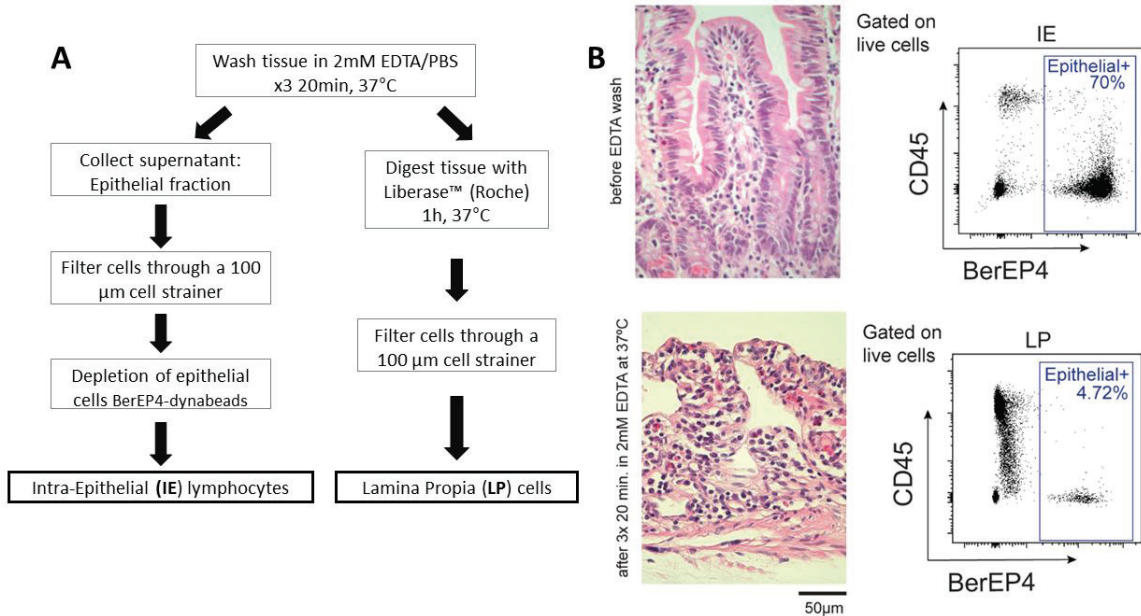
Figure 8. Intestinal tissue dissociation protocol. (A) Sample preparation workflow. (B) Representative H&E staining of tissue sections before (above) and after 3 sequential washes with EDTA buffer (below). (C) Representative flow cytometric staining showing the percentage of epithelial cells in IE and LP fractions.

overnight.

4.3 Flow cytometry analysis

Flow cytometry (FC) has been extensively used to analyze the immunophenotype and function of different cell populations in the studies included in this thesis. FC is a highly sensitive analytical technique that allows a multiparametric characterization on single cells. The basic principle of FC is the hydrodynamic focusing of cells, which means that cells are aligned one by one in front of a set of detectors while are excited by a light source, nowadays consisting of 3-4 laser beams. This way, several cell parameters on each cell can be simultaneously measured: the light scattering, which gives information about the size of the cell and its internal complexity; and the fluorescence, either intrinsic (auto-fluorescence) or derived from different fluorochrome-conjugated monoclonal antibodies. Over the last years, advances in technology have led to new detector options, additional lasers, and new fluorochromes, which together have considerably increased the number of parameters (colors) that can be simultaneously analyzed in a FC experiment.

Appropriate sample preparation and instrument setup are fundamental for a successful FC experiment, because, according to Shapiro's seventh law of flow-cytometry: "No data analysis technique can make good data out of bad data" (Shapiro, 2005). The quality of the single-cell suspension dramatically affects the data. Cells from digested tissue tend to clump easily, so they need to be filtered before the acquisition to prevent clogging the instrument or unstable flow. It is also essential to discriminate the dead cells (using a viability dye) and the doublets (by light scatter) in order to avoid artifacts in the data. The emission spectra of the different fluorochromes present certain overlap. Spillover occurs when the fluorescence emission of one fluorochrome is detected in a detector that is designed to measure the signal from another fluorochrome. The amount of spillover is a linear function that can be corrected through compensation and to optimally calculate these compensation values, compensation controls are prepared (normally using beads) with the same antibodies used in the experiment. Care must be taken to ensure that the peak of the positive control is as bright (or brighter) than the sample, and the background of the positive and negative controls are the same. The spillover correction leads to spread in the data, which reduces the sensitivity. For this reason, in order to optimize the sensitivity when designing a multicolor panel is important to match antibodies conjugated to bright fluorochromes for the dim markers and avoid using markers co-expressed in the same cell type in combinations of colors that present high spillover values. In the instrument setup, the voltages of each detector (PMT) need to be optimized to achieve the maximum sensitivity in each channel. Nowadays this is normally done with the aid of calculations (e.g. electronic noise) obtained by software, such as the BD Biosciences Cytometer Setup and Tracking system, which also allows tracking the reproducibility of the instrument over time (Cossarizza et al., 2019). In order to properly adjust the "gates" for the analysis, florescence-minus-one (FMO) and isotype controls (for intracellular staining) are prepared to determine the threshold for positive staining.
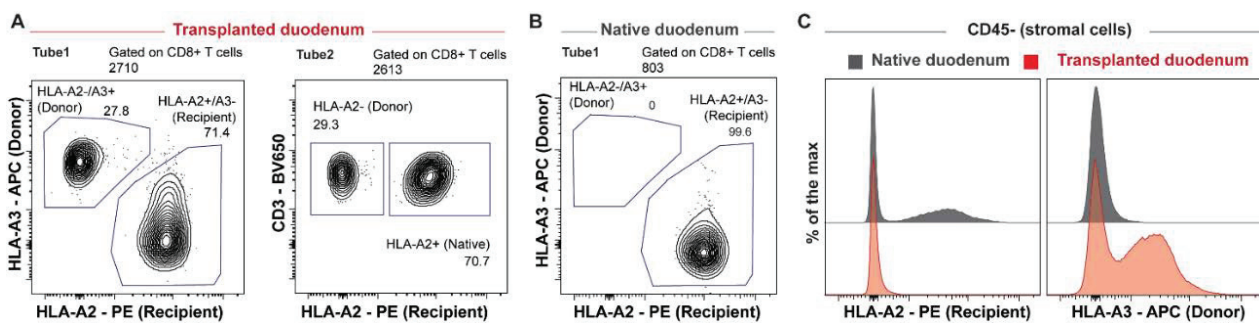
Figure 9. Representative flow-cytometric analysis of donor and recipient-derived cells in transplanted and native duodenum. (A) The percentages of donor and recipient-derived cells are similar when the flow experiment includes two antibodies (left) or only one antibody (right) against donor/recipient HLA-I molecules. **(B)** The staining of donor/recipient cells in native duodenum ensures precision in the sampling. **(C)** Stromal cells are used as intrinsic control in each sample.

A large part of the work in this thesis is based on the discrimination of donor-derived from recipient-derived cells in a transplant setting. For each patient, the HLA-typing was provided and duodenal biopsies from HLA-I mismatched pancreas transplanted recipients were collected. Antibodies against the specific donor and recipient HLA-I molecules were used to distinguish the origin of the cells and biopsies from the native (non-transplanted) duodenum and stromal cells (CD45-) in each sample were used as a control (**Figure 9**).

4.4 Flow cytometry cell sorting and magnetic cell separation

Some experiments included in this thesis required isolated populations of cells as starting material. All the sorting methods demand some previous knowledge about the target cells and the "unwanted" cells to discard. The choice of the separation technique mainly depends on the balance between the scale of the cellular output, purity, yield and the "gentleness" of the isolation method, which directly affects the viability and functionally of the sorted cells. For those experiments targeting a very specific population of cells (determined by combinations of several surface markers) and low numbers of sorted cells, FC cell sorting is the preferred option. To use this technique, one should take into account all the considerations mentioned before regarding FC analysis plus several factors derived from the sorting process itself. The user must establish some electronic gates as separation criteria, which together determine the deflection of each cell contained in a droplet (BD Fluorescence-Activated Cell Sorting, FACS system). The size of the cells determines the speed of the sort. Smaller cells can be sorted faster because a smaller nozzle can be used. The advantages of the FC sorting are that target cells can be selected based on multiple parameters, it gives high purities, and allows to sort in multiple devices, for example, to deposit one cell per well in a 96 well-plate for single-cell assays. However, the main limitations are the long time needed for sorting large numbers of cells (which results in lower viabilities) and that requires relatively high expertise.

For the reasons mentioned above, separation methods based on antibody-coated magnetic beads are the best option when large numbers of cells are required. Moreover, these methods are normally gentler with the cells than the FACS. The disadvantages are that the purities are usually lower than the FACS, and it is necessary to check the purity by staining a small aliquot and analyzing by FC. The purity of the resulting cell preparation must be verified by staining with antibodies against the unwanted cells and the target cells (using different epitopes or markers that the ones used for the separation). In this thesis, several bead-based strategies have been used to enrich cells (depletion of epithelial cells to get a higher proportion

of IELs, depletion of apoptotic cells with Annexin-V beads) or to positively isolate cells. Two commercially available beads were used: Dynabeads, which are superparamagnetic beads of about 4.5 μm diameter, and MACS microbeads, which are smaller beads (0.05 μm diameter) that use a column-based system for magnetic isolation. Isolation kits allowing the release of the beads bound to the target cells (for example, using biotinylated antibodies for the capture and releasing by competitive binding of biotin with higher affinity) enable further consecutive rounds of isolation using new cell markers. This strategy makes possible to combine several depletion and positive isolation steps to get the cells of interest with a high purity (**Figure 10**).
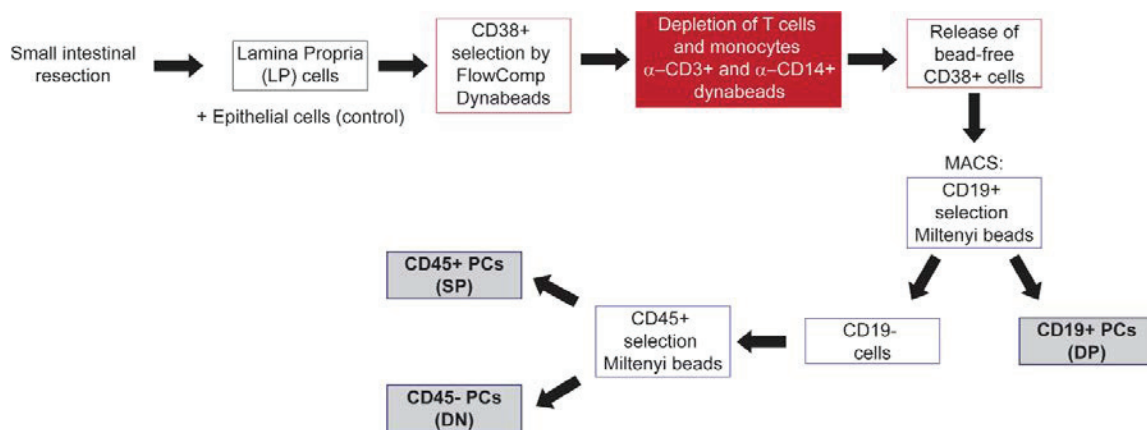
Figure 10. Workflow for the magnetic separation of different populations of PCs from intestinal single-cell suspensions.

4.5   Analysis of T-cell function

In the **papers I and II** of this thesis, we analyzed the cytokine production by intestinal CD8+ T cells, CD4+ T cells and CD4+ Foxp3+ T_{Reg} cells. Tissue-derived single cells were activated *in vitro,* and intracellular immunostaining was performed with monoclonal antibodies against specific cytokines in combination with surface cell markers. The method used for T-cell activation may affect the cytokine secretion profile by T cells *in vitro* (Olsen and Sollid, 2013). We assessed the cytokine production by intestinal T cells after stimulation with phorbol 12-myristate 13-acetate (PMA, 1.5 ng/mL) together with Ionomycin (1μg/mL) for 4h. Protein transport was blocked by adding monensin (BD GolgiStop) for the last 3h. PMA/Ionomycin activation is the most robust stimuli for most T cell cytokines. PMA is an activator of the protein kinase C and ionomycin is a Ca^{2+} ionophore, and the combination of both activates T cells by circumventing TCR activation (Yin et al., 2015). One pitfall of this stimulation method is that CD3 and CD4 tend to be downregulated after PMA/Ionomycin–mediated activation. PMA/Ionomycin

and monensin can be toxic for cells at high concentrations and long incubation times are not recommended. CD3/CD28 activation is a more physiological stimuli, and for this reason it was used for the analysis of the production of cytotoxic proteins. The production of granzyme-B and perforin was evaluated by intracellular staining after 21h incubation with anti-CD3/CD28 beads (Dynabeads human T-cell activator) at a 1:1 (beads : cells) ratio, or with control medium (basal expression levels). Activation of T cells is associated with an increase in size (forward light scatter signal) and downregulation of CD3.

To test the functional capacity of intestinal T_{Reg} cells in **paper III**, *in vitro* suppression assays were performed following standard protocols (Collison and Vignali, 2011). We sorted intestinal CD25+ CD127- CD4+ T_{Reg} cells and we tested their ability to inhibit the proliferation of autologous CD25-CD127+ CD45-RA+ naïve CD4+ T cells isolated from blood (responder cells). Responder cells were labelled with 5,6-carboxyfluorescein succinimidyl ester (CFSE, 1.5 μM) and T_{Reg} cells were first pre-activated for 48h with anti-CD3/CD28 beads. T responder cells were cultured alone or in the presence of T_{Reg} cells at a 1:2 ratio (T_{Reg} cells: T responder cells), and stimulated with anti-CD3/CD28 beads in a 1:2 ratio (beads:cells). After 4 days of co-culture, the inhibition of the proliferation of T responder cells was analyzed by CFSE dilution using FC.

4.6   Immunohistochemistry and immunofluorescence microscopy

Immunohistochemistry (IHC) or Immunofluorescence (IF) microscopy methods provide information regarding tissue architecture, spatial relationships of a cell with the neighboring cells and relevant information of where the markers are localized in the cell. This information is missing in FC, which in contrast provides a better quantification and characterization of cell populations by using 12-15 or more parameters. In IF the number of colors (and therefore, parameters to be analyzed) is usually limited to 4, and the interpretation of the results is more subjective. Recent reports have found that tissue-isolation protocols normally underestimate the numbers of resident cells and distort the representation of certain populations that are more efficiently extracted (Steinert et al., 2015). To overcome this limitation, imaging-based methods serve as a complementary approach to FC for the study of tissue-derived cell populations.

In the **papers I and II** of this thesis, *in situ* T cell counts were performed by IHC to verify the maintenance of total CD8+ and CD4+ T cells in transplanted duodenum during the one-year follow-up period. As a control, tissue sections from native (non-transplanted) duodenum were also stained and counted. For the analysis, biopsies were formalin-fixed and paraffin-embedded

and 4μm sections were prepared. Dewaxed and rehydrated sections were subjected to heat-induced antigen retrieval using a low pH buffer. Immunostaining was performed with primary antibodies against CD3 or CD8 and secondary antibodies conjugated to alkaline-phosphatase enzyme, and subsequently incubated with a chromogen. Stained sections were scanned, and positive cells were automatically counted. The results were similar as given as a fraction of total nucleated cells and per tissue density.

In **papers I, II and IV** of this thesis, analysis of chimerism was performed by in situ X/Y FISH (fluorescence in situ hybridization) and IF in tissue sections from intestinal biopsies of gender-mismatched pancreas transplanted recipients. Tissue sections of endoscopic biopsies from transplanted duodenum were prepared as described above. Sections were then incubated with FISH probes annealing to specific regions of the sex chromosomes (X/Y). Subsequently, standard immunostaining was performed using primary antibodies of different isotypes or species targeting T-cell markers (CD3, CD4 or CD8) and detection with fluorochrome-conjugated secondary antibodies. A confocal microscope was used for image acquisition. Confocal microscopy offers several advantages over conventional widefield fluorescence microscopy, including the creation of sharp images by eliminating the background away from the focal plane and the capability to collect and stack serial optical sections from different optical planes. The last one is especially important in order to properly detect both X/Y probes in the same cell, given that the chromosomes can be located in different planes of the tissue.

4.7 Immune repertoire analysis

All the immune repertoire studies included in this thesis (**papers I and IV**) used mRNA as starting material to prepare sequencing libraries. This method offers the advantages that is less biased by PCR artifacts because the amplified fragments are smaller (do not contain introns) and detects only the adaptive immune receptor that is productively arranged and post-transcriptionally processed (the TCR /BCR that is going to be expressed on the cell). In addition, it is possible to detect low abundant sequences, given that mRNA transcripts are found in larger numbers than their templates of genomic DNA. However, the use of genomic DNA as starting material offers the advantage that is more stable than mRNA and that the presence of only one template per cell (instead of several transcripts in cells presenting different transcriptional activity) allows more robust quantifications of the different clones.

In the **paper I** of this thesis we performed single-cell and bulk TCR sequencing of different populations of intestinal CD8+ T cells. First, we aimed to study the clonotype overlap between donor CD8+ T$_{RM}$ cells isolated from samples at the day of the transplantation surgery and those isolated one-year post-transplantation. For this analysis we chose a single-cell TCR sequencing protocol, for several reasons. First, the numbers of donor CD8+ T$_{RM}$ cells isolated from biopsies were quite low, and single-cell approaches give better recovery from low cell inputs. Moreover, single-cell sequencing has the advantage that provides information about the paring of TCR-α and TCR-β chains. However, this method presents low-throughput, is quite labor-intensive and expensive (requires large amounts of primers and reagents), making difficult the analysis of more than several few samples. We analyzed biopsies of donor duodenum from two different patients at the two mentioned time points, and we also included biopsies of the recipient duodenum of one of the patients, as a control. Single cells were sorted into 96-well PCR plates and library preparation was performed following the protocol described by Risnes et al. (Risnes et al., 2018), using cDNA synthesis and nested PCR reactions with sets of multiplexed TCR primers. Pairing information was important for us because we wanted to be sure that we were able to identify exactly the same clonotypes one year apart. Therefore, the clonotypes were defined based on the complete similarity of the CDR3 nucleotide sequence and V and J gene segment usage for both TCR-α and TCR-β chains. Some clones were detected expressing dual TCR-α chains (≈10%), and few cells that were found containing more than three chains (for either dual TCR-α and/or TCR-β chain) were discarded from the analysis.

In the **paper I** we also aimed to compare the TCR repertoire of different populations of intestinal CD8+ T cells (IE and LP CD103+ cells, as well as LP CD103- KLRG1+ and KLRG1- cells). For this analysis, we sorted 5000 cells of each CD8+ T-cell subset from 5 individuals, and we prepared bulk-TCR sequencing libraries by semi-nested PCR targeting both TCR-α and TCR-β genes, according to the protocol detailed in (Risnes et al., 2018). The quantity of the input (mRNA) and the sequencing depth directly determine the TCR diversity that the method can capture. In this protocol, we included three cDNA replicates for each TCR chain, and we found that the correlation of the read counts for the clonotypes in the three replicates was high, which indicates reproducibility of the TCR repertoire sequencing (Greiff et al., 2014). For downstream analysis, the reads of the three replicates were collapsed, and only clonotypes (defined by similar V and J gene usage and CDR3 nucleotide sequence) with a minimal read count of 10 were used.

In the **paper IV**, 10.000 IgA+ PCs of each PC subset (CD45+ CD19+, CD45+ CD19- and CD45- CD19-) were sorted and high-throughput sequencing of the IgH region was performed from cDNA, according to the protocol described by Snir et al. (Snir et al., 2015). Given the complexity of these immune repertoire sequencing workflows and the possibility that batch effects can influence the analysis, it is crucial to process the samples in a very standardized way: similar numbers of cells as starting material, similar concentrations of the final product to sequence, etc. in order to get comparable numbers of reads in all the subsets and individuals.

4.8   Retrospective carbon-14 dating of human cells

Traditional ^{3}H-thymidine and BrdU incorporation methods have been extensively used in mice to measure the turnover of cell populations *in vivo*, during relatively short periods of time. Ki67 intracellular staining allows the quantification of the cells in cycle at a given time but lacks information regarding the proportion of cells that have been exchanged over a long period.

At the laboratory of professor Jonas Frisén at Karolinska Institutet (Stockholm) a new method inspired in the ^{14}C measurements used in archeology have been developed to retrospectively determine the age of humans cells (Spalding et al., 2005). The testing of nuclear weapons during the 1950-60 generated massive levels of ^{14}C in the atmosphere, and after the ban treaty in 1963 the ^{14}C levels dropped exponentially. The atmospheric ^{14}C is fixated in the plants by photosynthesis, and then transmitted to humans through the food chain. DNA is a very stable molecule that does not exchange the carbon after division, therefore, reflecting the levels in the atmosphere at any given time point. The principle of this technique is that the measurement of the ^{14}C levels in genomic DNA can be used to retrospectively determine the birth date of cells in the human body (Bergmann et al., 2009; Spalding et al., 2008; Spalding et al., 2013). This analysis gives an average age of the cell population with a precision of ±2 years but requires large number of cells as starting material (around 10 million cells). The resolution of the technique (in time and number of cells) depends on when the cells were generated in relation to when the individual was born. For this reason, in order to get a high sensitivity for the analysis of the turnover of intestinal PCs we included samples from patients born both before and after the nuclear bomb test. In addition, we included epithelial cells (average life span ≈5 days) as a control for very short-lived cells.

4.9 Statistical analysis

In the bioinformatic analysis of the immune repertoires of the **papers I** and **IV**, paired-end raw sequencing reads were pre-processed (quality filtering, primer annotation, etc.) using selected steps of the pRESTO toolkit (Vander Heiden et al., 2014), as described in detailed for TCR and BCR repertoire analysis in (Risnes et al., 2018) and (Snir et al., 2015), respectively. Then, sequences were aligned using the ImMunoGeneTics database (IMGT/High V-Quest online tool) (Alamyar et al., 2012)) to identify the V,D, and J gene segments and the CDR3 region. Bulk TCR data in **paper I** were preprocessed (VDJ alignment and clonotyping), using the MIXCR software package (Bolotin et al., 2015), and the tcR package (Nazarov et al., 2015) was used for descriptive statistics of the TCR clonotypes. In **papers I** and **IV**, the convergence of two different immune repertoires was calculated using the Morisita Horn index, which quantifies the overlap of the clonotypes taking into account their relative abundance across the different samples (Greiff et al., 2015). TCR repertoire diversity was calculated using the Shannon Evenness index, which ranges between 1 (uniform clonal population) and 0 (repertoire completely skewed towards one clone) (Greiff et al., 2015).

Statistical analyses of flow-cytometric data were performed using versions 7 and 8 of GraphPad Prism (GraphPad Software). Paired t-test was applied to compare two groups of sample pairs (two cell subsets from the same patient sample, two time points, two experimental conditions, etc.), and comparisons between two independent groups were analyzed by unpaired t-test. Analysis of variance (ANOVA) was used to compare the means of three or more groups, with or without paired observations (repeated measures). Tukey's post hoc test was applied to all pairwise comparisons to identify significant comparisons. Post hoc test are adjusted to account for multiple comparisons, due to the increased chances of type I error (false positives) in multiple comparisons (Skinner, 2018). When the variables were affected by two factors, two-way ANOVA (with or without matching factors) and Tukey's post hoc test were applied. Both t-test and ANOVA require that the data in each group are normally distributed and that variability is the same in all the groups (homogeneity of variances). In the cases where this last assumption is not met, the Welch's correction for unequal variances can be applied (Skinner, 2018). In those experiments where the number of sample replicates was small, the normality of the data distribution cannot be assumed and non-parametric test (Wilcoxon Signed Rank test and Kruskal Wallis test) were used. For correlation analysis, Pearson correlation test was used. All tests were performed as two-tailed test and a p-value of <0.05 was considered significant.

5. DISCUSSION

The gut harbors the largest fraction of PCs and antigen-experienced T cells in the body (MacDonald, 2008; Pabst et al., 2008). In healthy intestine, T cells constitute one third of the immune cells in the LP, and PCs are almost as abundant as T cells. Intestinal T cells are seeded in the fetus as early as the second trimester of pregnancy, whereas intestinal PC development initiates later during infancy (Stras et al., 2019). During homeostasis, the intestinal mucosa is continuously exposed to a massive antigenic load derived from dietary products and microbiota, and the intestinal immune system must rapidly respond to this highly dynamic array of antigens. This rapid immune response was thought to be provided by intestinal IgA, secreted by PCs that were continuously generated in reaction to changes in the luminal content (Hapfelmeier et al., 2010; Mattioli and Tomasi, 1973). On the other hand, it was long known that intestinal T cells present an effector phenotype and display cytotoxic activity (Brandtzaeg et al., 1989; Lefrancois et al., 1997; Muller et al., 2000; Ruthlein et al., 1992). CD69 was found to be expressed on intestinal T cells, but it was considered indicative of early activation (Klein, 2004; Sancho et al., 2005). Thus, intestinal T cells were thought to constitute recently activated effectors, probably involved in current immune responses against intestinal pathogens or microbiota (Sheridan and Lefrancois, 2010). Interestingly, the distinctive phenotype of intestinal IE CD8+ T cells, characterized by CD69 and CD103 expression, was not observed on circulating T cells from blood, suggesting that intestinal IE CD8+ T cells could be retained without leaving the tissue (Masopust et al., 2006). This hypothesis was confirmed by subsequent studies in parabiotic mice, demonstrating that IE CD8+ T cells present low degree of equilibration with their circulating counterparts (Klein, 2004; Masopust et al., 2010).

In humans, the dynamics of intestinal T cell and PC populations in terms of recruitment, renewal, exit rates, and residence time has been largely unknown. In the articles included in this thesis, we performed a detailed characterization of the phenotype and the long-term persistence of different populations of adaptive immune cells in the human small intestine and we found that the majority of the intestinal PCs constitute long-lived cells with a lifespan of several decades (**paper IV**), and that stable residency and not recirculation is the main feature of most of the intestinal T cells (**papers I, II and III**).
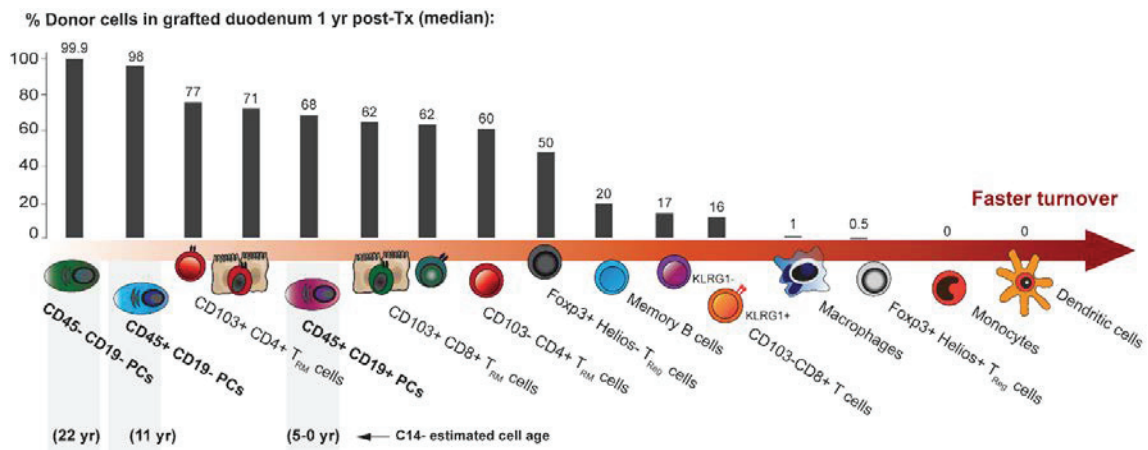
Figure 11. Turnover of immune cells in human small intestine. Above: Median values for the replacement kinetics of different immune subsets of the adaptive and innate system (for comparison) in transplanted duodenum. Below: Estimated cell age for the different PC populations measured by C-14 retrospective birth dating.

5.1 A chimeric system to study the *in vivo* turnover of immune cells in the human small intestine.

Knowledge about the stability, migration and renewal of tissue-derived immune cell populations in physiological and pathological conditions is fundamental in order to develop new therapeutic approaches. The major aim might be to create optimized immunization strategies to elicit durable humoral and T cell responses. However, experiments to decipher the longevity of immune cell populations from non-lymphoid tissues are not easily performed in humans.

In our lab, the discovery that most PCs remained of donor origin in biopsies from grafted duodenum at one-year after transplantation was initially evidenced by using X/Y FISH and immunofluorescence in gender mismatched donor transplanted patients (**paper IV**), and represented the first strong proof demonstrating that long-lived immune cells exist in the human gut. Then, a flow cytometric approach was optimized for the identification of persisting donor PCs and other immune cells in single-cell suspensions isolated from fresh duodenal biopsies of transplanted duodenum from patients showing disparity of HLA-type I molecules with their donors. This method offers more precise cell quantifications and the possibility to use additional phenotypic markers to discriminate different cell types (**Figure 11**). Applying this analysis to longitudinal samples, we found that intestinal PCs present very low replacement one-year post-transplantation, especially the populations lacking CD19 expression. After a detailed phenotypic classification of different populations of PCs was established, a strategy for large-scale PC isolation was developed in order to analyze the content of C-14 in the DNA of these cells and determine their absolute age (**paper I**).

Due to difficulties in obtaining enough cells from pure populations, C-dating was not applied to other immune cell types. However, the longitudinal analysis of biopsies from grafted duodenum in patients undergoing pancreas-duodenal transplantation represented a unique opportunity to track the maintenance and the *in vivo* generation of intestinal T_{RM} cells over time (**Figure 12**). Intestinal T cells were more dynamically replaced compared to PCs, but still we found that most of the CD8+ and CD4+ T cells persisted for at least one year in transplanted duodenum (**papers I and II**). The migratory and residency features of T_{reg} cells are less described than conventional T cells. By tracking the proportions of donor and recipient-derived cells over time we found that two populations of T_{reg} cells, distinguished by Helios expression, presented different turnover rates (**paper III**). Helios+ T_{reg} cells were almost absent in biopsies taken one-year post-transplantation, whereas considerable numbers of donor Helios- T_{reg} cells remained after one year, comparable to the persisting cells observed for CD4+ T_{RM} cells.
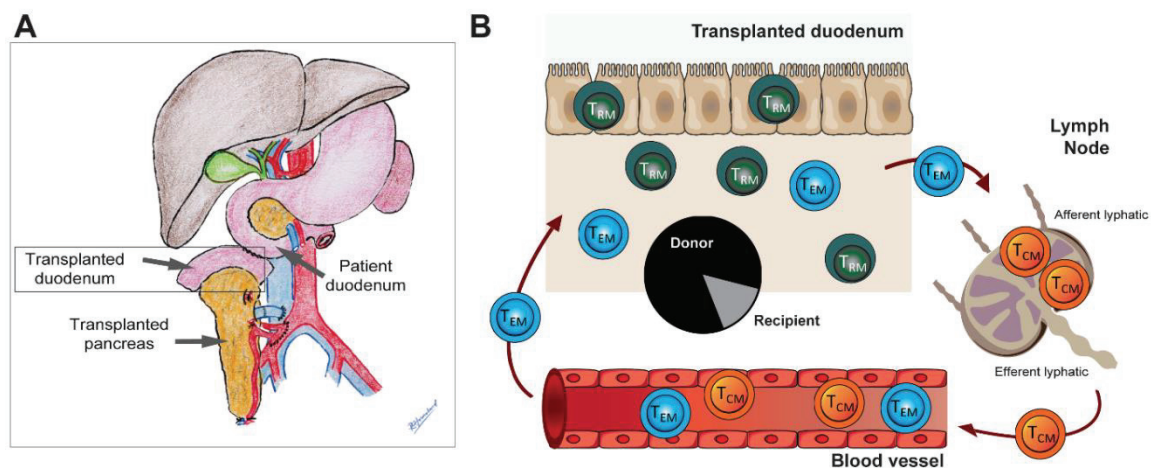
Figure 12. T cell dynamics in grafted duodenum of pancreas transplanted patients. (A) Depiction of the pancreas transplantation showing the duodenostomy anastomosis, as described in (Horneland et al., 2015). Credits: Rune Horneland, reprinted with his permission. **(B)** T cell migration patterns. Central memory T cells (T_{CM}) preferentially recirculate between the secondary lymph organs and blood whereas effector memory T cells (T_{EM}) circulate through blood and non-lymphoid tissues. We found that a large fraction of donor T cells were maintained for one year in human duodenum, suggesting that they constitute T_{RM} cell populations.

To study the population dynamics of T_{RM} cells, the individual contributions of recruitment, self-renewal and cell loss must be addressed (Morris et al., 2019). The recruitment rate can be estimated by the fraction of incoming recipient cells in intestinal biopsies over time. It is likely that, compared to the steady state situation, our results derived from transplanted duodenum overestimate the physiological recruitment rate. It is been shown that ischemia and reperfusion injury caused during the transplantation surgery may increase the recruitment of leukocytes to the graft (Eguiluz-Gracia et al., 2016). In addition, it is likely that the

immunosuppressive treatment, which includes ATG and drastically depletes T cells in blood, might reduce the numbers of some populations of T cells (with recirculating potential) lodged in the graft or might affect the physiological recruitment rate. Furthermore, we have found that the replacement of intestinal immune cells increases (and it is almost complete) in those patients experiencing graft rejection (unpublished results), in line with observations reported in other transplantation studies (de Leur et al., 2019; Snyder et al., 2019; Zuber et al., 2016). However, all the specimens included in the studies of this thesis were blindly evaluated by experienced pathologists, and patients exhibiting histological or clinical signs of rejection in any transplanted organ were excluded from the analysis. In contrast to whole bowel or multivisceral transplantations, which are frequently associated with rejection episodes (Zuber et al., 2016), pancreas transplantation presents lower frequency of rejections in the duodenum (Nordheim et al., 2018). We have previously reported that DCs and some Mφs are rapidly replaced in transplanted duodenum (Bujko et al., 2018; Richter et al., 2018), which might increase the risk of local alloreactivity. All the patients included in our studies presented chimerism in the graft, although we found considerable interindividual variability in the fractions of recipient cells for the different immune cell subsets. Therefore, it is likely that low-grade rejection might occur in some cases without being detected at the clinical or histological level.

To account for the contribution of self-renewal in the homeostatic maintenance of PCs and T_{RM} cells, we measured the expression of the proliferative marker Ki67 in cells isolated from healthy intestinal resections and eventually in transplanted biopsies, as a control. We found that intestinal PCs exhibited extremely low proliferation (<1%), in line with their long lifespan calculated by C-14 dating. The proliferative activity of intestinal CD8+ T cells and CD4+ T cells was also low (median <5% and <4%, respectively).

Our turnover data correspond to static "snapshots" at different times (3 weeks, 6 weeks and 52 weeks after transplantation) of a dynamic process that occurs continuously over time, and caution must be taken in their interpretation. To investigate the contribution of T_{RM} precursors to the T_{RM} pool, we tracked the phenotypic changes of the graft-infiltrating recipient cells *in vivo* during the one-year follow-up period. We found that incoming recipient cells progressively acquired a T_{RM} phenotype over time, demonstrating that *in situ* differentiation occurs, in agreement with other observations in transplanted lung (Snyder et al., 2019). Donor T cells surviving for more than 600 days in non-rejected intestinal grafts have been previously reported (Zuber et al., 2016). In this study, patients were subjected to whole bowel transplantation or multivisceral transplantation, which in both cases includes gut-associated lymphoid tissue (such as Peyer's patches) and MLNs. These organized lymphoid structures in the

graft can release donor T cells and stem cells that enter the circulation and are often detected in the blood of these patients long after transplantation (Fu et al., 2019). In our studies, the patients received only the proximal part of the duodenum lacking GALT or lymph nodes and, therefore, the contribution from lymphoid donor cells to the renewal of T cells in the graft is negligible.

Finally, the contribution of the cell loss, including exit from the tissue and cell death, must be evaluated to completely describe T_{RM} cell homeostasis (Morris et al., 2019). We did not find any significant reduction in the *in-situ* T cell counts from biopsies before and one year after transplantation and neither detect T cell chimerism in blood from the transplanted patients, together suggesting that the fraction of intestinal T cells leaving the tissue or dying is low.

5.2 Human T_{RM} cells in small intestine recapitulate many of the features described for murine T_{RM} cells.

Most of our knowledge about T_{RM} phenotype and function derives from studies of antigen-specific T cells in different mice models of infection. However, it has been reported that mice kept in specific pathogen free (SPF) conditions contain lower numbers of T_{RM} cells in peripheral tissues compared to humans. In contrast, mice co-housed with pet-store mice ("dirty mice") present higher numbers of T_{RM} cells compared to SPF mice, highlighting the importance of the exposure to environmental antigens in the development of T_{RM} cells (Beura et al., 2016; Reese et al., 2016). These differences represent one of the major challenges to translate the T_{RM} data from mice studies into humans.

Knowledge about T_{RM} cells in humans is still scarce, mainly due to difficulties in sampling human tissues, for example from surgical resections. In general, both murine and human T_{RM} cells share a common phenotype, characterized by the expression of CD69 and CD103, the last one mainly expressed on CD8+ T_{RM} cells (Masopust and Soerens, 2019; Szabo et al., 2019).

CD69 is a C-type lectin receptor that has been traditionally considered an early leukocyte activation marker, due to its rapid induction after TCR engagement or cytokine stimulation (Cibrian and Sanchez-Madrid, 2017; Sancho et al., 2005). In the human small intestine, virtually all the CD4+ and CD8+ T cells express CD69, and most of the LP CD8+ T cells (≈80%) and virtually all the IE CD8+ T cells express CD103. In contrast, only a fraction of the LP and IE CD4+ T cells express CD103 (≈20% and 60%, respectively). We found that recipient T cells infiltrating the graft as early as 3 weeks after transplantation already expressed high levels of CD69, and this

expression was further increased over time. CD69 is induced by local TGF-β (Casey et al., 2012; Zhang and Bevan, 2013), and is upregulated soon after arrival into the intestinal mucosa in parabiotic mice (Klonowski et al., 2004). CD69 plays a key role in preventing tissue egress and favoring tissue residency by antagonizing with S1PR1 (Mackay et al., 2015a; Shiow et al., 2006; Skon et al., 2013). In addition, transcriptional downregulation of both S1PR1 and KLF2, the last one being a transcription factor that controls S1PR1 expression, is required for T_{RM} cell establishment (Skon et al., 2013). Interestingly, some *bona fide* T_{RM} populations lacking CD69 expression have been identified in parabiotic mice (Steinert et al., 2015), and Walsh and colleagues have recently found that CD69 is dispensable for the establishment and maintenance of stable CD8+ T_{RM} cells in certain non-lymphoid tissues, such as the intestinal LP and epithelium (Walsh et al., 2019).

On the other hand, almost all the donor CD8+ T cells surviving for one year in the graft were CD103+, highlighting the importance of this integrin in the retention of CD8+ T_{RM} cells by binding to E-cadherin and tethering to epithelial cells (Cepek et al., 1994). However, we found that 15% of the CD103- CD8+ T cells remained still of donor origin one year after transplantation, which might indicate that the requirement for CD103 is not absolute. Supporting this notion, a population of small intestinal CD103- CD8+ T_{RM} cells has been described in a mouse model of oral infection with *Yersinia pseudotuberculosis*. (Bergsbaken and Bevan, 2015).

Tissue residency and migratory patterns of CD4+ T cells have been less well characterized compared to CD8+ T cells. CD4+ T_{RM} cells have been identified in several non-lymphoid tissues, such as the skin (Glennie et al., 2015; Watanabe et al., 2015), lung (Hondowicz et al., 2018; Teijaro et al., 2011) and reproductive tract (Iijima and Iwasaki, 2014). However, some studies showed that skin CD4+ T-cell immunosurveillance rely more on continuous recirculation rather than permanent residency (Collins et al., 2016; Gebhardt et al., 2011). Moreover, the numbers of antigen-specific CD4+ T cells seemed to decline faster than CD8+ T cells in mice models (Cauley et al., 2002; Homann et al., 2001; Seder and Ahmed, 2003), and pulmonary CD4+ T cells are more rapidly replaced than CD8+ T cells in lung transplanted patients (Snyder et al., 2019); together indicating that memory CD4+ T cells are less durable than CD8+ T cells. We found that intestinal CD4+ T cells remained of donor-origin in grafted duodenum at similar or even higher numbers than CD103+ CD8+ cells at one-year post-transplantation. In addition, both CD103- and CD103+ CD4+ T cells persisted in the graft at similar rates, thereby both can be functionally defined as T_{RM} cells. In agreement with these results, intestinal CD4+ T cell response after oral infection with *Listeria monocytogenes* was dominated by long-lived CD103- CD4+ T cells in mice (Romagnoli et al., 2017), indicating that a large fraction of CD4+ T

cell might be maintained by mechanisms independent of CD103. In a recent study, Klicznik and colleagues reported that a distinct population of skin CD4+ T_{RM} cells being CLA+ CD69+ CD103+ was able to downregulate CD69, exit the tissue and enter the circulation as CLA+ CD69- CD103+ cells in the steady-state (Klicznik et al., 2019). This study adds to the growing evidence that T_{RM} cells are highly heterogeneous (Bergsbaken and Bevan, 2015; Cheuk et al., 2017; Kumar et al., 2018b; Kumar et al., 2017; Watanabe et al., 2015), revealing that few T_{RM} cells might still conserved enough developmental plasticity to display migratory capacity under certain conditions.

Small intestinal T_{reg} cells induced in response to dietary antigens in mice have been considered short-lived cells, showing continuous replenishment from circulating precursors (Kim et al., 2016). We found that T_{reg} cells comprise two functionally distinct populations in human small intestine, distinguished by their expression of the transcription factor Helios. Both populations of intestinal T_{reg} cells expressed CD69, but at lower levels (≈40-50%) compared to conventional CD4+ T cells. Interestingly, T_{reg} cells presented higher fraction of CCR7+ cells than conventional CD4+ T cells, which are predominantly CCR7- in human small intestine. The Helios+ T_{reg} subset was completely replaced in donor duodenum at one-year post-transplantation and lacked CD103 expression. In contrast, Helios- T_{reg} cells were maintained in the graft after one year, and this subset showed comparable CD103 expression than conventional CD4 T cells.

Transcriptomic profiling studies have demonstrated that CD69+ T_{RM} cells are enriched for expression of adhesion/homing molecules, including CD49a and CXCR6, and negative regulators of activation such as PD-1 and CD101; which together form part of a core signature in multiple tissues in humans (Kumar et al., 2018a; Kumar et al., 2017). Furthermore, T_{RM} cells from different anatomic regions present tissue-restricted phenotypic features, reflecting the functional adaptations to each tissue environment (Cantero-Perez et al., 2019; Hayward et al., 2020; Pallett et al., 2017; Smolders et al., 2018). In this regard, we found that both intestinal CD8+ and CD4+ T cells exhibited high expression of NK-cell receptors, including CD161 and 2B4 (CD244), and reduced expression of CD28 compared to effector memory cells from blood. This phenotype suggests that activation of intestinal T cells (specially IE T cells) is tightly controlled by immunomodulatory markers responding to tissue-derived signals (Cabinian et al., 2018; Jabri and Ebert, 2007), thus preventing tissue pathology. Unlike T_{RM} cells from other tissues, including brain, lung or pancreas (Hombrink et al., 2016; Kumar et al., 2017; Shwetank et al., 2017; Wakim et al., 2010; Weisberg et al., 2019), PD-1 was expressed at reduced levels on intestinal CD103+ CD8+ T_{RM} cells compared to blood effector memory CD8+ T cells. This may reflect that the

environmental cues required for PD-1 upregulation on T$_{RM}$ cells depend on each particular tissue or organ.

KLRG1, a NK-cell receptor highly expressed on terminally differentiated T cells (Henson and Akbar, 2009), was expressed at variable levels on intestinal CD103- CD8+ and CD4+ T cells but completely absent on CD103+ T cells. KLRG1 acts as a co-inhibitory receptor on T cells (Rosshart et al., 2008), and can be used together with CD127 (IL7-R) to distinguish short-lived memory precursor cells (SLPCs, KLRG1+ CD127- cells) from memory precursor cells (MPECs, KLRG1- CD127+ cells) within the memory CD8+ T-cell population (Chang et al., 2014; Joshi et al., 2007). KLRG1 and CD103 share a common ligand, E-cadherin (Schwartzkopff et al., 2015); besides, the expression of both markers is regulated by TGF-β (Rosshart et al., 2008; Zhang and Bevan, 2013). The action of TGF-β on T cells is dual, being required to induce CD103 expression and to downregulate KLRG1 (Schwartzkopff et al., 2015). This duality might explain the mutually-exclusive expression pattern that we found for these two markers on intestinal T cells. Although both molecules share the same ligand, the binding of E-cadherin to CD103 or KLRG1 influence the interactions of CD8+ T cells and their targets in different ways: whereas KLRG1 inhibits T-cell effector function (Henson et al., 2009; Rosshart et al., 2008; Schwartzkopff et al., 2015), CD103 promotes cell-cell interactions and cytolysis (Le Floc'h et al., 2007).

Despite the substantial overlap in the phenotype of T$_{RM}$ cells in humans and mice, some differences have been found in the transcriptional factors regulating T$_{RM}$ development. Compared to circulating T cells, T$_{RM}$ cells express low levels of KLF2, Eomes and intermediate levels of T-bet and Blimp-1 (Mackay and Kallies, 2017; Mackay et al., 2015b). Hobit, a transcription factor homolog to Blimp-1, has been proposed as a master regulation of resident leukocytes in mice (Mackay and Kallies, 2017; Mackay et al., 2016). However, several studies in humans have reported low expression of this marker in T$_{RM}$ cells (Hombrink et al., 2016; Kumar et al., 2017). In addition, Notch1 and Runx3 have been shown to play a role in T$_{RM}$ generation in mice (Hombrink et al., 2016; Milner et al., 2017) and were found upregulated in lung T$_{RM}$ cells compared to circulating cells by transcriptomic analysis in human samples (Hombrink et al., 2016; Kumar et al., 2017; Oja et al., 2018; Snyder et al., 2019).

In mice models, antigen-specific CD4+ and CD8+ T$_{RM}$ cells isolated from the same tissue have exhibited similar transcriptional and phenotypic features, but also equivalent functional capabilities after reinfection (Beura et al., 2019). In agreement with this, when stimulated with PMA/ionomycin, a large fraction of both CD8+ and CD4+ T$_{RM}$ cells in LP produced high amounts of IFN-γ, IL-2 and TNF-α simultaneously. Polyfunctional T cells strongly correlate with enhanced

protection after infection in mice, non-human primates and humans (Darrah et al., 2007; Seder et al., 2008), and greater anti-tumor responses (Ding et al., 2012; Wimmers et al., 2016). These cytokines secreted by T_{RM} cells mediate direct pathogen elimination and induce other neighboring cells ("sensing-and-alarm" function) to recruit circulating cells and promote immune protection in the tissue (described in detail in **Figure 13**) (Ariotti et al., 2014; Iijima and Iwasaki, 2014; Schenkel et al., 2014). During infection, this sensing-and-alarm function can be triggered in bystander T_{RM} cells by antigen-independent mechanisms, resulting in protection against unrelated pathogens (Ariotti et al., 2014; Ge et al., 2019). Given the abundance of bystander CD8+ T cells in tumors (Rosato et al., 2019; Simoni et al., 2018), activated T_{RM} cells specific for unrelated antigens might synergize with neo-antigen specific CD8+ T cells to promote tumor rejection.
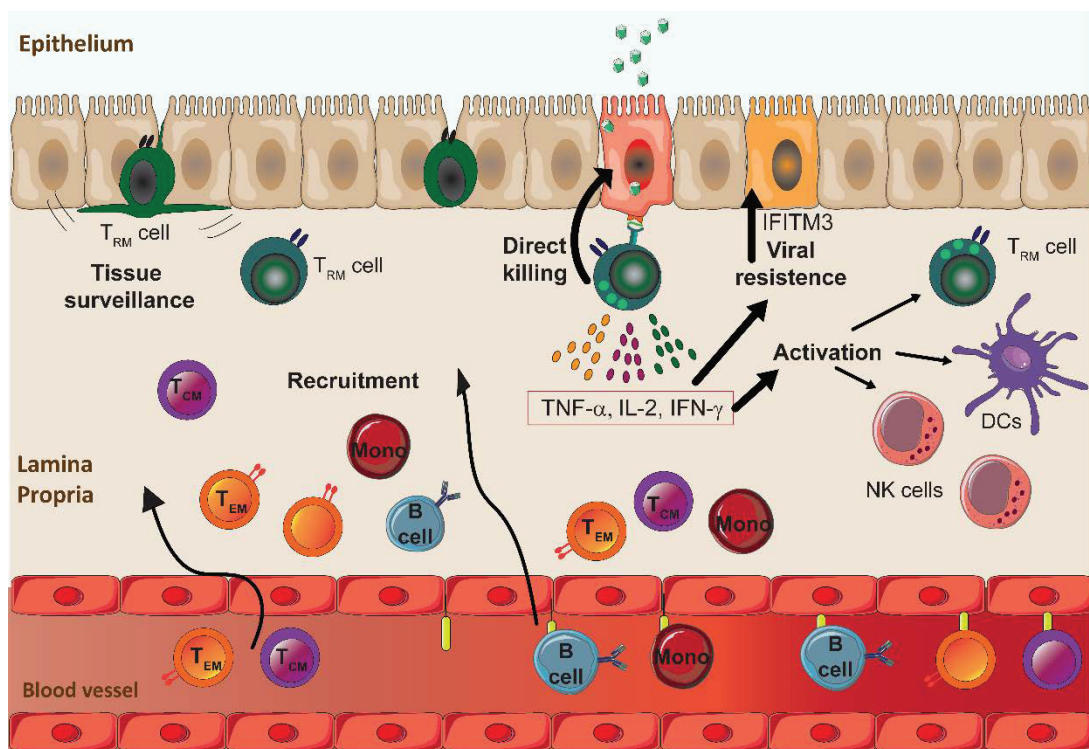
Figure 13. Protective recall responses mediated by CD8 T_{RM} cells. Intraepithelial T_{RM} cells are continuously patrolling their local environment. Immediately after infection (hours), reactivated CD8+ T_{RM} cells expressing high levels of granzyme-B, may directly eliminate infected epithelial cells. Upon recognition of their cognate antigen, activated CD8+ T_{RM} cells can secrete high levels of pro-inflammatory cytokines (such as IFN-γ, IL-2, TNF-α) that act at different levels on the neighboring cells. These cytokines mediate the upregulation of interferon stimulated genes (such as IFITM3) in the surrounding epithelial cells, which increases their resistance to viral infection. In addition, these cytokines mediated the upregulation of chemokines and VCAM-1 to activate the endothelium and recruit circulating B cells, T_{EM} and T_{CM} CD8+ and CD4+ T cells and monocytes into the tissue. Furthermore, these cytokines promote the maturation of local dendritic cells and induce the activation of bystander memory CD8+ T cells and natural killer cells, which in turn may also upregulate granzyme-B and promote the proliferation of CD8+ T_{RM} cells. Together, CD8+ T_{RM} cells can trigger a cascade of events to alarm neighboring cells and promote protective responses at the sites of pathogen encounter. Adapted from (Behr et al., 2018; Rosato et al., 2017).

A fraction of the CD103- CD4 T$_{RM}$ cells (mean 3%) and CD103+ CD4+ CD4 T$_{RM}$ cells (7%) produced IL-17 in human small intestine at the steady state. IL-17 has been shown to play a critical role in promoting intestinal homeostasis by maintaining the integrity of the epithelial barrier (Maloy and Kullberg, 2008; Martinez-Lopez et al., 2019). Interestingly, increased numbers of proinflammatory T$_H$17 cells displaying a T$_{RM}$ phenotype (CD69+ CD103+) have been found in biopsies of IBD patients (Zundler et al., 2019).

In addition to their cytokine secretion, when LP CD8+ T$_{RM}$ cells were stimulated with anti-CD3/CD28 beads, they expressed high levels of granzyme-B and perforin, suggesting that they can directly kill infected cells. In addition, a fraction of LP CD4+ T cells (≈40%) also displayed production of granzyme-B after stimulation. In contrast to their LP counterparts, IE CD8+ T$_{RM}$ cells were less responsive to the stimuli used in these studies, producing less cytokines and cytotoxic mediators. This hyporesponsiveness of IE T cells can be explained to some extent by their higher rate of apoptosis *ex vivo* (Brunner et al., 2001), and their abundant expression of immunomodulatory markers, such as 2B4, CD161 (showed in **paper I**) and CD101 (Russell et al., 1996), which might inhibition T cell activation and proliferation.

5.3 Adaptability to a highly dynamic antigenic environment is provided by short-lived populations in human small intestine

Long-term B-cell and T-cell protection depends on the generation of durable memory populations able to respond against reinfections. This persistent memory can be static or dynamic. Static memory is provided by populations with long lifespan and presents low plasticity. In contrast, dynamic memory is conferred by populations of cells with shorter longevity but that can be perpetuated at the clonal level (by homeostatic proliferation or differentiation from precursor cells), providing long-term memory with more flexibility to different contexts (Macallan et al., 2017). Competition for space, homeostatic resources, etc. may dictate how new specificities are incorporated into the niche of long-lived cells (Morris et al., 2019).

In human small intestine, CD19+ PCs presented higher turnover and secreted more IgA than the two other CD19- PC subsets, suggesting that they constitute a more dynamic PC subset reacting against ongoing antigenic challenge. In contrast, CD19- PCs (including CD45- and CD45+ subsets) showed a lifespan of several decades and were enriched in rotavirus-specific cells.

Rotavirus infection most often causes diarrheal disease in infants and young children, indicating that CD19- PCs constitute static subsets that might provide almost life-long protection to intestinal pathogens. CD45+ PCs showed intermediate turnover and phenotypic characteristics compared to the other two PC subsets. In agreement with this, immunoglobulin repertoire analysis revealed high clonal overlap between CD45+ PCs and the other two subsets, suggesting that CD45+ PCs represent a transitional developmental stage between CD19- PCs and CD45+ PCs.

Large numbers of intestinal CD8+ and CD4+ T cells were maintained for one year in transplanted duodenum, however the high variability in the replacement rates among patients suggests that they constitute more dynamic populations compared to PCs. In order to study whether long-term memory was conferred through clonal propagation, we examined the conservation of the repertoire of donor CD8+ CD103+ T_{RM} cells in biopsies from transplanted duodenum of the same patient at baseline and one year after transplantation. Overlapping clones (defined by paired TCRα and β chains) were detected across biopsies taken from different sites (several centimeters aside) one-year apart from donor duodenum in the two patients analyzed and recipient duodenum of one of the patients. This indicates that CD8+ T_{RM} repertoire is extremely stable and polarized towards expanded clones, in agreement with previous reports showing oligoclonal expansions of intestinal T cells widely dispersed throughout the human intestine (Gross et al., 1994). Comparing the TCR repertoire of different populations of intestinal CD8+ T cells we found high similarity in the repertoires of LP and IE CD103+ CD8+ T cells, suggesting that these two subsets were closely interconnected. In line with these results, the turnover values of both subsets were strongly correlated, reinforcing the notion that both populations constitute the same cell type located at different tissue compartments. In agreement with this, a recent study using *in vivo* imaging demonstrated that murine intestinal CD8+ T cells are constantly moving between the LP and the epithelium and vice versa (Thompson et al., 2019).

In transplanted small intestine, incoming recipient CD8+ T cells early after transplantation were mainly CD103- and acquired CD103 expression over time. This suggest that CD103- CD8+ T cells constitute recently recruited cells and some of them might differentiate into CD103+ T_{RM} cells *in situ*. Around 60% of the intestinal CD103- CD8+ T cells expressed KLRG1, a marker of short-lived effector cells (Joshi et al., 2007); and several studies in mouse have evidenced that CD8+ T_{RM} cells are generated from KLRG1- precursors (Mackay et al., 2013; Sheridan et al., 2014). To better understand the relationship among the different intestinal CD8+ T-cell subsets, we compared their TCR repertoire and we found that CD103- KLRG1- cells were

more closely related to CD103+ T$_{RM}$ cells than CD103- KLRG1+ cells. In addition, the KLRG1- subset was more similar to CD103+ T$_{RM}$ cells in terms of phenotype and function (cytokine profile and cytotoxic granule production), together indicating that they might constitute the progenitors of CD103+ T$_{RM}$ cells also in humans (**Figure 14**). However, exposure to the abundant local TGF-β might contribute to downregulate this marker (Schwartzkopff et al., 2015). Furthermore, a population of KLRG1+ cells has been shown to lose KLRG1 expression and differentiated into CD103+ CD8+ T$_{RM}$ cells in mice (Herndler-Brandstetter et al., 2018), arguing against the stability of this marker to distinguish between terminally differentiated cells and memory precursor that retained enough plasticity to give rise to T$_{RM}$ cells.
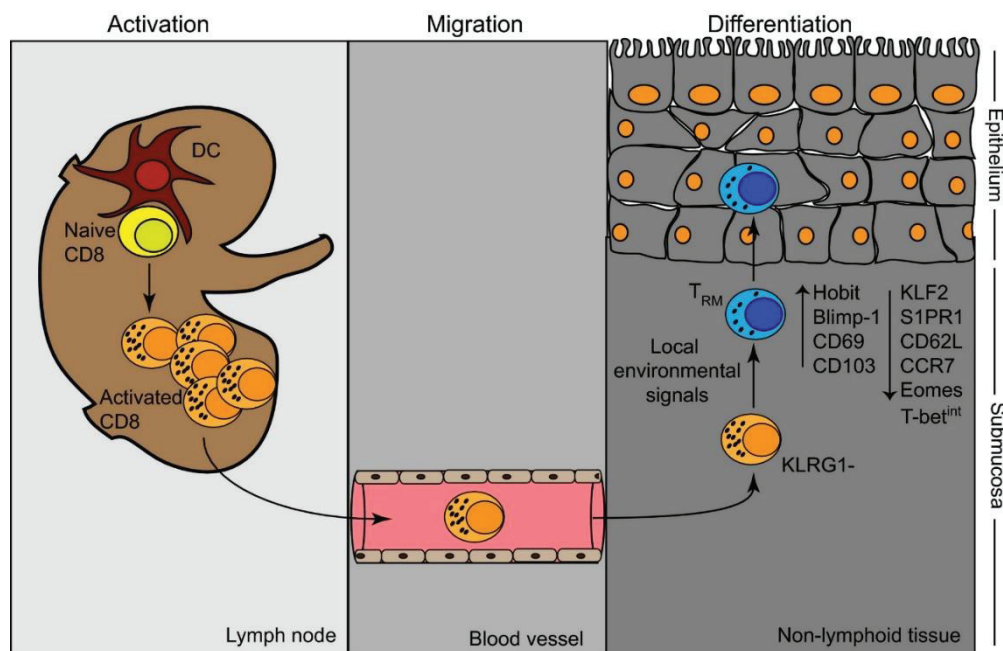
Figure 14. T$_{RM}$ differentiation. Activated T cells migrate from the secondary lymphoid organs to the sites of infection, where they collaborate in eradicating the pathogen. Once the infection is resolved, a fraction of these T cells lacking KLRG1 expression differentiated to T$_{RM}$ after exposure to the local environmental signals, such as TGF-β. T$_{RM}$ differentiation program includes upregulation of molecules that promote the retention in the tissue and downregulation of molecules involved in tissue egress. Reprinted from American Journal of Transplantation, Volume: 17, Issue: 5, Pages: 1167-1175, First published: 02 November 2016, DOI: (10.1111/ajt.14101) © 2016, with permission from Wiley.

The combination of different factors including TCR signal strength, environmental cues, co-stimulation, asymmetric division and cell metabolic state, plays a crucial role in determining T$_{RM}$ fate (Chang et al., 2014). However, how these inputs are regulated and integrated to imprint a specific T$_{RM}$ epigenetic program in precursor cells is not entirely elucidated yet. Priming of committed precursors by specific DC subsets in the lymph nodes might also influence T$_{RM}$ cell formation. In this regard, crosspriming by DNGR-1-expressing cDC1 cells was required to generate T$_{RM}$ precursors in a model of vaccinia infection (Iborra et al., 2016).

Little is known about the transcription factors involved in CD4+ T_{RM} generation or which type of effector subsets constitute the precursors of CD4+ T_{RM} cells. Nonetheless, there is evidence indicating that the requirements for CD4+ T_{RM} formation might differ from those observed for CD8+ T_{RM} cells in the same tissue. For example, pull and prime vaccination recruited CD4+ and CD8+ effector T cells to the female reproductive tract and established CD8+ T_{RM} cells in this site but not CD4+ T_{RM} cells (Shin and Iwasaki, 2012). Moreover, in a model of cytomegalovirus infection, antigen recognition was required for the generation of CD4+ T_{RM} cells but not for CD8+ T_{RM} cells in the salivary gland (Thom et al., 2015). CD4+ T_{RM} maintenance was found to be dependent on the formation of clusters with other resident immune cells, including CD8+ T_{RM} cells and macrophages, in skin and female reproductive tract (Collins et al., 2016; Iijima and Iwasaki, 2014). On the other hand, CD4+T-cell help was found to be necessary for the development of CD103+ CD8+ T_{RM} cells after influenza infection in the lung (Laidlaw et al., 2014).

6. FUTURE PERSPECTIVES

The advances in our understanding of turnover and retention of intestinal adaptive immune cells have profound implications for the treatment of intestinal diseases and the design of new therapeutic interventions, such as mucosal vaccines to elicit long-lived antibody and T-cell mediated responses.

Intestinal secreted IgA directly interacts with commensal bacteria and regulates the composition of the intestinal microbiota. In this regard, long-lived PCs could be crucial players to promote a healthy microbiota by ensuring its stability and diversity over time (Jahnsen et al., 2018). Targeting long-lived PCs in oral vaccines or immunological therapeutic settings could be a promising approach for those diseases caused by dysbiosis in the gut. Furthermore, emerging evidence reveals the central role of microbiome modulating human immunity, for example in the contexts of cancer immunotherapy (Mullard, 2018) and vaccination (Hagan et al., 2019). This opens up the possibility for the implementation of new therapeutic approaches targeting IgA-producing PCs to modulate the microbiota before other immunotherapeutic treatments or vaccines are administered.

Since their discovery in the last decade, the study of tissue-resident memory T cells has been a very active area of research. There is compelling evidence showing that T_{RM} cells provide protective responses and long-term immunity against a broad variety of viral, bacterial, fungal and parasitic infections, reviewed in (Muruganandah et al., 2018). This knowledge is fostering the development of new immunization strategies using optimized routes of administration (e.g. "prime-and-pull" vaccines) to establish pathogen-specific T_{RM} cells at target locations. Among those approaches, T_{RM}-mediated protection has been generated against herpes simplex virus type-2 (HSV-2), *Salmonella enterica* serovar Typhi (S. Typhi), human papillomavirus, malaria and simian/human immunodeficiency virus (SHIV) (Bernstein et al., 2019; Booth et al., 2019; Cuburu et al., 2019; Fernandez-Ruiz et al., 2016; Petitdemange et al., 2019; Shin and Iwasaki, 2012). Interestingly, vaccination strategies inducing both CD8+ T_{RM} cells and antibody responses provided superior protection against mucosal SHIV-infection in macaques (Petitdemange et al., 2019).

Several studies have demonstrated that T_{RM} cells play a significant role in immunity against cancer (Enamorado et al., 2017; Malik et al., 2017; Nizard et al., 2017; Park et al., 2018b). Adoptive cell therapy using chimeric antigen receptor (CAR) T cells or tumor-infiltrating lymphocytes have shown limited success in solid tumors, mainly due to difficulties in reaching the tumors and surviving long-term in the tumor microenvironment (D'Aloia et al., 2018). Single-cell transcriptomic analysis of infused tumor-infiltrating lymphocytes from a metastatic colorectal cancer patient experiencing partial response revealed a distinct signature characterized by increased expression of *ITGB1*, *IL-7R* (CD127) and *ZNF683* (Hobit) in those T-cell clones persisting long-term in blood (Lu et al., 2019). This suggests that the identification of tumor-infiltrating lymphocytes with the potential to migrate and survive long-term (in blood and preferably in the tumor) might lead to improved adoptive cell therapies for solid tumors. In addition, T_{RM} cells infiltrating tumors often present high PD-1 expression (often as part of their intrinsic tissue-residency program), making them sensitive to checkpoint blockade immunotherapy (Park and Mackay, 2017). Furthermore, bystander CD8+ T_{RM} cells with specificities against previous viral infections can be activated and repurposed to promote immune activation in the tumor microenvironment (Rosato et al., 2019).

There is increasing evidence showing that T_{RM} cells are involved in the pathogenesis of tissue-specific autoimmune and inflammatory diseases, such as psoriasis (Cheuk et al., 2017; Clark, 2011), inflammatory bowel disease (Noble et al., 2019; Zundler et al., 2019) and others, recently reviewed in (Sasson et al., 2020). Moreover, pathologic T_H2 resident memory cells can

be established after inhaled exposure to allergens in a mouse model of asthma (Hondowicz et al., 2016). Better knowledge about the factors driving T_{RM} cell development and maintenance will stimulate the development of new therapeutic targets used to selectively deplete T_{RM} cells while keeping the systemic immunity intact.

T_{RM} cells constitute the vast majority of the total T-cell compartment in the body, whereas blood T cells comprise only a small fraction of the total T-cell pool (Thome et al., 2014). Unlike circulating T cells, T_{RM} cells in peripheral tissues are highly resistant to immunosuppressive and conditioning regimens (Lutter et al., 2018b; Turner et al., 2014). The implications of the long-term persistence of donor T_{RM} cells in the graft outcome are still uncertain, because T_{RM} cells involved in both protective and inflammatory responses have been described in transplantation settings. For example, passenger donor T_{RM} cells persisting in face transplants have been found associated with tissue injury in rejected allografts (Lian et al., 2014). However, donor T_{RM} cells might also provide protection against infections in grafts of immunocompromised transplanted patients through sensing and alarm functions (Beura et al., 2017) (**Figure 15**). This way, persistent donor T_{RM} cells could prevent inflammation caused by cross-reactive pathogenic antigens and promote longer graft survival. In line with this hypothesis, studies in lung and whole bowel (or multivisceral) transplanted patients have revealed that rejection cases correlate with lower numbers of donor T_{RM} cells in the graft (Snyder et al., 2019; Zuber et al., 2016); and our observations also agree with this (unpublished results).

On the other hand, potentially alloreactive host T cells might migrate to the graft and differentiate into T_{RM} cells, incrementing the risk of late rejection. It is well established that lymphopenic conditions promote the proliferation of naïve T cells, in a mechanism dependent on IL-7 and self-peptide MHC-recognition (Jameson, 2002). This naïve T cells undergoing homeostatic proliferation can reach the peripheral tissues and differentiate into T_{RM} cells (Casey et al., 2012). Thus, it might be the case that immunosuppressive regimens to prevent graft rejection became part of the problem by promoting proliferation and differentiation of alloreactive host T cells, establishing them as persistent T_{RM} cells in the graft (Beura et al., 2017). The contribution of host T cells to graft-versus-host-disease (GVHD) pathogenesis in skin and colon has been reported in a recent study from our group, revealing a mechanism that involves activation by adjacent donor-derived APCs (Divito et. al J Clin Invest, in press).
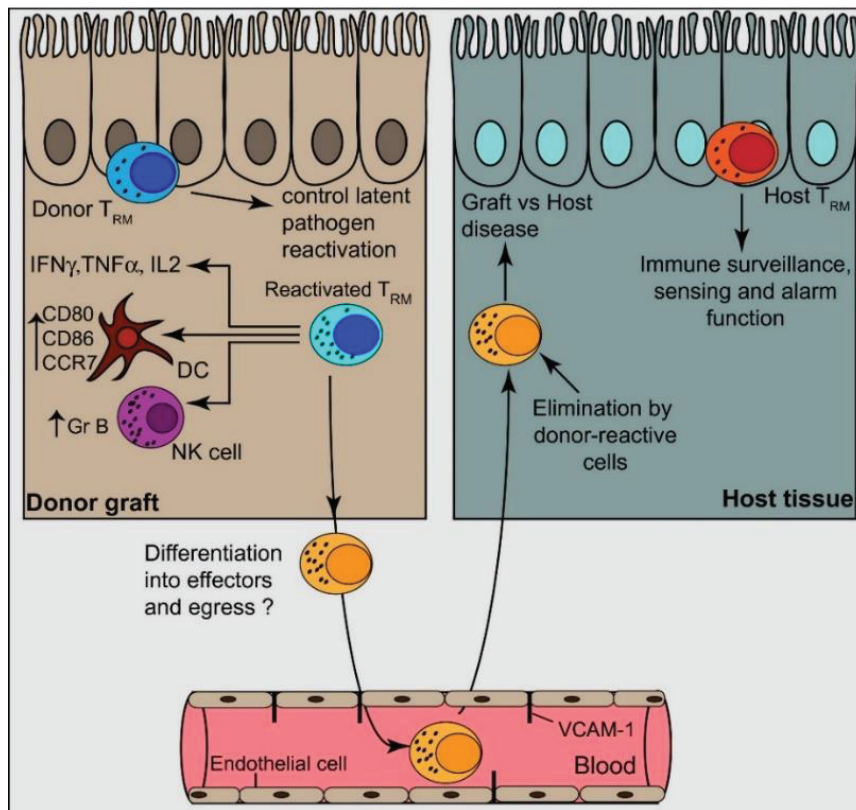
Figure 15. Role of T$_{RM}$ cells in transplantation. Reprinted from American Journal of Transplantation, Volume: 17, Issue: 5, Pages: 1167-1175, First published: 02 November 2016, DOI: (10.1111/ajt.14101) © 2016, with permission from Wiley.

Remaining challenges in the field:

To decipher T-cell immune surveillance in peripheral tissues, extrapolations of analysis from blood are not possible, making necessary to sample the tissues directly. This approach presents technical difficulties, including sample availability, time consuming protocols, blood contamination, poor isolation efficiencies and poor cell viability. Technical improvements in microscopy methods, such as quantitative immunofluorescence or highly multiplexed immunofluorescence protocols (e.g. CODEX) will improve the characterization and quantification of tissue-resident populations. In addition, the broad application of single-cell spatial transcriptomic methods will circumvent the artifacts caused by tissue digestion, providing valuable information about the interactions between T$_{RM}$ cells, T$_{reg}$ cells, PCs and their neighboring cells in the context of the tissue architecture.

There is increasing evidence showing the risk of using CD69, alone or together with CD103, to infer tissue residency. Hence, dissecting T$_{RM}$ cell heterogeneity and identifying reliable and unambiguous markers to correctly distinguish T$_{RM}$ cells from circulating T cells or from "ex- T$_{RM}$ cells" re-differentiated into circulating cells, is one of the major challenges in the field.These

markers might be restrained to specific tissues, or to certain species (different in mice versus humans). However, perhaps these differences between *bona fide* T$_{RM}$ cells and "T$_{RM}$-but still circulating cells" are not found in the phenotype but imprinted as epigenetic marks.

A recent report has revealed a crucial role of TGF-β in the epigenetic pre-conditioning of resting naïve CD8+ T cells, preparing them to undergo T$_{RM}$ cell differentiation (Mani et al., 2019). Approaches applying epigenetic analysis, such as ATAC-seq, to specific populations of T$_{RM}$ cells and precursor T cells will aid to elucidate the signatures for T$_{RM}$ cell differentiation and the interconnection with committed precursors. Knowledge about CD4+ T$_{RM}$ cell development and ontogeny is very incomplete compared to that of CD8+ T$_{RM}$ cells, and efforts must be done to advance also in this area.

Information about the specificities of T$_{RM}$ cells and T$_{reg}$ cells in different human tissues is lacking. Methods to analyze antigen-specific T cells, such as MHC multimers, applied together with TCR sequencing analysis will provide new insights to the understanding of T$_{RM}$ cell / T$_{reg}$ cell selection and differentiation, and will aid to investigate how clones of different specificities compete for their survival in the tissue. Of particular interest is the relationship between intestinal T cells and the microbiota members, which might be untangled by developing new functional assays to study the specificities of T cells against a broad array of commensals.

Resident immune cells need to adapt to their particular tissue environment, for example to oxygen tension and available metabolites. These tissue-specific adaptations are probably shared among T$_{RM}$ cells and other residents, such as PCs, Treg cells, γδ-T cells, iNKT cells and ILCs. Metabolic adaptations are also needed for the transition from effectors to memory cells, and the impact of the metabolic profile in the maintenance of T$_{RM}$ cells in the tissues is starting to be elucidated. Finally, the implementation of *in vitro* systems recapitulating these tissue conditions, such as organoids, might provide novel insights about the functional adaptations of tissue-derived cells.

7. BIBLIOGRAPHY

Abadie, V., V. Discepolo, and B. Jabri. 2012. Intraepithelial lymphocytes in celiac disease immunopathology. *Semin Immunopathol* 34:551-566.

Ackerman, A.L., A. Giodini, and P. Cresswell. 2006. A role for the endoplasmic reticulum protein retrotranslocation machinery during crosspresentation by dendritic cells. *Immunity* 25:607-617.

Agace, W.W. 2008. T-cell recruitment to the intestinal mucosa. *Trends Immunol* 29:514-522.

Agace, W.W., and K.D. McCoy. 2017. Regionalized Development and Maintenance of the Intestinal Adaptive Immune Landscape. *Immunity* 46:532-548.

Ai, T.L., B.D. Solomon, and C.S. Hsieh. 2014. T-cell selection and intestinal homeostasis. *Immunol Rev* 259:60-74.

Akimova, T., U.H. Beier, L. Wang, M.H. Levine, and W.W. Hancock. 2011. Helios expression is a marker of T cell activation and proliferation. *PLoS One* 6:e24226.

Alamyar, E., P. Duroux, M.P. Lefranc, and V. Giudicelli. 2012. IMGT((R)) tools for the nucleotide analysis of immunoglobulin (IG) and T cell receptor (TR) V-(D)-J repertoires, polymorphisms, and IG mutations: IMGT/V-QUEST and IMGT/HighV-QUEST for NGS. *Methods Mol Biol* 882:569-604.

Almeida, A., A.L. Mitchell, M. Boland, S.C. Forster, G.B. Gloor, A. Tarkowska, T.D. Lawley, and R.D. Finn. 2019. A new genomic blueprint of the human gut microbiota. *Nature* 568:499-504.

Anderson, G., and E.J. Jenkinson. 2001. Lymphostromal interactions in thymic development and function. *Nat Rev Immunol* 1:31-40.

Annunziato, F., C. Romagnani, and S. Romagnani. 2015. The 3 major types of innate and adaptive cell-mediated effector immunity. *J Allergy Clin Immunol* 135:626-635.

Ariotti, S., M.A. Hogenbirk, F.E. Dijkgraaf, L.L. Visser, M.E. Hoekstra, J.Y. Song, H. Jacobs, J.B. Haanen, and T.N. Schumacher. 2014. T cell memory. Skin-resident memory CD8(+) T cells trigger a state of tissue-wide pathogen alert. *Science* 346:101-105.

Arstila, T.P., A. Casrouge, V. Baron, J. Even, J. Kanellopoulos, and P. Kourilsky. 1999. A direct estimate of the human alphabeta T cell receptor diversity. *Science* 286:958-961.

Barry, M., and R.C. Bleackley. 2002. Cytotoxic T lymphocytes: all roads lead to death. *Nat Rev Immunol* 2:401-409.

Basso, A.S., H. Cheroutre, and D. Mucida. 2009. More stories on Th17 cells. *Cell Res* 19:399-411.

Baxter, A.G., and P.D. Hodgkin. 2002. Activation rules: the two-signal theories of immune activation. *Nat Rev Immunol* 2:439-446.

Behr, F.M., A. Chuwonpad, R. Stark, and K. van Gisbergen. 2018. Armed and Ready: Transcriptional Regulation of Tissue-Resident Memory CD8 T Cells. *Front Immunol* 9:16.

Bekiaris, V., E.K. Persson, and W.W. Agace. 2014. Intestinal dendritic cells in the regulation of mucosal immunity. *Immunol Rev* 260:86-101.

Bennett, M.S., J.L. Round, and D.T. Leung. 2015. Innate-like lymphocytes in intestinal infections. *Curr Opin Infect Dis* 28:457-463.

Benoun, J.M., N.G. Peres, N. Wang, O.H. Pham, V.L. Rudisill, Z.N. Fogassy, P.G. Whitney, D. Fernandez-Ruiz, T. Gebhardt, Q.M. Pham, L. Puddington, S. Bedoui, R.A. Strugnell, and S.J. McSorley. 2018. Optimal protection against Salmonella infection requires noncirculating memory. *Proc Natl Acad Sci U S A* 115:10416-10421.

Berard, M., and D.F. Tough. 2002. Qualitative differences between naive and memory T cells. *Immunology* 106:127-138.

Bergmann, O., R.D. Bhardwaj, S. Bernard, S. Zdunek, F. Barnabe-Heider, S. Walsh, J. Zupicich, K. Alkass, B.A. Buchholz, H. Druid, S. Jovinge, and J. Frisen. 2009. Evidence for cardiomyocyte renewal in humans. *Science* 324:98-102.

Bergsbaken, T., and M.J. Bevan. 2015. Proinflammatory microenvironments within the intestine regulate the differentiation of tissue-resident CD8(+) T cells responding to infection. *Nat Immunol* 16:406-414.

Bergsbaken, T., M.J. Bevan, and P.J. Fink. 2017. Local Inflammatory Cues Regulate Differentiation and Persistence of CD8(+) Tissue-Resident Memory T Cells. *Cell Rep* 19:114-124.

Bernstein, D.I., R.D. Cardin, F.J. Bravo, S. Awasthi, P. Lu, D.A. Pullum, D.A. Dixon, A. Iwasaki, and H.M. Friedman. 2019. Successful application of prime and pull strategy for a therapeutic HSV vaccine. *NPJ Vaccines* 4:33.

Beura, L.K., N.J. Fares-Frederickson, E.M. Steinert, M.C. Scott, E.A. Thompson, K.A. Fraser, J.M. Schenkel, V. Vezys, and D. Masopust. 2019. CD4+ resident memory T cells dominate immunosurveillance and orchestrate local recall responses. *The Journal of Experimental Medicine*

Beura, L.K., S.E. Hamilton, K. Bi, J.M. Schenkel, O.A. Odumade, K.A. Casey, E.A. Thompson, K.A. Fraser, P.C. Rosato, A. Filali-Mouhim, R.P. Sekaly, M.K. Jenkins, V. Vezys, W.N. Haining, S.C. Jameson, and D. Masopust. 2016. Normalizing the environment recapitulates adult human immune traits in laboratory mice. *Nature* 532:512-516.

Beura, L.K., J.S. Mitchell, E.A. Thompson, J.M. Schenkel, J. Mohammed, S. Wijeyesinghe, R. Fonseca, B.J. Burbach, H.D. Hickman, V. Vezys, B.T. Fife, and D. Masopust. 2018. Intravital mucosal imaging of CD8(+) resident memory T cells shows tissue-autonomous recall responses that amplify secondary memory. *Nat Immunol* 19:173-182.

Beura, L.K., P.C. Rosato, and D. Masopust. 2017. Implications of Resident Memory T Cells for Transplantation. *Am J Transplant* 17:1167-1175.

Blattman, J.N., R. Antia, D.J. Sourdive, X. Wang, S.M. Kaech, K. Murali-Krishna, J.D. Altman, and R. Ahmed. 2002. Estimating the precursor frequency of naive antigen-specific CD8 T cells. *J Exp Med* 195:657-664.

Blum, J.S., P.A. Wearsch, and P. Cresswell. 2013. Pathways of antigen processing. *Annu Rev Immunol* 31:443-473.

Bolotin, D.A., S. Poslavsky, I. Mitrophanov, M. Shugay, I.Z. Mamedov, E.V. Putintseva, and D.M. Chudakov. 2015. MiXCR: software for comprehensive adaptive immunity profiling. *Nat Methods* 12:380-381.

Booth, J.S., E. Goldberg, S.A. Patil, R.S. Barnes, B.D. Greenwald, and M.B. Sztein. 2019. Effect of the live oral attenuated typhoid vaccine, Ty21a, on systemic and terminal ileum mucosal CD4+ T memory responses in humans. *Int Immunol* 31:101-116.

Brandtzaeg, P. 2013. Secretory IgA: designed for anti-microbial defense. *Front Immunol* 4:

Brandtzaeg, P., V. Bosnes, T.S. Halstensen, H. Scott, L.M. Sollid, and K.N. Valnes. 1989. T lymphocytes in human gut epithelium preferentially express the alpha/beta antigen receptor and are often CD45/UCHL1-positive. *Scand J Immunol* 30:123-128.

Brandtzaeg, P., I.N. Farstad, F.E. Johansen, H.C. Morton, I.N. Norderhaug, and T. Yamanaka. 1999. The B-cell system of human mucosae and exocrine glands. *Immunol Rev* 171:45-87.

Brandtzaeg, P., and R. Pabst. 2004. Let's go mucosal: communication on slippery ground. *Trends Immunol* 25:570-577.

Breitfeld, D., L. Ohl, E. Kremmer, J. Ellwart, F. Sallusto, M. Lipp, and R. Forster. 2000. Follicular B helper T cells express CXC chemokine receptor 5, localize to B cell follicles, and support immunoglobulin production. *J Exp Med* 192:1545-1552.

Brucklacher-Waldert, V., E.J. Carr, M.A. Linterman, and M. Veldhoen. 2014. Cellular Plasticity of CD4+ T Cells in the Intestine. *Front Immunol* 5:488.

Brunner, T., D. Arnold, C. Wasem, S. Herren, and C. Frutschi. 2001. Regulation of cell death and survival in intestinal intraepithelial lymphocytes. *Cell Death Differ* 8:706-714.

Bujko, A., N. Atlasy, O.J.B. Landsverk, L. Richter, S. Yaqub, R. Horneland, O. Oyen, E.M. Aandahl, L. Aabakken, H.G. Stunnenberg, E.S. Baekkevold, and F.L. Jahnsen. 2018. Transcriptional and functional profiling defines human small intestinal macrophage subsets. *J Exp Med* 215:441-458.

Bunker, J.J., and A. Bendelac. 2018. IgA Responses to Microbiota. *Immunity* 49:211-224.

Cabinian, A., D. Sinsimer, M. Tang, Y. Jang, B. Choi, Y. Laouar, and A. Laouar. 2018. Gut symbiotic microbes imprint intestinal immune cells with the innate receptor SLAMF4 which contributes to gut immune protection against enteric pathogens. *Gut* 67:847-859.

Call, M.E., J. Pyrdol, M. Wiedmann, and K.W. Wucherpfennig. 2002. The organizing principle in the formation of the T cell receptor-CD3 complex. *Cell* 111:967-979.

Cantero-Perez, J., J. Grau-Exposito, C. Serra-Peinado, D.A. Rosero, L. Luque-Ballesteros, A. Astorga-Gamaza, J. Castellvi, T. Sanhueza, G. Tapia, B. Lloveras, M.A. Fernandez, J.G. Prado, J.M. Sole-Sedeno, A. Tarrats, C. Lecumberri, L. Manalich-Barrachina, C. Centeno-Mediavilla, V. Falco, M.J. Buzon, and M. Genesca. 2019. Resident memory T cells are a cellular reservoir for HIV in the cervical mucosa. *Nat Commun* 10:4739.

Casey, K.A., K.A. Fraser, J.M. Schenkel, A. Moran, M.C. Abt, L.K. Beura, P.J. Lucas, D. Artis, E.J. Wherry, K. Hogquist, V. Vezys, and D. Masopust. 2012. Antigen-independent differentiation and maintenance of effector-like resident memory T cells in tissues. *J Immunol* 188:4866-4875.

Cauley, L.S., T. Cookenham, T.B. Miller, P.S. Adams, K.M. Vignali, D.A. Vignali, and D.L. Woodland. 2002. Cutting edge: virus-specific CD4+ memory T cells in nonlymphoid tissues express a highly activated phenotype. *J Immunol* 169:6655-6658.

Cauley, L.S., and L. Lefrancois. 2013. Guarding the perimeter: protection of the mucosa by tissue-resident memory T cells. *Mucosal Immunol* 6:14-23.

Cepek, K.L., S.K. Shaw, C.M. Parker, G.J. Russell, J.S. Morrow, D.L. Rimm, and M.B. Brenner. 1994. Adhesion between epithelial cells and T lymphocytes mediated by E-cadherin and the alpha E beta 7 integrin. *Nature* 372:190-193.

Cerovic, V., C.C. Bain, A.M. Mowat, and S.W. Milling. 2014. Intestinal macrophages and dendritic cells: what's the difference? *Trends Immunol* 35:270-277.

Cerovic, V., S.A. Houston, J. Westlund, L. Utriainen, E.S. Davison, C.L. Scott, C.C. Bain, T. Joeris, W.W. Agace, R.A. Kroczek, A.M. Mowat, U. Yrlid, and S.W. Milling. 2015. Lymph-borne CD8alpha+ dendritic cells are uniquely able to cross-prime CD8+ T cells with antigen acquired from intestinal epithelial cells. *Mucosal Immunol* 8:38-48.

Chang, J.T., E.J. Wherry, and A.W. Goldrath. 2014. Molecular regulation of effector and memory T cell differentiation. *Nat Immunol* 15:1104-1115.

Chen, L., and D.B. Flies. 2013. Molecular mechanisms of T cell co-stimulation and co-inhibition. *Nat Rev Immunol* 13:227-242.

Cheroutre, H., and F. Lambolez. 2008. Doubting the TCR coreceptor function of CD8alphaalpha. *Immunity* 28:149-159.

Cheroutre, H., F. Lambolez, and D. Mucida. 2011. The light and dark sides of intestinal intraepithelial lymphocytes. *Nat Rev Immunol* 11:445-456.

Cherrier, D.E., N. Serafini, and J.P. Di Santo. 2018. Innate Lymphoid Cell Development: A T Cell Perspective. *Immunity* 48:1091-1103.

Cheuk, S., H. Schlums, I. Gallais Serezal, E. Martini, S.C. Chiang, N. Marquardt, A. Gibbs, E. Detlofsson, A. Introini, M. Forkel, C. Hoog, A. Tjernlund, J. Michaelsson, L. Folkersen, J. Mjosberg, L. Blomqvist, M. Ehrstrom, M. Stahle, Y.T. Bryceson, and L. Eidsmo. 2017. CD49a Expression Defines Tissue-Resident CD8(+) T Cells Poised for Cytotoxic Function in Human Skin. *Immunity* 46:287-300.

Chowdhury, D., and J. Lieberman. 2008. Death by a thousand cuts: granzyme pathways of programmed cell death. *Annu Rev Immunol* 26:389-420.

Cibrian, D., and F. Sanchez-Madrid. 2017. CD69: from activation marker to metabolic gatekeeper. *Eur J Immunol* 47:946-953.

Clark, R.A. 2011. Gone but not forgotten: lesional memory in psoriatic skin. *J Invest Dermatol* 131:283-285.

Clark, R.A. 2015. Resident memory T cells in human health and disease. *Sci Transl Med* 7:269rv261.

Collin, M., and V. Bigley. 2018. Human dendritic cell subsets: an update. *Immunology* 154:3-20.

Collins, N., X. Jiang, A. Zaid, B.L. Macleod, J. Li, C.O. Park, A. Haque, S. Bedoui, W.R. Heath, S.N. Mueller, T.S. Kupper, T. Gebhardt, and F.R. Carbone. 2016. Skin CD4(+) memory T cells exhibit combined cluster-mediated retention and equilibration with the circulation. *Nat Commun* 7:11514.

Collison, L.W., and D.A. Vignali. 2011. In vitro Treg suppression assays. *Methods Mol Biol* 707:21-37.

Commins, S.P., L. Borish, and J.W. Steinke. 2010. Immunologic messenger molecules: cytokines, interferons, and chemokines. *J Allergy Clin Immunol* 125:S53-72.

Coombes, J.L., and F. Powrie. 2008. Dendritic cells in intestinal immune regulation. *Nat Rev Immunol* 8:435-446.

Cossarizza, A., H.D. Chang, A. Radbruch, A. Acs, D. Adam, S. Adam-Klages, W.W. Agace, N. Aghaeepour, M. Akdis, M. Allez, L.N. Almeida, G. Alvisi, G. Anderson, I. Andra, F. Annunziato, A. Anselmo, P. Bacher, C.T. Baldari, S. Bari, V. Barnaba, J. Barros-Martins, L. Battistini, W. Bauer, S. Baumgart, N. Baumgarth, D. Baumjohann, B. Baying, M. Bebawy, B. Becher, W. Beisker, V. Benes, R. Beyaert, A. Blanco, D.A. Boardman, C. Bogdan, J.G. Borger, G. Borsellino, P.E. Boulais, J.A. Bradford, D. Brenner, R.R. Brinkman, A.E.S. Brooks, D.H. Busch, M. Buscher, T.P. Bushnell, F. Calzetti, G. Cameron, I. Cammarata, X. Cao, S.L. Cardell, S. Casola, M.A. Cassatella, A. Cavani, A. Celada, L. Chatenoud, P.K. Chattopadhyay, S. Chow, E. Christakou, L. Cicin-Sain, M. Clerici, F.S. Colombo, L. Cook, A. Cooke, A.M. Cooper, A.J. Corbett, A. Cosma, L. Cosmi, P.G. Coulie, A. Cumano, L. Cvetkovic, V.D. Dang, C. Dang-Heine, M.S. Davey, D. Davies, S. De Biasi, G. Del Zotto, G.V. Dela Cruz, M. Delacher, S. Della Bella, P. Dellabona, G. Deniz, M. Dessing, J.P. Di Santo, A. Diefenbach, F. Dieli, A. Dolf, T. Dorner, R.J. Dress, D. Dudziak, M. Dustin, C.A. Dutertre, F. Ebner, S.B.G. Eckle, M. Edinger, P. Eede, G.R.A. Ehrhardt, M. Eich, P. Engel, B. Engelhardt, A. Erdei, C. Esser, B. Everts,

M. Evrard, C.S. Falk, T.A. Fehniger, M. Felipo-Benavent, H. Ferry, M. Feuerer, A. Filby, K. Filkor, S. Fillatreau, M. Follo, I. Forster, J. Foster, G.A. Foulds, B. Frehse, P.S. Frenette, S. Frischbutter, W. Fritzsche, D.W. Galbraith, A. Gangaev, N. Garbi, B. Gaudilliere, R.T. Gazzinelli, J. Geginat, W. Gerner, N.A. Gherardin, K. Ghoreschi, L. Gibellini, F. Ginhoux, K. Goda, D.I. Godfrey, C. Goettlinger, J.M. Gonzalez-Navajas, C.S. Goodyear, A. Gori, J.L. Grogan, D. Grummitt, A. Grutzkau, C. Haftmann, J. Hahn, H. Hammad, G. Hammerling, L. Hansmann, G. Hansson, C.M. Harpur, S. Hartmann, A. Hauser, A.E. Hauser, D.L. Haviland, D. Hedley, D.C. Hernandez, G. Herrera, M. Herrmann, C. Hess, T. Hofer, P. Hoffmann, K. Hogquist, T. Holland, T. Hollt, R. Holmdahl, P. Hombrink, J.P. Houston, B.F. Hoyer, B. Huang, F.P. Huang, J.E. Huber, J. Huehn, M. Hundemer, C.A. Hunter, W.Y.K. Hwang, A. Iannone, F. Ingelfinger, S.M. Ivison, H.M. Jack, P.K. Jani, B. Javega, S. Jonjic, T. Kaiser, T. Kalina, T. Kamradt, S.H.E. Kaufmann, B. Keller, S.L.C. Ketelaars, A. Khalilnezhad, S. Khan, J. Kisielow, P. Klenerman, J. Knopf, H.F. Koay, K. Kobow, J.K. Kolls, W.T. Kong, M. Kopf, T. Korn, K. Kriegsmann, H. Kristyanto, T. Kroneis, A. Krueger, J. Kuhne, C. Kukat, D. Kunkel, H. Kunze-Schumacher, T. Kurosaki, C. Kurts, P. Kvistborg, I. Kwok, J. Landry, O. Lantz, P. Lanuti, F. LaRosa, A. Lehuen, S. LeibundGut-Landmann, M.D. Leipold, L.Y.T. Leung, M.K. Levings, A.C. Lino, F. Liotta, V. Litwin, Y. Liu, H.G. Ljunggren, M. Lohoff, G. Lombardi, L. Lopez, M. Lopez-Botet, A.E. Lovett-Racke, E. Lubberts, H. Luche, B. Ludewig, E. Lugli, S. Lunemann, H.T. Maecker, L. Maggi, O. Maguire, F. Mair, K.H. Mair, A. Mantovani, R.A. Manz, A.J. Marshall, A. Martinez-Romero, G. Martrus, I. Marventano, W. Maslinski, G. Matarese, A.V. Mattioli, C. Maueroder, A. Mazzoni, J. McCluskey, M. McGrath, H.M. McGuire, I.B. McInnes, H.E. Mei, F. Melchers, S. Melzer, D. Mielenz, S.D. Miller, K.H.G. Mills, H. Minderman, J. Mjosberg, J. Moore, B. Moran, L. Moretta, T.R. Mosmann, S. Muller, G. Multhoff, L.E. Munoz, C. Munz, T. Nakayama, M. Nasi, K. Neumann, L.G. Ng, A. Niedobitek, S. Nourshargh, G. Nunez, J.E. O'Connor, A. Ochel, A. Oja, D. Ordonez, A. Orfao, E. Orlowski-Oliver, W. Ouyang, A. Oxenius, R. Palankar, I. Panse, K. Pattanapanyasat, M. Paulsen, D. Pavlinic, L. Penter, P. Peterson, C. Peth, J. Petriz, F. Piancone, W.F. Pickl, S. Piconese, M. Pinti, A.G. Pockley, M.J. Podolska, Z. Poon, K. Pracht, I. Prinz, C.E.M. Pucillo, S.A. Quataert, L. Quatrini, K.M. Quinn, H. Radbruch, T. Radstake, S. Rahmig, H.P. Rahn, B. Rajwa, G. Ravichandran, Y. Raz, J.A. Rebhahn, D. Recktenwald, D. Reimer, E.S.C. Reis, E.B.M. Remmerswaal, L. Richter, L.G. Rico, A. Riddell, A.M. Rieger, J.P. Robinson, C. Romagnani, A. Rubartelli, J. Ruland, A. Saalmuller, Y. Saeys, T. Saito, S. Sakaguchi, F. Sala-de-Oyanguren, Y. Samstag, S. Sanderson, I. Sandrock, A. Santoni, R.B. Sanz, M. Saresella, C. Sautes-Fridman, B. Sawitzki, L. Schadt, A. Scheffold, H.U. Scherer, M. Schiemann, F.A. Schildberg, E. Schimisky, A. Schlitzer, J. Schlosser, S. Schmid, S. Schmitt, K. Schober, D. Schraivogel, W. Schuh, T. Schuler, R. Schulte, A.R. Schulz, S.R. Schulz, C. Scotta, D. Scott-Algara, D.P. Sester, T.V. Shankey, B. Silva-Santos, A.K. Simon, K.M. Sitnik, S. Sozzani, D.E. Speiser, J. Spidlen, A. Stahlberg, A.M. Stall, N. Stanley, R. Stark, C. Stehle, T. Steinmetz, H. Stockinger, Y. Takahama, K. Takeda, L. Tan, A. Tarnok, G. Tiegs, G. Toldi, J. Tornack, E. Traggiai, M. Trebak, T.I.M. Tree, J. Trotter, J. Trowsdale, M. Tsoumakidou, H. Ulrich, S. Urbanczyk, W. van de Veen, M. van den Broek, E. van der Pol, S. Van Gassen, G. Van Isterdael, R.A.W. van Lier, M. Veldhoen, S. Vento-Asturias, P. Vieira, D. Voehringer, H.D. Volk, A. von Borstel, K. von Volkmann, A. Waisman, R.V. Walker, P.K. Wallace, S.A. Wang, X.M. Wang, M.D. Ward, K.A. Ward-Hartstonge, K. Warnatz, G. Warnes, S. Warth, C. Waskow, J.V. Watson, C. Watzl, L. Wegener, T. Weisenburger, A. Wiedemann, J. Wienands, A. Wilharm, R.J. Wilkinson, G. Willimsky, J.B. Wing, R. Winkelmann, T.H. Winkler, O.F. Wirz, A. Wong, P. Wurst, J.H.M. Yang, J. Yang, M. Yazdanbakhsh, L. Yu, A. Yue, H. Zhang, Y. Zhao, S.M. Ziegler, C. Zielinski, J. Zimmermann, and A. Zychlinsky. 2019. Guidelines for the use of flow cytometry and cell sorting in immunological studies (second edition). *Eur J Immunol* 49:1457-1973.

Cox, M.A., S.M. Kahan, and A.J. Zajac. 2013. Anti-viral CD8 T cells and the cytokines that they love. *Virology* 435:157-169.

Crosby, C.M., and M. Kronenberg. 2018. Tissue-specific functions of invariant natural killer T cells. *Nat Rev Immunol* 18:559-574.

Crotty, S., and R. Ahmed. 2004. Immunological memory in humans. *Semin Immunol* 16:197-203.

Cuburu, N., R. Kim, G.C. Guittard, C.D. Thompson, P.M. Day, D.E. Hamm, Y.S. Pang, B.S. Graham, D.R. Lowy, and J.T. Schiller. 2019. A Prime-Pull-Amplify Vaccination Strategy To Maximize Induction of Circulating and Genital-Resident Intraepithelial CD8(+) Memory T Cells. *J Immunol* 202:1250-1264.

BIBLIOGRAPHY

Curtsinger, J.M., and M.F. Mescher. 2010. Inflammatory cytokines as a third signal for T cell activation. *Curr Opin Immunol* 22:333-340.

D'Aloia, M.M., I.G. Zizzari, B. Sacchetti, L. Pierelli, and M. Alimandi. 2018. CAR-T cells: the long and winding road to solid tumors. *Cell Death Dis* 9:282.

Darrah, P.A., D.T. Patel, P.M. De Luca, R.W. Lindsay, D.F. Davey, B.J. Flynn, S.T. Hoff, P. Andersen, S.G. Reed, S.L. Morris, M. Roederer, and R.A. Seder. 2007. Multifunctional TH1 cells define a correlate of vaccine-mediated protection against Leishmania major. *Nat Med* 13:843-850.

Davis, M.M. 1990. T cell receptor gene diversity and selection. *Annu Rev Biochem* 59:475-496.

Davis, M.M., and P.J. Bjorkman. 1988. T-cell antigen receptor genes and T-cell recognition. *Nature* 334:395-402.

de Leur, K., M. Dieterich, D.A. Hesselink, O.B.J. Corneth, F. Dor, G.N. de Graav, A.M.A. Peeters, A. Mulder, H. Kimenai, F.H.J. Claas, M.C. Clahsen-van Groningen, L.J.W. van der Laan, R.W. Hendriks, and C.C. Baan. 2019. Characterization of donor and recipient CD8+ tissue-resident memory T cells in transplant nephrectomies. *Sci Rep* 9:5984.

De Simone, M., G. Rossetti, and M. Pagani. 2018. Single Cell T Cell Receptor Sequencing: Techniques and Future Challenges. *Front Immunol* 9:1638.

den Braber, I., T. Mugwagwa, N. Vrisekoop, L. Westera, R. Mogling, A.B. de Boer, N. Willems, E.H. Schrijver, G. Spierenburg, K. Gaiser, E. Mul, S.A. Otto, A.F. Ruiter, M.T. Ackermans, F. Miedema, J.A. Borghans, R.J. de Boer, and K. Tesselaar. 2012. Maintenance of peripheral naive T cells is sustained by thymus output in mice but not humans. *Immunity* 36:288-297.

Dijkgraaf, F.E., T.R. Matos, M. Hoogenboezem, M. Toebes, D.W. Vredevoogd, M. Mertz, B. van den Broek, J.Y. Song, M.B.M. Teunissen, R.M. Luiten, J.B. Beltman, and T.N. Schumacher. 2019. Tissue patrol by resident memory CD8(+) T cells in human skin. *Nat Immunol* 20:756-764.

Ding, Z.C., L. Huang, B.R. Blazar, H. Yagita, A.L. Mellor, D.H. Munn, and G. Zhou. 2012. Polyfunctional CD4(+) T cells are essential for eradicating advanced B-cell lymphoma after chemotherapy. *Blood* 120:2229-2239.

Dogra, P., H.E. Ghoneim, H.A. Abdelsamed, and B. Youngblood. 2016. Generating long-lived CD8(+) T-cell memory: Insights from epigenetic programs. *Eur J Immunol* 46:1548-1562.

Dustin, M.L. 2014. The immunological synapse. *Cancer Immunol Res* 2:1023-1033.

Eguiluz-Gracia, I., H.H. Schultz, L.I. Sikkeland, E. Danilova, A.M. Holm, C.J. Pronk, W.W. Agace, M. Iversen, C. Andersen, F.L. Jahnsen, and E.S. Baekkevold. 2016. Long-term persistence of human donor alveolar macrophages in lung transplant recipients. *Thorax* 71:1006-1011.

Enamorado, M., S. Iborra, E. Priego, F.J. Cueto, J.A. Quintana, S. Martinez-Cano, E. Mejias-Perez, M. Esteban, I. Melero, A. Hidalgo, and D. Sancho. 2017. Enhanced anti-tumour immunity requires the interplay between resident and circulating memory CD8(+) T cells. *Nat Commun* 8:16073.

Ettersperger, J., N. Montcuquet, G. Malamut, N. Guegan, S. Lopez-Lastra, S. Gayraud, C. Reimann, E. Vidal, N. Cagnard, P. Villarese, I. Andre-Schmutz, R. Gomes Domingues, C. Godinho-Silva, H. Veiga-Fernandes, L. Lhermitte, V. Asnafi, E. Macintyre, C. Cellier, K. Beldjord, J.P. Di Santo, N. Cerf-Bensussan, and B. Meresse. 2016. Interleukin-15-Dependent T-Cell-like Innate Intraepithelial Lymphocytes Develop in the Intestine and Transform into Lymphomas in Celiac Disease. *Immunity* 45:610-625.

Eyerich, S., K. Eyerich, D. Pennino, T. Carbone, F. Nasorri, S. Pallotta, F. Cianfarani, T. Odorisio, C. Traidl-Hoffmann, H. Behrendt, S.R. Durham, C.B. Schmidt-Weber, and A. Cavani. 2009. Th22 cells represent a distinct human T cell subset involved in epidermal immunity and remodeling. *J Clin Invest* 119:3573-3585.

Fagarasan, S., K. Kinoshita, M. Muramatsu, K. Ikuta, and T. Honjo. 2001. In situ class switching and differentiation to IgA-producing cells in the gut lamina propria. *Nature* 413:639-643.

Farber, D.L., M.G. Netea, A. Radbruch, K. Rajewsky, and R.M. Zinkernagel. 2016. Immunological memory: lessons from the past and a look to the future. *Nat Rev Immunol* 16:124-128.

Farber, D.L., N.A. Yudanin, and N.P. Restifo. 2014. Human memory T cells: generation, compartmentalization and homeostasis. *Nat Rev Immunol* 14:24-35.

Faria, A.M.C., B.S. Reis, and D. Mucida. 2017. Tissue adaptation: Implications for gut immunity and tolerance. *J Exp Med* 214:1211-1226.

Fenton, T.M., A. Kelly, E.E. Shuttleworth, C. Smedley, A. Atakilit, F. Powrie, S. Campbell, S.L. Nishimura, D. Sheppard, S. Levison, J.J. Worthington, M.J. Lehtinen, and M.A. Travis. 2017. Inflammatory cues enhance TGFbeta activation by distinct subsets of human intestinal dendritic cells via integrin alphavbeta8. *Mucosal Immunol* 10:624-634.

74

Ferguson, A. 1977. Intraepithelial lymphocytes of the small intestine. *Gut* 18:921-937.

Fernandez-Ruiz, D., W.Y. Ng, L.E. Holz, J.Z. Ma, A. Zaid, Y.C. Wong, L.S. Lau, V. Mollard, A. Cozijnsen, N. Collins, J. Li, G.M. Davey, Y. Kato, S. Devi, R. Skandari, M. Pauley, J.H. Manton, D.I. Godfrey, A. Braun, S.S. Tay, P.S. Tan, D.G. Bowen, F. Koch-Nolte, B. Rissiek, F.R. Carbone, B.S. Crabb, M. Lahoud, I.A. Cockburn, S.N. Mueller, P. Bertolino, G.I. McFadden, I. Caminschi, and W.R. Heath. 2016. Liver-Resident Memory CD8(+) T Cells Form a Front-Line Defense against Malaria Liver-Stage Infection. *Immunity* 45:889-902.

Fu, J., J. Zuber, M. Martinez, B. Shonts, A. Obradovic, H. Wang, S.P. Lau, A. Xia, E.E. Waffarn, K. Frangaj, T.M. Savage, M.T. Simpson, S. Yang, X.V. Guo, M. Miron, T. Senda, K. Rogers, A. Rahman, S.H. Ho, Y. Shen, A. Griesemer, D.L. Farber, T. Kato, and M. Sykes. 2019. Human Intestinal Allografts Contain Functional Hematopoietic Stem and Progenitor Cells that Are Maintained by a Circulating Pool. *Cell Stem Cell* 24:227-239 e228.

Fujita, H. 2013. The role of IL-22 and Th22 cells in human skin diseases. *J Dermatol Sci* 72:3-8.

Gagliani, N., C.F. Magnani, S. Huber, M.E. Gianolini, M. Pala, P. Licona-Limon, B. Guo, D.R. Herbert, A. Bulfone, F. Trentini, C. Di Serio, R. Bacchetta, M. Andreani, L. Brockmann, S. Gregori, R.A. Flavell, and M.G. Roncarolo. 2013. Coexpression of CD49b and LAG-3 identifies human and mouse T regulatory type 1 cells. *Nat Med* 19:739-746.

Gattinoni, L., E. Lugli, Y. Ji, Z. Pos, C.M. Paulos, M.F. Quigley, J.R. Almeida, E. Gostick, Z. Yu, C. Carpenito, E. Wang, D.C. Douek, D.A. Price, C.H. June, F.M. Marincola, M. Roederer, and N.P. Restifo. 2011. A human memory T cell subset with stem cell-like properties. *Nat Med* 17:1290-1297.

Ge, C., I.R. Monk, A. Pizzolla, N. Wang, J.G. Bedford, T.P. Stinear, G.P. Westall, and L.M. Wakim. 2019. Bystander Activation of Pulmonary Trm Cells Attenuates the Severity of Bacterial Pneumonia by Enhancing Neutrophil Recruitment. *Cell Rep* 29:4236-4244 e4233.

Gebhardt, T., L.M. Wakim, L. Eidsmo, P.C. Reading, W.R. Heath, and F.R. Carbone. 2009. Memory T cells in nonlymphoid tissue that provide enhanced local immunity during infection with herpes simplex virus. *Nature Immunology* 10:524-530.

Gebhardt, T., P.G. Whitney, A. Zaid, L.K. Mackay, A.G. Brooks, W.R. Heath, F.R. Carbone, and S.N. Mueller. 2011. Different patterns of peripheral migration by memory CD4+ and CD8+ T cells. *Nature* 477:216-219.

Gensollen, T., S.S. Iyer, D.L. Kasper, and R.S. Blumberg. 2016. How colonization by microbiota in early life shapes the immune system. *Science* 352:539-544.

Georgiev, P., L.M. Charbonnier, and T.A. Chatila. 2019. Regulatory T Cells: the Many Faces of Foxp3. *J Clin Immunol* 39:623-640.

Glennie, N.D., V.A. Yeramilli, D.P. Beiting, S.W. Volk, C.T. Weaver, and P. Scott. 2015. Skin-resident memory CD4+ T cells enhance protection against Leishmania major infection. *J Exp Med* 212:1405-1414.

Greiff, V., U. Menzel, U. Haessler, S.C. Cook, S. Friedensohn, T.A. Khan, M. Pogson, I. Hellmann, and S.T. Reddy. 2014. Quantitative assessment of the robustness of next-generation sequencing of antibody variable gene repertoires from immunized mice. *BMC Immunol* 15:40.

Greiff, V., E. Miho, U. Menzel, and S.T. Reddy. 2015. Bioinformatic and Statistical Analysis of Adaptive Immune Repertoires. *Trends Immunol* 36:738-749.

Gross, G.G., V.L. Schwartz, C. Stevens, E.C. Ebert, R.S. Blumberg, and S.P. Balk. 1994. Distribution of dominant T cell receptor beta chains in human intestinal mucosa. *J Exp Med* 180:1337-1344.

Gutzeit, C., G. Magri, and A. Cerutti. 2014. Intestinal IgA production and its role in host-microbe interaction. *Immunol Rev* 260:76-85.

Hagan, T., M. Cortese, N. Rouphael, C. Boudreau, C. Linde, M.S. Maddur, J. Das, H. Wang, J. Guthmiller, N.Y. Zheng, M. Huang, A.A. Uphadhyay, L. Gardinassi, C. Petitdemange, M.P. McCullough, S.J. Johnson, K. Gill, B. Cervasi, J. Zou, A. Bretin, M. Hahn, A.T. Gewirtz, S.E. Bosinger, P.C. Wilson, S. Li, G. Alter, S. Khurana, H. Golding, and B. Pulendran. 2019. Antibiotics-Driven Gut Microbiome Perturbation Alters Immunity to Vaccines in Humans. *Cell* 178:1313-1328 e1313.

Halle, S., O. Halle, and R. Forster. 2017. Mechanisms and Dynamics of T Cell-Mediated Cytotoxicity In Vivo. *Trends Immunol* 38:432-443.

Hapfelmeier, S., M.A. Lawson, E. Slack, J.K. Kirundi, M. Stoel, M. Heikenwalder, J. Cahenzli, Y. Velykoredko, M.L. Balmer, K. Endt, M.B. Geuking, R. Curtiss, 3rd, K.D. McCoy, and A.J. Macpherson. 2010. Reversible microbial colonization of germ-free mice reveals the dynamics of IgA immune responses. *Science* 328:1705-1709.

Hayday, A., E. Theodoridis, E. Ramsburg, and J. Shires. 2001. Intraepithelial lymphocytes: exploring the Third Way in immunology. *Nat Immunol* 2:997-1003.

Hayward, S.L., C.D. Scharer, E.K. Cartwright, S. Takamura, Z.T. Li, J.M. Boss, and J.E. Kohlmeier. 2020. Environmental cues regulate epigenetic reprogramming of airway-resident memory CD8(+) T cells. *Nat Immunol*

Henson, S.M., and A.N. Akbar. 2009. KLRG1--more than a marker for T cell senescence. *Age (Dordr)* 31:285-291.

Henson, S.M., O. Franzese, R. Macaulay, V. Libri, R.I. Azevedo, S. Kiani-Alikhan, F.J. Plunkett, J.E. Masters, S. Jackson, S.J. Griffiths, H.P. Pircher, M.V. Soares, and A.N. Akbar. 2009. KLRG1 signaling induces defective Akt (ser473) phosphorylation and proliferative dysfunction of highly differentiated CD8+ T cells. *Blood* 113:6619-6628.

Herndler-Brandstetter, D., H. Ishigame, R. Shinnakasu, V. Plajer, C. Stecher, J. Zhao, M. Lietzenmayer, L. Kroehling, A. Takumi, K. Kometani, T. Inoue, Y. Kluger, S.M. Kaech, T. Kurosaki, T. Okada, and R.A. Flavell. 2018. KLRG1(+) Effector CD8(+) T Cells Lose KLRG1, Differentiate into All Memory T Cell Lineages, and Convey Enhanced Protective Immunity. *Immunity* 48:716-729 e718.

Herzog, S., M. Reth, and H. Jumaa. 2009. Regulation of B-cell proliferation and differentiation by pre-B-cell receptor signalling. *Nat Rev Immunol* 9:195-205.

Homann, D., L. Teyton, and M.B. Oldstone. 2001. Differential regulation of antiviral T-cell immunity results in stable CD8+ but declining CD4+ T-cell memory. *Nat Med* 7:913-919.

Hombrink, P., C. Helbig, R.A. Backer, B. Piet, A.E. Oja, R. Stark, G. Brasser, A. Jongejan, R.E. Jonkers, B. Nota, O. Basak, H.C. Clevers, P.D. Moerland, D. Amsen, and R.A. van Lier. 2016. Programs for the persistence, vigilance and control of human CD8(+) lung-resident memory T cells. *Nat Immunol* 17:1467-1478.

Hondowicz, B.D., D. An, J.M. Schenkel, K.S. Kim, H.R. Steach, A.T. Krishnamurty, G.J. Keitany, E.N. Garza, K.A. Fraser, J.J. Moon, W.A. Altemeier, D. Masopust, and M. Pepper. 2016. Interleukin-2-Dependent Allergen-Specific Tissue-Resident Memory Cells Drive Asthma. *Immunity* 44:155-166.

Hondowicz, B.D., K.S. Kim, M.J. Ruterbusch, G.J. Keitany, and M. Pepper. 2018. IL-2 is required for the generation of viral-specific CD4(+) Th1 tissue-resident memory cells and B cells are essential for maintenance in the lung. *Eur J Immunol* 48:80-86.

Hooper, L.V., and A.J. Macpherson. 2010. Immune adaptations that maintain homeostasis with the intestinal microbiota. *Nat Rev Immunol* 10:159-169.

Horneland, R., V. Paulsen, J.P. Lindahl, K. Grzyb, T.J. Eide, K. Lundin, L. Aabakken, T. Jenssen, E.M. Aandahl, A. Foss, and O. Oyen. 2015. Pancreas transplantation with enteroanastomosis to native duodenum poses technical challenges--but offers improved endoscopic access for scheduled biopsies and therapeutic interventions. *Am J Transplant* 15:242-250.

Iborra, S., M. Martinez-Lopez, S.C. Khouili, M. Enamorado, F.J. Cueto, R. Conde-Garrosa, C. Del Fresno, and D. Sancho. 2016. Optimal Generation of Tissue-Resident but Not Circulating Memory T Cells during Viral Infection Requires Crosspriming by DNGR-1(+) Dendritic Cells. *Immunity* 45:847-860.

Iijima, N., and A. Iwasaki. 2014. T cell memory. A local macrophage chemokine network sustains protective tissue-resident memory CD4 T cells. *Science* 346:93-98.

Jabri, B., and E. Ebert. 2007. Human CD8+ intraepithelial lymphocytes: a unique model to study the regulation of effector cytotoxic T lymphocytes in tissue. *Immunol Rev* 215:202-214.

Jahnsen, F.L., E.S. Baekkevold, J.R. Hov, and O.J. Landsverk. 2018. Do Long-Lived Plasma Cells Maintain a Healthy Microbiota in the Gut? *Trends Immunol* 39:196-208.

Jameson, S.C. 2002. Maintaining the norm: T-cell homeostasis. *Nat Rev Immunol* 2:547-556.

Janeway, C.A., Jr. 1992. The immune system evolved to discriminate infectious nonself from noninfectious self. *Immunol Today* 13:11-16.

Jiang, X., R.A. Clark, L. Liu, A.J. Wagers, R.C. Fuhlbrigge, and T.S. Kupper. 2012. Skin infection generates non-migratory memory CD8+ T(RM) cells providing global skin immunity. *Nature* 483:227-231.

Joeris, T., K. Muller-Luda, W.W. Agace, and A.M. Mowat. 2017. Diversity and functions of intestinal mononuclear phagocytes. *Mucosal Immunol* 10:845-864.

Joshi, N.S., W. Cui, A. Chandele, H.K. Lee, D.R. Urso, J. Hagman, L. Gapin, and S.M. Kaech. 2007. Inflammation directs memory precursor and short-lived effector CD8(+) T cell fates via the graded expression of T-bet transcription factor. *Immunity* 27:281-295.

Kaech, S.M., and W. Cui. 2012. Transcriptional control of effector and memory CD8+ T cell differentiation. *Nat Rev Immunol* 12:749-761.

Kaech, S.M., E.J. Wherry, and R. Ahmed. 2002. Effector and memory T-cell differentiation: implications for vaccine development. *Nat Rev Immunol* 2:251-262.

Kamran, P., K.I. Sereti, P. Zhao, S.R. Ali, I.L. Weissman, and R. Ardehali. 2013. Parabiosis in mice: a detailed protocol. *J Vis Exp*

Kapsenberg, M.L. 2003. Dendritic-cell control of pathogen-driven T-cell polarization. *Nat Rev Immunol* 3:984-993.

Kim, K.S., S.W. Hong, D. Han, J. Yi, J. Jung, B.G. Yang, J.Y. Lee, M. Lee, and C.D. Surh. 2016. Dietary antigens limit mucosal immunity by inducing regulatory T cells in the small intestine. *Science* 351:858-863.

Kinnear, E., L. Lambert, J.U. McDonald, H.M. Cheeseman, L.J. Caproni, and J.S. Tregoning. 2018. Airway T cells protect against RSV infection in the absence of antibody. *Mucosal Immunol* 11:249-256.

Klein, J.R. 2004. T-cell activation in the curious world of the intestinal intraepithelial lymphocyte. *Immunol Res* 30:327-337.

Klicznik, M.M., P.A. Morawski, B. Höllbacher, S.R. Varkhande, S.J. Motley, L. Kuri-Cervantes, E. Goodwin, M.D. Rosenblum, S.A. Long, G. Brachtl, T. Duhen, M.R. Betts, D.J. Campbell, and I.K. Gratz. 2019. Human CD4+CD103+ cutaneous resident memory T cells are found in the circulation of healthy individuals. *Science Immunology* 4:

Klonowski, K.D., K.J. Williams, A.L. Marzo, D.A. Blair, E.G. Lingenheld, and L. Lefrançois. 2004. Dynamics of Blood-Borne CD8 Memory T Cell Migration In Vivo. *Immunity* 20:551-562.

Koch, S., N. Sopel, and S. Finotto. 2017. Th9 and other IL-9-producing cells in allergic asthma. *Semin Immunopathol* 39:55-68.

Konig, R., L.Y. Huang, and R.N. Germain. 1992. MHC class II interaction with CD4 mediated by a region analogous to the MHC class I binding site for CD8. *Nature* 356:796-798.

Kopf, M., M.F. Bachmann, and B.J. Marsland. 2010. Averting inflammation by targeting the cytokine environment. *Nat Rev Drug Discov* 9:703-718.

Kumar, B.V., T.J. Connors, and D.L. Farber. 2018a. Human T Cell Development, Localization, and Function throughout Life. *Immunity* 48:202-213.

Kumar, B.V., R. Kratchmarov, M. Miron, D.J. Carpenter, T. Senda, H. Lerner, A. Friedman, S.L. Reiner, and D.L. Farber. 2018b. Functional heterogeneity of human tissue-resident memory T cells based on dye efflux capacities. *JCI Insight* 3:

Kumar, B.V., W. Ma, M. Miron, T. Granot, R.S. Guyer, D.J. Carpenter, T. Senda, X. Sun, S.H. Ho, H. Lerner, A.L. Friedman, Y. Shen, and D.L. Farber. 2017. Human Tissue-Resident Memory T Cells Are Defined by Core Transcriptional and Functional Signatures in Lymphoid and Mucosal Sites. *Cell Rep* 20:2921-2934.

Kurd, N., and E.A. Robey. 2016. T-cell selection in the thymus: a spatial and temporal perspective. *Immunol Rev* 271:114-126.

Laidlaw, B.J., J.E. Craft, and S.M. Kaech. 2016. The multifaceted role of CD4(+) T cells in CD8(+) T cell memory. *Nat Rev Immunol* 16:102-111.

Laidlaw, B.J., N. Zhang, H.D. Marshall, M.M. Staron, T. Guan, Y. Hu, L.S. Cauley, J. Craft, and S.M. Kaech. 2014. CD4+ T cell help guides formation of CD103+ lung-resident memory CD8+ T cells during influenza viral infection. *Immunity* 41:633-645.

Lambrecht, B.N., and H. Hammad. 2003. The other cells in asthma: dendritic cell and epithelial cell crosstalk. *Curr Opin Pulm Med* 9:34-41.

Le Floc'h, A., A. Jalil, I. Vergnon, B. Le Maux Chansac, V. Lazar, G. Bismuth, S. Chouaib, and F. Mami-Chouaib. 2007. Alpha E beta 7 integrin interaction with E-cadherin promotes antitumor CTL activity by triggering lytic granule polarization and exocytosis. *J Exp Med* 204:559-570.

Lefranc, M.P. 2001. Nomenclature of the human T cell receptor genes. *Curr Protoc Immunol* Appendix 1:Appendix 1O.

Lefrancois, L., B. Fuller, J.W. Huleatt, S. Olson, and L. Puddington. 1997. On the front lines: Intraepithelial lymphocytes as primary effectors of intestinal immunity. *Springer Semin Immun* 18:463-475.

Lemke, A., M. Kraft, K. Roth, R. Riedel, D. Lammerding, and A.E. Hauser. 2016. Long-lived plasma cells are generated in mucosal immune responses and contribute to the bone marrow plasma cell pool in mice. *Mucosal Immunol* 9:83-97.

León, F., E. Roldán, L. Sanchez, C. Camarero, A. Bootello, and G. Roy. 2003. Human small-intestinal epithelium contains functional natural killer lymphocytes. *Gastroenterology* 125:345-356.

Li, P., R. Spolski, W. Liao, and W.J. Leonard. 2014. Complex interactions of transcription factors in mediating cytokine biology in T cells. *Immunol Rev* 261:141-156.

BIBLIOGRAPHY

Lian, C.G., E.M. Bueno, S.R. Granter, A.C. Laga, A.P. Saavedra, W.M. Lin, J.S. Susa, Q. Zhan, A.K. Chandraker, S.G. Tullius, B. Pomahac, and G.F. Murphy. 2014. Biomarker evaluation of face transplant rejection: association of donor T cells with target cell injury. *Mod Pathol* 27:788-799.

Lieberman, J. 2003. The ABCs of granule-mediated cytotoxicity: new weapons in the arsenal. *Nat Rev Immunol* 3:361-370.

Lu, Y.C., L. Jia, Z. Zheng, E. Tran, P.F. Robbins, and S.A. Rosenberg. 2019. Single-cell transcriptome analysis reveals gene signatures associated with T-cell persistence following adoptive cell therapy. *Cancer Immunol Res*

Lutter, L., D.P. Hoytema van Konijnenburg, E.C. Brand, B. Oldenburg, and F. van Wijk. 2018a. The elusive case of human intraepithelial T cells in gut homeostasis and inflammation. *Nat Rev Gastroenterol Hepatol* 15:637-649.

Lutter, L., J. Spierings, F.C.C. van Rhijn-Brouwer, J.M. van Laar, and F. van Wijk. 2018b. Resetting the T Cell Compartment in Autoimmune Diseases With Autologous Hematopoietic Stem Cell Transplantation: An Update. *Front Immunol* 9:767.

Ma, C.S., G.Y. Chew, N. Simpson, A. Priyadarshi, M. Wong, B. Grimbacher, D.A. Fulcher, S.G. Tangye, and M.C. Cook. 2008. Deficiency of Th17 cells in hyper IgE syndrome due to mutations in STAT3. *J Exp Med* 205:1551-1557.

Macallan, D.C., J.A. Borghans, and B. Asquith. 2017. Human T Cell Memory: A Dynamic View. *Vaccines (Basel)* 5:

MacDonald, T.T. 2008. The gut is still the biggest lymphoid organ in the body. *Mucosal Immunology* 1:246-247.

Mackay, L.K., A. Braun, B.L. Macleod, N. Collins, C. Tebartz, S. Bedoui, F.R. Carbone, and T. Gebhardt. 2015a. Cutting edge: CD69 interference with sphingosine-1-phosphate receptor function regulates peripheral T cell retention. *J Immunol* 194:2059-2063.

Mackay, L.K., and A. Kallies. 2017. Transcriptional Regulation of Tissue-Resident Lymphocytes. *Trends Immunol* 38:94-103.

Mackay, L.K., M. Minnich, N.A. Kragten, Y. Liao, B. Nota, C. Seillet, A. Zaid, K. Man, S. Preston, D. Freestone, A. Braun, E. Wynne-Jones, F.M. Behr, R. Stark, D.G. Pellicci, D.I. Godfrey, G.T. Belz, M. Pellegrini, T. Gebhardt, M. Busslinger, W. Shi, F.R. Carbone, R.A. van Lier, A. Kallies, and K.P. van Gisbergen. 2016. Hobit and Blimp1 instruct a universal transcriptional program of tissue residency in lymphocytes. *Science* 352:459-463.

Mackay, L.K., A. Rahimpour, J.Z. Ma, N. Collins, A.T. Stock, M.L. Hafon, J. Vega-Ramos, P. Lauzurica, S.N. Mueller, T. Stefanovic, D.C. Tscharke, W.R. Heath, M. Inouye, F.R. Carbone, and T. Gebhardt. 2013. The developmental pathway for CD103(+)CD8+ tissue-resident memory T cells of skin. *Nat Immunol* 14:1294-1301.

Mackay, L.K., E. Wynne-Jones, D. Freestone, D.G. Pellicci, L.A. Mielke, D.M. Newman, A. Braun, F. Masson, A. Kallies, G.T. Belz, and F.R. Carbone. 2015b. T-box Transcription Factors Combine with the Cytokines TGF-beta and IL-15 to Control Tissue-Resident Memory T Cell Fate. *Immunity* 43:1101-1111.

Mahnke, Y.D., T.M. Brodie, F. Sallusto, M. Roederer, and E. Lugli. 2013. The who's who of T-cell differentiation: human memory T-cell subsets. *Eur J Immunol* 43:2797-2809.

Malik, B.T., K.T. Byrne, J.L. Vella, P. Zhang, T.B. Shabaneh, S.M. Steinberg, A.K. Molodtsov, J.S. Bowers, C.V. Angeles, C.M. Paulos, Y.H. Huang, and M.J. Turk. 2017. Resident memory T cells in the skin mediate durable immunity to melanoma. *Sci Immunol* 2:

Maloy, K.J., and M.C. Kullberg. 2008. IL-23 and Th17 cytokines in intestinal homeostasis. *Mucosal Immunol* 1:339-349.

Mani, V., S.K. Bromley, T. Aijo, R. Mora-Buch, E. Carrizosa, R.D. Warner, M. Hamze, D.R. Sen, A.Y. Chasse, A. Lorant, J.W. Griffith, R.A. Rahimi, C.P. McEntee, K.L. Jeffrey, F. Marangoni, M.A. Travis, A. Lacy-Hulbert, A.D. Luster, and T.R. Mempel. 2019. Migratory DCs activate TGF-beta to precondition naive CD8(+) T cells for tissue-resident memory fate. *Science* 366:

Marsal, J., and W.W. Agace. 2012. Targeting T-cell migration in inflammatory bowel disease. *J Intern Med* 272:411-429.

Martinez-Lopez, M., S. Iborra, R. Conde-Garrosa, A. Mastrangelo, C. Danne, E.R. Mann, D.M. Reid, V. Gaboriau-Routhiau, M. Chaparro, M.P. Lorenzo, L. Minnerup, P. Saz-Leal, E. Slack, B. Kemp, J.P. Gisbert, A. Dzionek, M.J. Robinson, F.J. Ruperez, N. Cerf-Bensussan, G.D. Brown, D. Bernardo, S. LeibundGut-Landmann, and D. Sancho. 2019. Microbiota Sensing by Mincle-Syk Axis in Dendritic

Cells Regulates Interleukin-17 and -22 Production and Promotes Intestinal Barrier Integrity. *Immunity* 50:446-461 e449.

Masopust, D., D. Choo, V. Vezys, E.J. Wherry, J. Duraiswamy, R. Akondy, J. Wang, K.A. Casey, D.L. Barber, K.S. Kawamura, K.A. Fraser, R.J. Webby, V. Brinkmann, E.C. Butcher, K.A. Newell, and R. Ahmed. 2010. Dynamic T cell migration program provides resident memory within intestinal epithelium. *Journal of Experimental Medicine* 207:553-564.

Masopust, D., K. Murali-Krishna, and R. Ahmed. 2007. Quantitating the magnitude of the lymphocytic choriomeningitis virus-specific CD8 T-cell response: it is even bigger than we thought. *J Virol* 81:2002-2011.

Masopust, D., and A.G. Soerens. 2019. Tissue-Resident T Cells and Other Resident Leukocytes. *Annu Rev Immunol*

Masopust, D., V. Vezys, A.L. Marzo, and L. Lefrancois. 2001. Preferential localization of effector memory cells in nonlymphoid tissue. *Science* 291:2413-2417.

Masopust, D., V. Vezys, E.J. Wherry, D.L. Barber, and R. Ahmed. 2006. Cutting edge: gut microenvironment promotes differentiation of a unique memory CD8 T cell population. *J Immunol* 176:2079-2083.

Mattioli, C.A., and T.B. Tomasi, Jr. 1973. The life span of IgA plasma cells from the mouse intestine. *J Exp Med* 138:452-460.

Matzinger, P. 2002. The danger model: a renewed sense of self. *Science* 296:301-305.

Mayassi, T., and B. Jabri. 2018. Human intraepithelial lymphocytes. *Mucosal Immunol* 11:1281-1289.

Mazzini, E., L. Massimiliano, G. Penna, and M. Rescigno. 2014. Oral tolerance can be established via gap junction transfer of fed antigens from CX3CR1(+) macrophages to CD103(+) dendritic cells. *Immunity* 40:248-261.

McDonald, B.D., B. Jabri, and A. Bendelac. 2018. Diverse developmental pathways of intestinal intraepithelial lymphocytes. *Nat Rev Immunol* 18:514-525.

Medzhitov, R., and C.A. Janeway, Jr. 2002. Decoding the patterns of self and nonself by the innate immune system. *Science* 296:298-300.

Milner, J.J., C. Toma, B. Yu, K. Zhang, K. Omilusik, A.T. Phan, D. Wang, A.J. Getzler, T. Nguyen, S. Crotty, W. Wang, M.E. Pipkin, and A.W. Goldrath. 2017. Runx3 programs CD8(+) T cell residency in non-lymphoid tissues and tumours. *Nature* 552:253-257.

Moor, A.E., Y. Harnik, S. Ben-Moshe, E.E. Massasa, M. Rozenberg, R. Eilam, K. Bahar Halpern, and S. Itzkovitz. 2018. Spatial Reconstruction of Single Enterocytes Uncovers Broad Zonation along the Intestinal Villus Axis. *Cell* 175:1156-1167 e1115.

Morabito, K.M., T.R. Ruckwardt, A.J. Redwood, S.M. Moin, D.A. Price, and B.S. Graham. 2017. Intranasal administration of RSV antigen-expressing MCMV elicits robust tissue-resident effector and effector memory CD8+ T cells in the lung. *Mucosal Immunol* 10:545-554.

Morris, S.E., D.L. Farber, and A.J. Yates. 2019. Tissue-Resident Memory T Cells in Mice and Humans: Towards a Quantitative Ecology. *J Immunol* 203:2561-2569.

Moskowitz, D.M., D.W. Zhang, B. Hu, S. Le Saux, R.E. Yanes, Z. Ye, J.D. Buenrostro, C.M. Weyand, W.J. Greenleaf, and J.J. Goronzy. 2017. Epigenomics of human CD8 T cell differentiation and aging. *Sci Immunol* 2:

Mosmann, T.R., and R.L. Coffman. 1989. TH1 and TH2 cells: different patterns of lymphokine secretion lead to different functional properties. *Annu Rev Immunol* 7:145-173.

Mowat, A.M. 2003. Anatomical basis of tolerance and immunity to intestinal antigens. *Nat Rev Immunol* 3:331-341.

Mowat, A.M. 2018. To respond or not to respond - a personal perspective of intestinal tolerance. *Nat Rev Immunol* 18:405-415.

Mowat, A.M., and W.W. Agace. 2014. Regional specialization within the intestinal immune system. *Nat Rev Immunol* 14:667-685.

Mucida, D., and H. Cheroutre. 2010. The many face-lifts of CD4 T helper cells. *Adv Immunol* 107:139-152.

Mueller, S.N., T. Gebhardt, F.R. Carbone, and W.R. Heath. 2013. Memory T cell subsets, migration patterns, and tissue residence. *Annu Rev Immunol* 31:137-161.

Mueller, S.N., and L.K. Mackay. 2016. Tissue-resident memory T cells: local specialists in immune defence. *Nat Rev Immunol* 16:79-89.

Mullard, A. 2018. Oncologists tap the microbiome in bid to improve immunotherapy outcomes. *Nat Rev Drug Discov* 17:153-155.

Muller, S., M. Buhler-Jungo, and C. Mueller. 2000. Intestinal intraepithelial lymphocytes exert potent protective cytotoxic activity during an acute virus infection. *J Immunol* 164:1986-1994.

Murphy, K.M., and S.L. Reiner. 2002. The lineage decisions of helper T cells. *Nat Rev Immunol* 2:933-944.

Murphy, K.M., and B. Stockinger. 2010. Effector T cell plasticity: flexibility in the face of changing circumstances. *Nat Immunol* 11:674-680.

Muruganandah, V., H.D. Sathkumara, S. Navarro, and A. Kupz. 2018. A Systematic Review: The Role of Resident Memory T Cells in Infectious Diseases and Their Relevance for Vaccine Development. *Front Immunol* 9:1574.

Nair, N., E.W. Newell, C. Vollmers, S.R. Quake, J.M. Morton, M.M. Davis, X.S. He, and H.B. Greenberg. 2016. High-dimensional immune profiling of total and rotavirus VP6-specific intestinal and circulating B cells by mass cytometry. *Mucosal Immunol* 9:68-82.

Napier, R.J., E.J. Adams, M.C. Gold, and D.M. Lewinsohn. 2015. The Role of Mucosal Associated Invariant T Cells in Antimicrobial Immunity. *Front Immunol* 6:344.

Nazarov, V.I., M.V. Pogorelyy, E.A. Komech, I.V. Zvyagin, D.A. Bolotin, M. Shugay, D.M. Chudakov, Y.B. Lebedev, and I.Z. Mamedov. 2015. tcR: an R package for T cell receptor repertoire advanced data analysis. *BMC Bioinformatics* 16:175.

Nemazee, D. 2017. Mechanisms of central tolerance for B cells. *Nat Rev Immunol* 17:281-294.

Netea, M.G., and L.A.B. Joosten. 2018. Trained Immunity and Local Innate Immune Memory in the Lung. *Cell* 175:1463-1465.

Nizard, M., H. Roussel, M.O. Diniz, S. Karaki, T. Tran, T. Voron, E. Dransart, F. Sandoval, M. Riquet, B. Rance, E. Marcheteau, E. Fabre, M. Mandavit, M. Terme, C. Blanc, J.B. Escudie, L. Gibault, F.L.P. Barthes, C. Granier, L.C.S. Ferreira, C. Badoual, L. Johannes, and E. Tartour. 2017. Induction of resident memory T cells enhances the efficacy of cancer vaccine. *Nat Commun* 8:15221.

Noble, A., L. Durant, L. Hoyles, A.L. McCartney, R. Man, J. Segal, S.P. Costello, P. Hendy, D. Reddi, S. Bouri, D.N.F. Lim, T. Pring, M.J. O'Connor, P. Datt, A. Wilson, N. Arebi, A. Akbar, A.L. Hart, S.R. Carding, and S.C. Knight. 2019. Deficient Resident Memory T-Cell and Cd8 T-Cell Response to Commensals in Inflammatory Bowel Disease. *J Crohns Colitis*

Nordheim, E., R. Horneland, E.M. Aandahl, K. Grzyb, L. Aabakken, V. Paulsen, K. Midtvedt, A. Hartmann, and T. Jenssen. 2018. Pancreas transplant rejection episodes are not revealed by biopsies of the donor duodenum in a prospective study with paired biopsies. *Am J Transplant* 18:1256-1261.

Oja, A.E., B. Piet, C. Helbig, R. Stark, D. van der Zwan, H. Blaauwgeers, E.B.M. Remmerswaal, D. Amsen, R.E. Jonkers, P.D. Moerland, M.A. Nolte, R.A.W. van Lier, and P. Hombrink. 2018. Trigger-happy resident memory CD4(+) T cells inhabit the human lungs. *Mucosal Immunol* 11:654-667.

Olsen, I., and L.M. Sollid. 2013. Pitfalls in determining the cytokine profile of human T cells. *J Immunol Methods* 390:106-112.

Ott, P.A., Z. Hu, D.B. Keskin, S.A. Shukla, J. Sun, D.J. Bozym, W. Zhang, A. Luoma, A. Giobbie-Hurder, L. Peter, C. Chen, O. Olive, T.A. Carter, S. Li, D.J. Lieb, T. Eisenhaure, E. Gjini, J. Stevens, W.J. Lane, I. Javeri, K. Nellaiappan, A.M. Salazar, H. Daley, M. Seaman, E.I. Buchbinder, C.H. Yoon, M. Harden, N. Lennon, S. Gabriel, S.J. Rodig, D.H. Barouch, J.C. Aster, G. Getz, K. Wucherpfennig, D. Neuberg, J. Ritz, E.S. Lander, E.F. Fritsch, N. Hacohen, and C.J. Wu. 2017. An immunogenic personal neoantigen vaccine for patients with melanoma. *Nature* 547:217-221.

Pabst, O., and E. Slack. 2019. IgA and the intestinal microbiota: the importance of being specific. *Mucosal Immunology*

Pabst, R., M.W. Russell, and P. Brandtzaeg. 2008. Tissue distribution of lymphocytes and plasma cells and the role of the gut. *Trends Immunol* 29:206-208; author reply 209-210.

Pallett, L.J., J. Davies, E.J. Colbeck, F. Robertson, N. Hansi, N.J.W. Easom, A.R. Burton, K.A. Stegmann, A. Schurich, L. Swadling, U.S. Gill, V. Male, T. Luong, A. Gander, B.R. Davidson, P.T.F. Kennedy, and M.K. Maini. 2017. IL-2(high) tissue-resident T cells in the human liver: Sentinels for hepatotropic infection. *J Exp Med* 214:1567-1580.

Park, C.O., X. Fu, X. Jiang, Y. Pan, J.E. Teague, N. Collins, T. Tian, J.T. O'Malley, R.O. Emerson, J.H. Kim, Y. Jung, R. Watanabe, R.C. Fuhlbrigge, F.R. Carbone, T. Gebhardt, R.A. Clark, C.P. Lin, and T.S. Kupper. 2018a. Staged development of long-lived T-cell receptor alphabeta TH17 resident memory T-cell population to Candida albicans after skin infection. *J Allergy Clin Immunol* 142:647-662.

Park, C.O., and T.S. Kupper. 2015. The emerging role of resident memory T cells in protective immunity and inflammatory disease. *Nat Med* 21:688-697.

Park, S.L., A. Buzzai, J. Rautela, J.L. Hor, K. Hochheiser, M. Effern, N. McBain, T. Wagner, J. Edwards, R. McConville, J.S. Wilmott, R.A. Scolyer, T. Tuting, U. Palendria, D. Gyorki, S.N. Mueller, N.D.

Huntington, S. Bedoui, M. Holzel, L.K. Mackay, J. Waithman, and T. Gebhardt. 2018b. Tissue-resident memory CD8(+) T cells promote melanoma-immune equilibrium in skin. *Nature*

Park, S.L., T. Gebhardt, and L.K. Mackay. 2019. Tissue-Resident Memory T Cells in Cancer Immunosurveillance. *Trends Immunol* 40:735-747.

Park, S.L., and L.K. Mackay. 2017. PD-1: always on my mind. *Immunol Cell Biol* 95:857-858.

Park, S.L., A. Zaid, J.L. Hor, S.N. Christo, J.E. Prier, B. Davies, Y.O. Alexandre, J.L. Gregory, T.A. Russell, T. Gebhardt, F.R. Carbone, D.C. Tscharke, W.R. Heath, S.N. Mueller, and L.K. Mackay. 2018c. Local proliferation maintains a stable pool of tissue-resident memory T cells after antiviral recall responses. *Nat Immunol* 19:183-191.

Paul, W.E., and J. Zhu. 2010. How are T(H)2-type immune responses initiated and amplified? *Nat Rev Immunol* 10:225-235.

Pepper, M., J.L. Linehan, A.J. Pagan, T. Zell, T. Dileepan, P.P. Cleary, and M.K. Jenkins. 2010. Different routes of bacterial infection induce long-lived TH1 memory cells and short-lived TH17 cells. *Nat Immunol* 11:83-89.

Petitdemange, C., S.P. Kasturi, P.A. Kozlowski, R. Nabi, C.F. Quarnstrom, P.B.J. Reddy, C.A. Derdeyn, L.M. Spicer, P. Patel, T. Legere, Y.O. Kovalenkov, C.C. Labranche, F. Villinger, M. Tomai, J. Vasilakos, B. Haynes, C.Y. Kang, J.S. Gibbs, J.W. Yewdell, D. Barouch, J. Wrammert, D. Montefiori, E. Hunter, R.R. Amara, D. Masopust, and B. Pulendran. 2019. Vaccine induction of antibodies and tissue-resident CD8+ T cells enhances protection against mucosal SHIV-infection in young macaques. *JCI Insight* 4:

Piet, B., G.J. de Bree, B.S. Smids-Dierdorp, C.M. van der Loos, E.B. Remmerswaal, J.H. von der Thusen, J.M. van Haarst, J.P. Eerenberg, A. ten Brinke, W. van der Bij, W. Timens, R.A. van Lier, and R.E. Jonkers. 2011. CD8(+) T cells with an intraepithelial phenotype upregulate cytotoxic function upon influenza infection in human lung. *J Clin Invest* 121:2254-2263.

Qi, Q., Y. Liu, Y. Cheng, J. Glanville, D. Zhang, J.Y. Lee, R.A. Olshen, C.M. Weyand, S.D. Boyd, and J.J. Goronzy. 2014. Diversity and clonal selection in the human T-cell repertoire. *Proc Natl Acad Sci U S A* 111:13139-13144.

Raki, M., A.C. Beitnes, K.E. Lundin, J. Jahnsen, F.L. Jahnsen, and L.M. Sollid. 2013. Plasmacytoid dendritic cells are scarcely represented in the human gut mucosa and are not recruited to the celiac lesion. *Mucosal Immunol* 6:985-992.

Reese, T.A., K. Bi, A. Kambal, A. Filali-Mouhim, L.K. Beura, M.C. Burger, B. Pulendran, R.P. Sekaly, S.C. Jameson, D. Masopust, W.N. Haining, and H.W. Virgin. 2016. Sequential Infection with Common Pathogens Promotes Human-like Immune Gene Expression and Altered Vaccine Response. *Cell Host Microbe* 19:713-719.

Reinhardt, R.L., A. Khoruts, R. Merica, T. Zell, and M.K. Jenkins. 2001. Visualizing the generation of memory CD4 T cells in the whole body. *Nature* 410:101-105.

Rescigno, M. 2014. Dendritic cell-epithelial cell crosstalk in the gut. *Immunol Rev* 260:118-128.

Restifo, N.P., and L. Gattinoni. 2013. Lineage relationship of effector and memory T cells. *Curr Opin Immunol* 25:556-563.

Richter, L., O.J.B. Landsverk, N. Atlasy, A. Bujko, S. Yaqub, R. Horneland, O. Oyen, E.M. Aandahl, K.E.A. Lundin, H.G. Stunnenberg, E.S. Baekkevold, and F.L. Jahnsen. 2018. Transcriptional profiling reveals monocyte-related macrophages phenotypically resembling DC in human intestine. *Mucosal Immunol*

Risnes, L.F., A. Christophersen, S. Dahal-Koirala, R.S. Neumann, G.K. Sandve, V.K. Sarna, K.E. Lundin, S.W. Qiao, and L.M. Sollid. 2018. Disease-driving CD4+ T cell clonotypes persist for decades in celiac disease. *J Clin Invest* 128:2642-2650.

Robertson, R.C., A.R. Manges, B.B. Finlay, and A.J. Prendergast. 2019. The Human Microbiome and Child Growth - First 1000 Days and Beyond. *Trends Microbiol* 27:131-147.

Roche, P.A., and K. Furuta. 2015. The ins and outs of MHC class II-mediated antigen processing and presentation. *Nat Rev Immunol* 15:203-216.

Romagnoli, P.A., H.H. Fu, Z. Qiu, C. Khairallah, Q.M. Pham, L. Puddington, K.M. Khanna, L. Lefrancois, and B.S. Sheridan. 2017. Differentiation of distinct long-lived memory CD4 T cells in intestinal tissues after oral Listeria monocytogenes infection. *Mucosal Immunol* 10:520-530.

Roncarolo, M.G., and S. Gregori. 2008. Is FOXP3 a bona fide marker for human regulatory T cells? *Eur J Immunol* 38:925-927.

Roncarolo, M.G., S. Gregori, M. Battaglia, R. Bacchetta, K. Fleischhauer, and M.K. Levings. 2006. Interleukin-10-secreting type 1 regulatory T cells in rodents and humans. *Immunol Rev* 212:28-50.

Rosato, P.C., L.K. Beura, and D. Masopust. 2017. Tissue resident memory T cells and viral immunity. *Curr Opin Virol* 22:44-50.

Rosato, P.C., S. Wijeyesinghe, J.M. Stolley, C.E. Nelson, R.L. Davis, L.S. Manlove, C.A. Pennell, B.R. Blazar, C.C. Chen, M.A. Geller, V. Vezys, and D. Masopust. 2019. Virus-specific memory T cells populate tumors and can be repurposed for tumor immunotherapy. *Nat Commun* 10:567.

Rosshart, S., M. Hofmann, O. Schweier, A.K. Pfaff, K. Yoshimoto, T. Takeuchi, E. Molnar, W.W. Schamel, and H. Pircher. 2008. Interaction of KLRG1 with E-cadherin: new functional and structural insights. *Eur J Immunol* 38:3354-3364.

Rovedatti, L., T. Kudo, P. Biancheri, M. Sarra, C.H. Knowles, D.S. Rampton, G.R. Corazza, G. Monteleone, A. Di Sabatino, and T.T. Macdonald. 2009. Differential regulation of interleukin 17 and interferon gamma production in inflammatory bowel disease. *Gut* 58:1629-1636.

Rudd, B.D., V. Venturi, M.P. Davenport, and J. Nikolich-Zugich. 2011. Evolution of the antigen-specific CD8+ TCR repertoire across the life span: evidence for clonal homogenization of the old TCR repertoire. *J Immunol* 186:2056-2064.

Ruiz, P., H. Takahashi, V. Delacruz, E. Island, G. Selvaggi, S. Nishida, J. Moon, L. Smith, T. Asaoka, D. Levi, A. Tekin, and A.G. Tzakis. 2010. International grading scheme for acute cellular rejection in small-bowel transplantation: single-center experience. *Transplant Proc* 42:47-53.

Russell, G.J., C.M. Parker, A. Sood, E. Mizoguchi, E.C. Ebert, A.K. Bhan, and M.B. Brenner. 1996. p126 (CDw101), a costimulatory molecule preferentially expressed on mucosal T lymphocytes. *J Immunol* 157:3366-3374.

Ruthlein, J., G. Heinze, and I.O. Auer. 1992. Anti-CD2 and anti-CD3 induced T cell cytotoxicity of human intraepithelial and lamina propria lymphocytes. *Gut* 33:1626-1632.

Sakaguchi, S., T. Yamaguchi, T. Nomura, and M. Ono. 2008. Regulatory T cells and immune tolerance. *Cell* 133:775-787.

Sakai, S., K.D. Kauffman, J.M. Schenkel, C.C. McBerry, K.D. Mayer-Barber, D. Masopust, and D.L. Barber. 2014. Cutting edge: control of Mycobacterium tuberculosis infection by a subset of lung parenchyma-homing CD4 T cells. *J Immunol* 192:2965-2969.

Sallusto, F. 2016. Heterogeneity of Human CD4(+) T Cells Against Microbes. *Annu Rev Immunol* 34:317-334.

Sallusto, F., D. Lenig, R. Forster, M. Lipp, and A. Lanzavecchia. 1999. Two subsets of memory T lymphocytes with distinct homing potentials and effector functions. *Nature* 401:708-712.

Sancho, D., M. Gomez, and F. Sanchez-Madrid. 2005. CD69 is an immunoregulatory molecule induced following activation. *Trends Immunol* 26:136-140.

Sasson, S.C., C.L. Gordon, S.N. Christo, P. Klenerman, and L.K. Mackay. 2020. Local heroes or villains: tissue-resident memory T cells in human health and disease. *Cellular & Molecular Immunology*

Sathaliyawala, T., M. Kubota, N. Yudanin, D. Turner, P. Camp, J.J. Thome, K.L. Bickham, H. Lerner, M. Goldstein, M. Sykes, T. Kato, and D.L. Farber. 2013. Distribution and compartmentalization of human circulating and tissue-resident memory T cell subsets. *Immunity* 38:187-197.

Schattgen, S.A., J.C. Crawford, L.-A. Van de Velde, H. Chu, S.K. Mazmanian, P. Bradley, and P.G. Thomas. 2019. Intestinal Intraepithelial Lymphocyte Repertoires are Imprinted Clonal Structures Selected for MHC Reactivity. *Immunity* D-19:

Schatz, D.G., and Y. Ji. 2011. Recombination centres and the orchestration of V(D)J recombination. *Nat Rev Immunol* 11:251-263.

Schenkel, J.M., K.A. Fraser, L.K. Beura, K.E. Pauken, V. Vezys, and D. Masopust. 2014. Resident memory CD8 T cells trigger protective innate and adaptive immune responses. *Science* 1254536.

Schenkel, J.M., K.A. Fraser, K.A. Casey, L.K. Beura, K.E. Pauken, V. Vezys, and D. Masopust. 2016. IL-15-Independent Maintenance of Tissue-Resident and Boosted Effector Memory CD8 T Cells. *J Immunol* 196:3920-3926.

Schenkel, J.M., K.A. Fraser, V. Vezys, and D. Masopust. 2013. Sensing and alarm function of resident memory CD8(+) T cells. *Nat Immunol* 14:509-513.

Schenkel, J.M., and D. Masopust. 2014. Tissue-resident memory T cells. *Immunity* 41:886-897.

Schlissel, M.S. 2003. Regulating antigen-receptor gene assembly. *Nat Rev Immunol* 3:890-899.

Schon, M.P., A. Arya, E.A. Murphy, C.M. Adams, U.G. Strauch, W.W. Agace, J. Marsal, J.P. Donohue, H. Her, D.R. Beier, S. Olson, L. Lefrancois, M.B. Brenner, M.J. Grusby, and C.M. Parker. 1999.

Mucosal T lymphocyte numbers are selectively reduced in integrin alpha E (CD103)-deficient mice. *J Immunol* 162:6641-6649.

Schroeder, H.W., Jr., and L. Cavacini. 2010. Structure and function of immunoglobulins. *J Allergy Clin Immunol* 125:S41-52.

Schulz, O., and O. Pabst. 2013. Antigen sampling in the small intestine. *Trends Immunol* 34:155-161.

Schwartzkopff, S., S. Woyciechowski, U. Aichele, T. Flecken, N. Zhang, R. Thimme, and H. Pircher. 2015. TGF-beta downregulates KLRG1 expression in mouse and human CD8(+) T cells. *Eur J Immunol* 45:2212-2217.

Sedda, S., I. Marafini, M.M. Figliuzzi, F. Pallone, and G. Monteleone. 2014. An overview of the role of innate lymphoid cells in gut infections and inflammation. *Mediators Inflamm* 2014:235460.

Seder, R.A., and R. Ahmed. 2003. Similarities and differences in CD4+ and CD8+ effector and memory T cell generation. *Nat Immunol* 4:835-842.

Seder, R.A., P.A. Darrah, and M. Roederer. 2008. T-cell quality in memory and protection: implications for vaccine design. *Nat Rev Immunol* 8:247-258.

Sewell, A.K. 2012. Why must T cells be cross-reactive? *Nat Rev Immunol* 12:669-677.

Shale, M., C. Schiering, and F. Powrie. 2013. CD4(+) T-cell subsets in intestinal inflammation. *Immunol Rev* 252:164-182.

Shapiro, H.M. 2005. Practical Flow Cytometry. Wiley, 736 pp.

Sheridan, B.S., and L. Lefrancois. 2010. Intraepithelial lymphocytes: to serve and protect. *Curr Gastroenterol Rep* 12:513-521.

Sheridan, B.S., Q.M. Pham, Y.T. Lee, L.S. Cauley, L. Puddington, and L. Lefrancois. 2014. Oral infection drives a distinct population of intestinal resident memory CD8(+) T cells with enhanced protective function. *Immunity* 40:747-757.

Shin, H., and A. Iwasaki. 2012. A vaccine strategy that protects against genital herpes by establishing local memory T cells. *Nature* 491:463-467.

Shiow, L.R., D.B. Rosen, N. Brdickova, Y. Xu, J. An, L.L. Lanier, J.G. Cyster, and M. Matloubian. 2006. CD69 acts downstream of interferon-alpha/beta to inhibit S1P1 and lymphocyte egress from lymphoid organs. *Nature* 440:540-544.

Shwetank, H.A. Abdelsamed, E.L. Frost, H.M. Schmitz, T.E. Mockus, B.A. Youngblood, and A.E. Lukacher. 2017. Maintenance of PD-1 on brain-resident memory CD8 T cells is antigen independent. *Immunol Cell Biol* 95:953-959.

Simoni, Y., E. Becht, M. Fehlings, C.Y. Loh, S.L. Koo, K.W.W. Teng, J.P.S. Yeong, R. Nahar, T. Zhang, H. Kared, K. Duan, N. Ang, M. Poidinger, Y.Y. Lee, A. Larbi, A.J. Khng, E. Tan, C. Fu, R. Mathew, M. Teo, W.T. Lim, C.K. Toh, B.H. Ong, T. Koh, A.M. Hillmer, A. Takano, T.K.H. Lim, E.H. Tan, W. Zhai, D.S.W. Tan, I.B. Tan, and E.W. Newell. 2018. Bystander CD8(+) T cells are abundant and phenotypically distinct in human tumour infiltrates. *Nature* 557:575-579.

Singh, K., M. Hjort, L. Thorvaldson, and S. Sandler. 2015. Concomitant analysis of Helios and Neuropilin-1 as a marker to detect thymic derived regulatory T cells in naive mice. *Sci Rep* 5:7767.

Skinner, J. 2018. Statistics for Immunologists. *Curr Protoc Immunol* 122:54.

Skon, C.N., J.Y. Lee, K.G. Anderson, D. Masopust, K.A. Hogquist, and S.C. Jameson. 2013. Transcriptional downregulation of S1pr1 is required for the establishment of resident memory CD8(+) T cells. *Nature Immunology* 14:1285-+.

Smith, N.M., G.A. Wasserman, F.T. Coleman, K.L. Hilliard, K. Yamamoto, E. Lipsitz, R. Malley, H. Dooms, M.R. Jones, L.J. Quinton, and J.P. Mizgerd. 2018. Regionally compartmentalized resident memory T cells mediate naturally acquired protection against pneumococcal pneumonia. *Mucosal Immunol* 11:220-235.

Smolders, J., K.M. Heutinck, N.L. Fransen, E.B.M. Remmerswaal, P. Hombrink, I.J.M. Ten Berge, R.A.W. van Lier, I. Huitinga, and J. Hamann. 2018. Tissue-resident memory T cells populate the human brain. *Nat Commun* 9:4593.

Snir, O., L. Mesin, M. Gidoni, K.E. Lundin, G. Yaari, and L.M. Sollid. 2015. Analysis of celiac disease autoreactive gut plasma cells and their corresponding memory compartment in peripheral blood using high-throughput sequencing. *J Immunol* 194:5703-5712.

Snyder, M.E., M.O. Finlayson, T.J. Connors, P. Dogra, T. Senda, E. Bush, D. Carpenter, C. Marboe, L. Benvenuto, L. Shah, H. Robbins, J.L. Hook, M. Sykes, F. D'Ovidio, M. Bacchetta, J.R. Sonett, D.J. Lederer, S. Arcasoy, P.A. Sims, and D.L. Farber. 2019. Generation and persistence of human tissue-resident memory T cells in lung transplantation. *Sci Immunol* 4:

Sorini, C., R.F. Cardoso, N. Gagliani, and E.J. Villablanca. 2018. Commensal Bacteria-Specific CD4(+) T Cell Responses in Health and Disease. *Front Immunol* 9:2667.

Spalding, K.L., E. Arner, P.O. Westermark, S. Bernard, B.A. Buchholz, O. Bergmann, L. Blomqvist, J. Hoffstedt, E. Naslund, T. Britton, H. Concha, M. Hassan, M. Ryden, J. Frisen, and P. Arner. 2008. Dynamics of fat cell turnover in humans. *Nature* 453:783-787.

Spalding, K.L., O. Bergmann, K. Alkass, S. Bernard, M. Salehpour, H.B. Huttner, E. Bostrom, I. Westerlund, C. Vial, B.A. Buchholz, G. Possnert, D.C. Mash, H. Druid, and J. Frisen. 2013. Dynamics of hippocampal neurogenesis in adult humans. *Cell* 153:1219-1227.

Spalding, K.L., R.D. Bhardwaj, B.A. Buchholz, H. Druid, and J. Frisen. 2005. Retrospective birth dating of cells in humans. *Cell* 122:133-143.

Spencer, J., and L.M. Sollid. 2016. The human intestinal B-cell response. *Mucosal Immunol* 9:1113-1124.

Spits, H. 2002. Development of alphabeta T cells in the human thymus. *Nat Rev Immunol* 2:760-772.

Stary, G., A. Olive, A.F. Radovic-Moreno, D. Gondek, D. Alvarez, P.A. Basto, M. Perro, V.D. Vrbanac, A.M. Tager, J. Shi, J.A. Yethon, O.C. Farokhzad, R. Langer, M.N. Starnbach, and U.H. von Andrian. 2015. VACCINES. A mucosal vaccine against Chlamydia trachomatis generates two waves of protective memory T cells. *Science* 348:aaa8205.

Steinbach, K., I. Vincenti, M. Kreutzfeldt, N. Page, A. Muschaweckh, I. Wagner, I. Drexler, D. Pinschewer, T. Korn, and D. Merkler. 2016. Brain-resident memory T cells represent an autonomous cytotoxic barrier to viral infection. *J Exp Med* 213:1571-1587.

Steinert, E.M., J.M. Schenkel, K.A. Fraser, L.K. Beura, L.S. Manlove, B.Z. Igyarto, P.J. Southern, and D. Masopust. 2015. Quantifying Memory CD8 T Cells Reveals Regionalization of Immunosurveillance. *Cell* 161:737-749.

Stras, S.F., L. Werner, J.M. Toothaker, O.O. Olaloye, A.L. Oldham, C.C. McCourt, Y.N. Lee, E. Rechavi, D.S. Shouval, and L. Konnikova. 2019. Maturation of the Human Intestinal Immune System Occurs Early in Fetal Development. *Dev Cell* 51:357-373 e355.

Sun, J.C., and L.L. Lanier. 2018. Is There Natural Killer Cell Memory and Can It Be Harnessed by Vaccination? NK Cell Memory and Immunization Strategies against Infectious Diseases and Cancer. *Cold Spring Harb Perspect Biol* 10:

Sungnak, W., C. Wang, and V.K. Kuchroo. 2019. Multilayer regulation of CD4 T cell subset differentiation in the era of single cell genomics. *Adv Immunol* 141:1-31.

Suzuki, K., and S. Fagarasan. 2009. Diverse regulatory pathways for IgA synthesis in the gut. *Mucosal Immunol* 2:468-471.

Suzuki, K., S.A. Ha, M. Tsuji, and S. Fagarasan. 2007. Intestinal IgA synthesis: a primitive form of adaptive immunity that regulates microbial communities in the gut. *Semin Immunol* 19:127-135.

Swain, S.L., K.K. McKinstry, and T.M. Strutt. 2012. Expanding roles for CD4(+) T cells in immunity to viruses. *Nat Rev Immunol* 12:136-148.

Szabo, P.A., M. Miron, and D.L. Farber. 2019. Location, location, location: Tissue resident memory T cells in mice and humans. *Sci Immunol* 4:

Takamura, S. 2018. Niches for the Long-Term Maintenance of Tissue-Resident Memory T Cells. *Front Immunol* 9:1214.

Teijaro, J.R., D. Turner, Q. Pham, E.J. Wherry, L. Lefrancois, and D.L. Farber. 2011. Cutting edge: Tissue-retentive lung memory CD4 T cells mediate optimal protection to respiratory virus infection. *J Immunol* 187:5510-5514.

Thom, J.T., T.C. Weber, S.M. Walton, N. Torti, and A. Oxenius. 2015. The Salivary Gland Acts as a Sink for Tissue-Resident Memory CD8(+) T Cells, Facilitating Protection from Local Cytomegalovirus Infection. *Cell Rep* 13:1125-1136.

Thome, J.J., N. Yudanin, Y. Ohmura, M. Kubota, B. Grinshpun, T. Sathaliyawala, T. Kato, H. Lerner, Y. Shen, and D.L. Farber. 2014. Spatial map of human T cell compartmentalization and maintenance over decades of life. *Cell* 159:814-828.

Thompson, E.A., J.S. Mitchell, L.K. Beura, D.J. Torres, P. Mrass, M.J. Pierson, J.L. Cannon, D. Masopust, B.T. Fife, and V. Vezys. 2019. Interstitial Migration of CD8αβ T Cells in the Small Intestine Is Dynamic and Is Dictated by Environmental Cues. *Cell Reports* 26:2859-2867.e2854.

Thornton, A.M., P.E. Korty, D.Q. Tran, E.A. Wohlfert, P.E. Murray, Y. Belkaid, and E.M. Shevach. 2010. Expression of Helios, an Ikaros transcription factor family member, differentiates thymic-derived from peripherally induced Foxp3+ T regulatory cells. *J Immunol* 184:3433-3441.

Turner, D.L., C.L. Gordon, and D.L. Farber. 2014. Tissue-resident T cells, in situ immunity and transplantation. *Immunol Rev* 258:150-166.

van Aalderen, M.C., E.B. Remmerswaal, I.J. ten Berge, and R.A. van Lier. 2014. Blood and beyond: properties of circulating and tissue-resident human virus-specific alphabeta CD8(+) T cells. *Eur J Immunol* 44:934-944.

Vander Heiden, J.A., G. Yaari, M. Uduman, J.N. Stern, K.C. O'Connor, D.A. Hafler, F. Vigneault, and S.H. Kleinstein. 2014. pRESTO: a toolkit for processing high-throughput sequencing raw reads of lymphocyte receptor repertoires. *Bioinformatics* 30:1930-1932.

Vignali, D.A., L.W. Collison, and C.J. Workman. 2008. How regulatory T cells work. *Nat Rev Immunol* 8:523-532.

von Andrian, U.H., and C.R. Mackay. 2000. T-cell function and migration. Two sides of the same coin. *N Engl J Med* 343:1020-1034.

Vyas, J.M., A.G. Van der Veen, and H.L. Ploegh. 2008. The known unknowns of antigen processing and presentation. *Nat Rev Immunol* 8:607-618.

Wakim, L.M., A. Woodward-Davis, and M.J. Bevan. 2010. Memory T cells persisting within the brain after local infection show functional adaptations to their tissue of residence. *P Natl Acad Sci USA* 107:17872-17879.

Walsh, D.A., H. Borges da Silva, L.K. Beura, C. Peng, S.E. Hamilton, D. Masopust, and S.C. Jameson. 2019. The Functional Requirement for CD69 in Establishment of Resident Memory CD8(+) T Cells Varies with Tissue Location. *J Immunol* 203:946-955.

Wang, J., A. Ioan-Facsinay, E.I. van der Voort, T.W. Huizinga, and R.E. Toes. 2007. Transient expression of FOXP3 in human activated nonregulatory CD4+ T cells. *Eur J Immunol* 37:129-138.

Watanabe, R., A. Gehad, C. Yang, L.L. Scott, J.E. Teague, C. Schlapbach, C.P. Elco, V. Huang, T.R. Matos, T.S. Kupper, and R.A. Clark. 2015. Human skin is protected by four functionally and phenotypically discrete populations of resident and recirculating memory T cells. *Sci Transl Med* 7:279ra239.

Weisberg, S.P., D.J. Carpenter, M. Chait, P. Dogra, R.D. Gartrell-Corrado, A.X. Chen, S. Campbell, W. Liu, P. Saraf, M.E. Snyder, M. Kubota, N.M. Danzl, B.A. Schrope, R. Rabadan, Y. Saenger, X. Chen, and D.L. Farber. 2019. Tissue-Resident Memory T Cells Mediate Immune Homeostasis in the Human Pancreas through the PD-1/PD-L1 Pathway. *Cell Reports* 29:3916-3932.e3915.

Weng, N.P., Y. Araki, and K. Subedi. 2012. The molecular basis of the memory T cell response: differential gene expression and its epigenetic regulation. *Nat Rev Immunol* 12:306-315.

Whibley, N., A. Tucci, and F. Powrie. 2019. Regulatory T cell adaptation in the intestine and skin. *Nat Immunol* 20:386-396.

Wilk, M.M., A. Misiak, R.M. McManus, A.C. Allen, M.A. Lynch, and K.H.G. Mills. 2017. Lung CD4 Tissue-Resident Memory T Cells Mediate Adaptive Immunity Induced by Previous Infection of Mice with Bordetella pertussis. *J Immunol* 199:233-243.

Williams, M.A., and M.J. Bevan. 2007. Effector and memory CTL differentiation. *Annu Rev Immunol* 25:171-192.

Wimmers, F., E.H. Aarntzen, T. Duiveman-deBoer, C.G. Figdor, J.F. Jacobs, J. Tel, and I.J. de Vries. 2016. Long-lasting multifunctional CD8(+) T cell responses in end-stage melanoma patients can be induced by dendritic cell vaccination. *Oncoimmunology* 5:e1067745.

Wu, T., Y. Hu, Y.T. Lee, K.R. Bouchard, A. Benechet, K. Khanna, and L.S. Cauley. 2014. Lung-resident memory CD8 T cells (TRM) are indispensable for optimal cross-protection against pulmonary virus infection. *J Leukoc Biol* 95:215-224.

Xu, Z., H. Zan, E.J. Pone, T. Mai, and P. Casali. 2012. Immunoglobulin class-switch DNA recombination: induction, targeting and beyond. *Nat Rev Immunol* 12:517-531.

Yang, J., M.S. Sundrud, J. Skepner, and T. Yamagata. 2014. Targeting Th17 cells in autoimmune diseases. *Trends Pharmacol Sci* 35:493-500.

Yen, H.R., T.J. Harris, S. Wada, J.F. Grosso, D. Getnet, M.V. Goldberg, K.L. Liang, T.C. Bruno, K.J. Pyle, S.L. Chan, R.A. Anders, C.L. Trimble, A.J. Adler, T.Y. Lin, D.M. Pardoll, C.T. Huang, and C.G. Drake. 2009. Tc17 CD8 T cells: functional plasticity and subset diversity. *J Immunol* 183:7161-7168.

Yin, Y., A. Mitson-Salazar, and C. Prussin. 2015. Detection of Intracellular Cytokines by Flow Cytometry. *Curr Protoc Immunol* 110:6 24 21-26 24 18.

Zhang, N., and M.J. Bevan. 2011. CD8(+) T cells: foot soldiers of the immune system. *Immunity* 35:161-168.

Zhang, N., and M.J. Bevan. 2013. Transforming growth factor-beta signaling controls the formation and maintenance of gut-resident memory T cells by regulating migration and retention. *Immunity* 39:687-696.

Zhang, Z., W. Zhang, J. Guo, Q. Gu, X. Zhu, and X. Zhou. 2017. Activation and Functional Specialization of Regulatory T Cells Lead to the Generation of Foxp3 Instability. *J Immunol* 198:2612-2625.

Zhu, J., and W.E. Paul. 2008. CD4 T cells: fates, functions, and faults. *Blood* 112:1557-1569.

Zhu, J., H. Yamane, and W.E. Paul. 2010. Differentiation of effector CD4 T cell populations (*). *Annu Rev Immunol* 28:445-489.

Zuber, J., B. Shonts, S.P. Lau, A. Obradovic, J. Fu, S. Yang, M. Lambert, S. Coley, J. Weiner, J. Thome, S. DeWolf, D.L. Farber, Y. Shen, S. Caillat-Zucman, G. Bhagat, A. Griesemer, M. Martinez, T. Kato, and M. Sykes. 2016. Bidirectional intragraft alloreactivity drives the repopulation of human intestinal allografts and correlates with clinical outcome. *Sci Immunol* 1:

Zundler, S., E. Becker, M. Spocinska, M. Slawik, L. Parga-Vidal, R. Stark, M. Wiendl, R. Atreya, T. Rath, M. Leppkes, K. Hildner, R. Lopez-Posadas, S. Lukassen, A.B. Ekici, C. Neufert, I. Atreya, K. van Gisbergen, and M.F. Neurath. 2019. Hobit- and Blimp-1-driven CD4(+) tissue-resident memory T cells control chronic intestinal inflammation. *Nat Immunol*

8. SCIENTIFIC PAPERS

JEM | Journal of Experimental Medicine

ARTICLE

Resident memory CD8 T cells persist for years in human small intestine

Raquel Bartolomé-Casado[1], Ole J.B. Landsverk[1], Sudhir Kumar Chauhan[1,2], Lisa Richter[1,3], Danh Phung[1], Victor Greiff[4], Louise F. Risnes[5,6], Ying Yao[4,6], Ralf S. Neumann[4,6], Sheraz Yaqub[7], Ole Øyen[8], Rune Horneland[8], Einar Martin Aandahl[2,8], Vemund Paulsen[9], Ludvig M. Sollid[4,5,6], Shuo-Wang Qiao[4,6], Espen S. Baekkevold[1], and Frode L. Jahnsen[1]

Resident memory CD8 T (Trm) cells have been shown to provide effective protective responses in the small intestine (SI) in mice. A better understanding of the generation and persistence of SI CD8 Trm cells in humans may have implications for intestinal immune-mediated diseases and vaccine development. Analyzing normal and transplanted human SI, we demonstrated that the majority of SI CD8 T cells were bona fide CD8 Trm cells that survived for >1 yr in the graft. Intraepithelial and lamina propria CD8 Trm cells showed a high clonal overlap and a repertoire dominated by expanded clones, conserved both spatially in the intestine and over time. Functionally, lamina propria CD8 Trm cells were potent cytokine producers, exhibiting a polyfunctional (IFN-γ+ IL-2+ TNF-α+) profile, and efficiently expressed cytotoxic mediators after stimulation. These results suggest that SI CD8 Trm cells could be relevant targets for future oral vaccines and therapeutic strategies for gut disorders.

Introduction

Studies in mice have shown that the intestine contains high numbers of resident memory CD8 T (Trm) cells (Steinert et al., 2015). CD8 Trm cells are persistent, noncirculatory cells that provide particularly rapid and efficient protection against recurrent infections (Ariotti et al., 2014). In addition to their cytotoxic activity, CD8 Trm cells are efficient producers of proinflammatory cytokines that rapidly trigger both innate and adaptive protective immune responses (Schenkel et al., 2014). Thus, CD8 Trm cells are attractive targets for vaccine development against intracellular pathogens (Gola et al., 2018) and cancer immunotherapy (Park et al., 2019).

Although studies in mice have significantly advanced our understanding of CD8 Trm cell function in the intestine (Jabri and Ebert, 2007; Sheridan et al., 2014; Konjar et al., 2018), translation of mouse data into humans should be implemented with caution. Specifically, the generation of T cell memory in humans occurs after exposure to a broad variety of pathogens and commensals over many decades of life, which cannot be recapitulated in mouse models. Most mice are maintained in specific pathogen–free conditions that reduce their microbiome

diversity, which in turn influences the immune homeostasis and response to pathogens in the intestine (Maynard et al., 2012; Tao and Reese, 2017). Moreover, murine intraepithelial (IE) CD8 T cells constitute a heterogeneous population of unconventional CD8αα+ and conventional CD8αβ+ T cells, with partially overlapping effector properties but different developmental origins (McDonald et al., 2018). In contrast, their human counterparts mainly consist of conventional CD8αβ-expressing cells (Jabri and Ebert, 2007).

Under steady state conditions, the human small intestine (SI) is densely populated by CD8 T cells, in both the lamina propria (LP) and the epithelium. However, most studies of human SI CD8 T cells have focused exclusively on IE CD8 T cells (Abadie et al., 2012). Therefore, there is currently very limited knowledge about several functional aspects of SI CD8 T cells. For example, is the CD8 T cell population heterogeneous? Are the CD8 T cells persistent or circulating cells? What are their cytotoxic and cytokine-producing capacity? To what extent are LP and IE CD8 T cells clonally related? To consider using SI CD8 T cells as targets to design effective oral vaccines and to understand

[1]Department of Pathology, Oslo University Hospital and University of Oslo, Oslo, Norway; [2]Department of Cancer Immunology, Institute for Cancer Research, Oslo University Hospital, Oslo, Norway; [3]Core Facility Flow Cytometry, Biomedical Center, Ludwig-Maximilians-University Munich, Munich, Germany; [4]Department of Immunology, Institute of Clinical Medicine, University of Oslo, Oslo, Norway; [5]Department of Immunology, Oslo University Hospital, Rikshospitalet, Oslo, Norway; [6]K.G. Jebsen Coeliac Disease Research Centre, University of Oslo, Oslo, Norway; [7]Department of Gastrointestinal Surgery, Oslo University Hospital, Rikshospitalet, Oslo, Norway; [8]Department of Transplantation Medicine, Section for Transplant Surgery, Oslo University Hospital, Rikshospitalet, Oslo, Norway; [9]Department of Gastroenterology, Oslo University Hospital, Rikshospitalet, Oslo, Norway.

Correspondence to Raquel Bartolomé-Casado: r.b.casado@medisin.uio.no; Frode L. Jahnsen: f.l.jahnsen@medisin.uio.no.

their involvement in immune-mediated diseases, these are critical questions to address.

Analyzing the CD8 T cell compartment in the normal SI as well as in a unique transplantation setting in humans, we report that most SI CD8 T cells are Trm cells that persist for >1 yr in the epithelium and LP. High-throughput TCR sequencing (TCR-seq) showed a polarized immune repertoire and high clonal relatedness between IE and LP CD8 Trm cells. Functionally, the minor population of LP CD103⁻ CD8 T cells was transient in the tissue and produced fewer cytokines but had more preformed cytotoxic granules. In contrast, we demonstrate that activated CD8 Trm cells expressed high levels of multiple cytokines (polyfunctional) and showed de novo production of cytotoxic granules. Thus, SI CD8 Trm cells have potent protective capabilities and present functional roles similar to CD8 Trm cells described in mice.

Results

Most CD8 T cells in the human SI express a resident memory phenotype

To determine whether the human SI contains persisting CD8 T cells, we first examined biopsies from donor duodenum after pancreatic-duodenal transplantation (Tx) of type I diabetic patients (Horneland et al., 2015). Using fluorescent in situ hybridization probes specific for X/Y chromosomes on tissue sections where patient and donor were of different gender, we could precisely distinguish donor and recipient cells and consistently detected a high fraction of persisting donor CD8 T cells 1 yr after Tx (Fig. 1 A).

This finding encouraged us to further characterize SI CD8 T cells, and to this end we examined resections of proximal SI obtained from pancreatic cancer surgery (Whipple procedure) and from donors and recipients during pancreatic-duodenal Tx (baseline samples). All tissue samples were evaluated by pathologists, and only histologically normal SI was included. Peripheral blood (PB) was collected from Tx recipients and pancreatic cancer patients, and PB mononuclear cells (PBMCs) were isolated and analyzed by flow cytometry together with single-cell suspensions from enzyme-digested LP and IE. The cross-contamination between IE and LP fractions was negligible, attested by complete removal of epithelial cells assessed by histology (Fig. S1 A) and by low numbers of epithelial cells in the LP fraction detected by flow cytometry (Fig. S1 B). We found that, in blood and SI-LP, CD8 T cells constituted about a third of the CD3 T cells, while CD8 T cells dominated (>75%) in the epithelium (Fig. S1 C). Almost all SI CD8 T cells were TCRαβ⁺ (≈99.8% in LP and 98.7% in epithelium; Fig. S1 D), and virtually all expressed the coreceptor CD8αβ (Fig. S1 E). The vast majority of SI CD8 T cells exhibited a CD45RO⁺ CD45RA⁻ L-Sel⁻ CCR7⁻ effector memory phenotype (Fig. 1 B), whereas PB also contained a substantial fraction of naive (CD45RO⁻ CD45RA⁺ CCR7⁺ L-Sel⁺) and central memory (CD45RO⁺ CD45RA⁻ CCR7⁺ L-Sel⁺) CD8 T cells (Fig. 1 B).

To further define and compare LP and IE CD8 T cells with PB CD8 T cells, we performed t-distributed stochastic neighbor embedding (t-SNE) analysis including classic Trm markers and

functional (e.g., costimulatory and inhibitory) receptors associated with a Trm phenotype (Mackay et al., 2013; Thome et al., 2014; Fergusson et al., 2016; Kumar et al., 2017). LP and IE CD8 T cells clustered together and were distinct from PB CD8 T cells (Fig. 1 C, left). By visualizing the expression pattern for each marker, we confirmed that cells expressing CD45RA and CCR7 were confined to the PB clusters, whereas the Trm markers CD69 and CD103 were expressed only on tissue-derived CD8 T cells. SI CD8 T cells also showed high expression of the coinhibitory receptor 2B4 (SLAMF4) and the C-type lectin natural killer receptor CD161, whereas CD28 and killer-cell lectin like receptor G1 (KLRG1) were expressed at higher levels on PB CD8 T cells. CD127 (IL7 receptor-α), NKG2D, and PD-1 did not show any clustered expression (Fig. 1 C).

Virtually all LP and IE CD8 T cells expressed CD69 (97.15% and 99.6%, respectively). CD103 was expressed by most (76%) LP CD8 T cells and by all IE CD8 T cells (Fig. 1 D), whereas the minor population of LP CD8 T cells lacking CD103 was more similar to PB CD8 T cells (Fig. 1 C). Given that CD103 is the currently most established marker to infer residency at mucosal surfaces (Beura et al., 2018b), we evaluated the phenotypic profiles of CD103⁺ and CD103⁻ SI CD8 T cells in a larger cohort of donors (Fig. 2 A). CD127 was expressed by a larger fraction of LP CD103⁺ CD8 T cells than IE CD103⁺ and LP CD103⁻ CD8 T cells (Fig. 2 A). However, IE CD103⁺ CD8 T cells had higher expression of 2B4 and CD161 compared with CD103⁻ CD8 T cells. NKG2D was broadly expressed on all SI CD8 T cell subsets, but showed significantly higher expression in the CD103⁻ compartment. In addition, we found consistently higher numbers of cells positive for CD28, PD-1, and KLRG1 within the CD103⁻ CD8 T population compared with both LP and IE CD103⁺ cells (Fig. 2 A). Interestingly, approximately half of the CD103⁻ CD8 T cells expressed KLRG1, whereas most CD103⁺ CD8 T cells were KLRG1⁻, and plotting CD103 versus KLRG1 divided LP CD8 T cells into three distinct subsets (Fig. 2 B). The distribution of these three LP CD8 T cell subsets was conserved lengthwise in the SI, as demonstrated by their similar representation in mucosal biopsies taken several centimeters apart in the same SI (Fig. S2 B). We also analyzed the expression of the proliferation marker Ki67 by intracellular staining and flow cytometry. We detected few Ki67-positive cells (median <5%) in all CD8 T cell subsets from normal SI samples (Fig. 2 C), indicating that the proliferative activity of SI CD8 T cells under steady state conditions is low. To summarize, we showed that the majority of LP CD8 T cells and nearly all IE CD8 T cells express a Trm phenotype (CD103⁺ KLRG1⁻), whereas a minor fraction in the LP was more similar to PB CD8 effector memory cells, being CD103⁻ KLRG1⁺/⁻.

CD8 Trm cells persist for ≥1 yr in transplanted SI

Next, we wanted to determine whether CD8 T cells expressing a Trm phenotype were maintained over time in the human SI. The in vivo replacement kinetics of CD8 T cells in duodenal biopsies obtained by endoscopy was examined at 3, 6, and 52 wk after Tx (Horneland et al., 2015; for details, see Fig. S3 A). Most donors and patients express different HLA type I molecules, making it possible to accurately distinguish persisting donor cells from newly recruited incoming recipient cells in the graft by flow
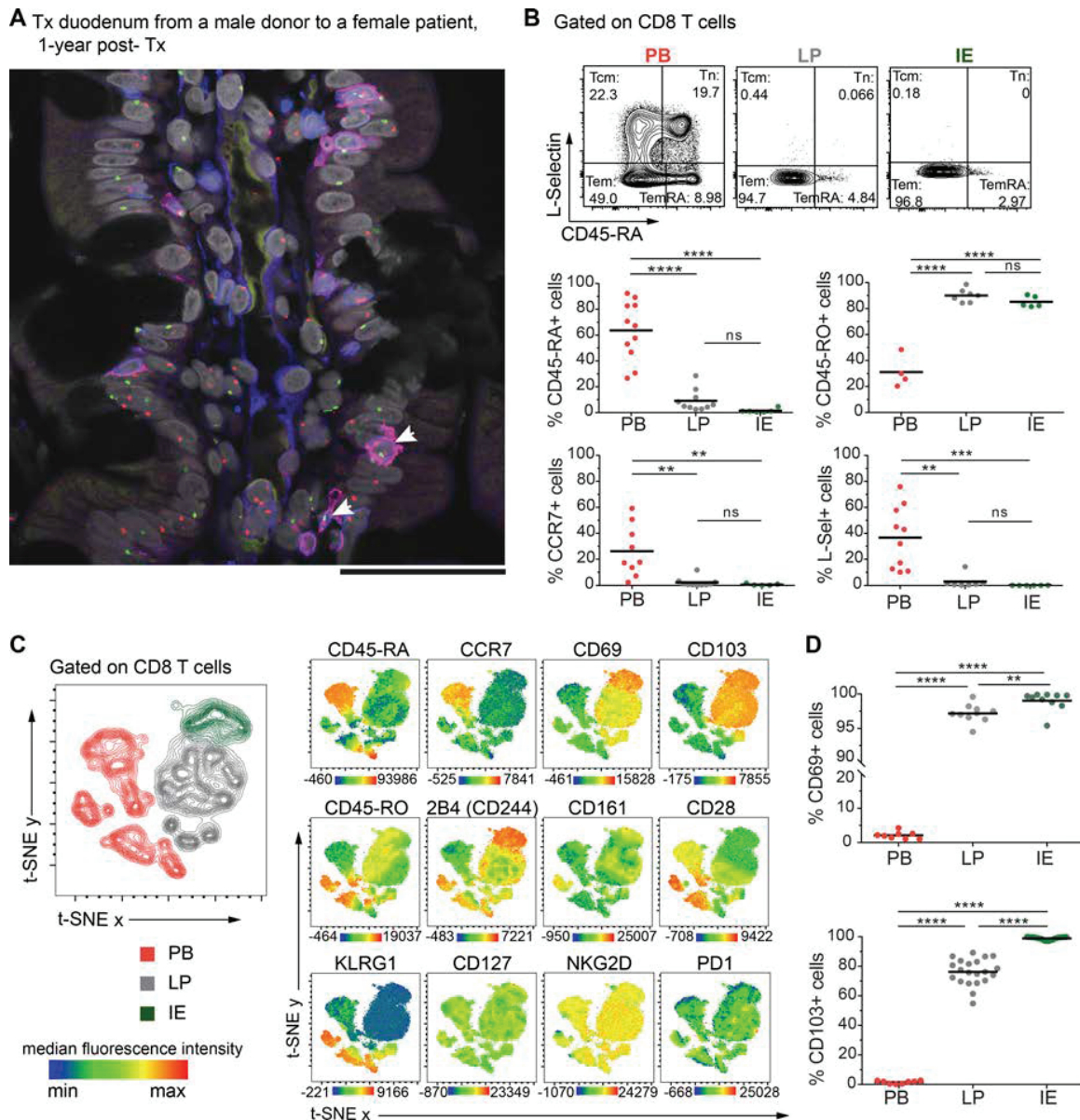
Bartolomé-Casado et al.
Persisting human intestinal CD8 Trm cells

Journal of Experimental Medicine 2
https://doi.org/10.1084/jem.20190414

Figure 1. **Human SI mucosa harbors a substantial population of CD8 T cells with a Trm phenotype. (A)** Representative confocal image of a tissue section from a male donor duodenum 1 yr after Tx into a female patient stained with X/Y chromosome fluorescent in situ hybridization probes (Y, green; X, red) and antibodies against CD8 (red) and CD3 (blue). Hoechst (gray) stains individual nuclei, and white arrows indicate donor (male) CD8 T cells ($n = 8$). Scale bar, 50 µm. **(B)** Expression of classic lymph node homing and memory markers on PB, LP, and IE CD8 T cells. Representative contour plots and compiled data for each marker are given. Tcm, central memory CD8 T cell; Tem, effector memory CD8 T cell; Tn, naive CD8 T cell. **(C)** t-SNE map showing the distribution of PB (red), LP (gray), and IE (green) CD8 T cell clusters (left). Overlay of the t-SNE map with expression levels for each marker, color-coded based on the median fluorescence intensity values, representative of three samples. See Fig. S2 A for details on preprocessing of flow data for t-SNE analysis. **(D)** Compiled data for the expression of CD69 and CD103 on PB, LP, and IE CD8 T cells. Black bars in B and D indicate mean values. Statistical analysis was performed using one-way ANOVA with Tukey's multiple comparisons test. ns, not significant; **, $P \le 0.01$; ***, $P \le 0.001$; ****, $P \le 0.0001$.

cytometry (Landsverk et al., 2017; Fig. 3 A). Only patients without histological or clinical signs of rejection were included ($n = 32$). At 3 and 6 wk after Tx, the vast majority of LP and IE CD103^{+} CD8 T cells were still of donor origin (Fig. 3 B). Of note, on average >60% of both LP and IE CD103^{+} CD8 T cells were still of donor origin 1 yr after Tx, although there was considerable interindividual variation, with some patients showing hardly any replacement at all (Fig. 3 B).

Immunophenotyping showed that the persisting donor CD103^{+} CD8 T cells expressed a Trm phenotype similar to the baseline situation (Fig. S3 B). LP CD103^{−} CD8 T cells were more rapidly replaced by recipient CD8 T cells, and at 6 wk after Tx, only 34% of the cells were of donor origin; however, after 1 yr, the LP CD103^{−} CD8 T cell compartment still contained ~15% donor cells (Fig. 3 B).

Within the LP CD103^{−} CD8 T cell population, the percentages of donor KLRG1^{+} and KLRG1^{−} cells were highly correlated ($r^2 = 0.67$,
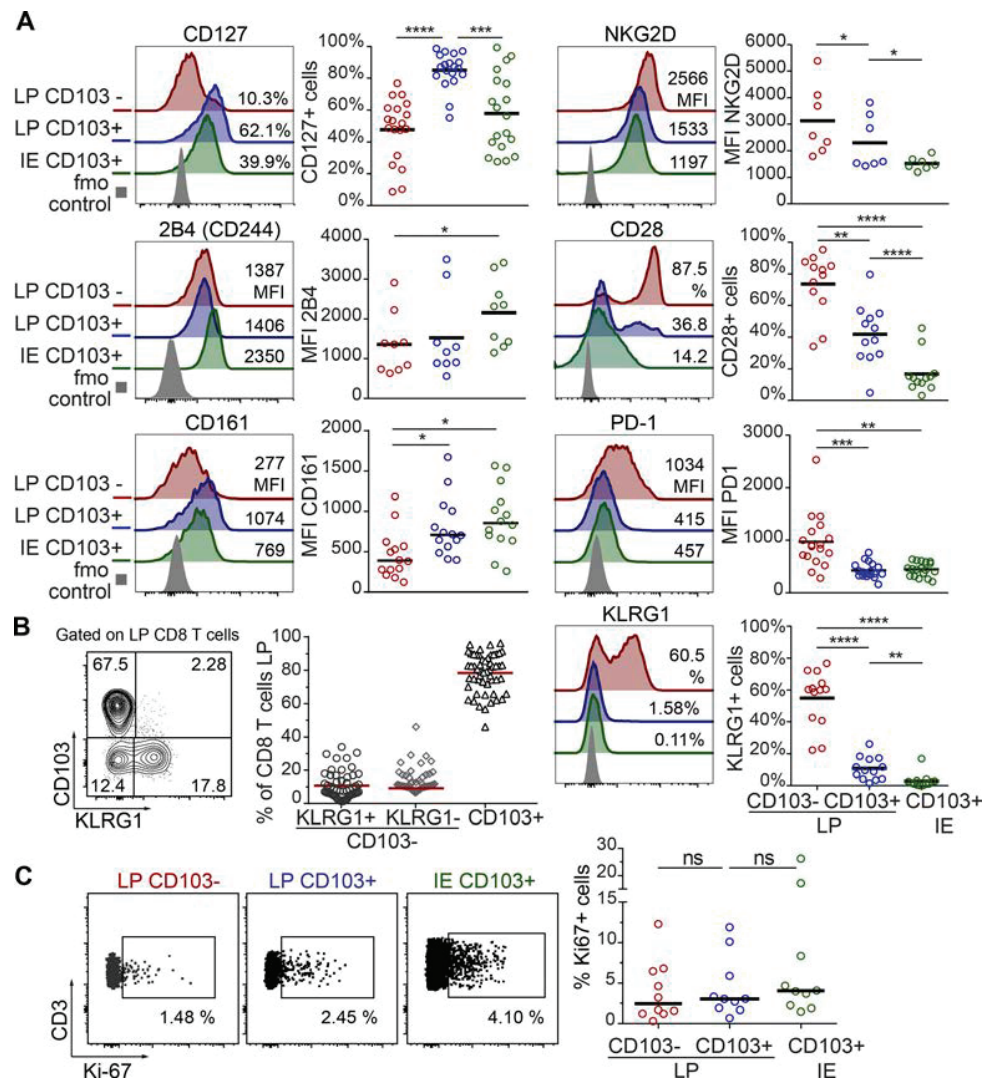
Figure 2. **LP and IE CD103⁺ CD8 T cells are phenotypically distinct from LP CD103⁻ CD8 T cells in normal human SI. (A)** Percentage of positive cells or median fluorescence intensity (MFI) values for various markers on LP CD103⁻, LP CD103⁺, and IE CD103⁺ CD8 T cells in histologically normal SI. Representative histograms for all markers are given with color codes (left): LP CD103⁻ (red), LP CD103⁺ (blue), IE CD103⁺ (green) CD8 T cells, and fluorescence minus one (fmo) control (gray). Black bars indicate mean values. **(B)** Representative contour plot (left) and fraction of LP CD103⁺ and CD103⁻ CD8 T cells expressing KLRG1 (right, n = 54). Red bars indicate mean values. **(C)** Representative dot plot (left) and percentage of LP CD103⁺, LP CD103⁻, and IE CD103⁺ CD8 T cells expressing Ki67 (right graph, n = 10). Black bars indicate median values. Statistical analysis was performed using one-way ANOVA for repeated measures with Tukey's multiple comparisons test. ns, not significant; *, $P \leq 0.05$; **, $P \leq 0.01$; ***, $P \leq 0.001$; ****, $P \leq 0.0001$.

$P < 0.0001$), suggesting a comparable replacement rate (Fig. 3 C). A similar replacement correlation was also found for CD103⁺ CD8 T cell subsets in LP and IE ($r^2 = 0.82$, $P < 0.0001$; Fig. S3 C). Analyzing recipient CD8 T cells, we found that 60–70% of incoming LP CD8 T cells were CD103⁻ KLRG1⁺/⁻ at 3 and 6 wk after Tx (Fig. 3, D and E). However, 1 yr after Tx, more than half of recipient LP CD8 T cells expressed a Trm phenotype (CD103⁺ KLRG1⁻), whereas the relative fractions of CD8 T cell phenotypes were stable at all the time points in the native duodenum (Fig. 3, D and E). This suggested that incoming CD103⁻ CD8 T cells gradually differentiated into CD103⁺ Trm cells, and that the relative distribution of the CD103⁺ subset within the total recipient CD8 T cell compartment at 1 yr after Tx became similar to the steady state situation (Figs. 2 B and 3, D and E). Flow-cytometric analysis of biopsies obtained

from the adjacent recipient duodenum did not show any donor-derived CD8 T cells, indicating that lateral migration or propagation from any residual lymphoid tissue in the graft was not occurring (Fig. S3 D).

To evaluate whether the surgical trauma, immunosuppressive treatment, and leukocyte chimerism was influencing the absolute numbers of SI CD8 T cells in the transplanted duodenum, we performed immunohistochemical staining of biopsies obtained at different time points from the same patients. Notably, we found that the overall density of CD8 T cells in transplanted duodenum was stable throughout the 1-yr follow-up period (Fig. S3 E). Moreover, flow-cytometric analysis of Tx tissue showed very few Ki67⁺ cells among the donor LP and IE CD103⁺ CD8 T cells (Fig. S3, F and G), similar to steady state
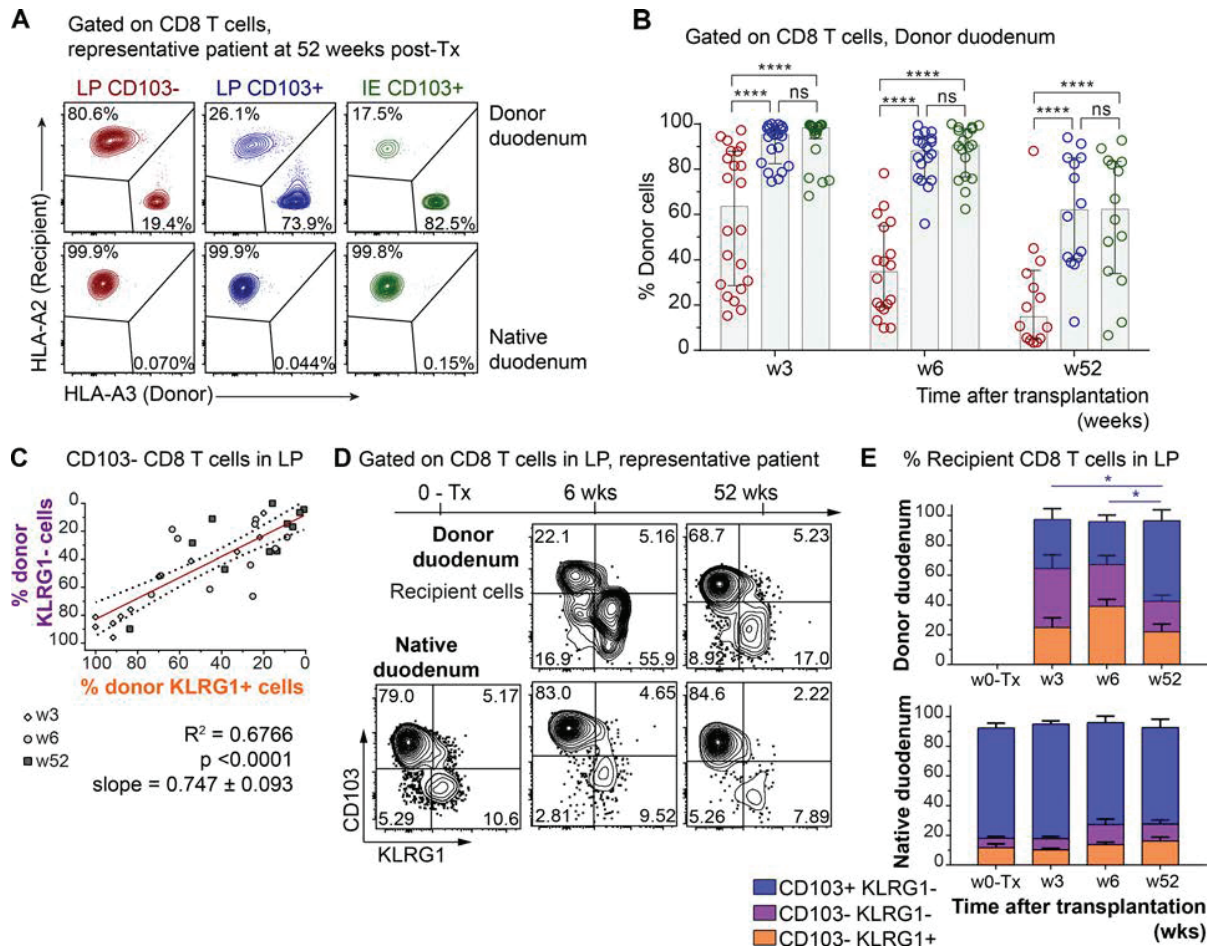
Bartolomé-Casado et al.
Persisting human intestinal CD8 Trm cells

Journal of Experimental Medicine
https://doi.org/10.1084/jem.20190414

4

Figure 3. **CD103⁺ CD8 T cells persist for ≥1 yr, while CD103⁻ CD8 T cells are dynamically exchanged in transplanted SI. (A)** Representative contour plots showing the percentage of donor and recipient LP CD103⁺, LP CD103⁻, and IE CD103⁺ CD8 T cells in donor duodenum 52 wk after Tx (n = 14). **(B)** Percentage of donor cells in the LP CD103⁻ (left, red), LP CD103⁺ (center, blue), and IE CD103⁺ (right, green) CD8 T cell subsets at 3 (n = 21), 6 (n = 18), and 52 wk after Tx (n = 14) as determined by HLA class I expression (as in A). Gray columns indicate median values. w, week. **(C)** Pearson correlation of percentages of donor-derived cells in KLRG1⁺ and KLRG1⁻ CD103⁻ CD8 T cell subsets in LP after Tx. Statistics performed using two-tailed P value (95% confidence interval, n = 33). **(D)** Distribution of recipient-derived CD8 T cells in the LP in different subsets according to the expression of KLRG1 and CD103, in donor (top) and native duodenum (bottom), before (0-Tx) and 3, 6, and 52 wk after Tx. One representative patient sample is shown (n = 33). **(E)** Compiled data for recipient CD8 T cell subset representation in native and donor duodenum before (w0-Tx) and after (w3-52) Tx. Mean with SD is shown. Statistical analysis was performed using two-way ANOVA with repeated measures across subsets and Tukey's multiple comparisons test of CD103⁺ KLRG1⁻ subset with time. ns, not significant; *, P ≤ 0.05; ****, P ≤ 0.0001.

levels (Fig. 2 C), indicating that proliferation was not a major contributing factor to the persistence of donor T cells in transplanted intestine. Taken together, these results show that SI CD103⁺ CD8 T cells can survive for ≥1 yr in the tissue and suggest that CD103⁻ CD8 T cells recruited to the SI may differentiate into Trm cells in situ.

Single-cell TCR repertoire analysis supports long-term persistence of CD103⁺ CD8 T cells in transplanted intestine
To further explore and verify the long-term persistence of SI CD8 Trm cells in Tx, we studied the conservation of the immune repertoire of SI CD103⁺ CD8 T cells over time at the single-cell level. Specifically, we performed single-cell high-throughput TCR-seq of donor LP CD103⁺ CD8 T cells sorted from the grafted duodenum before and 1 yr after Tx. To determine if the

degree of chimerism might affect the TCR repertoire, we included samples from one patient exhibiting high T cell replacement 1 yr after Tx (Ptx#1; 5% donor CD8 T cells) and one patient with low replacement (Ptx#2; 70% donor CD8 T cells; for sorting gating strategy, see Fig. S4 A). As a control, we also performed single-cell TCR-seq of LP CD103⁺ CD8 T cells from biopsies of the native (i.e., autologous, nontransplanted) duodenum of one patient (Ptx#2).

First, we investigated how many cells with the same clonotype (defined by identical nucleotide TCRα-β chains) were present in samples from the same individual taken before and 1 yr after Tx. Strikingly, despite the limited sampling, we detected overlapping clonotypes in biopsies obtained 1 yr apart in both transplanted and nontransplanted tissue. We found that 12% of the clonotypes identified at baseline were present 1 yr

Bartolomé-Casado et al.
Persisting human intestinal CD8 Trm cells

Journal of Experimental Medicine
https://doi.org/10.1084/jem.20190414

5

after Tx in patient Ptx#1, whereas a 50 and 37% overlap was detected in patient Ptx#2 (donor and native duodenum, respectively; Fig. 4 A). The frequency distribution of the TCRα-β clonotypes at both time points was similar in all the paired samples, and the first 10 clones with higher clonal size (8 of 21 clonotypes and 10 of 35 clonotypes on average, at week 0 and week 52, respectively) represented approximately half of the repertoire in all the cases, indicating significant clonal expansion (Fig. 4 B). Most of the unique TCRα-β sequences were derived from relatively small clones (expressed only by one cell), whereas a higher proportion of expanded clones were found among those shared at both time points (Fig. 4 C).

In agreement with other reports (Han et al., 2014), we found that TCR-seq efficiency was consistently lower for TCRα. To analyze a larger number of cells, we therefore calculated the clonal overlap using only the TCRβ chain sequence. In all paired samples, the percentage of overlapping TCRβ clonotypes was comparable to that calculated for TCRα-β clonotypes (Fig. 4 D). Furthermore, TCRβ analysis showed that the shared clones were more expanded both at baseline and at 52 wk compared with the unique clones (Fig. 4 E). The degree of clonal overlap and the frequency of expanded clones were similar in the grafted and the native duodenum from the same patient (Ptx#2), suggesting that chimerism in the transplanted SI did not trigger an excessive allo-driven clonal expansion. This was substantiated by the finding that CD8 T cells showed low expression of the proliferation marker Ki67 (Fig. S3, F and G). Together, these results confirmed that persisting CD8 Trm cells survive for ≥1 yr in transplanted duodenum and showed that relatively few expanded clonotypes constitute a considerable fraction of the CD8 Trm repertoire.

LP and IE CD103+ Trm cells present similar immune repertoire

The replacement kinetics and phenotype of CD8 T cells in transplanted SI (Figs. 3 B and S3 B) suggested that both IE and LP CD103+ CD8 T cells are Trm cells, whereas CD103− KLRG1+/− CD8 T cells were more dynamic subsets that have the potential to differentiate into CD103+ CD8 T cells (Fig. 3, D and E). To further interrogate the relationship among the SI CD8 T cell subsets, we sorted LP and IE CD103+ CD8 T cells as well as KLRG1+ and KLRG1− LP CD103− subsets from five SI samples. RNA was isolated, and TCRα and TCRβ genes were amplified by seminested PCR, including three cDNA replicates for each TCR chain (Fig. S4 B). Correlation of the read counts for the clonotypes found within the three molecular replicates was high (Fig. S4 D), indicating reproducibility of the TCR repertoire sequencing (Greiff et al., 2014). To determine whether different SI CD8 T cell subsets shared a common clonal origin, we calculated the percentage of overlapping clones and the Morisita–Horn similarity index for all the pairwise comparisons of both TCRα and TCRβ clonotypes. We found that the repertoire of LP and IE CD103+ CD8 T cells was very similar, with a clonal overlap of 35.6 and 37.5% and Morisita–Horn indexes of 0.66 and 0.71, respectively (Fig. 5, A and B). Both CD103− CD8 T cell subsets had a relatively low degree of similarity with the CD103+ subsets. However, notably, the Morisita–Horn index was 10-fold higher comparing LP and IE

CD103+ CD8 T cells with the KLRG1− subset than with the KLRG1+ subset (Fig. 5 B).

To better understand the extent of clonal overlap within the SI CD8 T cell population, we measured overlapping clones across all the SI CD8 T cell subsets. Interestingly, we found that some clones were shared among three or even all four CD8 T cell subsets (representative sample in Fig. 5 C), suggesting that the same progenitor cell can give rise to all memory CD8 T cell subsets. We next assessed the clonal diversity for each subset by calculating the Shannon evenness index, which describes the extent to which a distribution of clonotypes is distanced from the uniform distribution, with values ranging from 0 (least diverse, clonal dominance) to 1 (highly diverse, all clones have the same frequency; Greiff et al., 2015b). We found that all four SI CD8 T cell subsets displayed relatively low evenness values (Fig. S4 F), indicating a polarized repertoire with prevalence of certain clones. Fig. 5 D shows the abundance of the 10 most expanded TCRα and TCRβ clonotypes in each sample. Notably, a few dominant clones constituted a large fraction of the total repertoire in all of the subsets (≤40% of the total reads in some cases). In line with their similarity values (Fig. 5 B), LP and IE CD103+ T cells showed an analogous distribution of 10-top ranked clones in all five donors (Fig. 5 D).

To summarize, these data show that LP and IE CD103+ Trm cells have a very similar TCR repertoire. In both cases, this repertoire is biased toward a few expanded clones, and it is more closely related to the LP CD103− CD8 T cell subset lacking KLRG1 expression.

Activated SI CD8 T cell subsets produce different levels of cytokines and cytotoxic mediators

CD8 T cells exert their effector functions through activation-induced cytotoxicity involving targeted secretion of perforin and granzyme-B and cytokine secretion. In the absence of stimulation, significantly more CD103− CD8 T cells expressed granzyme-B and perforin compared with LP and IE CD103+ T cells (Fig. 6 A). However, after activation with anti-CD3/CD28 beads, both CD103− CD8 T cells and LP CD103+ CD8 T cells significantly increased their expression of granzyme-B and perforin, although the level of perforin was still higher in the CD103− CD8 T cell subset (Fig. 6 B). Within the CD103− population, KLRG1+ cells expressed higher levels of perforin after stimulation compared with KLRG1− cells (Fig. S5, A and B). Interestingly, induction of cytolytic molecules was hardly detectable in IE CD8 T cells, suggesting that TCR stimulation is not sufficient to activate their cytolytic function (Fig. 6 B).

To investigate their cytokine production profiles, SI CD8 T cell subsets were subjected to short-term stimulation with PMA and ionomycin, followed by intracellular flow-cytometric cytokine detection. Most (88%) LP CD103+ CD8 T cells produced one or more of the cytokines tested, whereas 75% of the LP CD103− CD8 T cells and 45% of the IE CD8 T cells were positive (Fig. 6, C and D). LP CD103+ CD8 T cells had a significantly higher proportion of dual IFN-γ+ IL-2+ cells and triple-producing (IFN-γ+ IL-2+ TNF-α+) cells compared with the other subsets (Fig. 6 C). Moreover, triple-producing CD8 T cells expressed

Bartolomé-Casado et al.
Persisting human intestinal CD8 Trm cells

Journal of Experimental Medicine
https://doi.org/10.1084/jem.20190414

6

Figure 4. **Persisting clonotypes of CD103+ CD8 Trm cells are detected in SI samples 1 yr after Tx. (A)** Clonotype overlap analysis by single-cell TCR-seq of donor CD103+ CD8 Trm cells derived from donor duodenum (Ptx#1- and Ptx#2-Donor) at baseline (w0, black) and 52 wk after Tx (w52, red) and of native CD103+ CD8 Trms from native duodenum (Ptx#2-Native). In italics (gray), number of unique clonotypes. Clonotype overlap was calculated as follows: % overlap(X,Y) = [(|X ∩Y|)/(|X| or |Y|)] × 100, where X represents the total clonotypes at week 0 (% in black), and Y represents the total clonotypes at week 52 (% in red). w, week. **(B)** Frequency (freq.) distribution of LP CD103+ CD8 Trm clonotypes at baseline (w0, black line) and 1 yr after Tx (w52, red line). Clonotype index is ordered by decreasing clonotype size. **(C)** Clonal dominance and preferential *TRAV/TRBV* pairing. Each slice of the column represents a different *TRAV/TRBV* pair, and the number of cells expressing them is shown (for more than one cell). Unique and overlapping *TRAV/TRBV* clones are shown separately. **(D)** Clonotype overlap analysis of total TCRβ clonotypes in the same samples as described in A. **(E)** Correlation of the TCRβ clonotypes found at baseline (w0) and 1 yr after Tx (w52). The samples are color-coded, and clonal size is represented by circle size. M-H, Morisita–Horn index.

Bartolomé-Casado et al.
Persisting human intestinal CD8 Trm cells

Journal of Experimental Medicine
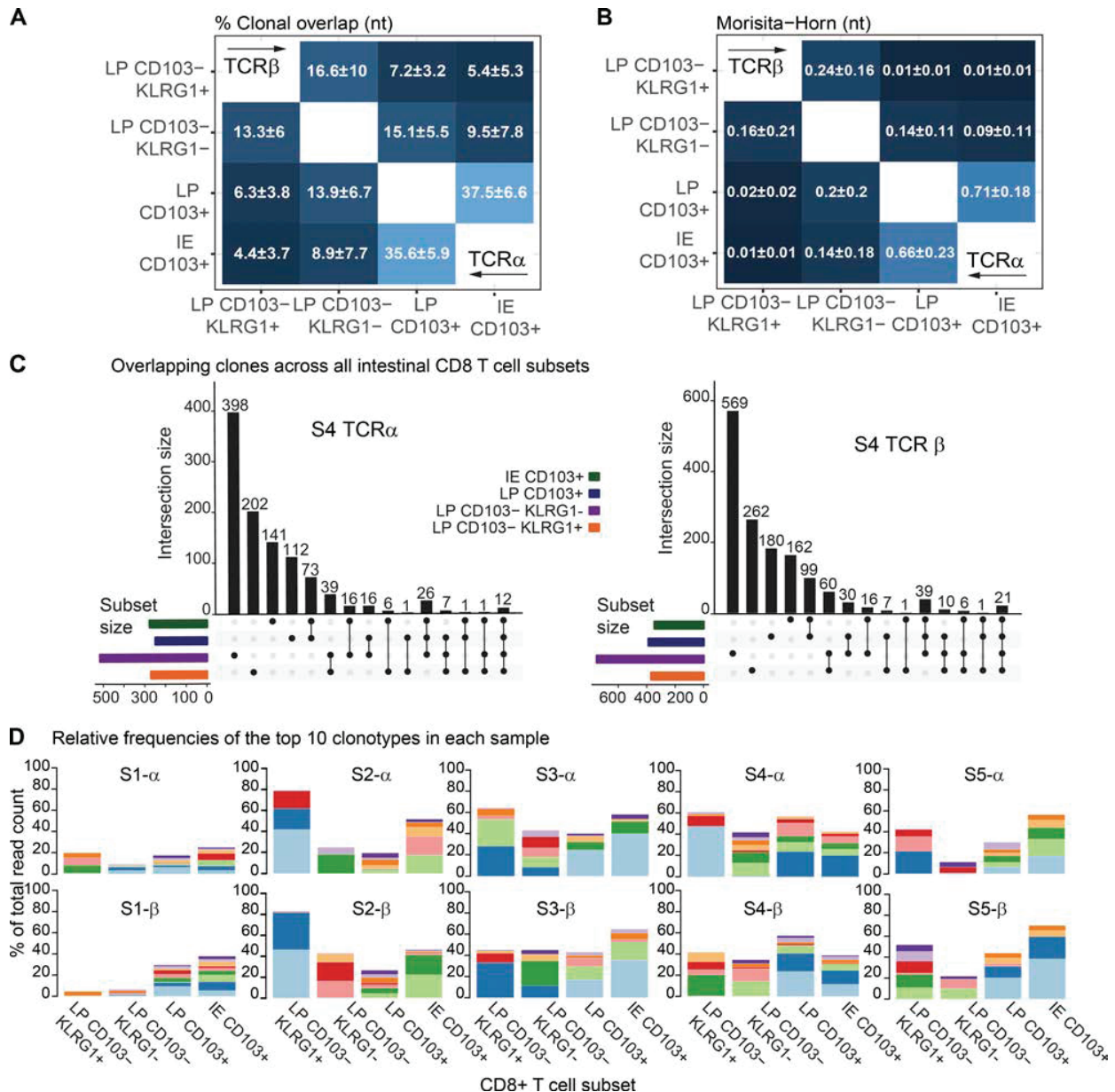https://doi.org/10.1084/jem.20190414

7

Figure 5. **High clonal overlap between IE and LP CD103⁺ CD8 T cells. (A and B)** Mean percentage of clonal overlap (A) and Morisita–Horn similarity indexes (B) applied to all the pairwise combinations of CD8 T cell subsets for TCRα (right corner) and TCRβ clonotypes (left corner) derived from normal SI (*n* = 5). The Morisita–Horn index ranges from 0 (no similarity) to 1 (identical). **(C)** Overlapping clones among the different intestinal CD8 T cell subsets for TCRα and TCRβ in one representative sample (*n* = 5). Intersections are represented below the x axis (black circles), the number of overlapping clonotypes is represented on the histogram, and the total amounts of clonotypes per subset are represented as color-coded horizontal bars. **(D)** Size of the read counts for the 10 most expanded clonotypes relative to the total reads in each subset. Shared clones are represented with the same color within the same sample (S) and TCR chain.

significantly higher levels of the individual cytokines compared with single cytokine–producing cells ([Fig. 6, E and F](#)). Within the CD103⁻ CD8 T cell population, we found that KLRG1⁻ cells contained significantly higher numbers of triple-producing cells than their KLRG1⁺ counterpart (Fig. S5 C).

Taken together, these data showed that CD8 Trm cells in LP are more potent cytokine-producing cells than CD103⁻ CD8 T cells. All LP CD8 T cell subsets efficiently produced cytotoxic molecules after activation, whereas IE CD8 Trm cells produced significantly fewer cytokines and cytotoxic molecules.

Discussion

Here we show that the human SI contains several phenotypically, functionally, and clonally distinct CD8 T cell subsets. Virtually all IE CD8 T cells and the majority of LP CD8 T cells expressed a Trm phenotype and were persistent cells (>1 yr) with a very similar immune repertoire. When activated, all subsets contained cytokine-producing cells, with LP CD8 Trm cells being particularly efficient. The two minor CD103⁻ CD8 T cell subsets were phenotypically more similar to PB CD8 T cells, presented an immune repertoire more different from the
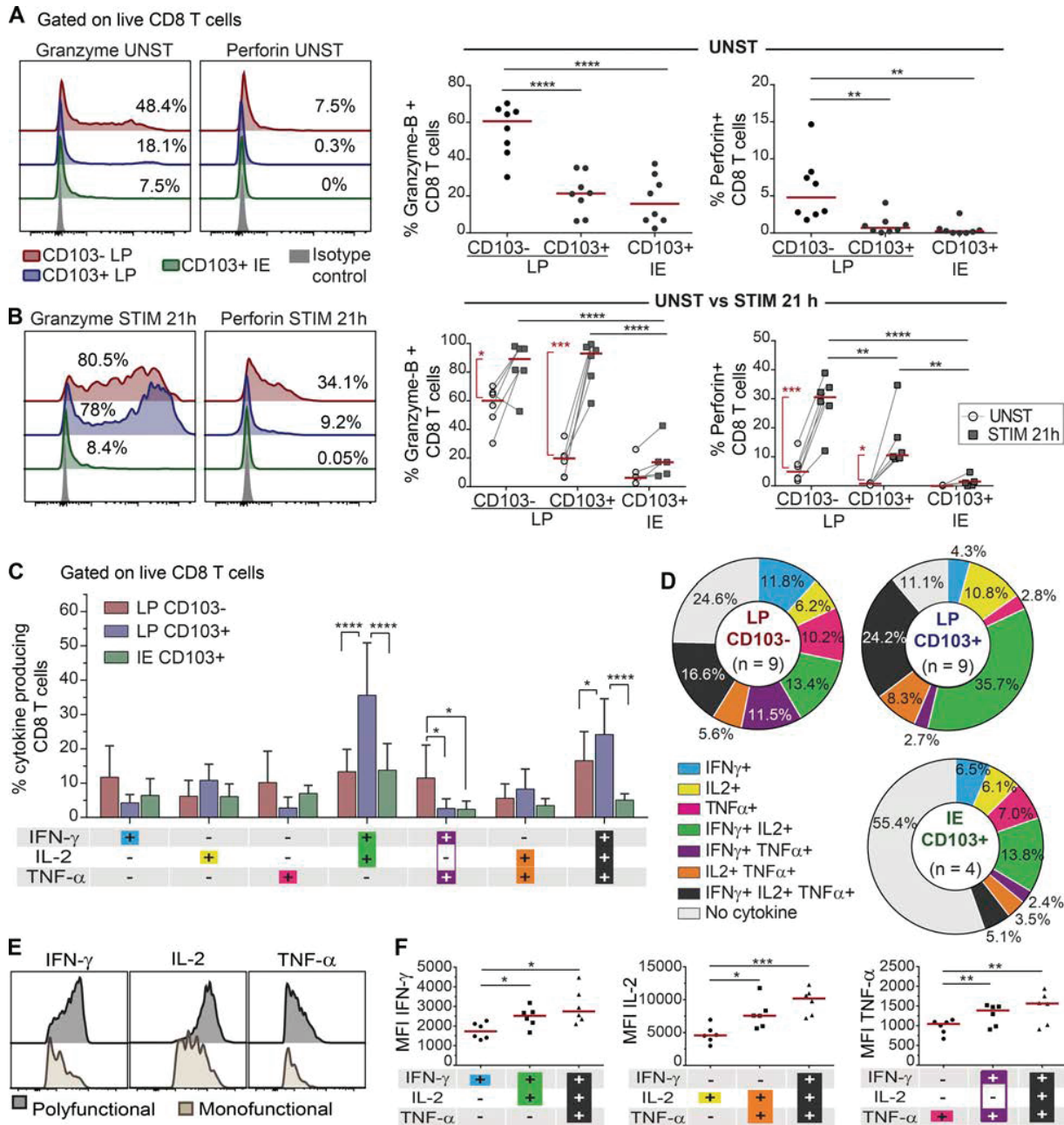
Bartolomé-Casado et al.
Persisting human intestinal CD8 Trm cells

Journal of Experimental Medicine 8
https://doi.org/10.1084/jem.20190414

Figure 6. **SI CD8 T cell subsets produce different levels of cytokines and cytotoxic molecules in response to activation. (A and B)** Representative flow-cytometric histogram (left) and compiled data (right, $n = 8$) for the intracellular expression of granzyme-B and perforin in CD8 T cell subsets without (A; UNST) and after (B; STIM) stimulation with anti-CD3/CD28 beads for 21 h ($n = 6$). Red lines indicate median values. **(C)** Flow-cytometric analysis of PMA/ionomycin-induced cytokine production by LP CD103⁻, LP CD103⁺, and IE CD103⁺ CD8 T cells. The mean percentages of cytokine-producing cells with SD are given by bars. **(D)** Relative representation of specific cytokine production profiles for LP CD103⁻ ($n = 9$), LP CD103⁺ ($n = 9$), and IE CD103⁺ ($n = 4$) CD8 T cells are represented on pie charts with color codes (C). Mean values of indicated experiments. **(E and F)** Representative histograms (E) and compiled median fluorescence intensity (MFI; F) values for single, dual, and triple cytokine-producing CD8 T cells ($n = 6$). Red lines indicate median values. Statistical analysis was performed using one-way (A and F) and two-way (B and C) repeated-measures ANOVA with Tukey's multiple comparisons test. For CD3/CD28 stimulation in B, Student's t test was applied to compare unstimulated and stimulated cells (red vertical lines and asterisks). *, $P \le 0.05$; **, $P \le 0.01$; ***, $P \le 0.001$; ****, $P \le 0.0001$. Red horizontal lines on graphs represent median values.

Trm cells, and produced higher levels of granzyme-B and perforin.

Experiments to accurately determine the longevity of lymphocytes are not readily performed in human tissues (Landsverk et al., 2017); however, by studying the replacement kinetics in a Tx setting, we were able to determine the persistence of CD8 T cells in grafted human duodenum. By multiparameter flow-cytometric analysis of CD8 T cells derived from normal

(nontransplanted) SI, we found that LP CD8 T cells could be divided into three distinct subsets depending on their expression of CD103 and KLRG1. Most of CD8 T cells displayed a Trm phenotype (CD103+ KLRG1−). We found that LP and IE CD103+ CD8 T cells expressed low levels of CD28, especially in the epithelium. In contrast, LP and IE CD103+ CD8 T cells expressed high levels of natural killer cell receptors, such as 2B4 (SLAM4) and CD161, and high levels of CD127. High PD-1 expression has been reported on CD8 Trm from human lung (Hombrink et al., 2016; Kumar et al., 2017). However, we found that intestinal LP and IE CD103+ express low levels of PD-1, in line with previous studies in mice (Casey et al., 2012). In contrast, the two minor CD103− subsets in LP, either KLRG1− or KLRG1+, were more similar to the CD8 T cells in PB, presenting higher levels of CD28, PD1, and NKG2D and lower CD127 and CD161 expression. By following the turnover kinetics of the subsets in transplanted duodenum, we found in half of the patients that >60% of both IE and LP CD103+ CD8 T cells were of donor origin 1 yr after Tx, with no reduction in absolute numbers of CD8 T cells. The finding of persistent donor CD8 T cells was substantiated by single-cell TCR-seq showing a significant clonal overlap between donor LP CD103+ CD8 T cells obtained before and 1 yr after Tx. Donor CD103− CD8 T cells, in contrast, were more rapidly replaced by recipient cells. However, interestingly, a small fraction (15%) of the CD103− subsets were still of donor origin 1 yr after Tx.

Zuber et al. (2016) reported that donor CD8 T cells were present in some nonrejected intestinal transplants for >600 d. These patients received intestinal Tx alone or as part of multivisceral Tx, which in both situations included gut-associated lymphoid tissue (GALT, e.g., Peyer's patches) and mesenteric lymph nodes. Long-term mixed chimerism is observed in the blood of these patients (Fu et al., 2019), suggesting that organized lymphatic tissue in the graft continuously expand and release donor T cells that home to the intestinal mucosa. In our study, however, only the proximal part of the duodenum was transplanted, without GALT or lymph nodes, excluding the possibility of continuous replenishment of donor cells after Tx.

Our findings show that CD8 T clones have the capacity to survive for ≥1 yr and most probably many years in the human intestinal mucosa, thus demonstrating the existence of bona fide Trm cells in the human SI. In the steady state, Trm cells can be generated from circulating memory precursors (Gaide et al., 2015) or proliferate locally in response to cognate antigens (Beura et al., 2018a). The proliferation rate, as measured by Ki67 staining, was consistently low in the transplanted and nontransplanted SI. This is in agreement with previous reports (Thome et al., 2014), suggesting that the persistence of CD8 T cells was maintained by long-lived cells rather than local proliferation. The finding that there was no massive expansion of selected clones 1 yr after Tx compared with the situation at baseline and with the native duodenum supports this scenario. Most of the persistent CD8 T cells expressed the classical Trm marker CD103 (αE integrin), which binds E-cadherin on the surface of epithelial cells (Schön et al., 1999). However, a small population of CD103− CD8 T cells was also maintained for 1 yr in the transplanted duodenum, suggesting that CD103 is not an

obligate marker for all Trm cells, as has been also reported for intestinal CD8 T cells in mice (Bergsbaken and Bevan, 2015).

Translated to the steady state situation, it is likely that the turnover rate of CD8 T cells observed in transplanted SI underestimates their physiological longevity for several reasons. First, all patients received immunosuppressive treatment including anti-thymoglobulin, which rapidly depletes T cells in blood (Horneland et al., 2015). It is likely that this treatment also affects the T cell numbers in the periphery. Second, solid organ Tx surgery causes ischemia and reperfusion injury of the graft that increases the turnover of leukocytes (Eguíluz-Gracia et al., 2016); and third, our previous studies have shown that dendritic cells and some of the macrophage subsets are rapidly replaced in the transplanted duodenum (Bujko et al., 2018; Richter et al., 2018), thereby increasing the risk of local alloreactivity. As shown in other Tx settings (lung [Snyder et al., 2019], intestine [Zuber et al., 2016], and kidney [de Leur et al., 2019]), the turnover rate of resident T cells increases with graft rejection. Although patients with histological signs of rejection were excluded from the study, all included patients displayed T cell recipient chimerism in the graft, in which episodes of low-grade rejection cannot be excluded. Altogether, our results, derived from both transplanted and normal SI combined, strongly suggest that virtually all IE CD8 T cells and the majority of LP CD8 T cells under homeostatic conditions are long-lived Trm cells with low proliferative activity (<5% Ki67+ cells).

Most studies of SI CD8 T cells in humans have focused on the IE compartment, and there is less knowledge about the CD8 T cell population in LP. Here we show that IE and LP CD103+ CD8 T cells present a very similar immune repertoire, indicating a common origin. When stimulated with PMA/ionomycin, ~40% of IE CD8 T cells produced cytokines (IFN-γ, IL-2, or TNF-α), whereas nearly all LP CD8 Trm cells were cytokine producing, and more than a third of these cells produced IFN-γ, IL-2, and TNF-α simultaneously (polyfunctional). This enhanced ability of Trm to produce robust responses mediated by polyfunctional cytokine production have been associated with the role of Trm as sentinel cells in different barrier tissues, such as skin (Watanabe et al., 2015). When activated with anti-CD3/CD28 beads, LP CD8 Trm cells produced high amounts of granzyme-B and significant levels of perforin, whereas IE CD8 T cells expressed less of these cytotoxic mediators. This finding may to some extent be explained by the fact that IE CD8 T cells expressed high levels of immunomodulatory markers (CD244 and CD161, Fig. 2 A) and CD101 (Russell et al., 1996), which may inhibit T cell activation and proliferation. Although IE CD8 T cells were less responsive to the stimuli we used in this study, their TCR repertoire was similar to LP CD103+ CD8 T cells, indicating that they had been activated under similar antigenic conditions. Moreover, in the transplanted intestine, we found that the turnover kinetics of IE and LP CD103+ CD8 T cells were strongly correlated (Fig. S3 C), together suggesting that IE and LP CD8 Trm cells were interrelated populations rather than operating independently in different compartments. Recent reports have shown that murine intestinal T cells are very motile and can move back and forth between the LP and the epithelium (Thompson et al., 2019). In addition, epithelial cells are in

Bartolomé-Casado et al.
Persisting human intestinal CD8 Trm cells

Journal of Experimental Medicine
https://doi.org/10.1084/jem.20190414

10

continuous communication with IE CD8 T cells, and it is therefore plausible that epithelial cell signaling under steady state conditions might increase the threshold of TCR-mediated response as a mechanism to maintain the integrity of the epithelial barrier (Jabri and Ebert, 2007).

Approximately 20% of SI CD8 T cells in LP did not express CD103 under steady state conditions. They were phenotypically more similar to PB CD8 T cells than CD8 Trm cells, and the immune repertoire of CD103⁻ CD8 T cells showed low clonal overlap with their Trm counterparts. In transplanted intestine, incoming recipient CD8 T cells were mainly CD103⁻ at 3 and 6 wk after Tx, which is compatible with the notion that CD103⁻ CD8 T cells in the steady state are mostly recently recruited cells. However, 1 yr after Tx, most recipient CD8 T cells presented a Trm phenotype, indicating that CD103⁻ CD8 T cells differentiated into CD8 Trm cells in situ. Comparing the TCR repertoire, CD103⁻ KLRG1⁻ CD8 T cells were more similar to CD8 Trm cells than CD103⁻ KLRG1⁺ cells, which agrees with studies in mice showing that KLRG1⁻ CD8 T cells are Trm precursors (Mackay et al., 2013; Sheridan et al., 2014). The KLRG1⁻ subset was also more similar to Trm cells with regard to production of cytokines and cytotoxic molecules. Notwithstanding these findings, it has been shown that TGF-β, abundantly present in the intestinal microenvironment, induces down-regulation of KLRG1 (Schwartzkopff et al., 2015). Thus, it is possible that also KLRG1⁺ T cells can differentiate into Trm cells (Herndler-Brandstetter et al., 2018).

Interestingly, the immune repertoire in both CD103⁺ and CD103⁻ subsets was polarized toward few dominating expanded clones. Assuming that CD103⁻ CD8 T cells were recently recruited from the circulation, this finding suggests that the clonal expansion had occurred before disseminating into the tissue, most likely in GALT and mesenteric lymph nodes. In agreement with this concept, biopsies obtained from different sites (several centimeters apart) and at different time points in transplanted patients showed expansion of many of the same clones, suggesting that T cell clones were evenly distributed along the duodenal mucosa and less dependent on local proliferation. Thus, the maintenance of a polarized immune repertoire (likely specific to recurrent pathogens), conserved both longitudinally in the tissue and over time, represents an optimized strategy of protection.

There is increasing evidence that Trm cells play an important role in mediating protective responses and maintaining long-term immunity against a broad variety of infectious diseases (Muruganandah et al., 2018). These studies are mainly performed in mouse models, and studies investigating the existence and function of Trm cells in human tissue are still few. Here we provide evidence that the majority of SI CD8 T cells in the steady state are long-lived cells with very highly potent protective capabilities. These data indicate that Trm cells in the intestinal mucosa are attractive targets to design effective oral vaccines. Further, the knowledge that long-lived T cells exist in the gut should give incentive for the implementation of new therapeutic strategies in diseases where pathogenic T cells play an important role, such as inflammatory bowel disease, celiac disease, and gut graft-versus-host disease.

Materials and methods
Human biological material
SI samples were obtained either during pancreatic cancer surgery (Whipple procedure, n = 35; mean age 63 yr, range 40–81; 16 female) or from donors or patients during pancreas-duodenum Tx (donors, n = 52; mean age 31 yr, range 5–55; 24 female; patients, n = 36; mean age 41 yr, range 25–60; 14 female) as described previously (Landsverk et al., 2017; Richter et al., 2018). Cancer patients receiving neoadjuvant chemotherapy were excluded from the study. Endoscopic biopsies from donor and patient duodenum were obtained 3, 6, and 52 wk after Tx. All transplanted patients received a standard immunosuppressive regimen (Horneland et al., 2015). All tissue specimens were evaluated blindly by experienced pathologists, and only material with normal histology was included (Ruiz et al., 2010). Transplanted patients showing clinical or histological signs of rejection or other complications, as well as patients presenting pretransplant or de novo donor-specific antibodies, were excluded from the study. Blood samples were collected at the time of surgery, and buffy coats from healthy donors (Oslo University Hospital, Oslo, Norway).

Intestinal resections were opened longitudinally and rinsed with PBS, and mucosa was dissected in strips off the submucosa. For microscopy, small mucosal pieces were fixed in 4% formalin and embedded in paraffin according to standard protocols. Intestinal mucosa was washed three times in PBS containing 2 mM EDTA and 1% FCS at 37°C with shaking for 20 min and filtered through nylon 100-μm mesh to remove epithelial cells. Epithelial fractions in each washing step were pooled and filtered through 100-μm cell strainers (Falcon; BD). After three sequential washes with EDTA buffer, the epithelial layer was completely removed from the tissue, and the basal membrane remained intact as shown in Fig. S1 A. Epithelial cells in the EDTA fraction were depleted by incubation with anti-human epithelial antigen antibody (clone Ber-EP4; Dako) followed by anti-mouse IgG Dynabeads (Thermo Fisher Scientific) according to the manufacturer's protocol. A death cell removal kit (Miltenyi) was applied to the depleted IE cells before cell sorting and functional assays. LP was minced and digested in complete RPMI medium (supplemented with 10% FCS and 1% penicillin/streptomycin) containing 0.25 mg/ml Liberase TL and 20 U/ml DNase I (both from Roche), with stirring at 37°C for 1 h. Digested tissue was filtered twice through 100-μm cell strainers and washed three times in PBS. The purity of both IE and LP fractions was checked by flow cytometry. We found <5% BerEP4⁺ epithelial cells in LP and no expression of B cell/plasma cell markers (CD19 or CD27) in the IE (Fig. S1 B), confirming that the degree of cross-contamination between these fractions was very low. Intestinal biopsies from transplanted patients were processed according to the same protocol. PBMCs were isolated by Ficoll-based density gradient centrifugation (Lymphoprep; Axis-Shield). All participants gave their written informed consent. The study was approved by the Regional Committee for Medical Research Ethics in Southeast Norway and complies with the Declaration of Helsinki.

Microscopy
Analysis of chimerism was performed as described previously (Landsverk et al., 2017). Briefly, formalin-fixed 4-μm sections

Bartolomé-Casado et al.
Persisting human intestinal CD8 Trm cells

Journal of Experimental Medicine
https://doi.org/10.1084/jem.20190414

11

were washed sequentially in xylene, ethanol, and PBS. Heat-induced epitope retrieval was performed by boiling sections for 20 min in Dako buffer. Sections were incubated with CEP X SpectrumOrange/Y SpectrumGreen DNA Probes (Abbott Molecular) for 12 h at 37°C before immunostaining according to standard protocol with anti-CD3 (Polyclonal; Dako), anti-CD8 (clone 4B11; Novocastra) and secondary antibodies targeting rabbit IgG or mouse IgG2b conjugated to Alexa Fluor 647 and 555, respectively. Laser scanning confocal microscopy was performed on an Olympus FV1000 (BX61WI) system. Image z stacks were acquired at 1-μm intervals and combined using the Z project maximum-intensity function in ImageJ (National Institutes of Health). All microscopy images were assembled in Photoshop and Illustrator CC (Adobe).

CD8 immunoenzymatic staining was performed on formalin-fixed 4-μm sections, dewaxed in xylene and rehydrated in ethanol, and prepared with Vulcan Fast red kit (Biocare Medical) following standard protocols. In brief, heat-induced antigen retrieval was performed in Tris/EDTA pH 9 buffer, followed by staining with primary antibody (CD8 clone 4B11; Novocastra) and secondary anti-mouse AP-conjugated antibody and incubation with substrate (Fast Red Chromogen; Biocare Medical). Slides were counterstained with hematoxylin, and excess dye was removed by bluing in ammonia water. Tissue sections were scanned using Pannoramic Midi slide scanner (3DHISTECH), and counts were generated with QuPath software (Bankhead et al., 2017).

Flow cytometry and cell sorting

Immunophenotyping was performed on single-cell suspensions of LP and IE fractions and PBMCs using different multicolor combinations of directly conjugated monoclonal antibodies (Table S1). To assess the expression of L-selectin on digested tissue, cells were rested for 12 h at 37°C before immunostaining. Replacement of donor cells in duodenal biopsies of HLA-mismatched transplanted patients was assessed using different HLA type I allotype-specific antibodies targeting donor- and/or recipient-derived cells, and stroma cells were used as a control of specific staining. Dead cells were excluded based on propidium iodide staining (Molecular Probes; Life Technologies).

For analysis of cytokine production, LP and IE cell suspensions were stimulated for 4 h with control complete medium (RPMI supplemented with 10% FCS and 1% penicillin/streptomycin) or PMA (1.5 ng/ml) and ionomycin (1 μg/ml; both from Sigma-Aldrich) in the presence of monensin (Golgi Stop; BD Biosciences) added after 1 h of stimulation to allow intracellular accumulation of cytokines. Cells were stained using the BD Cytofix/Cytoperm kit (BD Biosciences) according to the manufacturer's instructions and stained with antibodies against TNFα, IFNγ, or IL-2 (Table S1). The mean percentage of live cells in the cytokine experiments, determined by flow-cytometric analysis using a fixable viability dye, was 77% for LP CD8 T cells (range 58.8–92.8%) and 70% for IE CD8 T cells (range 56.9–83.4%). For detection of cytotoxic granules, LP and IE cells were activated for 21 h with anti-CD3/CD28 beads (Dynabeads; Thermo Fisher Scientific) or control complete medium. For detection of intranuclear Ki67 expression, the FoxP3/transcription factor staining buffer set was used according to the manufacturer's instructions. eFluor-450 or eFluor-780 fixable viability dyes (eBioscience) were used before any intracellular/intranuclear staining procedure. All samples were acquired on LSR Fortessa flow cytometer (BD Biosciences), using FACSDiva software (BD Biosciences). Single-stained controls were prepared for compensation (UltraComp eBeads; eBioscience), and gates were adjusted by comparison with FMO controls or matched isotype controls.

Flow cytometry data were analyzed using FlowJo 10.4.2 (TreeStar). For Fig. 1 C, the expression of 16 phenotypic markers was analyzed at the single-cell level and compared for CD8 T cells in PB, LP, and IE (n = 5) using the merge and calculation functions of Infinicyt software (Cytognos), as described in detail elsewhere (Pedreira et al., 2013). The population within the CD8 T cell gate was downsampled for each compartment and exported to a new file, and then concatenated and subjected to t-SNE analysis using the plugin integrated in FlowJo 10.4.2 (see Fig. S2 A for more details). FACS sorting was performed on an Aria II Cell Sorter (BD Biosciences). A TCRγδ antibody was used to exclude these cells during sorting (see gating strategy in Fig. S4 A). All experiments were performed at the Flow Cytometry Core Facility, Oslo University Hospital.

Single-cell TCRα-β sequencing

Cell suspensions from two donors (Ptx#1 and Ptx#2) were prepared at the time of Tx and kept frozen in liquid nitrogen. 1 yr after Tx, biopsies from the same patients (donor and recipient tissue) were collected, and single-cell suspensions were prepared and processed together with the thawed baseline samples from the same patients. Donor CD103^{+} KLRG1^{−} CD8 T cells from LP of transplanted tissue were identified following the gating strategy in Fig. S4 A, and single cells were sorted into 96-well plates (Bio-Rad) containing 5 μl capture buffer (20 mM Tris-HCl, pH 8, 1% NP-40, and 1 U/μl RNase inhibitor). The plates were spun down and snap frozen immediately after sorting and stored at −80°C until cDNA synthesis. Paired TCRα and TCRβ sequences were obtained after three nested PCRs with multiplexed primers covering all TCRα and TCRβ V genes, as described before (Risnes et al., 2018). In brief, cDNA plates were stored at −20°C, and each of the three nested PCR steps was performed in a total volume of 10 μl using 1 μl cDNA/PCR template and KAPA HiFi HotStart ReadyMix (Kapa Biosystems). In the last PCR reaction, TRAC and TRBC barcoding primers were added together with Illumina PairedEnd primers. Cycling conditions, concentrations, and primer sequences for all three PCR reactions can be found in Risnes et al. (2018) and the original protocol in Han et al. (2014). Products in each well were combined, purified, and sequenced using the Illumina paired-end 250-bp MiSeq platform at the Norwegian Sequencing Centre, Oslo University Hospital. The resulting paired-end sequencing reads were processed in a multistep pipeline using selected steps of the pRESTO toolkit (Vander Heiden et al., 2014) according to Risnes et al. (2018). In short, high-purity reads (average Phred score >30) were deconvoluted using barcode identifiers and collapsed, and only the top three for each well were retained for further analysis. For identification of V, D, and J genes and the CDR3

Bartolomé-Casado et al.
Persisting human intestinal CD8 Trm cells

Journal of Experimental Medicine
https://doi.org/10.1084/jem.20190414

12

junctions, the International ImMunoGeneTics Information System (IMGT)/HighV-QUEST online tool (Alamyar et al., 2012) was used. The results were then filtered and collapsed. Paired TCR sequences were grouped in clonotypes, defined by identical V and J gene (subgroup level) together with identical CDR3 nucleotide sequence for both TCRα and TCRβ when that information was available (Brown et al., 2019). Only valid singleton cells containing no more than three chains (dual TCRα and TCRβ) with ≥100 reads were considered for downstream analysis.

Bulk TCR-seq

5,000 cells of each subset of CD8 T cells (CD103⁻ KLRG1⁺, CD103⁻ KLRG1⁻, and CD103⁺ from LP and CD103⁺ IELs) were sorted into tubes containing 100 µl of TCL lysis buffer (Qiagen) supplemented with 1% β-mercaptoethanol and stored at −80°C until cDNA synthesis (see Fig. S4 B). Total RNA was extracted using RNAclean XP beads (Agencourt) following the manufacturer's protocol. A modified SMART (switching mechanism at 5′ end of RNA template) protocol (Quigley et al., 2011) was used in first-strand cDNA synthesis, described in detail elsewhere (Risnes et al., 2018). In brief, TCRα and TCRβ genes were amplified in two rounds of seminested PCRs. In the first reaction, the cDNA from each sample was divided into three replicates and amplified with TRAC and TRBC primers, and in the second reaction, different indexed primers were used to barcode the samples and replicates. A third, final reaction was performed using Illumina Seq Primers R1/R2 for sequencing. TCRα and TCRβ PCR products were quantified using the KAPA library quantification kit for Illumina platforms (Kapa Biosystems) and pooled at the same concentrations. Subsequently, pooled TCRα and TCRβ products were cleaned and concentrated with MinElute PCR Purification Kit (Qiagen) and run on a 1.5% agarose gel. Bands of appropriate size (~650 bp) were gel-extracted (Fig. S4 C), purified using the Monarch Gel Extraction kit (New England Biolabs), and cleaned with MinElute PCR Purification Kit. The amplicon TCR library was sequenced using the paired-end 300-bp Illumina MiSeq; the approximate number of paired-end reads generated per CD8 T cell population was 35,000 reads for TCRα and 45,000 reads for TCRβ sequences. The total number of reads was 60 million (~20 million reads per library). Bulk TCR-seq data were preprocessed (VDJ alignment and clonotyping) using the MiXCR software package (Bolotin et al., 2015). Clonotypes were defined based on the V and J gene usage and the nucleotide sequence of the CDR3 region (Greiff et al., 2015b). Correlation of the read counts for the clonotypes found within the three molecular replicates was high (Fig. S4 D), indicating reproducibility of the TCR repertoire sequencing (Greiff et al., 2014). For downstream analysis, raw reads from molecular triplicates were cumulated, and only clonotypes with a minimal read count of 10 were used. Sample preparation and read statistics are summarized in Fig. S4 (B–E). tcR package was used for descriptive statistics (Nazarov et al., 2015). The percentage of overlapping clones shared between two CD8 T cell subsets was calculated as

$$\text{overlap}(X, Y) = \frac{|X \cap Y|}{\text{mean}(|X|, |Y|)} \times 100,$$

where $|X|$ and $|Y|$ are the clonal sizes (number of unique clones) of repertoires X and Y.

Statistical analysis

Statistical analyses were performed in Prism 7 (GraphPad Software). To assess statistical significance among SI CD8 T cell subsets, data were analyzed by one-way ANOVA (standard or repeated measures) followed by Tukey's multiple comparison tests. Replacement data and distribution of CD8 T cell subsets at different time points were analyzed by two-way ANOVA matching across subsets, followed by Tukey's multiple comparison tests. Correlations between replacement kinetics of different CD8 T cell subsets were calculated using Pearson correlation with two-tailed P value (95% confidence interval). P values of <0.05 were considered significant. TCR repertoire analysis was performed using the R statistical programming environment (R Development Core Team, 2018). Non-base R packages used for analyses were tcR (Nazarov et al., 2015), upsetR (Lex et al., 2014), ggplot2 (Wickham, 2009), and VennDiagram (Chen, 2018). The Morisita–Horn index was calculated using the R divo package (Sadee et al., 2017). Vegan package (Oksanen et al., 2018) was used to calculate the diversity (Shannon evenness index) as previously described (Greiff et al., 2015a).

Data and materials availability

Bulk and single-cell TCR raw sequences were deposited under a controlled data access at the European Genome-phenome Archive (https://www.ebi.ac.uk/ega/), with the accession no. EGAS00001003676 (datasets EGAD00001005049 and EGAD00001005050, respectively).

Online supplemental material

Fig. S1 shows some general considerations regarding sample preparation and characterization of intestinal CD8 T cells. Fig. S2 depicts extended features of the immunophenotypic analysis applied to PB, LP, and IE CD8 T cells. Fig. S3 summarizes additional data concerning the replacement kinetics of intestinal CD8 T cells in transplanted duodenum. Fig. S4 provides information about the TCR immune repertoire analysis: Gating strategy for sorting, bulk TCR-seq workflow, and read statistics. Fig. S5 shows functional characterization of LP KLRG1⁺ and KLRG1⁻ CD103⁻ CD8 T cell subsets. Table S1 lists all the antibodies used in the study.

References

Abadie, V., V. Discepolo, and B. Jabri. 2012. Intraepithelial lymphocytes in celiac disease immunopathology. *Semin. Immunopathol.* 34:551–566. https://doi.org/10.1007/s00281-012-0316-x

Alamyar, E., P. Duroux, M.P. Lefranc, and V. Giudicelli. 2012. IMGT(®) tools for the nucleotide analysis of immunoglobulin (IG) and T cell receptor (TR) V-(D)-J repertoires, polymorphisms, and IG mutations: IMGT/V-QUEST and IMGT/HighV-QUEST for NGS. *Methods Mol. Biol.* 882: 569–604. https://doi.org/10.1007/978-1-61779-842-9_32

Ariotti, S., M.A. Hogenbirk, F.E. Dijkgraaf, L.L. Visser, M.E. Hoekstra, J.Y. Song, H. Jacobs, J.B. Haanen, and T.N. Schumacher. 2014. T cell memory. Skin-resident memory CD8+ T cells trigger a state of tissue-wide pathogen alert. *Science.* 346:101–105. https://doi.org/10.1126/science.1254803

Bankhead, P., M.B. Loughrey, J.A. Fernández, Y. Dombrowski, D.G. McArt, P.D. Dunne, S. McQuaid, R.T. Gray, L.J. Murray, H.G. Coleman, et al. 2017. QuPath: Open source software for digital pathology image analysis. *Sci. Rep.* 7:16878. https://doi.org/10.1038/s41598-017-17204-5

Bergsbaken, T., and M.J. Bevan. 2015. Proinflammatory microenvironments within the intestine regulate the differentiation of tissue-resident CD8+ T cells responding to infection. *Nat. Immunol.* 16:406–414. https://doi.org/10.1038/ni.3108

Beura, L.K., J.S. Mitchell, E.A. Thompson, J.M. Schenkel, J. Mohammed, S. Wijeyesinghe, R. Fonseca, B.J. Burbach, H.D. Hickman, V. Vezys, et al. 2018a. Intravital mucosal imaging of CD8+ resident memory T cells shows tissue-autonomous recall responses that amplify secondary memory. *Nat. Immunol.* 19:173–182. https://doi.org/10.1038/s41590-017-0029-3

Beura, L.K., S. Wijeyesinghe, E.A. Thompson, M.G. Macchietto, P.C. Rosato, M.J. Pierson, J.M. Schenkel, J.S. Mitchell, V. Vezys, B.T. Fife, et al. 2018b. T Cells in Nonlymphoid Tissues Give Rise to Lymph-Node-Resident Memory T Cells. *Immunity.* 48:327–338.e5. https://doi.org/10.1016/j.immuni.2018.01.015

Bolotin, D.A., S. Poslavsky, I. Mitrophanov, M. Shugay, I.Z. Mamedov, E.V. Putintseva, and D.M. Chudakov. 2015. MiXCR: software for comprehensive adaptive immunity profiling. *Nat. Methods.* 12: 380–381. https://doi.org/10.1038/nmeth.3364

Brown, A.J., I. Snapkov, R. Akbar, M. Pavlović, E. Miho, G.K. Sandve, and V. Greiff. 2019. Augmenting adaptive immunity: progress and challenges in the quantitative engineering and analysis of adaptive immune receptor repertoires. *arXiv.* doi:arXiv:1904.04105v2 [q-bio.QM] (Preprint posted April 8, 2019)

Bujko, A., N. Atlasy, O.J.B. Landsverk, L. Richter, S. Yaqub, R. Horneland, O. Øyen, E.M. Aandahl, L. Aabakken, H.G. Stunnenberg, et al. 2018. Transcriptional and functional profiling defines human small intestinal macrophage subsets. *J. Exp. Med.* 215:441–458. https://doi.org/10.1084/jem.20170057

Casey, K.A., K.A. Fraser, J.M. Schenkel, A. Moran, M.C. Abt, L.K. Beura, P.J. Lucas, D. Artis, E.J. Wherry, K. Hogquist, et al. 2012. Antigen-independent differentiation and maintenance of effector-like resident memory T cells in tissues. *J. Immunol.* 188:4866–4875. https://doi.org/10.4049/jimmunol.1200402

Chen, H.2018. VennDiagram: Generate High-Resolution Venn and Euler Plots. Available at: https://rdrr.io/cran/VennDiagram/ (accessed July 17, 2018).

de Leur, K., M. Dieterich, D.A. Hesselink, O.B.J. Corneth, F.J.M.F. Dor, G.N. de Graav, A.M.A. Peeters, A. Mulder, H.J.A.N. Kimenai, F.H.J. Claas, et al. 2019. Characterization of donor and recipient CD8+ tissue-resident memory T cells in transplant nephrectomies. *Sci. Rep.* 9:5984. https://doi.org/10.1038/s41598-019-42401-9

Eguíluz-Gracia, I., H.H. Schultz, L.I. Sikkeland, E. Danilova, A.M. Holm, C.J. Pronk, W.W. Agace, M. Iversen, C. Andersen, F.L. Jahnsen, and E.S. Baekkevold. 2016. Long-term persistence of human donor alveolar macrophages in lung transplant recipients. *Thorax.* 71:1006–1011. https://doi.org/10.1136/thoraxjnl-2016-208292

Fergusson, J.R., M.H. Hühn, L. Swadling, L.J. Walker, A. Kurioka, A. Llibre, A. Bertoletti, G. Holländer, E.W. Newell, M.M. Davis, et al. 2016. CD161(int) CD8+ T cells: a novel population of highly functional, memory CD8+ T cells enriched within the gut. *Mucosal Immunol.* 9:401–413. https://doi.org/10.1038/mi.2015.69

Fu, J., J. Zuber, M. Martinez, B. Shonts, A. Obradovic, H. Wang, S.P. Lau, A. Xia, E.E. Waffarn, K. Frangaj, et al. 2019. Human intestinal allografts contain functional hematopoietic stem and progenitor cells that are maintained by a circulating pool. *Cell Stem Cell.* 24:227–239.e8. https://doi.org/10.1016/j.stem.2018.11.007

Gaide, O., R.O. Emerson, X. Jiang, N. Gulati, S. Nizza, C. Desmarais, H. Robins, J.G. Krueger, R.A. Clark, and T.S. Kupper. 2015. Common clonal origin of central and resident memory T cells following skin immunization. *Nat. Med.* 21:647–653. https://doi.org/10.1038/nm.3860

Gola, A., D. Silman, A.A. Walters, S. Sridhar, S. Uderhardt, A.M. Salman, B.R. Halbroth, D. Bellamy, G. Bowyer, J. Powlson, et al. 2018. Prime and target immunization protects against liver-stage malaria in mice. *Sci. Transl. Med.* 10:eaap9128. https://doi.org/10.1126/scitranslmed.aap9128

Greiff, V., U. Menzel, U. Haessler, S.C. Cook, S. Friedensohn, T.A. Khan, M. Pogson, I. Hellmann, and S.T. Reddy. 2014. Quantitative assessment of the robustness of next-generation sequencing of antibody variable gene repertoires from immunized mice. *BMC Immunol.* 15:40. https://doi.org/10.1186/s12865-014-0040-5

Greiff, V., P. Bhat, S.C. Cook, U. Menzel, W. Kang, and S.T. Reddy. 2015a. A bioinformatic framework for immune repertoire diversity profiling enables detection of immunological status. *Genome Med.* 7:49. https://doi.org/10.1186/s13073-015-0169-8

Greiff, V., E. Miho, U. Menzel, and S.T. Reddy. 2015b. Bioinformatic and Statistical Analysis of Adaptive Immune Repertoires. *Trends Immunol.* 36:738–749. https://doi.org/10.1016/j.it.2015.09.006

Han, A., J. Glanville, L. Hansmann, and M.M. Davis. 2014. Linking T-cell receptor sequence to functional phenotype at the single-cell level. *Nat. Biotechnol.* 32:684–692. https://doi.org/10.1038/nbt.2938

Herndler-Brandstetter, D., H. Ishigame, R. Shinnakasu, V. Plajer, C. Stecher, J. Zhao, M. Lietzenmayer, L. Kroehling, A. Takumi, K. Kometani, et al. 2018. KLRG1+ Effector CD8+ T Cells Lose KLRG1, Differentiate into All Memory T Cell Lineages, and Convey Enhanced Protective Immunity. *Immunity.* 48:716–729.e8. https://doi.org/10.1016/j.immuni.2018.03.015

Hombrink, P., C. Helbig, R.A. Backer, B. Piet, A.E. Oja, R. Stark, G. Brasser, A. Jongejan, R.E. Jonkers, B. Nota, et al. 2016. Programs for the persistence, vigilance and control of human CD8+ lung-resident memory T cells. *Nat. Immunol.* 17:1467–1478. https://doi.org/10.1038/ni.3589

Horneland, R., V. Paulsen, J.P. Lindahl, K. Grzyb, T.J. Eide, K. Lundin, L. Aabakken, T. Jenssen, E.M. Aandahl, A. Foss, and O. Øyen. 2015. Pancreas transplantation with enteroanastomosis to native duodenum

Bartolomé-Casado et al.
Persisting human intestinal CD8 Trm cells

Journal of Experimental Medicine
https://doi.org/10.1084/jem.20190414

14

poses technical challenges--but offers improved endoscopic access for scheduled biopsies and therapeutic interventions. *Am. J. Transplant.* 15: 242–250. https://doi.org/10.1111/ajt.12953

Jabri, B., and E. Ebert. 2007. Human CD8+ intraepithelial lymphocytes: a unique model to study the regulation of effector cytotoxic T lymphocytes in tissue. *Immunol. Rev.* 215:202–214. https://doi.org/10.1111/j.1600 -065X.2006.00481.x

Konjar, Š., U.C. Frising, C. Ferreira, R. Hinterleitner, T. Mayassi, Q. Zhang, B. Blankenhaus, N. Haberman, Y. Loo, J. Guedes, et al. 2018. Mitochondria maintain controlled activation state of epithelial-resident T lymphocytes. *Sci. Immunol.* 3:eaan2543. https://doi.org/10.1126/sciimmunol .aan2543

Kumar, B.V., W. Ma, M. Miron, T. Granot, R.S. Guyer, D.J. Carpenter, T. Senda, X. Sun, S.H. Ho, H. Lerner, et al. 2017. Human Tissue-Resident Memory T Cells Are Defined by Core Transcriptional and Functional Signatures in Lymphoid and Mucosal Sites. *Cell Reports.* 20:2921–2934. https://doi.org/10.1016/j.celrep.2017.08.078

Landsverk, O.J., O. Snir, R.B. Casado, L. Richter, J.E. Mold, P. Réu, R. Horneland, V. Paulsen, S. Yaqub, E.M. Aandahl, et al. 2017. Antibody-secreting plasma cells persist for decades in human intestine. *J. Exp. Med.* 214:309–317. https://doi.org/10.1084/jem.20161590

Lex, A., N. Gehlenborg, H. Strobelt, R. Vuillemot, and H. Pfister. 2014. UpSet: Visualization of Intersecting Sets. *IEEE Trans. Vis. Comput. Graph.* 20: 1983–1992. https://doi.org/10.1109/TVCG.2014.2346248

Mackay, L.K., A. Rahimpour, J.Z. Ma, N. Collins, A.T. Stock, M.L. Hafon, J. Vega-Ramos, P. Lauzurica, S.N. Mueller, T. Stefanovic, et al. 2013. The developmental pathway for CD103(+)CD8+ tissue-resident memory T cells of skin. *Nat. Immunol.* 14:1294–1301. https://doi.org/10.1038/ni .2744

Maynard, C.L., C.O. Elson, R.D. Hatton, and C.T. Weaver. 2012. Reciprocal interactions of the intestinal microbiota and immune system. *Nature.* 489:231–241. https://doi.org/10.1038/nature11551

McDonald, B.D., B. Jabri, and A. Bendelac. 2018. Diverse developmental pathways of intestinal intraepithelial lymphocytes. *Nat. Rev. Immunol.* 18:514–525. https://doi.org/10.1038/s41577-018-0013-7

Muruganandah, V., H.D. Sathkumara, S. Navarro, and A. Kupz. 2018. A Systematic Review: The Role of Resident Memory T Cells in Infectious Diseases and Their Relevance for Vaccine Development. *Front. Immunol.* 9:1574. https://doi.org/10.3389/fimmu.2018.01574

Nazarov, V.I., M.V. Pogorelyy, E.A. Komech, I.V. Zvyagin, D.A. Bolotin, M. Shugay, D.M. Chudakov, Y.B. Lebedev, and I.Z. Mamedov. 2015. tcR: an R package for T cell receptor repertoire advanced data analysis. *BMC Bioinformatics.* 16:175. https://doi.org/10.1186/s12859-015-0613-1

Oksanen, J., F.G. Blanchet, M. Friendly, R. Kindt, P. Legendre, D. McGlinn, P.R. Minchin, R.B. O'Hara, G.L. Simpson, P. Solymos, et al. 2018. vegan: Community Ecology Package. Available at: https://cran.r-project.org/ package=vegan (accessed July 17, 2018).

Park, S.L., A. Buzzai, J. Rautela, J.L. Hor, K. Hochheiser, M. Effern, N. McBain, T. Wagner, J. Edwards, R. McConville, et al. 2019. Tissue-resident memory CD8+ T cells promote melanoma-immune equilibrium in skin. *Nature.* 565:366–371. https://doi.org/10.1038/s41586 -018-0812-9

Pedreira, C.E., E.S. Costa, Q. Lecrevisse, J.J. van Dongen, and A. Orfao. EuroFlow Consortium. 2013. Overview of clinical flow cytometry data analysis: recent advances and future challenges. *Trends Biotechnol.* 31: 415–425. https://doi.org/10.1016/j.tibtech.2013.04.008

Quigley, M.F., J.R. Almeida, D.A. Price, and D.C. Douek. 2011. Unbiased molecular analysis of T cell receptor expression using template-switch anchored RT-PCR. *Curr. Protoc. Immunol.* Chapter 10:Unit 10.33.

R Development Core Team. 2018. R: A Language and Environment for Statistical Computing. R Foundation for Statistical Computing, Vienna, Austria.

Richter, L., O.J.B. Landsverk, N. Atlasy, A. Bujko, S. Yaqub, R. Horneland, O. Øyen, E.M. Aandahl, K.E.A. Lundin, H.G. Stunnenberg, et al. 2018. Transcriptional profiling reveals monocyte-related macrophages phenotypically resembling DC in human intestine. *Mucosal Immunol.* 11: 1512–1523. https://doi.org/10.1038/s41385-018-0060-1

Risnes, L.F., A. Christophersen, S. Dahal-Koirala, R.S. Neumann, G.K. Sandve, V.K. Sarna, K.E. Lundin, S.W. Qiao, and L.M. Sollid. 2018. Disease-driving CD4+ T cell clonotypes persist for decades in celiac disease. *J. Clin. Invest.* 128:2642–2650. https://doi.org/10.1172/JCI98819

Ruiz, P., H. Takahashi, V. Delacruz, E. Island, G. Selvaggi, S. Nishida, J. Moon, L. Smith, T. Asaoka, D. Levi, et al. 2010. International grading scheme for acute cellular rejection in small-bowel transplantation: single-center experience. *Transplant. Proc.* 42:47–53. https://doi.org/10.1016/j .transproceed.2009.12.026

Russell, G.J., C.M. Parker, A. Sood, E. Mizoguchi, E.C. Ebert, A.K. Bhan, and M.B. Brenner. 1996. p126 (CDw101), a costimulatory molecule preferentially expressed on mucosal T lymphocytes. *J. Immunol.* 157: 3366–3374.

Sadee, C., M. Pietrzak, M. Seweryn, and G. Rempala. 2017. divo: Tools for analysis of diversity and similarity in biological systems. Available at: https://rdrr.io/cran/divo/ (accessed July 17, 2018).

Schenkel, J.M., K.A. Fraser, L.K. Beura, K.E. Pauken, V. Vezys, and D. Masopust. 2014. T cell memory. Resident memory CD8 T cells trigger protective innate and adaptive immune responses. *Science.* 346:98–101. https://doi.org/10.1126/science.1254536

Schön, M.P., A. Arya, E.A. Murphy, C.M. Adams, U.G. Strauch, W.W. Agace, J. Marsal, J.P. Donohue, H. Her, D.R. Beier, et al. 1999. Mucosal T lymphocyte numbers are selectively reduced in integrin alpha E (CD103)-deficient mice. *J. Immunol.* 162:6641–6649.

Schwartzkopff, S., S. Woyciechowski, U. Aichele, T. Flecken, N. Zhang, R. Thimme, and H. Pircher. 2015. TGF-β downregulates KLRG1 expression in mouse and human CD8(+) T cells. *Eur. J. Immunol.* 45:2212–2217. https://doi.org/10.1002/eji.201545634

Sheridan, B.S., Q.M. Pham, Y.T. Lee, L.S. Cauley, L. Puddington, and L. Lefrançois. 2014. Oral infection drives a distinct population of intestinal resident memory CD8(+) T cells with enhanced protective function. *Immunity.* 40:747–757. https://doi.org/10.1016/j.immuni.2014.03.007

Snyder, M.E., M.O. Finlayson, T.J. Connors, P. Dogra, T. Senda, E. Bush, D. Carpenter, C. Marboe, L. Benvenuto, L. Shah, et al. 2019. Generation and persistence of human tissue-resident memory T cells in lung transplantation. *Sci. Immunol.* 4:eaav5581. https://doi.org/10.1126/sciimmunol .aav5581

Steinert, E.M., J.M. Schenkel, K.A. Fraser, L.K. Beura, L.S. Manlove, B.Z. Igyártó, P.J. Southern, and D. Masopust. 2015. Quantifying Memory CD8 T Cells Reveals Regionalization of Immunosurveillance. *Cell.* 161: 737–749. https://doi.org/10.1016/j.cell.2015.03.031

Tao, L., and T.A. Reese. 2017. Making Mouse Models That Reflect Human Immune Responses. *Trends Immunol.* 38:181–193. https://doi.org/10 .1016/j.it.2016.12.007

Thome, J.J., N. Yudanin, Y. Ohmura, M. Kubota, B. Grinshpun, T. Sathaliyawala, T. Kato, H. Lerner, Y. Shen, and D.L. Farber. 2014. Spatial map of human T cell compartmentalization and maintenance over decades of life. *Cell.* 159:814–828. https://doi.org/10.1016/j.cell.2014.10.026

Thompson, E.A., J.S. Mitchell, L.K. Beura, D.J. Torres, P. Mrass, M.J. Pierson, J.L. Cannon, D. Masopust, B.T. Fife, and V. Vezys. 2019. Interstitial Migration of CD8αβ T Cells in the Small Intestine Is Dynamic and Is Dictated by Environmental Cues. *Cell Reports.* 26:2859–2867.e4. https:// doi.org/10.1016/j.celrep.2019.02.034

Vander Heiden, J.A., G. Yaari, M. Uduman, J.N. Stern, K.C. O'Connor, D.A. Hafler, F. Vigneault, and S.H. Kleinstein. 2014. pRESTO: a toolkit for processing high-throughput sequencing raw reads of lymphocyte receptor repertoires. *Bioinformatics.* 30:1930–1932. https://doi.org/10 .1093/bioinformatics/btu138

Watanabe, R., A. Gehad, C. Yang, L.L. Scott, J.E. Teague, C. Schlapbach, C.P. Elco, V. Huang, T.R. Matos, T.S. Kupper, and R.A. Clark. 2015. Human skin is protected by four functionally and phenotypically discrete populations of resident and recirculating memory T cells. *Sci. Transl. Med.* 7:279ra39. https://doi.org/10.1126/scitranslmed.3010302

Wickham, H. 2009. *ggplot2: Elegant Graphics for Data Analysis*, vol. VIII. Springer-Verlag, New York, 213 pp. https://doi.org/10.1007/978-0-387 -98141-3

Zuber, J., B. Shonts, S.P. Lau, A. Obradovic, J. Fu, S. Yang, M. Lambert, S. Coley, J. Weiner, J. Thome, et al. 2016. Bidirectional intragraft alloreactivity drives the repopulation of human intestinal allografts and correlates with clinical outcome. *Sci. Immunol.* 1:eaah3732. https://doi .org/10.1126/sciimmunol.aah3732
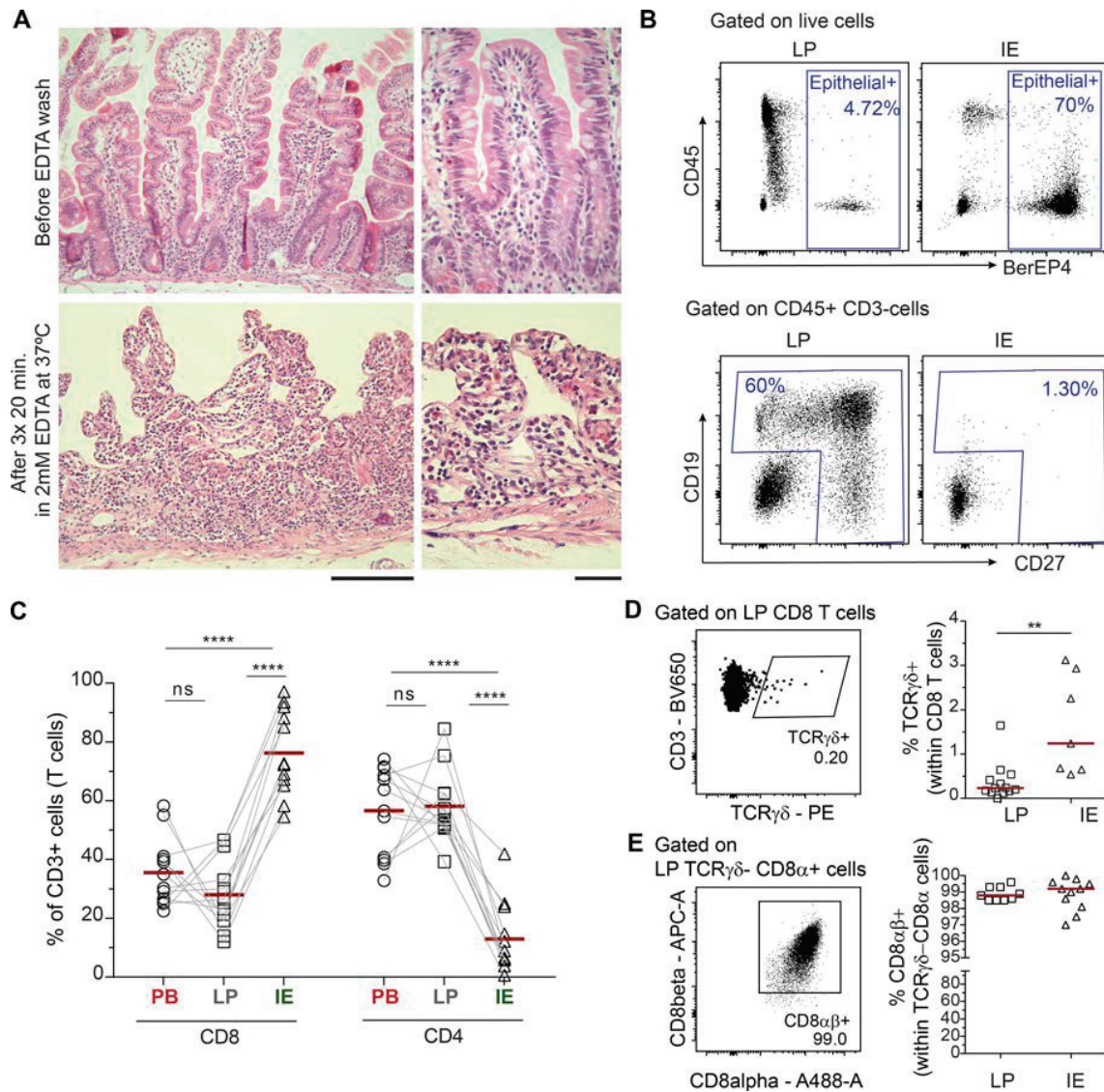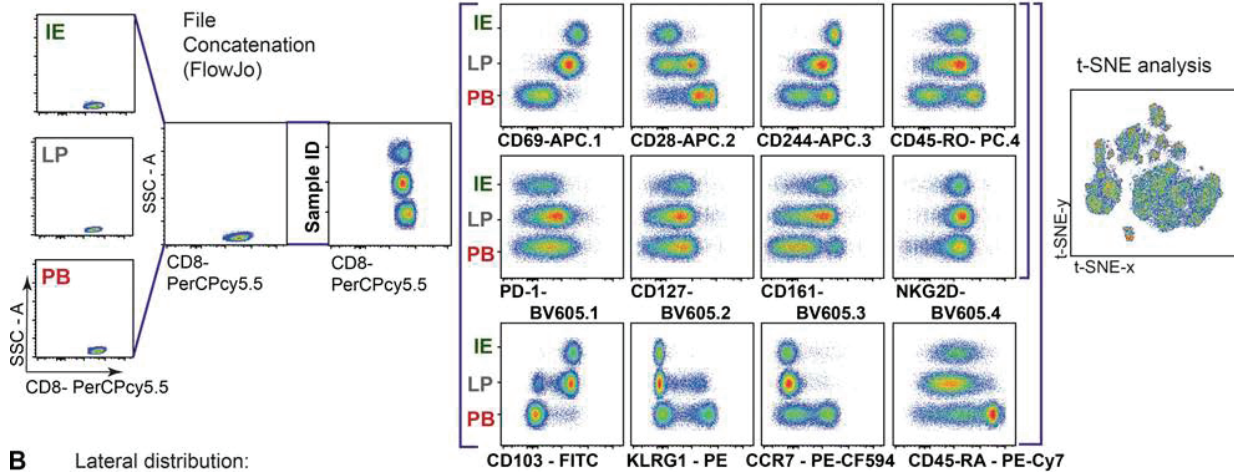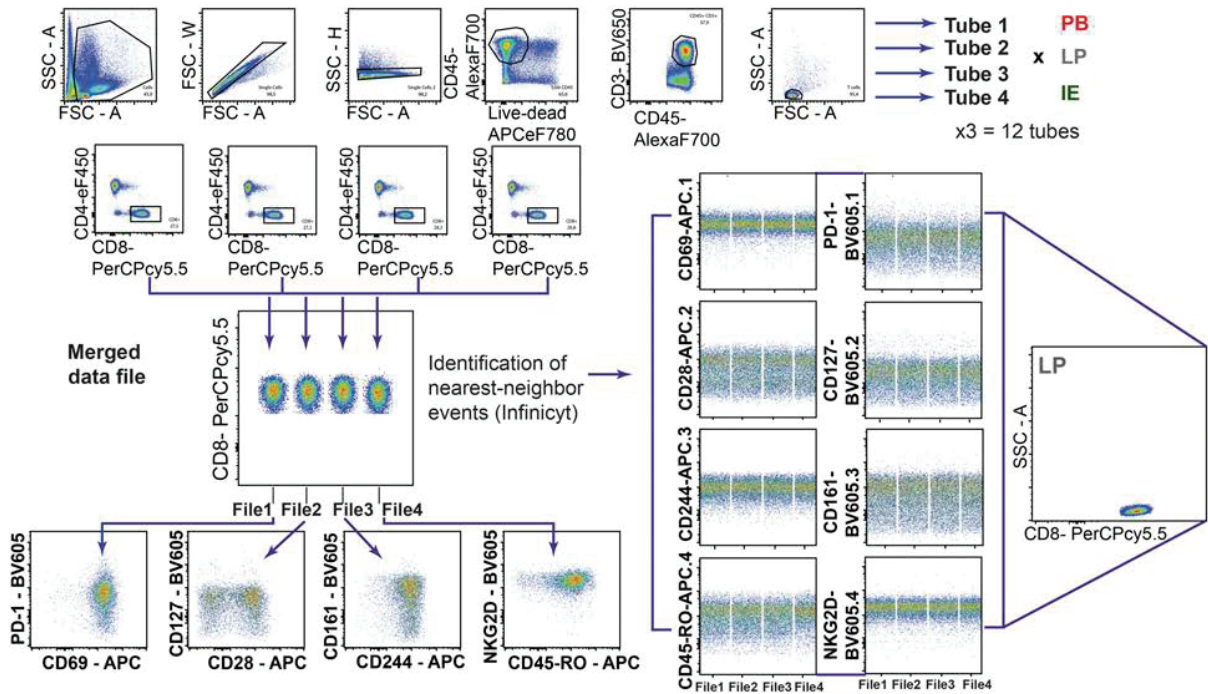
Figure S1. **General considerations regarding sample preparation and characterization of intestinal CD8 T cells. (A)** Confirmation of the absence of cross-contamination between LP and IE tissue fractions. Representative H&E staining of tissue sections obtained before and after three sequential washing steps with EDTA buffer (PBS containing 2 mM EDTA and 1% FCS) at 37°C with vigorous shaking. Scale bars represent 200 and 50 µm, respectively. **(B)** Representative flow cytometric plot showing the percentage of epithelial cells (BerEP4^{+} cells) and B cells within each fraction (*n* = 5; median = 1.25%; range = 0.15–4.72%). **(C)** Percentage of T cell subsets (CD4 and CD8) in PB, LP, and IE measured by flow cytometry. Red line indicates mean value. Statistics performed using two-way ANOVA, repeated measures matching both factors, and Tukey's multiple comparison test. **(D and E)** TCRγδ (D) and CD8β (E) expression on LP and IE CD8 T cells analyzed by flow cytometry. Red line indicates median value. Unpaired *t* test. ns, not significant; **, P ≤ 0.01; ****, P ≤ 0.0001.

Figure S2. Extended immunophenotypic analysis of LP and IE CD8 T cells. (A) Related to Fig. 1 C. Panel design, merging (as described in Pedreira et al., 2008, and concatenation of flow cytometric files before applying t-SNE analysis (FlowJo plugin). **(B)** Lateral distribution of LP CD8 T cell subsets. The lengthwise representation of the CD8 subsets in LP was determined by flow cytometric analysis of biopsies taken at intervals along resected duodenum-proximal jejunum from individual subjects after Whipple procedure. $n = 5$; paired Student's t test comparing 0 cm to the farthest distance. ns, not significant.

Bartolomé-Casado et al.
Persisting human intestinal CD8 Trm cells

Journal of Experimental Medicine   S2
https://doi.org/10.1084/jem.20190414

Figure S3. **Replacement kinetics of intestinal CD8 T cells in transplanted duodenum. (A)** Representation of pancreas Tx s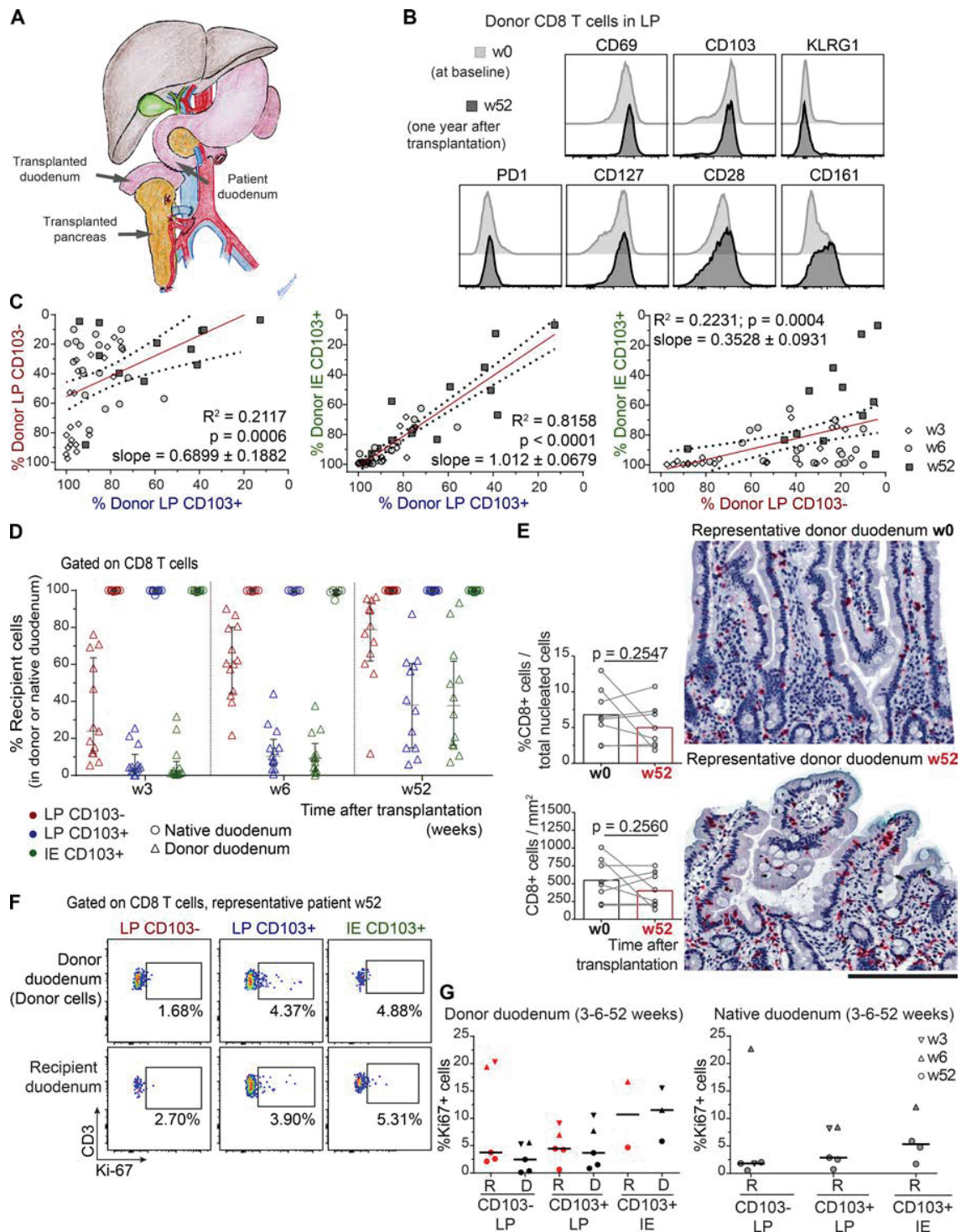howing the duodeno-duodenostomy anastomosis, as described in Horneland et al. (2015). **(B)** Expression profile of donor LP CD8 T cells derived from duodenal transplant at baseline (week 0 [w0]) versus 1 yr after Tx (w52). **(C)** Pearson correlation of the percentage of donor derived cells for CD103⁻ LP and IE CD103⁺ CD8 T cell subsets. Statistics performed using two-tailed P value (95% confidence interval). **(D)** Percentage of recipient CD8 T cells for each subset isolated from donor and recipient (native) duodenum of the same patients at different time points after Tx. Black horizontal lines represent median values, and error bars show interquartile ranges. **(E)** Representative immunohistochemistry staining of CD8 T cells (Fast-Red) on tissue sections from donor duodenum, before (w0) and 1 yr after Tx (w52). Scale bar, 200 µm. Left: Compiled data of CD8 T cell counts on tissue sections from donor duodenum of representative patients ($n = 8$) before (w0) and 1 yr after Tx (w52). Paired t test. **(F)** Representative dot plot showing Ki67 expression in CD8 T cell subsets derived from donor and native duodenum 1 yr after Tx. **(G)** Compiled data for the percentage of Ki67-positive cells in donor-derived (D) or recipient-derived (R) cells for each CD8 T cell subset at different time points after Tx in donor and native duodenum.
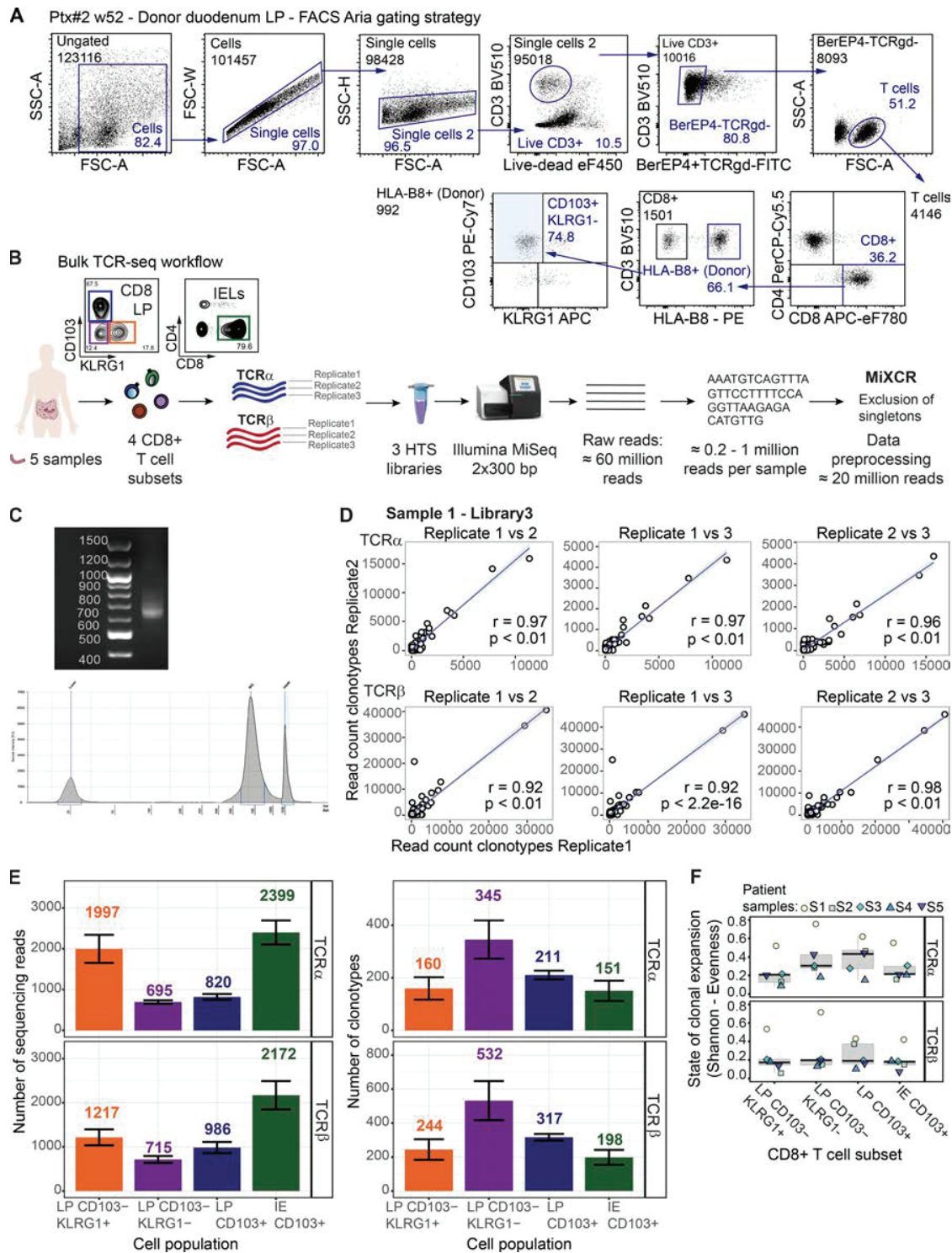
Bartolomé-Casado et al.
Persisting human intestinal CD8 Trm cells

Journal of Experimental Medicine
https://doi.org/10.1084/jem.20190414

S3

Figure S4. **TCR-seq: Gating strategy for sorting, bulk TCR-seq workflow, and read statistics. (A)** Gating strategy for flow cytometry analysis and single cell sorting of CD8 T cells from duodenal biopsies. Representative sample of grafted duodenum from a transplanted patient 1 yr after Tx is shown. SSC-A, side scatter (area); FSC-A/W, forward scatter (area/width). **(B)** Overview of sample processing, data acquisition, and data processing. Some graphical elements in the illustration were modified from Servier Medical Art (https://smart.servier.com/), licensed under a Creative Common Attribution 3.0 Generic License. IELs, intraepithelial lymphocytes; HTS, high-throughput sequencing. **(C)** Agarose gel shows representative library following the protocol explained in B. Expected band size ≈700 bp. **(D)** Correlation plots showing the correlation of the common clonotypes between the three replicates' representative samples. **(E)** Clone and sequence counts after MiXCR preprocessing are shown by CD8 T cell subset (mean ± SEM). The total number of sequencing reads used for the analysis was 20,692,061 (total number of raw reads: ≈62,317,193). Mean Phred scores of raw data were ≥30. **(F)** Evenness index is calculated for the TCRα and TCRβ repertoire of each CD8 T cell subset per sample. Values range from 0 (monoclonal distribution) to 1 (uniform distribution).

Bartolomé-Casado et al.
Persisting human intestinal CD8 Trm cells

Journal of Experimental Medicine
https://doi.org/10.1084/jem.20190414

S4
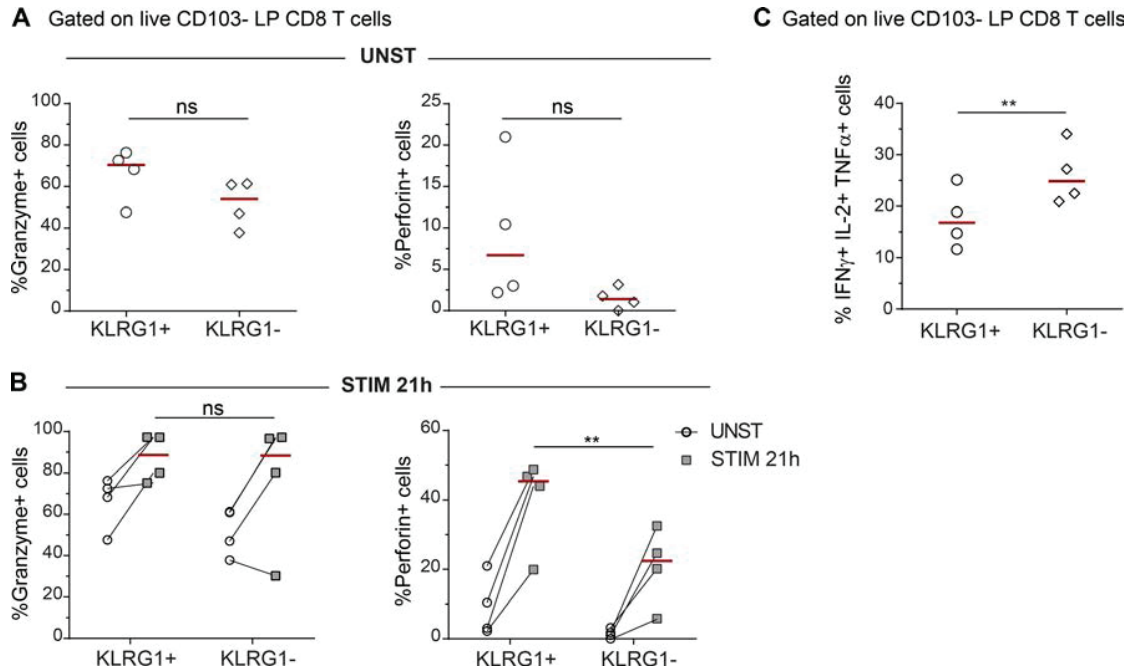
Figure S5. **Functional characterization of LP KLRG1+ and KLRG1− CD103− CD8 T cell subsets. (A and B)** Percentage of Granzyme-B– and perforin-positive cells in unstimulated samples (A; UNST) and after 21 h of activation with anti-CD3 beads (B; STIM) for the different CD103− CD8 T cell subsets (KLRG1+, KLRG1−) in LP (n = 4). **(C)** Percentage of polyfunctional (IL-2+, IFN-γ+, and TNF-α+) cells for the different CD103− CD8 T cell subsets (KLRG1+, KLRG1−) in LP (n = 4). Student's t test was applied to compare the two subsets. ns, not significant; **, P ≤ 0.01.

Bartolomé-Casado et al.
Persisting human intestinal CD8 Trm cells

Journal of Experimental Medicine   S5
https://doi.org/10.1084/jem.20190414

Target	Clone	Fluorophore	Company	Catalog no.	Phenotype Trm	PTx panel	Aria sorting	Ki67 nuclear	Cytotoxicity	Cytokines	X/Y FISH
CD3	OKT_3	BV650	BioLegend	317324	x	x		x			
CD3	OKT_3	APC-eF780	eBioscience	47-0037-42			x			x	
CD3	OKT_3	BV510	BioLegend	317332						x	
CD3	OKT_3	APC	BioLegend	317318			x				
CD3	OKT_3	PerCP-Cy5.5	BioLegend	317336				x			
CD3	Poly	Unconjugated	Dako	A0452							x
CD4	OKT_4	eF450	eBioscience	48-0048-42	x	x		x		x	
CD4	OKT_4	PerCP-Cy5.5	BioLegend	317428			x				
CD8	SK1	Alexa Fluor 488	BioLegend	344716	x	x					
CD8	SK1	APC-eF780	eBioscience	47-0087-42			x		x	x	
CD8	SK1	PerCP Cy5.5	BioLegend	344710	x					x	
CD8	SK1	PE	BD Biosciences	340046				x			
CD8	4B11	Unconjugated	Novocastra	NCL-L-CD8-4B11							x
CD8b/NHP	SIDI8BEE	eF660	eBioscience	50-5273-41	x	x					
CD28	CD28.2	BV605	BD Horizon	562976	x	x					
CD28	CD28.2	APC	BioLegend	302912	x	x					
CD28	CD28.2	PE	BioLegend	302908	x	x					
CD45	HI30	BV510	BioLegend	304036			x	x	x		
CD45	HI30	Ax700	BioLegend	304024	x						
CD45	2D1	APC-H7	BD Biosciences	560178	x	x				x	
CD45-RA	HI100	APC-eF780	eBioscience	47-0458-42	x					x	
CD45-RA	HI100	PE-Cy7	eBioscience	25-0458-42			x			x	
CD45-RO	UCHL1	APC	eBioscience	17-0457-42							
CD103	B-Ly7	PE-Cy7	BioLegend	350212	x	x	x	x	x		
CD103	Ber-ACT8	BV605	BioLegend	350218						x	
CD103	Ber-ACT8	PE-Cy7	BioLegend	350212						x	
CD103	B-Ly7	FITC	eBioscience	11-1038-42	x						
CD62-L (L-Sel)	SK11	FITC	BD Pharmingen	347443	x						
CD127 (IL7-R)	Hil7r-m21	PE	BD Pharmingen	561028	x	x				x	
CD127 (IL7-R)	Hil7r-m21	BV605	BD Horizon	562662	x	x					
CD161 (KLRB1)	HP-3G10	BV605	BioLegend	339915	x	x					
CD244 (SLAMF4)	2B4	APC	BioLegend	329511	x	x					
CCR7 (CD197)	G043H7	PE	BioLegend	353203	x						
CCR7 (CD197)	G043H7	PE-dazzle594	BioLegend	353235	x						
PD-1 (CD279)	EH12.1	BV605	BD Horizon	563245	x	x					
KLRG1	13F12F2	APC	eBioscience	17-9488-42	x	x	x	x	x	x	
KLRG1	13F12F2	PE	eBioscience	12-9488-42	x	x	x		x		
NKG2D	1D11	PE	BioLegend	320805	x	x					

References

Horneland, R., V. Paulsen, J.P. Lindahl, K. Grzyb, T.J. Eide, K. Lundin, L. Aabakken, T. Jenssen, E.M. Aandahl, A. Foss, and O. Øyen. 2015. Pancreas transplantation with enteroanastomosis to native duodenum poses technical challenges--but offers improved endoscopic access for scheduled biopsies and therapeutic interventions. *Am. J. Transplant.* 15:242–250. https://doi.org/10.1111/ajt.12953

Pedreira, C.E., E.S. Costa, S. Barrena, Q. Lecrevisse, J. Almeida, J.J. van Dongen, and A. Orfao. EuroFlow Consortium. 2008. Generation of flow cytometry data files with a potentially infinite number of dimensions. *Cytometry A.* 73:834–846. https://doi.org/10.1002/cyto.a.20608

II

CD4+ T cells persist for years in the human small intestine and mediate robust T_H1 immunity

Raquel Bartolomé Casado[1][*], Ole J.B. Landsverk[1], Sudhir Kumar Chauhan[1,2], Frank Sætre[1],

Kjersti Thorvaldsen Hagen[1], Sheraz Yaqub[3], Ole Øyen[4], Rune Horneland[4], Einar Martin

Aandahl[2,4], Lars Aabakken[5], Espen S. Bækkevold[1], Frode L. Jahnsen[1][*]

[1]*Department of Pathology, Oslo University Hospital and University of Oslo, Oslo, Norway.*
[2]*Department of Cancer Immunology, Institute for Cancer Research, Oslo University Hospital, Oslo, Norway*
[3]*Department of Gastrointestinal Surgery, Oslo University Hospital, Rikshospitalet, Oslo, Norway*
[4]*Department of Transplantation Medicine, Section for Transplant Surgery, Oslo University Hospital, Rikshospitalet, Oslo, Norway.*
[5]*Department of Gastroenterology, Oslo University Hospital - Rikshospitalet, Oslo, Norway*

[*] Correspondence: r.b.casado@medisin.uio.no ; f.l.jahnsen@medisin.uio.no

Abbreviations:

IE, intraepithelial

LP, lamina propria

RPMI, Roswell Park Memorial Institute medium

SI, small intestine

T_{RM}, resident memory T cell

Tx, pancreatic-duodenal transplantation (of diabetes mellitus patients)

Keywords: Tissue-resident lymphocytes; CD4+ T cells; memory T cells; human small intestine; longevity; transplantation

Abstract:

Studies in mice and humans have shown that CD8^{+} T cell immunosurveillance in non-lymphoid tissues is dominated by resident populations. Whether CD4^{+} T cells use the same strategies to survey peripheral tissues is less clear. Here, examining the turnover of CD4^{+} T cells in transplanted duodenum in humans, we demonstrate that the majority of CD4^{+} T cells were still donor-derived one year after transplantation. In contrast to memory CD4^{+} T cells in peripheral blood, intestinal CD4^{+} T_{RM} cells expressed CD69 and CD161, but only a minor fraction expressed CD103. Functionally, intestinal CD4^{+} T_{RM} cells were very potent cytokine producers; the vast majority being polyfunctional T_H1 cells, whereas a minor fraction produced IL-17. Interestingly, a fraction of intestinal CD4^{+} T cells produced granzyme-B and perforin after activation. Together, we show that the intestinal CD4^{+} T-cell compartment is dominated by resident populations that survive for more than 1 year. This finding is of high relevance for the development of oral vaccines and therapies for diseases in the gut.

Introduction

Studies of mouse models of infection have shown that CD8^{+} T cells remain in peripheral tissues long after pathogen clearance (Masopust et al., 2001). These long-lived CD8^{+} T cells have limited potential to recirculate and have been termed resident memory T (T_{RM}) cells (Masopust and Soerens, 2019; Mueller and Mackay, 2016; Szabo et al., 2019). Moreover, CD8^{+} T_{RM} cells show an extraordinary ability to mount rapid and potent *in situ* responses after infectious re-exposure (Beura et al., 2018; Park et al., 2018; Schenkel et al., 2013). The currently most established markers to identify CD8^{+} T_{RM} cells in barrier tissues are CD69 and CD103 (Bartolome-Casado et al., 2019; Mackay et al., 2013; Snyder et al., 2019) . CD69 is rapidly upregulated after arrival into the tissue (Klonowski et al., 2004), and plays a key role preventing tissue egress by antagonizing sphingosine 1-phosphate receptor (S1PR1) (Skon et al., 2013). CD103 (also known as α_E integrin) is highly expressed on intraepithelial lymphocytes (IELs) and the heterodimer $\alpha_E\beta_7$ binds E-cadherin on the surface of epithelial cells (Cepek et al., 1994; Schon et al., 1999), promoting the accumulation of IELs in the epithelium.

Although CD4^{+} T cells are more abundant than CD8^{+} T cells in most peripheral tissues (Sathaliyawala et al., 2013), studies to understand T_{RM} cell biology have mainly focused on CD8^{+} T cells. Over the last decade, CD4^{+} T_{RM} cells have been identified in lungs (Hondowicz et al., 2016; Teijaro et al., 2011), skin (Glennie et al., 2015; Watanabe et al., 2015) and the reproductive tract (Iijima and Iwasaki, 2014). However, the CD4^{+} T_{RM} population seems to be more heterogeneous and functionally plastic compared to CD8^{+} T_{RM} cells (Becattini et al., 2015; Brucklacher-Waldert et al., 2014), and whether CD4^{+} T cells in peripheral tissues are truly resident, non-circulatory cells is still a matter of debate (Carbone and Gebhardt, 2019).

CD103 as well as CD69 are induced by TGF-β, which is constitutively produced by gut epithelial cells (Zhang and Bevan, 2013). At human mucosal sites, most CD4^{+} T cells express CD69, but few express CD103 compared to CD8^{+} T_{RM} cells (Sathaliyawala et al., 2013), and both CD103^{-} and CD103^{+} CD4^{+} T subsets have been described in different tissues, such as lung (Oja et al., 2018; Snyder et al., 2019) and skin (Watanabe et al., 2015). Intestinal CD4^{+} T_{RM} cells have shown to play a critical role in protection against different pathogens, including *C. rodentium* (Bishu et al., 2019) and *Listeria* (Romagnoli et al., 2017) in mouse models. Although our knowledge about the role of intestinal CD4^{+} T-cell effector subsets in the pathogenesis of inflammatory bowel disease (IBD) (Kleinschek et al., 2009; Lamb et al., 2017; Zundler et al., 2019) and coeliac disease (Christophersen et al., 2019; Risnes et al., 2018) have substantially progressed over the last decade, our current understanding of CD4^{+} T-cell immunosurveillance and long-term persistence in the human intestine remains incomplete.

We have recently reported that the majority of CD8^{+} T cells persists for years in human small intestine (Bartolome-Casado et al., 2019), however, it is still unknown whether CD4^{+} T cells share these features with their CD8^{+} counterparts. Here, we present a comprehensive study of the longevity and phenotype of intestinal CD4^{+} T cells in humans. In a unique transplantation setting we followed the persistence of donor-derived CD4^{+} T cells in grafted duodenum over time and found that the majority of donor CD4^{+} T cells are maintained for at least one year in the graft. Furthermore, both CD103^{-} and CD103^{+} CD4^{+} T cell populations presented very similar turnover rates, suggesting that both constitute T_{RM} populations. Finally, we showed that the vast majority of both CD103^{-} and CD103^{+} CD4^{+} T_{RM} cells were polyfunctional T_H1 cells and a fraction produced cytotoxic granules after activation.

Results

Human intestinal CD4⁺ T cells are phenotypically distinct from their circulating counterparts

To identify CD4⁺ T cells with a T_{RM}-phenotype in the human small intestine (SI) we first studied the CD4⁺ T-cell compartment under steady state conditions. For this purpose we collected SI specimens from proximal duodenum-jejunum resections of patients undergoing pancreatic cancer surgery (Whipple procedure, n = 35; mean age 63yr; 16 female), and from donors and recipients during pancreatic-duodenal Tx (baseline samples, donors: n = 52; mean age 31yr; 24 female; patients: n = 36; mean age 41yr; 14 female). All tissue samples were evaluated by experienced pathologists and only histologically normal SI was included. Single-cell suspensions from epithelium and enzyme-digested lamina propria (LP) were obtained and analyzed by flow cytometry together with peripheral blood mononuclear cells (PBMCs) from the patients. To characterize the phenotypic profile of SI CD4⁺ T cells, we performed flow-cytometry analysis using a panel of antibodies that we recently implemented to study SI CD8⁺ T_{RM} cells (Bartolome-Casado et al., 2019). CD4⁺ T cells comprised almost 60% of LP T cells (with a CD4⁺: CD8⁺ ratio similar to PB), but constituted only 10% of T cells in the epithelium (**Figure S1A-B**). The relative distribution of T cell subsets was conserved in mucosal biopsies sampled up to 35 cm apart from the same intestinal resection (**Figure S1C**).

Applying a dimensionality reduction technique (UMAP, Uniform Manifold Approximation and Projection) on the compiled flow cytometry data we found that all SI CD4⁺ T cells clustered separate from PB CD4⁺ T cells (**Figure 1A, left**). The vast majority of the SI CD4⁺ T cells presented a CD45RA⁻ CD45RO⁺ L-Sel⁻ CCR7⁻ effector memory (T_{EM}) phenotype (**Figure 1A-C**). In contrast, PB CD4⁺ T cells contained a substantial fraction of naïve (T_N, CD45RO⁻ CD45RA⁺ CCR7⁺ L-Sel⁺) and central memory (T_{CM}, CD45RO⁺ CD45RA⁻ CCR7⁺ L-Sel⁺) CD4⁺ T cells (**Figure 1A-C**). Virtually all SI CD4⁺ T cells expressed the T_{RM} marker CD69 whereas all PB CD4⁺ T cells were CD69-negative (**Figure 1A, C**). The SI CD4⁺ T cells were separated into three clusters based on their differential expression of CD103 and KLRG1 (**Figure 1A**). The population expressing CD103 comprised on average 18% of the LP and 66% of IE CD4⁺ T cells (**Figure 1C, left**), whereas KLRG1 was expressed by 26% and 5% of LP and IE CD4⁺ T cells, respectively (**Figure 1D**). PB CD4⁺ T cells were completely negative for CD103, however a fraction (mean 19%) of PB CD4⁺ T_{EM} cells expressed KLRG1 (**Figure 1A and D**). PB CD4⁺ T_{EM} and

SI CD4$^+$ T cells showed similar expression of PD1, CD127 (IL-7 receptor- α) and NKG2D. In contrast, CD28 was significantly higher expressed on PB CD4$^+$ T$_{EM}$ cells, whereas CD161 was expressed at higher levels on SI CD4$^+$ T cells (**Figure 1A and D**). In addition, the immunomodulatory receptor CD244 (2B4) was expressed higher on the IE subset. In line with other reports (Kumar et al., 2017), we also found that the negative regulator CD101 was highly expressed by the SI CD4$^+$ T cells (**Figure 1S-D**). Given that one of the SI CD4$^+$ T-cell clusters was enriched in cells expressing the T$_{RM}$ marker CD103 (**Figure 1A**), we examined the differential phenotypic profile of CD103$^+$ and CD103$^-$ CD4$^+$ T cells in LP and in the epithelium. CD103$^-$ CD4$^+$ T cells presented a higher fraction of KLRG1 positive cells in both compartments, while IE CD103$^+$ CD4$^+$ T cells exhibited significantly higher expression of 2B4. Otherwise we found only small differences between the CD103$^+$ and CD103$^-$ subsets (representative histograms in **Figure 1E** and compiled data in **Figure S1E**).

Taken together, these results show that SI CD4$^+$ T cells were clearly different from their blood counterparts, being CD69$^+$ CD103$^{+/-}$ CD161$^+$ CD28^{low}. The phenotype of IE CD4$^+$ T cells was very similar to IE CD8$^+$ cells; the majority being CD103$^+$ KLRG1$^-$ 2B4$^+$.

CD4$^+$ T$_{RM}$ cells persist for >1 yr in the transplanted SI

To directly examine the longevity of CD4$^+$ T$_{RM}$ cells in human SI, we assessed the long-term persistence of donor CD4$^+$ T cells in endoscopic biopsies obtained from grafted duodenum at 3, 6 and 52 weeks after pancreatic-duodenal transplantation (Tx) of type I diabetic patients (Horneland et al., 2015). Only patients without histological or clinical signs of rejection were included (n=32). Most donors and recipients expressed different human leukocyte antigen (HLA) type I molecules rendering it possible to distinguish donor cells from incoming recipient cells in the graft by flow cytometry **(Figure 2A-B)**. The CD103$^-$ and CD103$^+$ CD4$^+$ T cells were analyzed separately. At 3 and 6 weeks, LP and IE CD4$^+$ T cells exhibited very low replacement (median >85% donor cells), with no significant differences between the CD103$^-$ and CD103$^+$ CD4$^+$ T subsets **(Figure 2B)**. Importantly, also 1-yr after Tx the majority of SI CD4$^+$ T cells in both the LP and IE compartments were donor-derived, the fraction being slightly higher for LP CD103$^+$ compared to CD103$^-$ CD4$^+$ T cells (medians 77% and 60%, respectively). However, the majority of CD103$^-$ CD4$^+$ T cells were still of donor origin at 1 yr post-Tx, demonstrating that CD103 expression is not required for the persistence of CD4$^+$ T$_{RM}$

cells in human SI. In line with this, the turnover of both IE and LP CD103$^+$ and CD103$^-$ cells was highly correlated at 1 yr post-Tx (**Figure 2C**). Moreover, at 1 yr post-Tx the CD103$^-$ and CD103$^+$ CD4$^+$ T-cell subsets contained a similar (or higher) proportion of donor cells compared to donor CD8$^+$ T cell subsets (**Figure 2D**) (Bartolome-Casado et al., 2019). To confirm the persistence of donor CD4$^+$ T cells we performed immunostaining with anti-CD3 and anti-CD4 antibodies combined with fluorescent *in situ* hybridization probes specific for X/Y-chromosomes on tissue sections where recipients and donors were of different gender and consistently observed donor-derived CD4$^+$ T cells in the graft 1-yr after Tx (**Figure 2E**).

These results showed that the majority of donor-derived SI CD4$^+$ T cells persisted at least 1 yr (possibly years) in the tissue. However, to exclude effects of the surgical trauma, immunosuppressive treatment and leukocyte chimerism on the SI CD4$^+$ T-cell population, we examined the absolute T-cell counts in SI over time. Serial tissue sections were stained for CD3 and CD8, scanned and counted. The density of CD4$^+$ T cells was determined by subtracting the number of CD8$^+$ cells from the total CD3$^+$ cell count. We found that the overall density of both CD4$^+$ and CD8$^+$ T cells in Tx duodenum was stable throughout the 1-yr follow-up period (**Figure S2A-B**). Intracellular staining of single cell suspensions from Tx biopsies with the proliferation marker Ki67 showed few Ki67-positive cells among the donor CD4$^+$ T cells (**Figure S2C-D**). The percentage of Ki67$^+$ CD4$^+$ T cells was similar to that seen in the native duodenum in Tx patients and in steady state controls (**Figure S2D**), indicating that proliferation did not contribute substantially to the large number of persisting donor CD4$^+$ T cells in transplanted SI. Finally, we confirmed that the CD4$^+$ T cells in the native (recipient) duodenum were exclusively recipient-derived (**Figure S3**), demonstrating that migration of donor cells out of the graft was not occurring.

In conclusion, these results show that the CD4$^+$ T$_{RM}$ cell population includes both CD103$^-$ and CD103$^+$ cells, and that CD4$^+$ T$_{RM}$ cells are at least as persistent as CD103$^+$ CD8$^+$ T$_{RM}$ cells (Bartolome-Casado et al., 2019) in the transplanted SI.

Incoming recipient CD4$^+$ T cells undergo gradual phenotypic changes over time in transplanted duodenum

Transplanted SI gives us a unique opportunity to study the differentiation of recruited incoming CD4$^+$ T cells and whether they acquire a T$_{RM}$ phenotype in SI mucosa. To this end,

we compared the expression of T$_{RM}$ associated markers on donor- and recipient- derived LP CD4$^+$ T cells from biopsies of transplanted duodenum over time. Already at 3 wk post-Tx, virtually all recipient LP CD4$^+$ T cells expressed CD69 (**Figure 3A**). More than half of recipient CD4$^+$ T cells expressed CD161 at 6 weeks and that was further increased at 1-yr post Tx to similar levels as donor CD4$^+$ T cells (**Figure 3B**). CD103 was expressed on a minor subset of recipient-derived CD4$^+$ T cells at both 6 and 52 weeks; slightly lower than that on donor CD4$^+$ T cells (**Figure 3C, E**). In contrast, the fraction of KLRG1-positive cells within donor and recipient-derived CD4$^+$ T cells remained almost unchanged (**Figure 3D-E**). Similarly to the steady state conditions (**Figure 1A**), the majority of the LP CD4$^+$ T cells were CD103$^-$ KLRG1$^-$ at all the time points regardless of their origin (**Figure 3E**). Furthermore, the turnover of donor LP CD103$^-$ KLRG1$^-$ and CD103$^-$ KLRG1$^+$ CD4$^+$ T cells were very similar, evidenced by the high correlation of donor-derived cells within both subsets over time (**Figure 3F**).

Together, we find that recipient CD4$^+$ T cells recruited to the transplanted duodenum rapidly acquire phenotypic features similar to persistent donor CD4$^+$ T cells (**Figure 2**), suggesting that they gradually differentiate into T$_{RM}$ *in situ*.

The majority of SI CD4$^+$ T cells exhibits a polyfunctional T$_H$1 profile

To examine the functional properties of SI CD4$^+$ T cells we studied their cytokine expression profile and ability to produce cytotoxic granules. First, LP CD4$^+$ T cells isolated from histologically normal SI were short-term stimulated with PMA and Ionomycin and intracellular staining was perform with antibodies targeting specific cytokines (**Table S1**). By flow-cytometric analysis we found that the majority of the LP CD4$^+$ T cells, both CD103$^-$ and CD103$^+$, produced IFN-γ, IL-2 and TNF-α **(Figure 4A)**. Almost half of the cells produced all these three cytokines simultaneously **(Figure 4B-C)**, and we did not find significant differences between CD103$^-$ KLRG1$^+$ and KLRG1$^-$ cells (**Figure S4A**). In contrast, triple-producing cells constituted only 4% of the memory CD4$^+$ T cells in PB **(Figure 4B-C)**. Comparing the LP CD103$^-$ and CD103$^+$ subsets, we found significantly higher fraction of IL-17 and MIP1-β-producing cells within the CD103$^+$ subset compared to CD103$^-$ CD4$^+$ T cell subset **(Figure 4A)**. Furthermore, CD103$^+$ CD4$^+$ T cells contained a higher fraction of IFN-γ$^+$ IL-17$^+$ double producing cells **(Figure 4D)**. In contrast, CD103$^-$ CD4$^+$ T cells presented higher numbers of IL-13-producing cells than their

CD103^{+} counterparts, whereas comparable expression of IL-10 and IL-22 was found in the two subsets **(Figure 4A)**.

Murine CD4^{+} T$_{RM}$ cells have exhibited upregulation of granzyme-B upon reactivation with their cognate antigen (Beura et al., 2019). We therefore analyzed the capacity of SI CD4^{+} T cells to produce granzyme-B or perforin at the steady state and after stimulation with anti-CD3/CD28 beads. In the absence of stimulation, very few cells expressed these cytolytic proteins, however, both LP CD103^{-} and CD103^{+} subsets increased their expression of granzyme-B and perforin after activation **(Figure 5)**. We found a significantly higher proportion of granzyme-B producing cells within the LP CD103^{+} subset as compared to the CD103^{-} CD4^{+} T cell subset **(Figure 5)**. On the other hand, no significant differences were found in the activation-induced production of perforin between either subsets. **(Figure 5).** Comparing the KLRG1^{+} and KLRG1^{-} cells in the LP CD103^{-} compartment, we found higher basal levels of granzyme-B among the KLRG1^{+} cells (**Figure S4B**), but similar levels of granzyme-B and perforin after stimulation (**Figure S4B-C**).

These data show that the majority of the SI CD4^{+} T$_{RM}$ cells are polyfunctional T$_H$1 cells, with a large fraction co-producing IFN-γ, IL-2 and TNF-α. A fraction of CD4[+] T$_{RM}$ cells also produces the cytotoxic proteins granzyme-B and perforin after stimulation.

Discussion

Over the last years it has been demonstrated that immunosurveillance by memory CD8^{+} T cell in barrier tissues is largely mediated by durable, resident cell populations. However, whether memory CD4^{+} T cells use similar surveillance strategies is less clear (Carbone and Gebhardt, 2019; Homann et al., 2001; Snyder et al., 2019; Watanabe et al., 2015). Here, we show that the majority of CD4^{+} T cells are persistent for at least for 1 yr in the human SI mucosa, where they exhibit robust effector functions including polyfunctional T$_H$1 responses.

There is conflicting evidence with regards to the long-term residency of memory CD4^{+} T cells in barrier tissues. Studies of CD4^{+} T$_{RM}$ cells using parabiotic mice have suggested that CD4^{+} T-cell surveillance in the skin was dependent on continuous recirculation rather than permanent residency (Collins et al., 2016; Gebhardt et al., 2011). However, evidence of CD4^{+} T$_{RM}$ cells persistence has been reported in other peripheral tissues, such as the reproductive

mucosa and lung (Iijima and Iwasaki, 2014; Teijaro et al., 2011). Similarly, Beura et al. recently demonstrated that residency is the dominant mechanism of memory CD4$^+$ T-cell immunosurveillance in non-lymphoid tissues, but they did not evaluate the longevity (Beura et al., 2019). Moreover, in a recent study Klicznik and colleagues discovered a population of skin CD103$^+$ CD69$^+$ CD4$^+$ T cells that were able to downregulate CD69 expression and enter the circulation, indicating that some CD4$^+$ T$_{RM}$ cells may retain migratory potential (Klicznik et al., 2019).

In mouse models of infection, the number of antigen-specific memory CD4$^+$ T cells in lymphoid and non-lymphoid tissues seem to decline faster than CD8$^+$ T cells (Cauley et al., 2002; Homann et al., 2001), suggesting that memory CD4$^+$ T cells are less durable. In line with these results, donor CD4$^+$ T cells in lung transplanted patients were more rapidly lost than CD8$^+$ T cells (Snyder et al., 2019). Here, we found that donor CD4$^+$ T cells were maintained in duodenal grafts at equal or even higher numbers than CD103$^+$ CD8$^+$ T cells 1 yr after transplantation, without any change in cell density. In fact, in several patients more than 80% of the CD4$^+$ T cells were donor-derived at 1 yr. It is reasonable to assume that the host response to an organ transplantation would increase, rather than decrease, the replacement kinetics of immune cells in the graft (Eguiluz-Gracia et al., 2016; Snyder et al., 2019; Zuber et al., 2016), together indicating that most CD4$^+$ T cells in human SI are non-circulating, resident cells that most likely perpetuate for years.

Similar to intestinal CD8$^+$ T$_{RM}$ cells (Bartolome-Casado et al., 2019), we found that virtually all the SI CD4$^+$ T cells expressed CD69 and CD161. However, unlike CD8$^+$ T cells, only a minor fraction of LP CD4$^+$ T cells expressed the α_E integrin, CD103. While CD103$^-$ CD8$^+$ T cells very rapidly turned over in transplanted duodenum (**Figure 2E** and (Bartolome-Casado et al., 2019)), both CD103$^-$ and CD103$^+$ CD4$^+$ T cells showed a similar persistence. These results show that retention of CD4$^+$ T cells is independent of CD103, in line with previous reports (Romagnoli et al., 2017).

Like murine CD4$^+$ T$_{RM}$ cells (Iijima and Iwasaki, 2014; Romagnoli et al., 2017), the vast majority of LP CD4$^+$ T$_{RM}$ cells exhibited a polyfunctional T$_H$1 profile, producing high amounts of IFN-γ, IL-2 and TNF-α . The fraction of polyfunctional T$_H$1 cells among SI CD4$^+$ T cells was much higher than among memory CD4$^+$ T cells in blood. Furthermore, >40% of the CD4$^+$ T$_{RM}$ cells expressed granzyme-B after stimulation. These results show that SI CD4$^+$ T$_{RM}$ cells, like

CD8+ T$_{RM}$ cells, undergo tissue-specific changes that make them poised to provide robust T$_H$1 immunity in response to reinfections (Beura et al., 2019; Pope et al., 2001). In addition to protection against pathogens (Romagnoli et al., 2017), long-lived CD4+ T cell responses to commensal bacteria have been found during acute gastrointestinal infection with *T. gondii* (Hand et al., 2012). Moreover, microbiota-specific CD4+ T cells have been identified in blood and intestinal biopsies from healthy humans (Hegazy et al., 2017), indicating that CD4+ T$_{RM}$ cells may actively contribute to intestinal homeostasis through interactions with the microbiota.

We found that a fraction of CD4+ T$_{RM}$ cells produced IL-17. T$_H$17 cells play an important role in intestinal inflammatory disorders (Kleinschek et al., 2009; Ouyang et al., 2008; Yang et al., 2014; Zundler et al., 2019), however IL-17 is also critical for maintaining mucosal barrier integrity (Martinez-Lopez et al., 2019; Ouyang et al., 2008). Recently it was reported that, in contrast to inflammatory T$_H$17 cells elicited by pathogens, gut commensal bacteria elicited tissue-resident homeostatic T$_H$17 cells, which showed limited capacity to produce inflammatory cytokines (Omenetti et al., 2019). In our study only a very small percentage of T$_H$17 cells co-produced the inflammatory cytokine IFN-γ, suggesting that the majority of SI T$_H$17 cells during homeostasis are non-inflammatory cells that support barrier integrity. However, further studies are needed to understand the role of SI T$_H$17 cells under homeostatic and inflammatory conditions.

Finally, we found, although marginally, that CD103+ T$_{RM}$ cells contained higher fractions of IL-17 single- and IL-17/IFN-γ double-producing cells than their CD103- counterparts. Moreover, CD103- and CD103+ CD4+ T cells also showed subtle phenotypic differences regarding their expression of KLRG1, CD28 and 2B4. However, to what extent the CD103+ and CD103- subsets represents distinct functional subsets needs further investigation.

In conclusion, we provide evidence that the majority of memory CD4+ T cells in the human SI are resident and may persist in the tissue for >1 year. This indicates that residency constitute the dominant mechanism for CD4+ memory T cell immunosurveillance in the human SI, and should be explored for the development of oral vaccines as well as for strategies to treat CD4+ T-cell mediated inflammatory intestinal diseases.

Materials and Methods

Patient samples.

Small intestinal samples were either obtained during pancreatic cancer surgery (Whipple procedure, n = 35; mean age 63yr; range 40-81yr; 16 female), or from donors and/or patients during pancreas-duodenum transplantation (donors: n = 52; mean age 31yr; range 5-55yr; 24 female; patients: n = 36; mean age 41yr; range 25-60yr; 14 female) as described previously (Bartolome-Casado et al., 2019). Cancer patients receiving neoadjuvant chemotherapy were excluded from the study. Endoscopic biopsies from donor and patient duodenum were collected at 3, 6 and 52 weeks after transplantation. All tissue specimens were evaluated blindly by experienced pathologists, and only material with normal histology was included (Ruiz et al., 2010). All transplanted patients received a standard immunosuppressive regimen (Horneland et al., 2015), and patients showing clinical or histological signs of rejection or other complications, as well as patients presenting pre-transplant or *de novo* donor specific antibodies (DSA) were excluded from the study. Blood samples were collected at the time of the surgery and buffy coats from healthy donors (Oslo University Hospital). All participants gave their written informed consent. The study was approved by the Regional Committee for Medical Research Ethics in Southeast Norway and complies with the Declaration of Helsinki.

Preparation of intestinal and peripheral blood single-cell suspensions

Intestinal resections were opened longitudinally and rinsed with PBS, and mucosa was dissected in strips off the submucosa. For microscopy, small mucosal pieces were fixed in 4% formalin and embedded in paraffin according to standard protocols. Intestinal mucosa was washed 3 times in PBS containing 2mM EDTA and 1% FCS at 37°C with shaking for 20 minutes and filtered through nylon 100-µm mesh to remove epithelial cells. Epithelial fractions in each washing step were pooled and filtered through 100-µm cell strainers (BD, Falcon). Epithelial cells in the EDTA fraction were depleted by incubation with anti-human epithelial antigen antibody (clone Ber-EP4, Dako) followed by anti-mouse IgG dynabeads (ThermoFisher) according to the manufacture's protocol. De-epithelialized LP was minced and digested in complete RPMI medium (supplemented with 1% Pen/Strep) containing 0.25 mg/mL Liberase TL and 20 U/mL DNase I (both from Roche), stirring at 37°C for 1h. Digested tissue was filtered twice through 100-µm cell strainers and washed tree times in PBS. Purity of both IE and LP

fractions was checked by flow-cytometry (Bartolome-Casado et al., 2019). Intestinal biopsies from transplanted patients were processed in the same way. PBMCs were isolated by Ficoll-based density gradient centrifugation (Lymphoprep™, Axis-Shield).

Flow cytometry

Single cell suspensions of intestinal LP and IE fractions and PBMCs were stained using different multicolor combinations of directly conjugated monoclonal antibodies (**Table S1**). To assess the expression of L-Selectin on digested tissue, cells were rested for 12h at 37°C before the immunostaining. Replacement of donor cells in duodenal biopsies of HLA mismatched transplanted patients was assessed using different HLA type I allotype-specific antibodies targeting donor- and/or recipient-derived cells, and stroma cells were used as a control of specific staining. Dead cells were excluded based on propidium iodide staining (Molecular Probes, Life Technologies). For analysis of cytokine production, LP and IE cell suspensions were stimulated for 4h with control complete medium (RPMI supplemented with 10% FCS, 1% Pen/Strep) or phorbol-12-myristate-13-acetate PMA (1.5 ng/mL) and ionomycin (1μg/mL; both from Sigma-Aldrich) in the presence of monensin (Golgi Stop, BD Biosciences) added after 1h of stimulation to allow intracellular accumulation of cytokines. Cells were stained using the BD Cytofix/Cytoperm kit (BD Biosciences) according to the manufacturer's instructions, and stained with antibodies against several cytokines (**Table S1**). For detection of cytotoxic granules, LP and IE cells were activated for 21h with anti-CD3/CD28 beads (Dynabeads, ThermoFisher) or control complete medium. For detection of intranuclear Ki67 expression the FoxP3/transcription factor staining buffer set was used according to the manufacturer's instructions. eFluor-450 or eFluor-780 fixable viability dyes (eBioscience) were used prior any intracellular/intranuclear staining procedure. All samples were acquired on LSR Fortessa flow cytometer (BD Biosciences), using FACSDiva software (BD Biosciences). Single stained controls were prepared for compensation (UltraComp eBeads™, eBioscience), and gates were adjusted by comparison with FMO controls or matched isotype controls. Flow cytometry data were analyzed using FlowJo 10.4.2 (Tree Star). For **Figure 1A**, the expression of 16 phenotypic markers was analyzed at the single cell-level and compared for CD4$^+$ T cells in PB, LP and IE (n=3) using the merge and calculation functions of Infinicyt software (Cytognos), as described in detail elsewhere (Pedreira et al., 2013). The population within the

CD4$^+$ T-cell gate was down-sampled for each compartment and exported to a new file, and then concatenated and subjected to UAMP analysis using the plugin integrated in FlowJo 10.5.3 as in (Bartolome-Casado et al., 2019). All experiments were performed at the Flow Cytometry Core Facility, Oslo University Hospital.

Microscopy.

Analysis of chimerism was performed as described previously (Landsverk et al., 2017). Briefly, formalin-fixed 4-μm sections were washed sequentially in xylene, ethanol, and PBS. Heat-induced epitope retrieval was performed by boiling sections for 20min in Dako buffer. Sections were incubated with CEP X SpectrumOrange/Y SpectrumGreen DNA Probes (Abbott Molecular Inc.) for 12h at 37°C before immunostaining according to standard protocol with anti-CD3 (Polyclonal; Dako), anti-CD4 (clone 1F6, Leica Biosystems) and secondary antibodies targeting rabbit IgG or mouse IgG2b conjugated to Alexa Fluor 647 and 555, respectively. Laser scanning confocal microscopy was performed on an Olympus FV1000 (BX61WI) system. Image z stacks were acquired at 1-μm intervals and combined using the Z project max intensity function in Image J (National Institutes of Health), and all microscopy images were assembled in Photoshop and Illustrator CC (Adobe).

CD8 and CD3 immunoenzymatic staining was performed on formalin-fixed 4-μm sections, dewaxed in xylene and rehydrated in ethanol, and prepared with Vulcan Fast red kit (Biocare Medical) following standard protocols. In brief, heat-induced antigen retrieval was performed in Tris/EDTA pH9 buffer (EnVision FLEX Dako kit, K8010), followed by staining with primary antibody (CD8 clone 4B11, Novocastra or CD3, polyclonal, Dako), secondary anti- mouse AP-conjugated antibody and incubation with substrate (Fast red chromogen, Biocare Medical). Slides were counterstained with hematoxylin and excess of dye was removed by bluing in ammoniac water. Tissue sections were scanned using Pannoramic Midi slide scanner (3DHISTECH) and counts generated with QuPath software (Bankhead et al., 2017).

Statistical analysis

Statistical analyses were performed in Prism 8 (GraphPad Software). To assess statistical significance among SI CD4$^+$ T cell subsets, data were analyzed by one-way ANOVA (standard or repeated measures, RM-ANOVA) followed by Tukey's multiple comparison tests.

Replacement data and distribution of CD4$^+$ T cell subsets at different time points were analyzed by two-way ANOVA matching across subsets followed by Tukey's multiple comparison tests. Correlations between replacement kinetics of different CD4$^+$ T cell subsets were calculated using Pearson correlation with two-tailed p-value (95% confidence interval). P-values of <0.05 were considered significant.

References:

Bankhead, P., M.B. Loughrey, J.A. Fernandez, Y. Dombrowski, D.G. McArt, P.D. Dunne, S. McQuaid, R.T. Gray, L.J. Murray, H.G. Coleman, J.A. James, M. Salto-Tellez, and P.W. Hamilton. 2017. QuPath: Open source software for digital pathology image analysis. *Sci Rep* 7:16878.

Bartolome-Casado, R., O.J.B. Landsverk, S.K. Chauhan, L. Richter, D. Phung, V. Greiff, L.F. Risnes, Y. Yao, R.S. Neumann, S. Yaqub, O. Oyen, R. Horneland, E.M. Aandahl, V. Paulsen, L.M. Sollid, S.W. Qiao, E.S. Baekkevold, and F.L. Jahnsen. 2019. Resident memory CD8 T cells persist for years in human small intestine. *J Exp Med*

Becattini, S., D. Latorre, F. Mele, M. Foglierini, C. De Gregorio, A. Cassotta, B. Fernandez, S. Kelderman, T.N. Schumacher, D. Corti, A. Lanzavecchia, and F. Sallusto. 2015. T cell immunity. Functional heterogeneity of human memory CD4(+) T cell clones primed by pathogens or vaccines. *Science* 347:400-406.

Beura, L.K., N.J. Fares-Frederickson, E.M. Steinert, M.C. Scott, E.A. Thompson, K.A. Fraser, J.M. Schenkel, V. Vezys, and D. Masopust. 2019. CD4+ resident memory T cells dominate immunosurveillance and orchestrate local recall responses. *The Journal of Experimental Medicine*

Beura, L.K., J.S. Mitchell, E.A. Thompson, J.M. Schenkel, J. Mohammed, S. Wijeyesinghe, R. Fonseca, B.J. Burbach, H.D. Hickman, V. Vezys, B.T. Fife, and D. Masopust. 2018. Intravital mucosal imaging of CD8(+) resident memory T cells shows tissue-autonomous recall responses that amplify secondary memory. *Nat Immunol* 19:173-182.

Bishu, S., G. Hou, M. El Zaatari, S.R. Bishu, D. Popke, M. Zhang, H. Grasberger, W. Zou, R.W. Stidham, P.D.R. Higgins, J.R. Spence, N. Kamada, and J.Y. Kao. 2019. Citrobacter rodentium Induces Tissue-Resident Memory CD4(+) T Cells. *Infect Immun* 87:

Brucklacher-Waldert, V., E.J. Carr, M.A. Linterman, and M. Veldhoen. 2014. Cellular Plasticity of CD4+ T Cells in the Intestine. *Front Immunol* 5:488.

Carbone, F.R., and T. Gebhardt. 2019. Should I stay or should I go-Reconciling clashing perspectives on CD4(+) tissue-resident memory T cells. *Sci Immunol* 4:

Cauley, L.S., T. Cookenham, T.B. Miller, P.S. Adams, K.M. Vignali, D.A. Vignali, and D.L. Woodland. 2002. Cutting edge: virus-specific CD4+ memory T cells in nonlymphoid tissues express a highly activated phenotype. *J Immunol* 169:6655-6658.

Cepek, K.L., S.K. Shaw, C.M. Parker, G.J. Russell, J.S. Morrow, D.L. Rimm, and M.B. Brenner. 1994. Adhesion between epithelial cells and T lymphocytes mediated by E-cadherin and the alpha E beta 7 integrin. *Nature* 372:190-193.

Christophersen, A., E.G. Lund, O. Snir, E. Sola, C. Kanduri, S. Dahal-Koirala, S. Zuhlke, O. Molberg, P.J. Utz, M. Rohani-Pichavant, J.F. Simard, C.L. Dekker, K.E.A. Lundin, L.M. Sollid, and M.M. Davis. 2019. Distinct phenotype of CD4(+) T cells driving celiac disease identified in multiple autoimmune conditions. *Nat Med* 25:734-737.

Collins, N., X. Jiang, A. Zaid, B.L. Macleod, J. Li, C.O. Park, A. Haque, S. Bedoui, W.R. Heath, S.N. Mueller, T.S. Kupper, T. Gebhardt, and F.R. Carbone. 2016. Skin CD4(+) memory T cells exhibit combined cluster-mediated retention and equilibration with the circulation. *Nat Commun* 7:11514.

Eguiluz-Gracia, I., H.H. Schultz, L.I. Sikkeland, E. Danilova, A.M. Holm, C.J. Pronk, W.W. Agace, M. Iversen, C. Andersen, F.L. Jahnsen, and E.S. Baekkevold. 2016. Long-term persistence of human donor alveolar macrophages in lung transplant recipients. *Thorax* 71:1006-1011.

Gebhardt, T., P.G. Whitney, A. Zaid, L.K. Mackay, A.G. Brooks, W.R. Heath, F.R. Carbone, and S.N. Mueller. 2011. Different patterns of peripheral migration by memory CD4+ and CD8+ T cells. *Nature* 477:216-219.

Glennie, N.D., V.A. Yeramilli, D.P. Beiting, S.W. Volk, C.T. Weaver, and P. Scott. 2015. Skin-resident memory CD4+ T cells enhance protection against Leishmania major infection. *J Exp Med* 212:1405-1414.

Hand, T.W., L.M. Dos Santos, N. Bouladoux, M.J. Molloy, A.J. Pagan, M. Pepper, C.L. Maynard, C.O. Elson, 3rd, and Y. Belkaid. 2012. Acute gastrointestinal infection induces long-lived microbiota-specific T cell responses. *Science* 337:1553-1556.

Hegazy, A.N., N.R. West, M.J.T. Stubbington, E. Wendt, K.I.M. Suijker, A. Datsi, S. This, C. Danne, S. Campion, S.H. Duncan, B.M.J. Owens, H.H. Uhlig, A. McMichael, I.B.D.C.I. Oxford, A. Bergthaler, S.A. Teichmann, S. Keshav, and F. Powrie. 2017. Circulating and Tissue-Resident CD4(+) T Cells With Reactivity to Intestinal Microbiota Are Abundant in Healthy Individuals and Function Is Altered During Inflammation. *Gastroenterology* 153:1320-1337 e1316.

Homann, D., L. Teyton, and M.B. Oldstone. 2001. Differential regulation of antiviral T-cell immunity results in stable CD8+ but declining CD4+ T-cell memory. *Nat Med* 7:913-919.

Hondowicz, B.D., D. An, J.M. Schenkel, K.S. Kim, H.R. Steach, A.T. Krishnamurty, G.J. Keitany, E.N. Garza, K.A. Fraser, J.J. Moon, W.A. Altemeier, D. Masopust, and M. Pepper. 2016. Interleukin-2-Dependent Allergen-Specific Tissue-Resident Memory Cells Drive Asthma. *Immunity* 44:155-166.

Horneland, R., V. Paulsen, J.P. Lindahl, K. Grzyb, T.J. Eide, K. Lundin, L. Aabakken, T. Jenssen, E.M. Aandahl, A. Foss, and O. Oyen. 2015. Pancreas transplantation with enteroanastomosis to native duodenum poses technical challenges--but offers improved endoscopic access for scheduled biopsies and therapeutic interventions. *Am J Transplant* 15:242-250.

Iijima, N., and A. Iwasaki. 2014. T cell memory. A local macrophage chemokine network sustains protective tissue-resident memory CD4 T cells. *Science* 346:93-98.

Kleinschek, M.A., K. Boniface, S. Sadekova, J. Grein, E.E. Murphy, S.P. Turner, L. Raskin, B. Desai, W.A. Faubion, R. de Waal Malefyt, R.H. Pierce, T. McClanahan, and R.A. Kastelein. 2009. Circulating and gut-resident human Th17 cells express CD161 and promote intestinal inflammation. *J Exp Med* 206:525-534.

Klicznik, M.M., P.A. Morawski, B. Höllbacher, S.R. Varkhande, S.J. Motley, L. Kuri-Cervantes, E. Goodwin, M.D. Rosenblum, S.A. Long, G. Brachtl, T. Duhen, M.R. Betts, D.J. Campbell, and I.K. Gratz. 2019. Human CD4+CD103+ cutaneous resident memory T cells are found in the circulation of healthy individuals. *Science Immunology* 4:

Klonowski, K.D., K.J. Williams, A.L. Marzo, D.A. Blair, E.G. Lingenheld, and L. Lefrançois. 2004. Dynamics of Blood-Borne CD8 Memory T Cell Migration In Vivo. *Immunity* 20:551-562.

Kumar, B.V., W. Ma, M. Miron, T. Granot, R.S. Guyer, D.J. Carpenter, T. Senda, X. Sun, S.H. Ho, H. Lerner, A.L. Friedman, Y. Shen, and D.L. Farber. 2017. Human Tissue-Resident Memory T Cells Are Defined by Core Transcriptional and Functional Signatures in Lymphoid and Mucosal Sites. *Cell Rep* 20:2921-2934.

Lamb, C.A., J.C. Mansfield, G.W. Tew, D. Gibbons, A.K. Long, P. Irving, L. Diehl, J. Eastham-Anderson, M.B. Price, G. O'Boyle, D.E.J. Jones, S. O'Byrne, A. Hayday, M.E. Keir, J.G. Egen, and J.A. Kirby. 2017. alphaEbeta7 Integrin Identifies Subsets of Pro-Inflammatory Colonic CD4+ T Lymphocytes in Ulcerative Colitis. *J Crohns Colitis* 11:610-620.

Landsverk, O.J., O. Snir, R.B. Casado, L. Richter, J.E. Mold, P. Reu, R. Horneland, V. Paulsen, S. Yaqub, E.M. Aandahl, O.M. Oyen, H.S. Thorarensen, M. Salehpour, G. Possnert, J. Frisen, L.M. Sollid, E.S. Baekkevold, and F.L. Jahnsen. 2017. Antibody-secreting plasma cells persist for decades in human intestine. *J Exp Med* 214:309-317.

Mackay, L.K., A. Rahimpour, J.Z. Ma, N. Collins, A.T. Stock, M.L. Hafon, J. Vega-Ramos, P. Lauzurica, S.N. Mueller, T. Stefanovic, D.C. Tscharke, W.R. Heath, M. Inouye, F.R. Carbone, and T. Gebhardt. 2013. The developmental pathway for CD103(+)CD8+ tissue-resident memory T cells of skin. *Nat Immunol* 14:1294-1301.

Martinez-Lopez, M., S. Iborra, R. Conde-Garrosa, A. Mastrangelo, C. Danne, E.R. Mann, D.M. Reid, V. Gaboriau-Routhiau, M. Chaparro, M.P. Lorenzo, L. Minnerup, P. Saz-Leal, E. Slack, B. Kemp, J.P. Gisbert, A. Dzionek, M.J. Robinson, F.J. Ruperez, N. Cerf-Bensussan, G.D. Brown, D. Bernardo, S. LeibundGut-Landmann, and D. Sancho. 2019. Microbiota Sensing by Mincle-Syk Axis in Dendritic Cells Regulates Interleukin-17 and -22 Production and Promotes Intestinal Barrier Integrity. *Immunity* 50:446-461 e449.

Masopust, D., and A.G. Soerens. 2019. Tissue-Resident T Cells and Other Resident Leukocytes. *Annu Rev Immunol*

Masopust, D., V. Vezys, A.L. Marzo, and L. Lefrancois. 2001. Preferential localization of effector memory cells in nonlymphoid tissue. *Science* 291:2413-2417.

Mueller, S.N., and L.K. Mackay. 2016. Tissue-resident memory T cells: local specialists in immune defence. *Nat Rev Immunol* 16:79-89.

Oja, A.E., B. Piet, C. Helbig, R. Stark, D. van der Zwan, H. Blaauwgeers, E.B.M. Remmerswaal, D. Amsen, R.E. Jonkers, P.D. Moerland, M.A. Nolte, R.A.W. van Lier, and P. Hombrink. 2018. Trigger-happy resident memory CD4(+) T cells inhabit the human lungs. *Mucosal Immunol* 11:654-667.

Omenetti, S., C. Bussi, A. Metidji, A. Iseppon, S. Lee, M. Tolaini, Y. Li, G. Kelly, P. Chakravarty, S. Shoaie, M.G. Gutierrez, and B. Stockinger. 2019. The Intestine Harbors Functionally Distinct Homeostatic Tissue-Resident and Inflammatory Th17 Cells. *Immunity*

Ouyang, W., J.K. Kolls, and Y. Zheng. 2008. The biological functions of T helper 17 cell effector cytokines in inflammation. *Immunity* 28:454-467.

Park, S.L., A. Zaid, J.L. Hor, S.N. Christo, J.E. Prier, B. Davies, Y.O. Alexandre, J.L. Gregory, T.A. Russell, T. Gebhardt, F.R. Carbone, D.C. Tscharke, W.R. Heath, S.N. Mueller, and L.K. Mackay. 2018. Local proliferation maintains a stable pool of tissue-resident memory T cells after antiviral recall responses. *Nat Immunol* 19:183-191.

Pedreira, C.E., E.S. Costa, Q. Lecrevisse, J.J. van Dongen, A. Orfao, and C. EuroFlow. 2013. Overview of clinical flow cytometry data analysis: recent advances and future challenges. *Trends Biotechnol* 31:415-425.

Pope, C., S.K. Kim, A. Marzo, D. Masopust, K. Williams, J. Jiang, H. Shen, and L. Lefrancois. 2001. Organ-specific regulation of the CD8 T cell response to Listeria monocytogenes infection. *J Immunol* 166:3402-3409.

Risnes, L.F., A. Christophersen, S. Dahal-Koirala, R.S. Neumann, G.K. Sandve, V.K. Sarna, K.E. Lundin, S.W. Qiao, and L.M. Sollid. 2018. Disease-driving CD4+ T cell clonotypes persist for decades in celiac disease. *J Clin Invest* 128:2642-2650.

Romagnoli, P.A., H.H. Fu, Z. Qiu, C. Khairallah, Q.M. Pham, L. Puddington, K.M. Khanna, L. Lefrancois, and B.S. Sheridan. 2017. Differentiation of distinct long-lived memory CD4 T cells in intestinal tissues after oral Listeria monocytogenes infection. *Mucosal Immunol* 10:520-530.

Ruiz, P., H. Takahashi, V. Delacruz, E. Island, G. Selvaggi, S. Nishida, J. Moon, L. Smith, T. Asaoka, D. Levi, A. Tekin, and A.G. Tzakis. 2010. International grading scheme for acute cellular rejection in small-bowel transplantation: single-center experience. *Transplant Proc* 42:47-53.

Sathaliyawala, T., M. Kubota, N. Yudanin, D. Turner, P. Camp, J.J. Thome, K.L. Bickham, H. Lerner, M. Goldstein, M. Sykes, T. Kato, and D.L. Farber. 2013. Distribution and compartmentalization of human circulating and tissue-resident memory T cell subsets. *Immunity* 38:187-197.

Schenkel, J.M., K.A. Fraser, V. Vezys, and D. Masopust. 2013. Sensing and alarm function of resident memory CD8(+) T cells. *Nat Immunol* 14:509-513.

Schon, M.P., A. Arya, E.A. Murphy, C.M. Adams, U.G. Strauch, W.W. Agace, J. Marsal, J.P. Donohue, H. Her, D.R. Beier, S. Olson, L. Lefrancois, M.B. Brenner, M.J. Grusby, and C.M. Parker. 1999. Mucosal T lymphocyte numbers are selectively reduced in integrin alpha E (CD103)-deficient mice. *J Immunol* 162:6641-6649.

Skon, C.N., J.Y. Lee, K.G. Anderson, D. Masopust, K.A. Hogquist, and S.C. Jameson. 2013. Transcriptional downregulation of S1pr1 is required for the establishment of resident memory CD8(+) T cells. *Nature Immunology* 14:1285-+.

Snyder, M.E., M.O. Finlayson, T.J. Connors, P. Dogra, T. Senda, E. Bush, D. Carpenter, C. Marboe, L. Benvenuto, L. Shah, H. Robbins, J.L. Hook, M. Sykes, F. D'Ovidio, M. Bacchetta, J.R. Sonett, D.J. Lederer, S. Arcasoy, P.A. Sims, and D.L. Farber. 2019. Generation and persistence of human tissue-resident memory T cells in lung transplantation. *Sci Immunol* 4:

Szabo, P.A., M. Miron, and D.L. Farber. 2019. Location, location, location: Tissue resident memory T cells in mice and humans. *Sci Immunol* 4:

Teijaro, J.R., D. Turner, Q. Pham, E.J. Wherry, L. Lefrancois, and D.L. Farber. 2011. Cutting edge: Tissue-retentive lung memory CD4 T cells mediate optimal protection to respiratory virus infection. *J Immunol* 187:5510-5514.

Watanabe, R., A. Gehad, C. Yang, L.L. Scott, J.E. Teague, C. Schlapbach, C.P. Elco, V. Huang, T.R. Matos, T.S. Kupper, and R.A. Clark. 2015. Human skin is protected by four functionally and phenotypically discrete populations of resident and recirculating memory T cells. *Sci Transl Med* 7:279ra239.

Yang, J., M.S. Sundrud, J. Skepner, and T. Yamagata. 2014. Targeting Th17 cells in autoimmune diseases. *Trends Pharmacol Sci* 35:493-500.

Zhang, N., and M.J. Bevan. 2013. Transforming growth factor-beta signaling controls the formation and maintenance of gut-resident memory T cells by regulating migration and retention. *Immunity* 39:687-696.

Zuber, J., B. Shonts, S.P. Lau, A. Obradovic, J. Fu, S. Yang, M. Lambert, S. Coley, J. Weiner, J. Thome, S. DeWolf, D.L. Farber, Y. Shen, S. Caillat-Zucman, G. Bhagat, A. Griesemer, M. Martinez, T. Kato, and M. Sykes. 2016. Bidirectional intragraft alloreactivity drives the repopulation of human intestinal allografts and correlates with clinical outcome. *Sci Immunol* 1:

Zundler, S., E. Becker, M. Spocinska, M. Slawik, L. Parga-Vidal, R. Stark, M. Wiendl, R. Atreya, T. Rath, M. Leppkes, K. Hildner, R. Lopez-Posadas, S. Lukassen, A.B. Ekici, C. Neufert, I. Atreya, K. van Gisbergen, and M.F. Neurath. 2019. Hobit- and Blimp-1-driven CD4(+) tissue-resident memory T cells control chronic intestinal inflammation. *Nat Immunol*

Author contributions:

R. Bartolomé-Casado, O.J.B. Landsverk, E.S. Bækkevold, and F.L. Jahnsen conceived the project. R. Bartolomé-Casado, O.J.B. Landsverk, and S.K. Chauhan processed samples, designed and performed experiments, and analyzed data. R. Bartolomé-Casado prepared figures. F. Sætre and K.Thorvaldsen Hagen assisted with experiments and data analysis. S. Yaqub and R. Horneland coordinated recruitment of patients and collection of biopsies. S. Yaqub, R. Horneland, O. Øyen, and E.M. Aandahl performed surgery and provided samples. L. Aabakken performed endoscopy and provided endoscopic biopsies. R. Bartolomé-Casado and F.L. Jahnsen wrote the manuscript. O.J.B. Landsverk, F. Sætre and E.S. Baekkevold contributed to writing the manuscript, E.S. Baekkevold, and F.L. Jahnsen supervised the study.
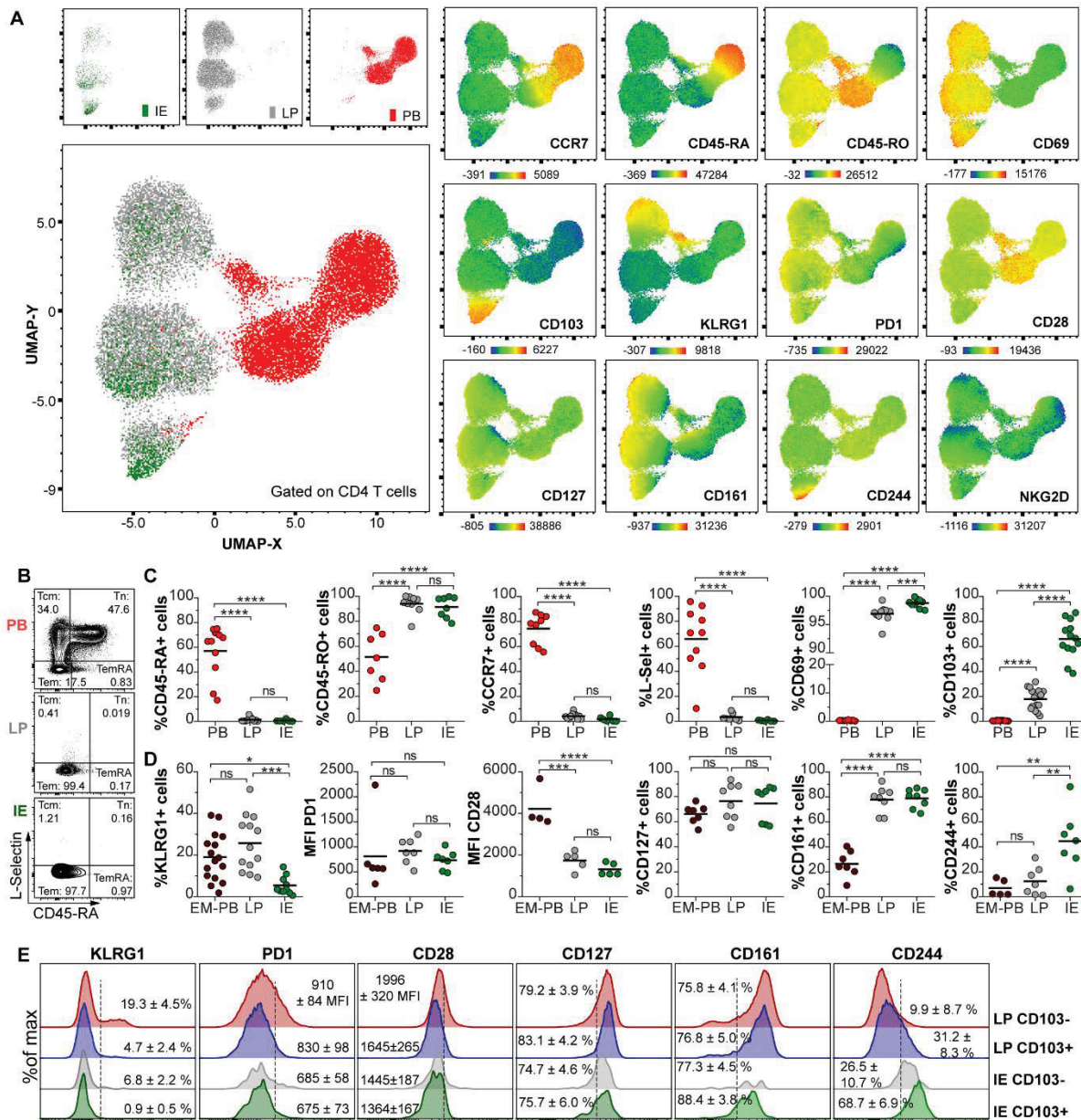
Figure 1. Human intestinal CD4⁺ T cells are phenotypically distinct from their circulating counterparts. (A) UMAP visualization after concatenation of flow-cytometric data from PB (red), LP (gray), and IE (green) CD4⁺ T cells, as described in (Bartolome-Casado et al., 2019). Representative of three samples. Map of the clusters and representation of each tissue compartment (left). Overlay of the UMAP clusters and the expression levels for each marker, color-coded based on the median fluorescence intensity values (MFI) (right). **(B)** Representative contour plots showing L-selectin and CD45RA expression on PB, LP and IE CD4⁺ T cells and classification of these cells into Tcm, central memory; Tem, effector memory; TemRA, effector memory re-expressing CD45RA; Tn, naïve. **(C)** Phenotypic comparison of total PB CD4⁺ T cells or **(D)** effector memory (EM) PB CD4⁺ T cells with intestinal LP, and IE CD4⁺ T cells. Compiled data for each marker are given and black bars indicate mean values. One-way ANOVA with Tukey's multiple comparisons test. ns, not significant; *, P ≤ 0.05; **, P ≤ 0.01 ***, P ≤ 0.001; ****, P ≤ 0.0001. **(E)**. Representative histograms showing the differential phenotypic profile of intestinal CD103⁻ and CD103⁺ CD4⁺ T cells from LP and IE for several T$_{RM}$-

related markers. Mean values and SEM is provided. Compiled data of all the experiments are shown in **Figure S1C**.
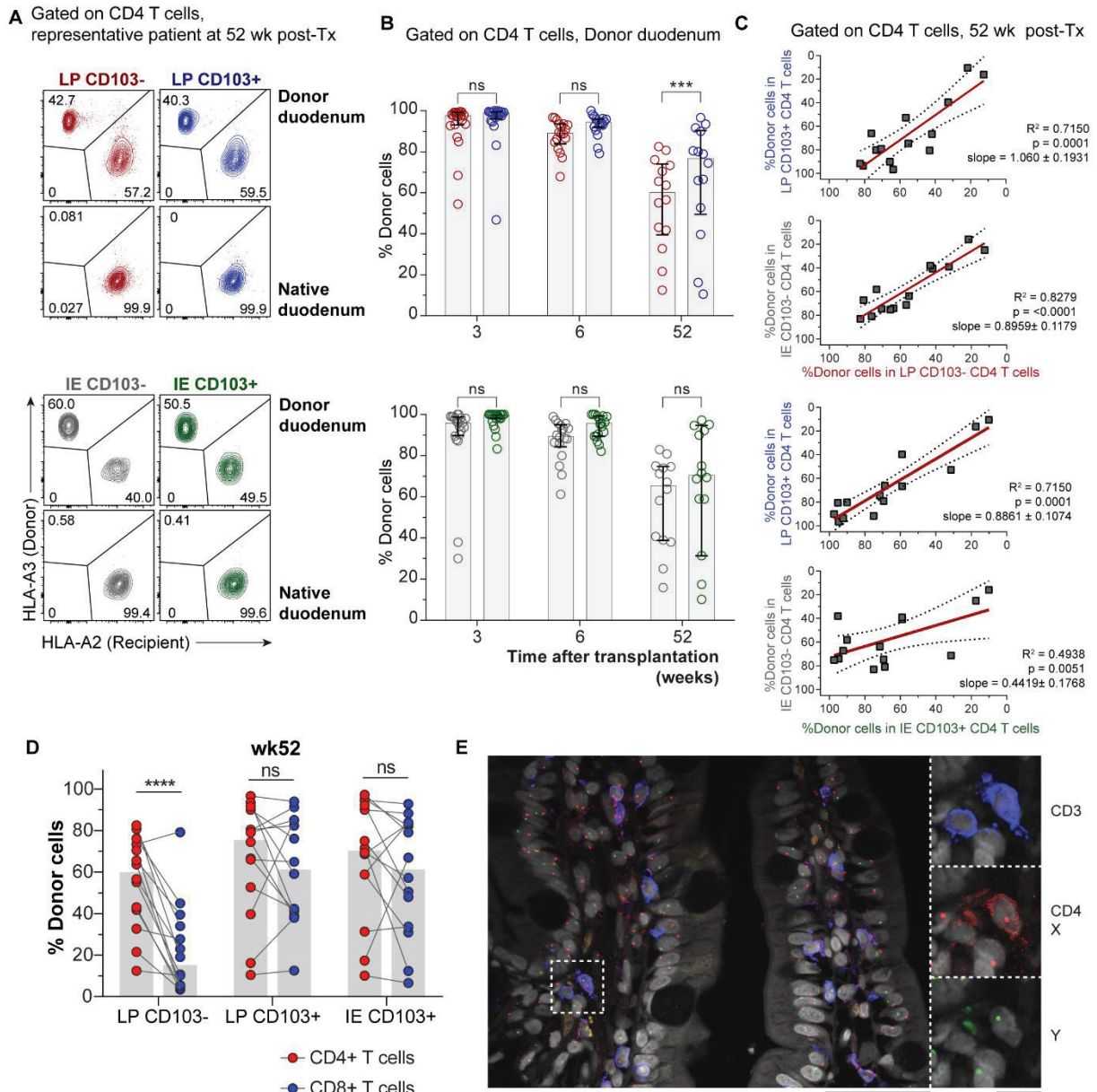

Figure 2. CD4⁺ T_RM cells persist for >1 yr in the transplanted SI

(A) Representative contour plots at 52 wk after Tx and **(B)** compile data for the fractions of donor-derived CD4⁺ T cells in LP CD103⁻ (red) and CD103⁺ (blue) compartments as well as IE CD103⁻ (grey) and CD103⁺ (green) at 3 (n = 20), 6 (n = 18), and 52 wk after Tx (n = 14) determined by HLA class I expression (as in A). Gray columns indicate median values. Statistical analysis was performed using two-way ANOVA for repeated measures (RM) with Tukey's multiple comparisons test. ns, not significant; ***, P ≤ 0.001; **(C)** Pearson correlation of the percentages of donor-derived cells in the above mentioned LP and IE CD4⁺ T cell subsets 1-yr after Tx. Statistics performed using two-tailed P value (95% confidence interval, n = 14). **(D)** Frequencies of persisting donor cells in different subsets of CD4⁺ and CD8⁺ T cells from the same biopsies of donor duodenum at 52 weeks (wk) post-Tx. Data for CD8⁺ T cells has been

previously published (Bartolome-Casado et al., 2019). Grey bars indicate median values. RM two-way ANOVA. ****, P ≤ 0.0001; ns, non-significant. **(E)** Representative confocal image of biopsies obtained from donor duodenum (male) of a female patient at one year post-transplantation. Tissue sections were stained with X/Y chromosome fluorescent in situ hybridization probes (Y, green; X, red) and antibodies against CD4 (red) and CD3 (blue). Hoechst (gray) stains individual nuclei. Scale bars, 50μm and 10μm, respectively.

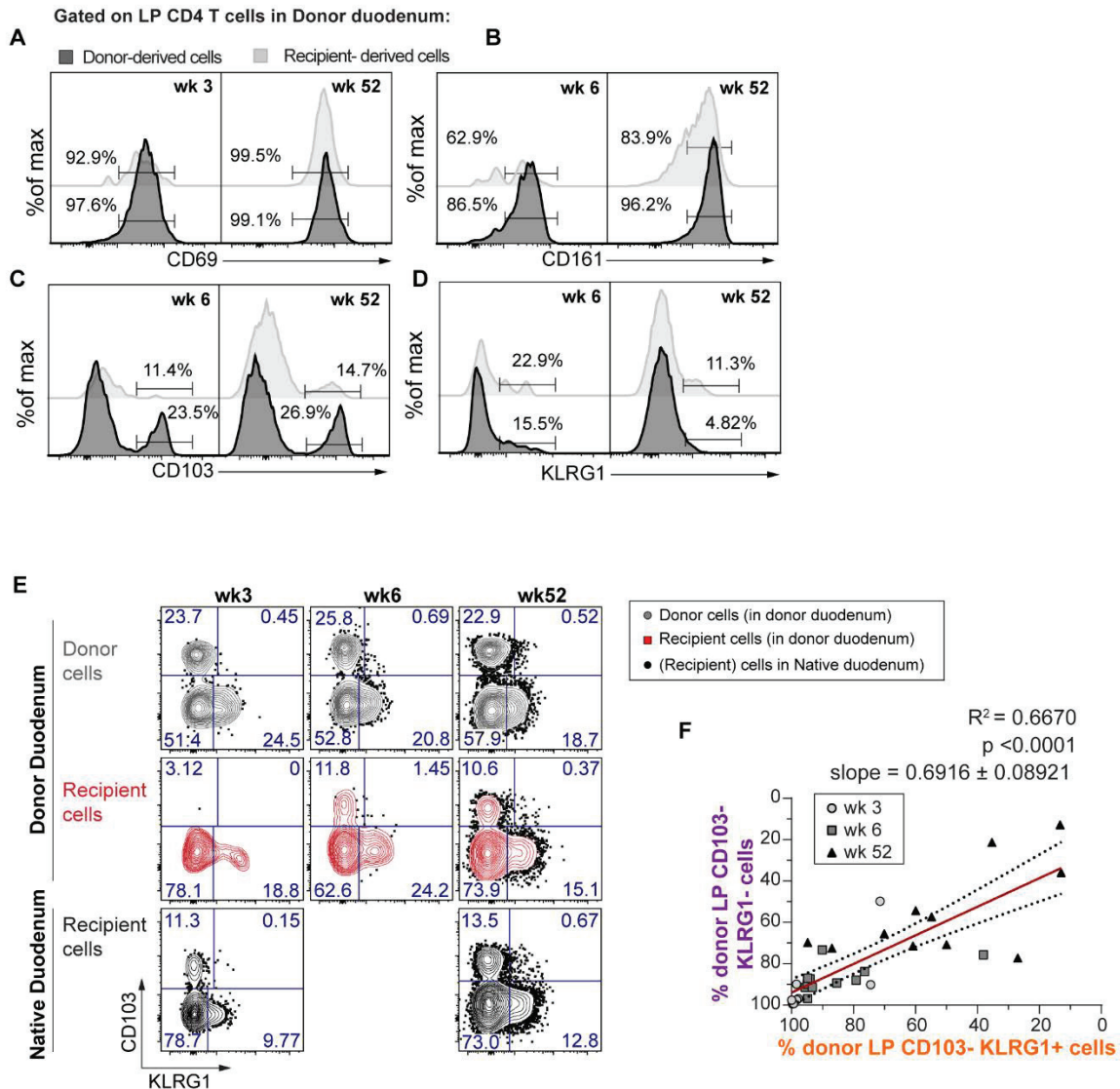**Figure 3. Incoming recipient CD4+ T cells undergo gradual phenotypic changes over time in transplanted duodenum (A-D)** Representative flow-cytometric analysis for the expression of different T_{RM} associated markers on donor-derived (black) and recipient- derived (light grey) LP CD4+ T cells from donor duodenum at the indicated weeks (wk) post-Tx. **(E)** Distribution of donor (grey) and recipient-derived (red) LP CD4+ T cells isolated from donor duodenum (above) and native duodenum (below, black) according to the expression of CD103 and KLRG1 at the indicated time-points after-Tx. **(F)** Pearson correlation of the percentages of donor-derived cells in LP CD103- KLRG1+ and KLRG1- CD4+ T cell subsets over time after Tx. Statistics performed using two-tailed P value (95% confidence interval, n = 32).
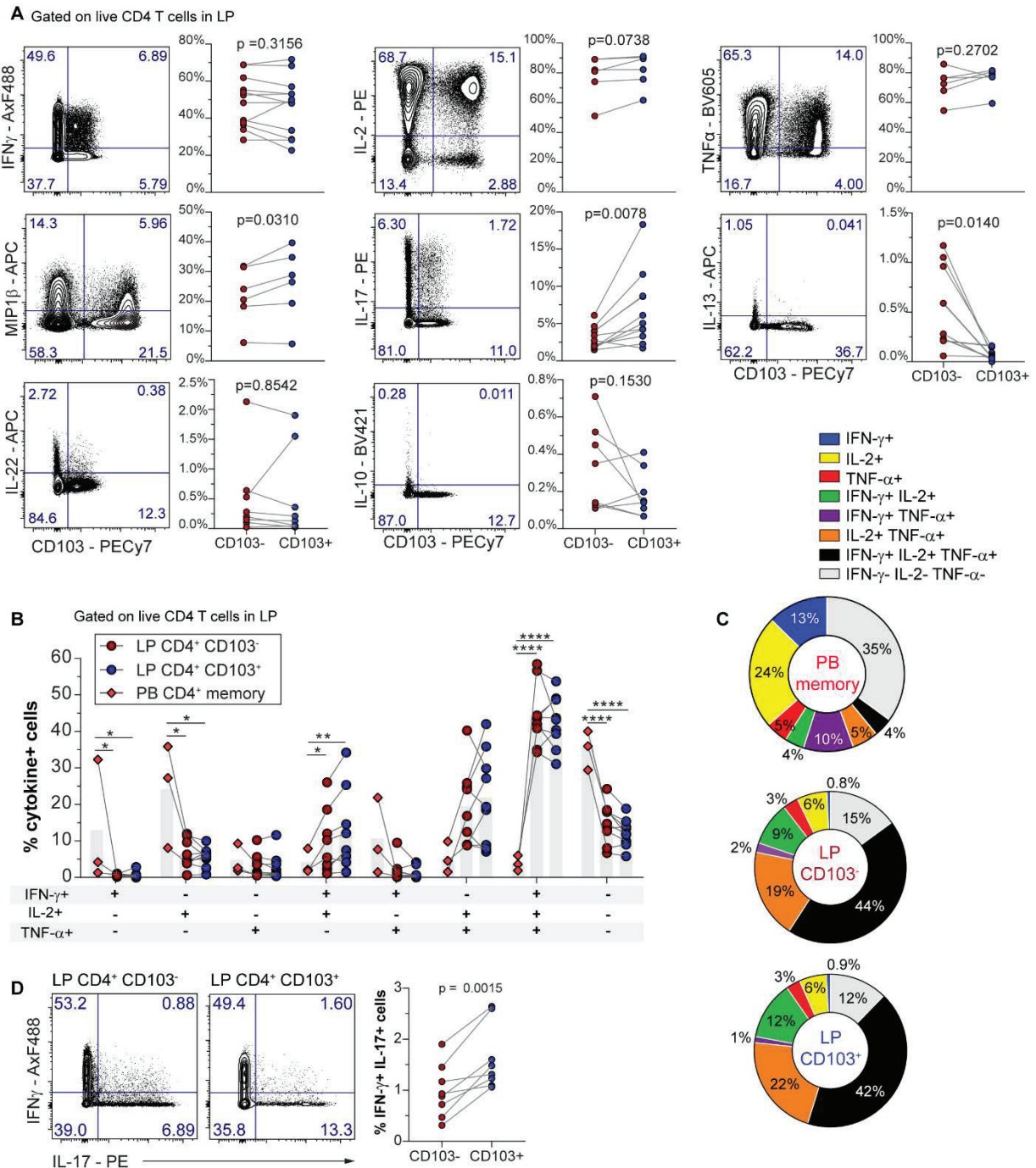
Figure 4. The majority of SI CD4⁺ T cells exhibits a polyfunctional T_H1 profile **(A)** Representative contour plots (left) and compiled data (right) showing PMA/ionomycin induced cytokine production by CD103⁻ compared to CD103⁺ LP CD4⁺ T cells. P values of paired t-test are displayed. **(B)** IFN-γ,IL-2 and TNF-α production by PB T_EM CD4⁺ T cells and intestinal LP CD103⁻, LP CD103⁺ CD4⁺ T cells. The bars indicate mean values. Statistics performed using one-way ANOVA for each combination of cytokines. **(C)** Relative fractions of each cytokine combination indicated in **(B)** by PB T_EM CD4⁺ T cells (n=3), and intestinal LP CD103⁻ (n=6) and LP CD103⁺ (n=6). CD4⁺ T cells represented on pie charts with color codes. Mean values of indicated experiments. **(D)** Representative contour plots (left) and compiled data (right) showing simultaneous IFN-γ and IL17 expression by LP CD103⁻ and CD103⁺ CD4⁺ T cells. Paired t-test.
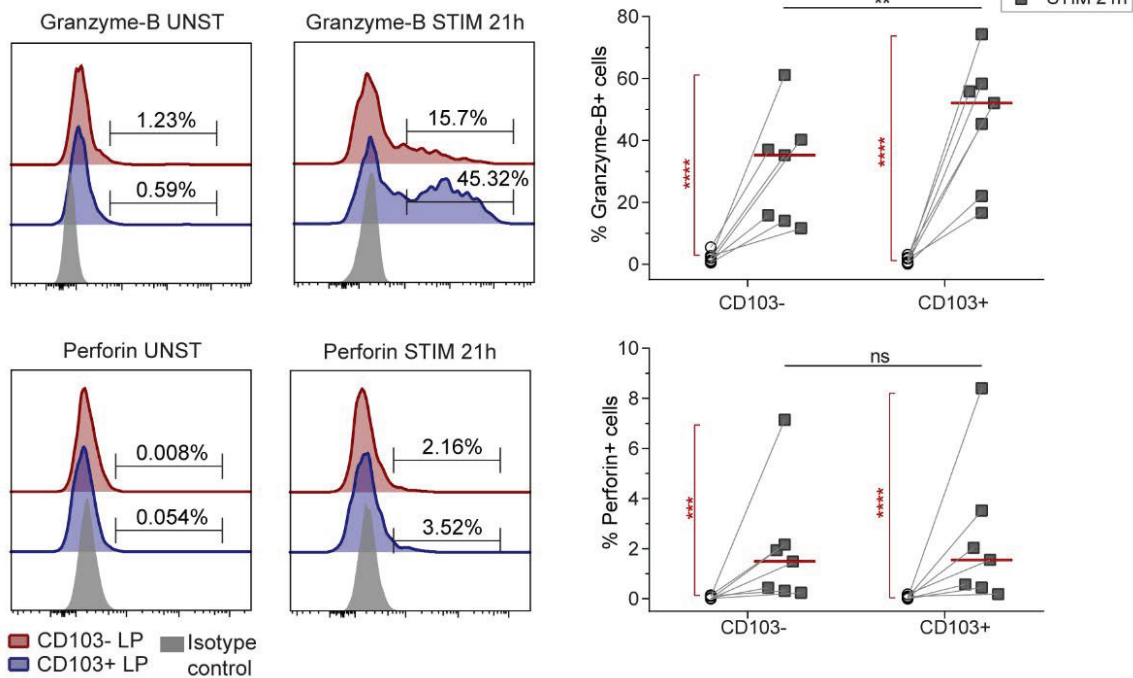
Figure 5. LP CD4$^+$ T cells produce cytotoxic granules after stimulation
Representative flow-cytometric histogram (left) and compiled data (right) for the intracellular expression of granzyme-B and perforin in LP CD103$^-$ and CD103$^+$ CD4$^+$ T cell subsets without (UNST) and after (STIM) stimulation with anti-CD3/CD28 beads for 21 h. Red lines indicate median values. Student's t test was applied to compare the expression of cytotoxic mediators by both subsets (black horizontal lines), and by unstimulated *versus* 21h stimulated cells (red vertical lines and asterisks). **, P ≤ 0.01; ns, not-significant.

Supplementary Materials

Table 1. Antibodies used in the study.

Figure S1. Extended phenotype of SI CD4$^+$ T cells, accompanies Figure 1.

Figure S2. Turnover of CD4$^+$ T cells in transplanted duodenum, accompanies Figure 2.

Figure S3. Absence of cross-contamination between donor and native (recipient) duodenum.

Figure S4. Comparative of the functional capabilities of LP CD103$^-$ KLRG1$^-$ and KLRG1$^+$ CD4$^+$ T cell subsets.

Table 1: Antibodies used in the study.

Target	Clone	Fluorophore	Company	Reference	Pheno-T$_{RM}$	PTx panel	Sorting	Ki67	Cyto-tox	Cytokines	X/Y FISH
CD3	OKT_3	BV650	Biolegend	317324	x	x		x			
CD3	OKT_3	APC-eF780	eBioscience	47-0037-42			x			x	
CD3	OKT_3	BV510	Biolegend	317332						x	
CD3	OKT_3	APC	Biolegend	317318			x				
CD3	OKT_3	PerCP-Cy5.5	Biolegend	317336				x			
CD3	Poly	unconj	Dako	A0452							x
CD4	OKT_4	eF450	eBioscience	48-0048-42	x	x		x		x	
CD4	OKT_4	PerCP-Cy5.5	Biolegend	317428			x				
CD4	1F6	unconj	Leica Biosystems	NCL-L-CD4-1F6							x
CD8	SK1	Alexa-Fluor488	Biolegend	344716	x	x					
CD8	SK1	APC-eF780	eBiosciences	47-0087-42			x		x	x	
CD8	SK1	PerCP Cy5.5	Biolegend	344710	x					x	
CD8	SK1	PE	BDB	340046				x			
CD8	4B11	unconj	Novocastra	NCL-L-CD8-4B11							x
CD8b /NHP	SIDI8BEE	eF660	eBioscience	50-5273-41	x	x					
CD28	CD28.2	BV605	BD Horizon	562976	x	x					
CD28	CD28.2	APC	Biolegend	302912	x	x					
CD28	CD28.2	PE	Biolegend	302908	x	x					
CD45	HI30	BV510	Biolegend	304036			x	x	x		
CD45	HI30	Ax700	Biolegend	304024	x						
CD45	2D1	APC-H7	BDB	560178	x	x				x	
CD45-RA	HI100	APC-eF780	eBiosciences	47-0458-42	x					x	
CD45-RA	HI100	PE-Cy7	eBiosciences	25-0458-42			x			x	
CD45-RO	UCHL1	APC	eBiosciences	17-0457-42	x						
CD62-L	SK11	FITC	BD Pharmingen	347443	x						
CD69	FN50	APC	Biolegend	310910	x						
CD103	B-Ly7	PE-Cy7	Biolegend	350212	x	x	x	x	x		
CD103	Ber-ACT8	BV605	Biolegend	350218						x	
CD103	Ber-ACT8	PE-Cy7	Biolegend	350212						x	
CD103	B-Ly7	FITC	eBioscience	11-1038-42	x					x	
CD127 (IL7-R)	Hil7r-m21	PE	BD-Pharm	561028	x	x				x	
CD127 (IL7-R)	Hil7r-m21	BV605	BD-Horizon	562662	x	x					
CD161 (KLRB1)	HP-3G10	BV605	Biolegend	339915	x	x					
CD244 (SLAMF4)	2B4	APC	Biolegend	329511	x	x					
CCR7 (CD197)	G043H7	PE	Biolegend	353203	x						
CCR7 (CD197)	G043H7	PE-dazzle594	Biolegend	353235	x						

Target	Clone	Fluorophore	Company	Reference	Pheno-T$_{RM}$	PTx panel	Sorting	Ki67	Cyto-tox	Cytokines	X/Y FISH
PD-1 (CD279)	EH12.1	BV605	BD-Horizon	563245	x	x					
KLRG1	13F12F2	APC	eBiosciences	17-9488-42	x	x	x	x	x	x	
KLRG1	13F12F2	PE	eBiosciences	12-9488-42	x	x	x		x		
NKG2D	1D11	PE	Biolegend	320805	x	x					
NKG2D	1D11	BV605	BDB	743559	x	x					
TCR-gd	5A6.E9	PE	Molecular Probes™, Invitrogen	MHGD04	x	x	x				
TCR-gd	5A6.E9	FITC	Molecular Probes™, Invitrogen	MHGD01		x	x				
Anti-Human Epithelial Ag	Ber-EP4	FITC	Dako	F0860			x				
HLA-A2	BB 7.2	PE	Abcam	ab79523		x					
HLA-A3	GAP.A3	FITC	eBioscience	11-5754-42		x					
HLA-A3	GAP.A3	APC	eBioscience	17-5754-42		x	x				
HLA-B7	BB7.1	PE	Millipore	MAB1288		x					
HLA-B8	REA145	PE	Miltenyi Biotech	130-118-960		x	x				
Granzyme-B	CLB-GB11	PE	SANQUIN (Dianova AS)	M2289					x		
Perforin	gG9	FITC	BD-Pharm	556577					x		
TNF-alpha	MAb11	BV605	Biolegend	502936						x	
IFNg	4S.B3	Ax488	Biolegend	502517						x	
IL-2	MQ1-17H12	PE	Biolegend	500306						x	
IL-10	JES3-9D7	BV421	BD-Horizon	564053						x	
IL-13	JES10-5A2	APC	Biolegend	501907						x	
IL-17	eBio64DEC17	PE	eBioscience	12-7179-41						x	
IL-22	22URTI	eF660	eBioscience	50-7229-41						x	
MIP1beta (CCL4)	FL3423L	APC	eBioscience	17-7540-41						x	
Ki67	B56	Ax488	BD-Pharm	558616				x			
Isotype mouse IgG1	MOPC-21	Ax488	BD-Pharm	555909				x	x		
Isotype mouse IgG2b	27-35	FITC	BD-Pharm	556577					x		
Isotype mouse IgG1	MOPC-31C	PE	BD-Pharm	550617					x		
Mouse IgG1	Polyclonal	Alexa 555	Molecular Probes™, Invitrogen	A-21147							x
Rabbit IgG (H+L)	Polyclonal	Alexa 647	Molecular Probes™, Invitrogen	A-31573							x

APC, allophycocyanin; Ax, Alexa Fluor; BV, brilliant violet; Cy7, cyanin7; eF, eFluor; FISH, fluorescence in situ hybridization; FITC, fluorescein isothiocyanate; H7, hilite7; PerCP-Cy5.5, peridinin–chlorophyll–protein cyanin5.5; unconj, unconjugated.
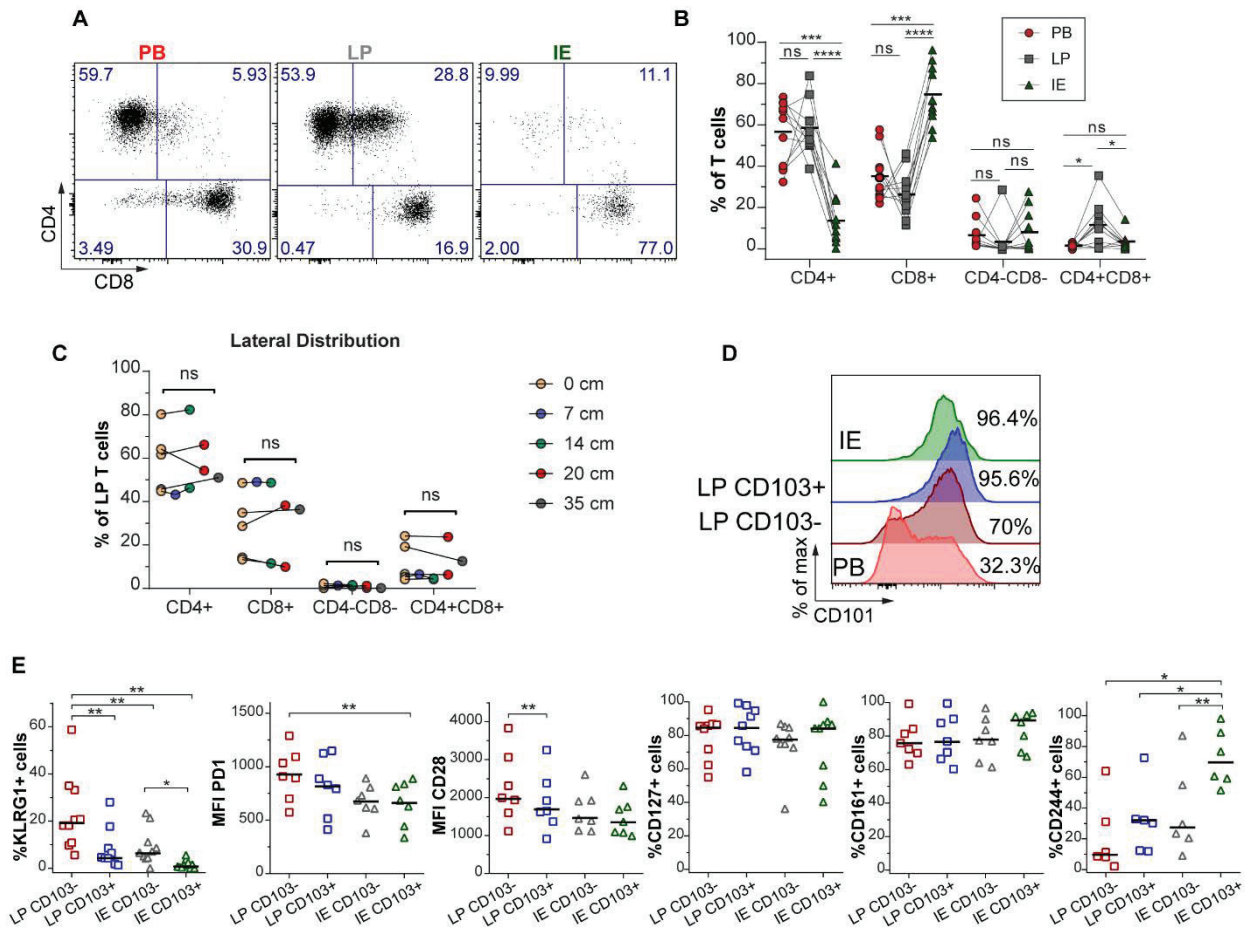
Figure S1. Extended phenotype of SI CD4+ T cells, accompanies Figure 1.
(A) Representative flow-cytometric dot-plot and **(B)** aggregated data for the distribution of T cell subsets in PB, LP, and IE fractions collected from the same patient. Black lines indicate mean value. Statistics performed using two-way ANOVA, repeated measures matching both factors, and Tukey's multiple comparison test. ns, not significant; *, P ≤ 0.05; ***, P ≤ 0.001; ****, P ≤ 0.0001. **(C)** Lengthwise representation of the CD4+ subsets in LP determined by flow cytometric analysis of biopsies taken at intervals along resected duodenum-proximal jejunum from individual subjects after Whipple procedure. n = 5; paired Student's t test comparing 0 cm to the farthest distance. ns, not significant. **(D)** Representative histogram showing the expression of CD101 on PB, CD103⁻ and CD103+ LP and IE CD4+ T cells. **(E)** Percentage of positive cells or MFI values for various markers on intestinal-derived CD103⁻ and CD103+ CD4+ T cells from LP and IE. Black bars indicate median values. Statistical analysis was performed using repeated-measures one-way ANOVA with Tukey's multiple comparisons test. *, P ≤ 0.05; **, P ≤ 0.01; all other comparisons are not significant.
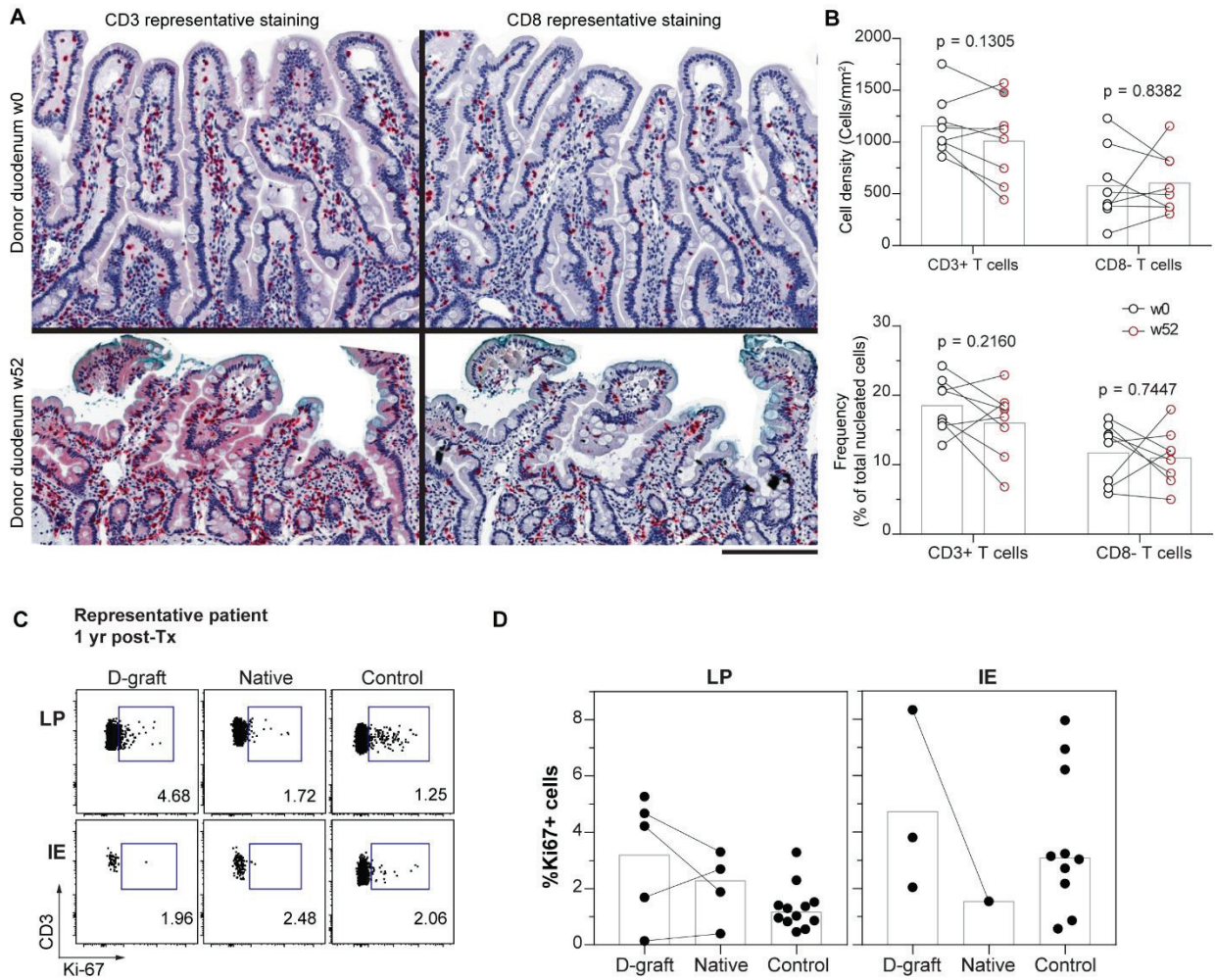
Figure S2. Turnover of CD4+ T cells in transplanted duodenum, accompanies Figure 2.
(A) Representative immunohistochemistry staining of CD3+ cells (left) and CD8+ T cells (right) on tissue sections from donor duodenum at baseline (w0) and 1-yr after Tx (w52). Scale bar, 200μm. **(B)** Compile data of CD3+ and CD8+ T cell counts on tissue sections from donor duodenum of representative patients (n=8) at baseline (w0, black) and 1-yr after Tx (w52, red). Paired t-test. **(C)** Representative dot plot showing Ki67 expression in donor- or recipient-derived CD4+ T cells in LP and epithelium (IE) isolated from biopsies of donor or native duodenum 1-yr after Tx and control intestinal resections. **(D)** Compiled data for the percentages of Ki67-positive cells in donor- or recipient-derived CD4+ T cells in LP and IE at different time points after Tx in donor or native duodenum and in control intestinal resections.

Fig. S3

Gated on CD4 T cells

Figure S3. Absence of cross-contamination between donor and native (recipient) duodenum. Frequencies of recipient cells within each CD4+ T-cell subset in biopsies from donor and recipient (native) duodenum of the same patients at different time points after Tx. Black horizontal lines represent median values, and error bars show interquartile ranges.

Figure S4. Comparative of the functional capabilities of LP CD103- KLRG1- and KLRG1+ CD4+ T cell subsets. (A) Frequency of polyfunctional (IL-2+, IFN-γ+ and TNF-α+) cells within LP CD103- KLRG1- and KLRG1+ subsets (n =4). **(B)** Frequencies of granzyme-B and **(C)** perforin positive cells in unstimulated samples (left) and after 21 h of activation with anti-CD3 beads (right) for the two subsets (KLRG1+, KLRG1−) of CD103- CD4+ T cells in LP. Paired student's t test between subsets (black) and unstimulated vs stimulated (red). Paired student's t test was applied to compare the two subsets. ns, not significant; **, P ≤ 0.01.

IV

JEM

Antibody-secreting plasma cells persist for decades in human intestine

Ole J.B. Landsverk,[1] Omri Snir,[2] Raquel Bartolomé Casado,[1]* Lisa Richter,[1]* Jeff E. Mold,[5] Pedro Réu,[5,6] Rune Horneland,[7] Vemund Paulsen,[7] Sheraz Yaqub,[8] Einar Martin Aandahl,[4,7] Ole M. Øyen,[7] Hildur Sif Thorarensen,[9] Mehran Salehpour,[10] Göran Possnert,[10] Jonas Frisén,[5] Ludvig M. Sollid,[3]** Espen S. Baekkevold,[1]** and Frode L. Jahnsen[1]**

[1]Department of Pathology, Centre for Immune Regulation, [2]Department of Immunology, Centre for Immune Regulation, [3]Department of Immunology, Centre for Immune Regulation and KG Jebsen Coeliac Disease Research Centre, and [4]Centre for Molecular Medicine Norway, Nordic European Molecular Biology Laboratory Partnership, Oslo University Hospital-Rikshospitalet and The University of Oslo, 0372 Oslo, Norway
[5]Department of Cell and Molecular Biology, Karolinska Institute, 171 77 Stockholm, Sweden
[6]Center for Neuroscience and Cell Biology, University of Coimbra, 3000-213 Coimbra, Portugal
[7]Department of Transplantation Medicine and [8]Department of Gastrointestinal Surgery, Oslo University Hospital-Rikshospitalet, 0372 Oslo, Norway
[9]Department of Informatics, University of Oslo, 0313 Oslo, Norway
[10]Department of Physics and Astronomy, Ion Physics, Uppsala University, 752 36 Uppsala, Sweden

Plasma cells (PCs) produce antibodies that mediate immunity after infection or vaccination. In contrast to PCs in the bone marrow, PCs in the gut have been considered short lived. In this study, we studied PC dynamics in the human small intestine by cell-turnover analysis in organ transplants and by retrospective cell birth dating measuring carbon-14 in genomic DNA. We identified three distinct PC subsets: a CD19+ PC subset was dynamically exchanged, whereas of two CD19− PC subsets, CD45+ PCs exhibited little and CD45− PCs no replacement and had a median age of 11 and 22 yr, respectively. Accumulation of CD45− PCs during ageing and the presence of rotavirus-specific clones entirely within the CD19− PC subsets support selection and maintenance of protective PCs for life in human intestine.

INTRODUCTION

Plasma cells (PCs) in the gut produce antibodies that are transported into the gut lumen and provide crucial protection against enteric microbiota. PCs are derived from B cells that have been primed and undergone class-switch recombination in gut-associated lymphoid tissues (Pabst, 2012). The intestine is exposed to a changing repertoire of microbial and dietary antigens and must continuously adapt by adjusting its immune repertoire. In an early study in mice, the half-life of gut PCs was estimated to be 4.7 d (Mattioli and Tomasi, 1973), leading to the prevailing notion that the intestinal PC repertoire is highly dynamic and temporally restricted in antigen specificity. However, in mice, specific antibodies could be detected 112 d after transient exposure to *Escherichia coli* (Hapfelmeier et al., 2010), and PCs generated after immunization with cholera toxin were found to persist in the lamina propria for up to 9 mo (Lemke et al., 2016). In humans, the existence of long-lived PCs in the gut is inferred from their survival in vitro for 4 wk in cultured small intestinal biopsies (Mesin et al., 2011), their phenotypic and transcriptomal

similarity with BM PCs (Nair et al., 2016), and the persistence of nonproliferating PCs in both ileum and colon for 234 d after CD19-directed chimeric antigen receptor T cell therapy (Bhoj et al., 2016). However, direct evidence of long-term persistence of human gut PCs is lacking.

RESULTS AND DISCUSSION

We used fluorescent in situ hybridization probes targeting X/Y chromosomes to discriminate between donor and recipient cells in biopsies from transplanted duodenum after mixed-gender pancreatic–duodenal transplantation (Ptx) of type I diabetes mellitus patients (Horneland et al., 2015) and found that most CD38+ PCs remained of donor origin 1 yr after transplantation (Fig. 1 A). To investigate the characteristics of these persisting PCs, we applied a flow cytometry–based strategy on single-cell suspensions from duodenal-proximal jejunum (small intestine [SI]). SI resections were obtained during Whipple procedure (pancreatoduodenectomy) or from donor and recipient during Ptx. PCs were identified as CD38hiCD27hiCD138+CD20− large cells, and we found that, in all adult subjects, they could be subdivided into three major subsets defined by selective expression of CD19 and CD45 (Fig. 1 B, top; Di Niro et al., 2010). For comparison,
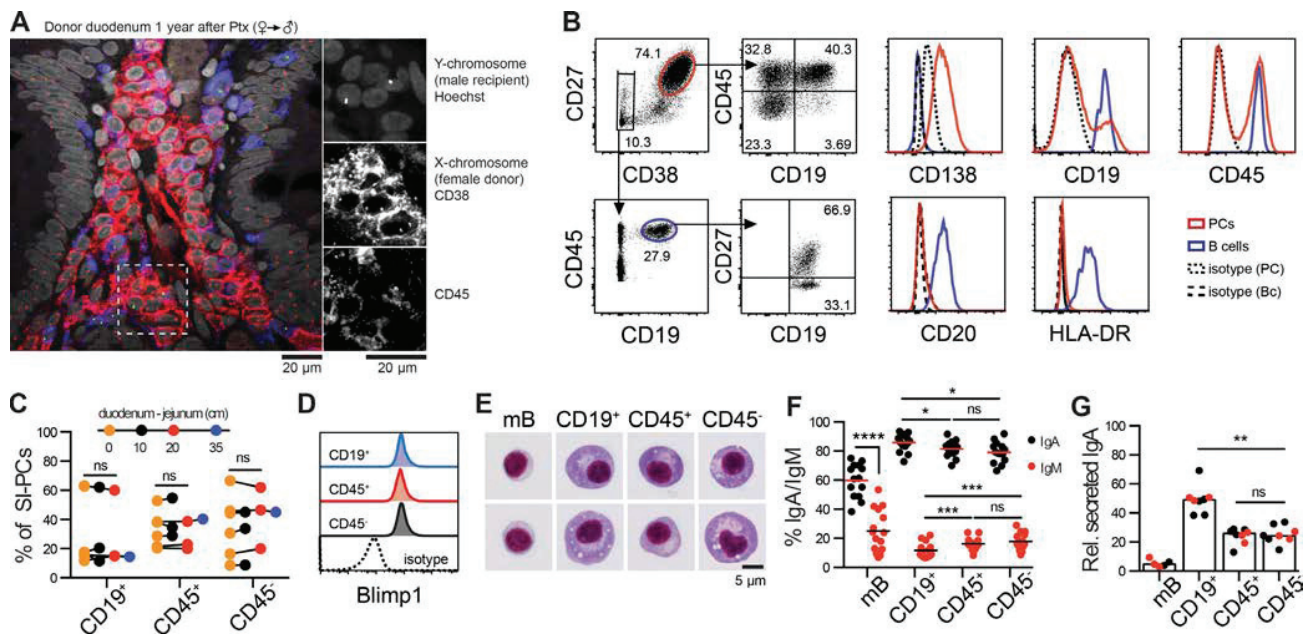

1

JEM

Figure 1. **PCs survive for 1 yr and comprise three distinct subsets in human SI.** (A) Immunofluorescence confocal micrograph of endoscopic biopsy from (female) donor duodenum 1 yr after Ptx into male recipient. Tissue sections were probed with X/Y chromosome fluorescent in situ hybridization probes (Y, green; X, red) and stained with anti-CD38 (red) and anti-CD45 (blue). Hoechst (gray) stains individual nuclei. The micrograph is representative of five gender-mismatched transplants. (B) Representative flow cytometric analysis of PCs (top) and B cells (bottom) from resected SI obtained during Whipple procedure or donor/recipient SI during Ptx. Dot plots and histograms are representative of all (CD27, CD38, CD19, and CD45), 4 (CD138), 19 (HLA-DR), and 5 (CD20) subjects. (C) The lengthwise representation of the PC subsets was determined by flow cytometric analysis of biopsies taken at intervals along resected duodenum-proximal jejunum from individual subjects after Whipple procedure. $n = 5$; paired Student's t test 0–20 cm ($n = 3$). (D) Blimp-1 expression among PC subsets was analyzed by intracellular staining and flow cytometry. The histogram is representative for 12 subjects (Whipple procedure). (E) Representative micrographs of memory B cells and PC subsets sorted by flow cytometry and stained with Hemacolor reagent. $n = 2$; Whipple procedure. (F) The percentage of memory B cells and PC subsets expressing cell surface IgA (black dots; $n = 14$) or IgM (red dots; $n = 15$) was determined by flow-cytometric analysis. Bars indicate median values. Dots represent individual subjects, SI resections from Whipple procedure, and Ptx. (G) IgA secretion from flow-sorted IgA$^+$ (black dots) or IgM$^-$ (red dots) memory B and PC subsets was determined by ELISA after 40-h culture in vitro and was normalized to the total for each subject. $n = 5$; Whipple procedure and Ptx. (F and G) One-way repeated measures ANOVA (RM-ANOVA), IgA$^+$ versus IgM$^+$ memory B cells in F; paired Student's t test. *, $P \leq 0.05$; **, $P \leq 0.01$; ***, $P \leq 0.001$; ****, $P \leq 0.0001$. Bc, B cell; mB, memory B cell; Rel., relative.

we also examined CD38$^-$CD20$^+$HLA-DR$^+$ B cells. These were dominantly CD27$^+$IgD$^-$ memory B cells, consistently present at low frequency in SI lamina propria, whereas CD27$^-$IgD$^+$IgM$^+$ naive-mature B cells represented a variable minor contribution from isolated lymphoid follicles (Fig. 1 B, bottom; and not depicted; Farstad et al., 2000). The CD19$^+$CD45$^+$ (hereafter CD19$^+$) and two CD19$^-$ PC subsets (hereafter CD45$^+$ and CD45$^-$) had a similar representation in mucosal biopsies taken at intervals along the upper SI of individual subjects (Fig. 1 C), expressed high levels of CD27, CD38, and the PC transcription factor Blimp-1, and had characteristic PC morphology (Figs. 1, D and E). The majority of cells were IgA$^+$ in all subsets (Fig. 1 F). However, CD19$^+$ PCs had a larger proportion of IgA$^+$ cells, and these secreted more IgA than either of the CD19$^-$ PC subsets when cultured in vitro (Fig. 1 G). This could indicate that CD19$^+$ PCs represented a more active PC subset potentially recently generated in response to current antigenic challenge.

To quantitatively determine the in vivo dynamics of the PC subsets, we exploited differences in HLA class I haplotype between donors and recipients after Ptx (Fig. 2 A). We found very few new (recipient) PCs in donor duodenum 3–6 wk after transplantation, and these were dominantly CD19$^+$ (Fig. 2 B). After 1 yr, a median 32% of the CD19$^+$ PCs was from the recipient, whereas the input into the CD45$^+$ PC subset remained minor (median 2.3%), and the contribution to the CD45$^-$ PC subset was negligible (median 0.01%). By comparison, B cells were largely replaced within 3–6 wk. However, some patients retained a few donor memory B cells even after 1 yr (Fig. 2, A and B, left), suggesting that these cells may also contribute to maintaining the clonal repertoire in humans (Lindner et al., 2012). We could not detect any donor B cells or PCs in the adjacent recipient duodenum (Fig. 2 C), demonstrating that there was no lateral mobility or propagation of donor PCs or B cells from solitary cells or from putative residual lymphoid tissue in the graft. To establish whether the new (recipient) PCs were adding to or
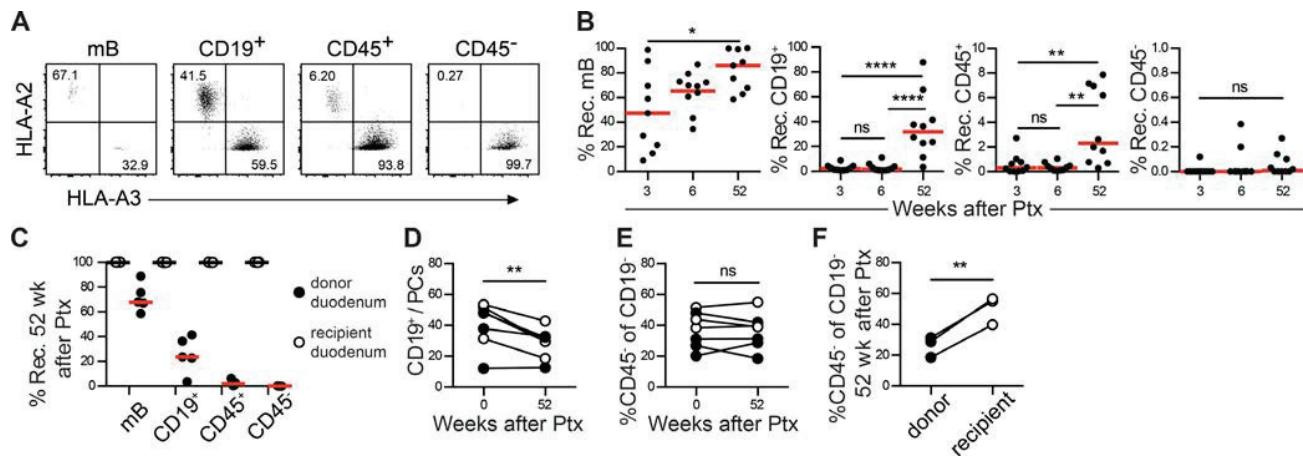
Figure 2. **SI–PC subsets have different replacement kinetics and in vivo stability.** (A) Representative flow cytometric analysis of memory B cell (mB) and PC subsets in endoscopic biopsies from donor duodenum 52 wk after Ptx (donor HLA-A2$^-$/A3$^+$; recipient HLA-A2$^+$/A3$^-$). (B) The percentage of recipient (Rec.) cells in each subset 3, 6, and 52 wk after Ptx was determined by HLA class I expression as in A. Each dot represents an individual donor. n = 10. One-way RM-ANOVA was used. (C) Chimerism was determined in endoscopic biopsies from donor duodenum (closed circles) and adjacent recipient duodenum (open circles) 52 wk after Ptx. n = 5. (D and E) The relative representation irrespective of origin of CD19$^+$ PCs among total PCs (D) and CD45$^-$ among CD19$^-$ PCs (E) was determined before and 52 wk after Ptx in donor (closed circles; n = 4) and adjacent recipient duodenum (open circles; n = 3). (F) Donor–recipients pairs with different CD19$^-$ PC subset representation before Ptx were examined 52 wk after transplantation (n = 3). Data points represent individual subjects; lines connect data from the same patients at different time points (D and E) or donor and recipient tissue at the same time point (F). Paired Student's t test was used. *, P ≤ 0.05; **, P ≤ 0.01; ****, P ≤ 0.0001.

replacing the preexisting donor CD19$^+$ PC population, we examined the relative representation of PC subsets (irrespective of origin) before and after Ptx. We observed a general decrease in CD19$^+$ PCs relative to the CD19$^-$ PC subsets after surgery in both donor and adjacent recipient duodenum (Fig. 2 D). However, the ratio between the CD19$^-$ PC subsets remained stable throughout the 1-yr follow-up (Fig. 2 E), and any difference in CD19$^-$ PC subset representation between donor and recipient before transplantation was maintained (Fig. 2 F). This demonstrates that CD19$^+$ PCs are dynamically exchanged in human SI and that the CD19$^-$ PC subsets represent stable populations with potentially very long lifespans that do not rapidly adapt to the environment of a new host.

The subdivision and dynamics of SI PCs are reminiscent of the recently reported division of BM PCs into static CD19$^-$ PCs that maintain long-term immunity and dynamic CD19$^+$ PCs that provide the transient response to new antigens (Halliley et al., 2015; Mei et al., 2015). In the BM, CD19$^-$ PCs have a prosurvival phenotype characterized by low expression of the proapoptotic receptor CD95, high expression of the antiapoptotic protein Bcl2, and low proliferation relative to CD19$^+$ PCs (Mei et al., 2015). We found that PCs in human SI had a similar phenotype: CD19$^+$ PCs expressed significantly more CD95, less Bcl-2, and contained more proliferating Ki67$^+$ cells relative to CD45$^-$ PCs, whereas CD45$^+$ PCs were intermediate in all regards (Fig. 3, A–C). BM PCs are maintained in a survival niche where a proliferation-inducing ligand (APRIL) binding to the B cell maturation antigen (BCMA) is a crucial survival factor (O'Connor et al., 2004;

Peperzak et al., 2013). APRIL is abundantly present in human intestine (Barone et al., 2009; Gustafson et al., 2014), and we found that BCMA was highly expressed by all SI PC subsets (Fig. 3 D). Furthermore, homotypic interactions between CD56$^+$ osteoblasts and/or mesenchymal stem cells and PCs may be involved in stable positioning within the BM survival niche, and CD80/86 interaction with CD28 can support the survival of long-lived BM PCs (see Mei et al., 2015). CD56 and CD28 are both enriched in CD19$^-$ relative to CD19$^+$ PCs in the BM (Mei et al., 2015), and we found a similar distinction in the SI, with CD45$^+$ PCs expressing intermediate levels of both markers (Fig. 3, E and F). To determine whether pathogen-specific clones were contained among the long-lived SI PCs, we measured reactivity against eGFP-labeled rotavirus particles (Di Niro et al., 2010). Rotavirus infects a high proportion of the population worldwide and is a major cause of diarrhea in young children. It has previously been demonstrated that the SI contain PCs specific for rotavirus (Di Niro et al., 2010), and we found that rotavirus-specific clones were predominantly present within the CD19$^-$ PC subsets in all subjects tested (Fig. 3 G).

The intermediate phenotype and dynamics suggested that CD45$^+$ PCs represented a developmental stage between CD19$^+$ PCs and CD45$^-$ PCs. To elucidate the relationship between the SI-PC subsets, we sorted IgA$^+$ PCs from SI resections obtained from Whipple procedure and performed high throughput sequencing of the heavy-chain variable region (IGHV) genes. All PC subsets displayed similar IGVH gene segment usage and number of IGHV somatic mutations
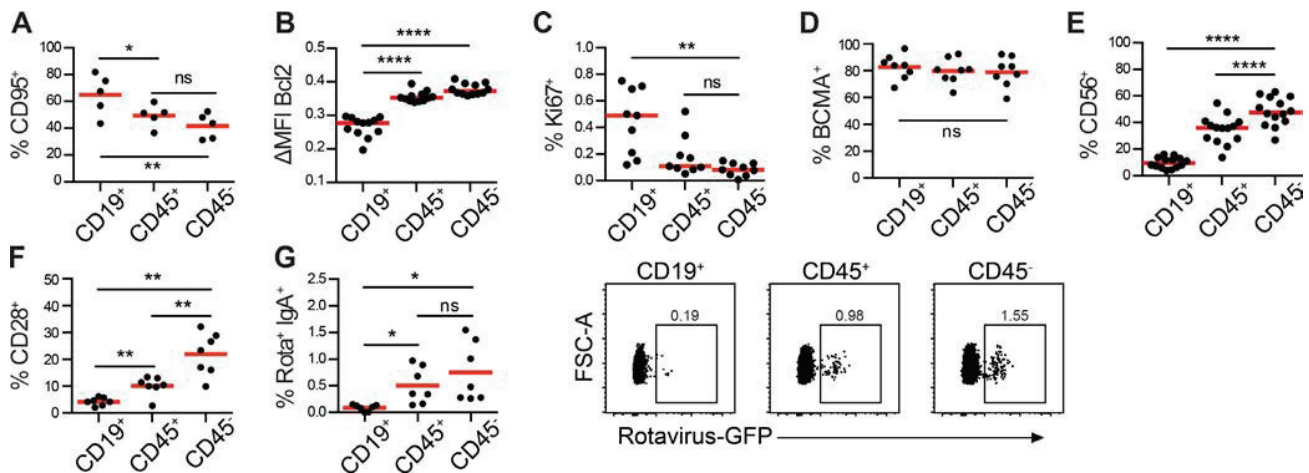
Figure 3. **CD19⁻ PCs exhibit features of advanced maturity and are enriched for rotavirus–specific clones.** (A) The percentage of CD95⁺ cells was determined relative to isotype control by flow cytometric analysis. $n = 5$; Whipple procedure. (B) The mean fluorescence intensity (MFI) of Bcl2 relative to isotype control staining (ΔMFI) on PC subsets was determined by flow cytometric analysis and presented as the fraction of total value for each subject. $n = 12$; Whipple procedure. (C–F) The percentage of Ki67⁺ ($n = 9$), BCMA⁺ ($n = 10$), CD56⁺ ($n = 14$), and CD28⁺ ($n = 7$) was determined relative to isotype control staining in SI resections (Whipple procedure and Ptx). (G) Rotavirus-reactive PCs were detected using eGFP-labeled VLPs relative to eGFP by flow cytometric analysis (SI resections from Whipple procedure [$n = 3$] or Ptx [$n = 4$]; median age 49 yr; range 7–74 yr; 2 female). Data points represent individual subjects. Red bars indicate mean values. FSC, forward side scatter. *, $P \leq 0.05$; **, $P \leq 0.01$; ****, $P \leq 0.0001$; one-way RM-ANOVA.

(Fig. 4, A and B). Application of the Morisita-Horn index showed an overall high degree of clonal sharing between the SI-PC subsets (Fig. 4 C). However, CD45⁻ PCs were consistently more closely related to CD45⁺ PCs than CD19⁺ PCs, and CD45⁺ PCs exhibited a higher level of clonal sharing with the other two subsets (Fig. 4, C and D), thus supporting an intermediate developmental stage of CD45⁺ PCs.

To investigate the development of the long-lived SI-PC compartment, we examined the representation of PC subsets in relation to age in SI resections obtained from donors ($n = 27$; age 7–51 yr; 17 female) and patients ($n = 18$; age 23–57 yr; 7 female) during Ptx and from patients undergoing Whipple procedure ($n = 27$; age 57–87 yr; 13 female). We found that whereas the CD19⁺ PCs were consistently present in all subjects, the CD19⁻ PC compartment was completely dominated by CD45⁺ PCs until late adolescence (Fig. 5, A and B). To directly determine the age of PCs in the SI, we sorted the PC subsets from resected SI (Whipple procedure) and measured carbon-14 in genomic DNA by accelerator mass spectrometry. The concentration of carbon-14 in DNA mirrors the level of atmospheric carbon-14, which peaked during the cold war and then decreased exponentially after the Limited Nuclear Test Ban Treaty in 1963 and can be used to retrospectively birth date cells in humans (Bergmann et al., 2009). We determined that the median age of CD45⁻ PCs was 22 yr among our subjects. CD45⁺ PCs were 11 yr old, whereas CD19⁺ PCs appeared to undergo constant renewal (Fig. 5 C). It is known that intestinal PCs are absent at birth but increase during the first few months to reach adult densities in early childhood (El Kaissouni et al., 1998; Gustafson et al., 2014). Therefore, subjects born before the bomb spike may have PCs formed early

in life that contain low concentrations of carbon-14, and thus, the determined ages for these subjects represent lower limits of the actual age of the cells (Fig. 5 D). Furthermore, as the individual carbon-14 values were derived from several million sorted cells and cells were added to the PC compartment over time (Fig. 2 B and Fig. 5 A), the oldest cells in the population would likely be considerably older than the quantified average. In agreement with our other results, this suggests that there is a gradual selection and conservation of clones from the CD19⁺ PC population into a CD19⁻ PC compartment initially as CD45⁺ PCs that, after some time, lose CD45 expression. It is highly probable that clones generated during childhood, such as during rotavirus infection (Fig. 3 G), are maintained within the CD45⁻ PC population. To our knowledge, the expression of CD45 by CD19⁺/⁻ BM PCs has not been addressed, but it is known that BM contains CD45⁺/⁻ PCs, and as both CD19⁻ and CD45⁻ BM PCs express more CD56 and proliferate less than their positive counterparts, it seems likely that a similar division of PCs exists in the BM (Pellat-Deceunynck and Bataille, 2004; Mei et al., 2015).

In conclusion, we have defined three subsets of SI PCs, which are functionally and phenotypically similar to BM PCs, and delineated their distinct replacement kinetics and developmental relationship. The presence and persistence of long-lived SI PCs deviates from the prevailing paradigm of humoral memory in the gut. Our data indicate that current antigenic challenge and attrition primarily affects the dynamic CD19⁺ PC compartment and show that distinct antibody specificities are conserved within a very long-lived CD19⁻ PC population that likely provides life-long protection against enteric pathogens. The existence of long-lived,
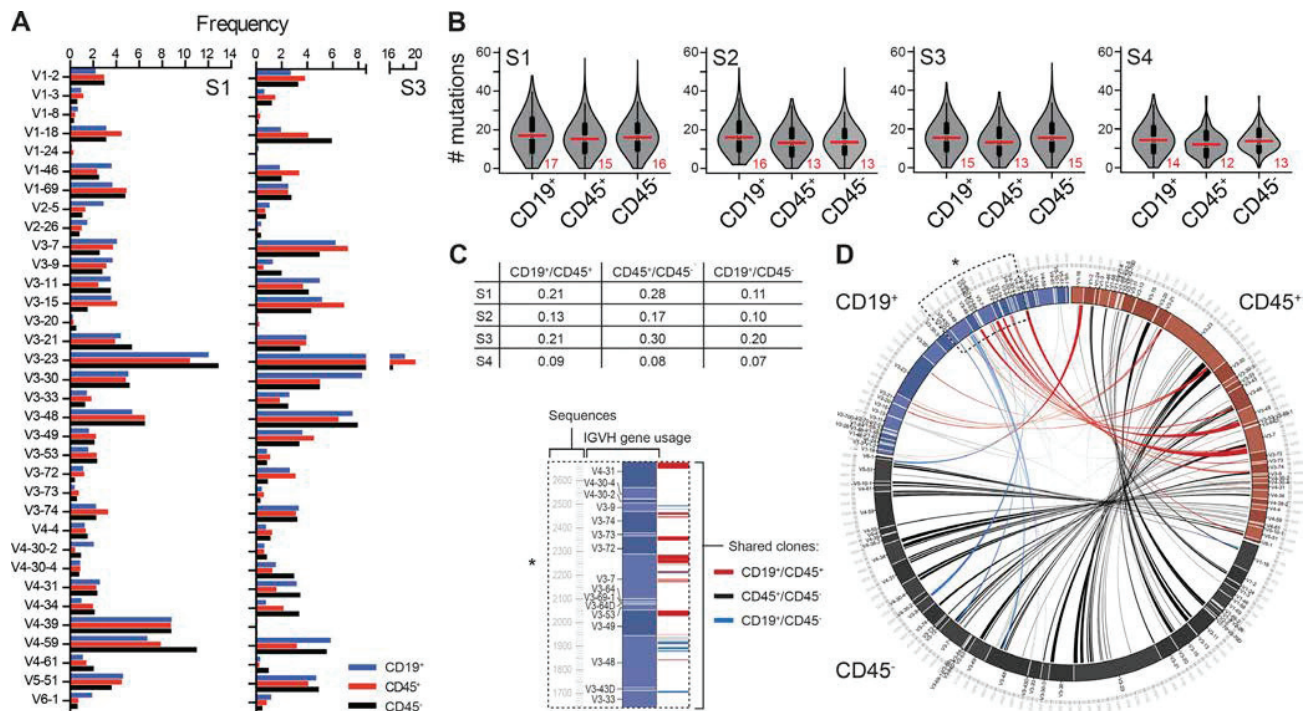
Figure 4. **Clonal relationships indicate selection and sequential development of SI PCs.** (A–D) High throughput sequencing was performed on FACS IgA+ PC subsets from SI resections (n = 4; 2 female; mean age 70 yr, range 61–77 yr; Whipple procedure) and analyzed as described in the High throughput sequencing of IGHV section of Materials and methods. (A) The frequency of IGHV gene segments used by the PC subsets is shown for two representative subjects (S1 and S3). (B) The level of somatic hypermutation among PC subsets for sequenced subjects (S1–S4) is presented in violin plots. The median number of mutations is indicated on plots in red bars and numbers. (C) The data table gives Morisita-Horn indices for clonal similarity between PC subsets in sequenced subjects (S1–S4). (D) Clonally related sequences assigned between PC subsets illustrated in a Circos plot. Lines represent clones shared between CD19+ and CD45+ (red), CD45+ and CD45− (black), CD19+, and CD45− (blue) or all PC subsets (gray) above a threshold of ≥10 unique sequences for one representative subject (S3). The width of the lines is proportional to the number of unique sequences within single clones. The asterisk marks the zoomed in region (left) describing figure elements in the Circos plot.

nonproliferating CD19− PCs in the gut gives promise for the development of oral vaccines but also needs to be addressed in clinical strategies targeting malignant or autoreactive PCs using chemotherapy, therapeutic antibodies, and chimeric antigen receptor T cell therapy.

MATERIALS AND METHODS
Human biological material
Duodenum-proximal jejunum tissue was resected from non–pathological SI during Whipple procedure (pancreaticoduodenectomy) of pancreatic cancer, distal bile duct cancer, or periampullary carcinoma patients (n = 35; mean age 70 yr; range 53–87 yr; 17 female) or from donor and patient duodenum during pancreas transplantation of type I diabetes mellitus patients (donors: n = 21, mean age 25 yr, range 7–51 yr, 11 female; patients: n = 15, mean age 40 yr, range 23–57 yr, 6 female; Horneland et al., 2015). Endoscopic biopsies were obtained from donor and patient duodenum by endoscopy 3, 6, and 52 wk after transplantation. All biological samples were evaluated blindly by an experienced pathologist (F.L. Jahnsen), and only material with normal histology was

included (Ruiz et al., 2010). Resected SI was opened longitudinally and rinsed thoroughly in PBS, and mucosal folds were dissected off the submucosa. Mucosal specimens for microscopy were fixed directly in formalin and paraffin embedded. To obtain single-cell suspensions for flow cytometry, cell sorting, and culture, epithelial cells were removed by washing in PBS containing 2 mM EDTA three times for 20 min at 37°C, and the lamina propria was minced and digested in RPMI medium containing 2.5 mg/ml Liberase and 20 U/ml DNase I (both from Roche) at 37°C for 1 h. Digested tissue was passed through 100-µm cell strainers (Falcon) and washed three times in PBS. The study was approved by the Regional Committee for Medical Research Ethics in Southeast Norway and the Privacy Ombudsman for Research at Oslo University Hospital–Rikshospitalet and complies with the Declaration of Helsinki. All participants gave their written informed consent.

Flow cytometry and FACS
Single-cell suspensions from lamina propria were analyzed by flow cytometry according to standard procedure using fluoro-
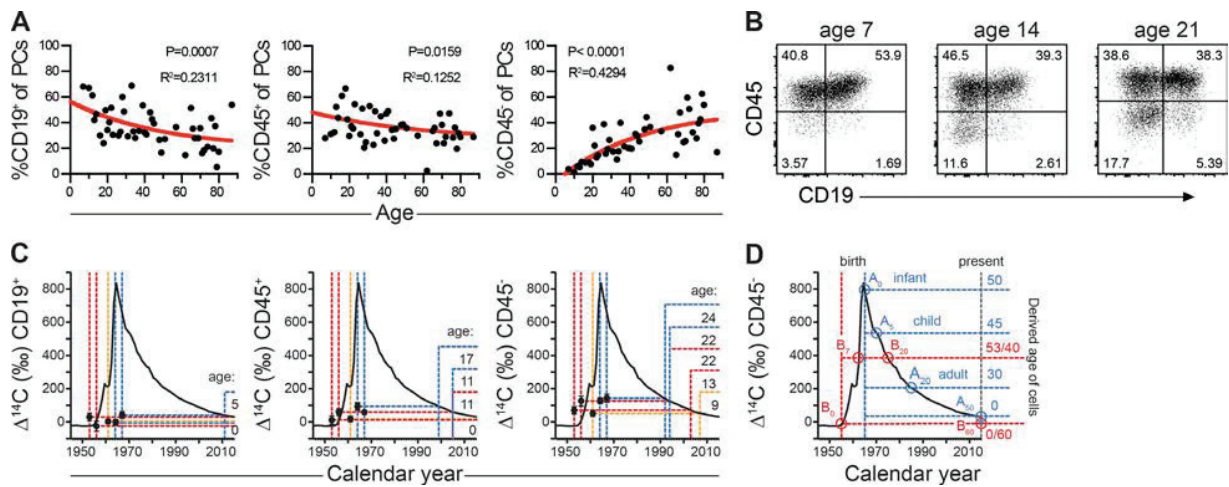
Figure 5. CD45⁻ PCs accumulate with age and persist for decades in human SI. (A) The representation of each SI-PC subset in SI resections ($n = 72$) obtained during Whipple procedure or donors and recipients during Ptx was determined by flow cytometric analysis and plotted against subject age. Lines represent nonlinear fitting (one-phase exponential decay). R^2 and two-tailed p-values of age and subset representation are shown on the graphs (Pearson correlation). (B) Dot plots show representative flow cytometric analysis of subjects with increasing age from A. (C) Carbon-14 concentrations in genomic DNA isolated from SI-PC subsets bead sorted from SI resections (Whipple procedure) were measured by accelerator mass spectrometry ($n = 5$; 1 female). The average age of cells in each PC subset was inferred from plotting the concentration of carbon-14 from each sample on the atmospheric carbon-14 curve, determining the corresponding year, and subtracting the year samples were acquired. Dots represent carbon-14 values and year of birth for individual donors. Vertical dashed red lines indicate data from subjects born before, yellow lines during the increase, and blue lines after the peak in atmospheric carbon-14. (D) Illustration of the strategy to infer age of cells based on amount of carbon-14 in genomic DNA relative to carbon-14 level in the atmosphere and subject age (hypothetical subject A [blue]; subscript gives age). Note that in subjects born prior to the bomb peak (red; B_0), cells generated during the bomb spike (i.e., B_7) will have higher carbon-14 concentration relative to their renewal rate, and cells generated post-bomb (i.e., B_{20} and B_{60}) will have lower carbon-14 concentration relative to their renewal rate.

chrome–conjugated antibodies targeting HLA-A2–PE (Abcam); CD20-FITC, CD45-APC-H7, and Ki67-FITC (BD); Bcl2–Alexa Fluor 488, BCMA-PE, CD3-APC, CD14-APC, CD19–Alexa Flour 488/PE-Cy7, CD20-PE, CD27-BV421/Pacific blue/APC-Cy7/PE-Cy7, CD28–Alexa Fluor 488, CD38-PE/APC-Cy7, CD45-BV510/APC-Cy7, CD56–Alexa Flour 488, CD95-PE, and HLA-DR–BV605/PerCP (BioLegend); CD138-FITC/PE-Cy7 and HLA-A3–FITC/APC (eBioscience); HLA-B7–PE (EMD Millipore); HLA-B8–PE (Miltenyi Biotec); IgA-FITC/PE, IgM-FITC/PE, and IgD-FITC/PE (Southern-Biotech); and Blimp-1–DyLight 488 (Thermo Fisher Scientific). For detection of intracellular antigens, cells were fixed in form-aldehyde and permeabilized using a Foxp3 staining buffer set (eBioscience). Detection of rotavirus–specific PCs was performed using eGFP-tagged virus–like particle 2 (VLP2)–eGFP/VLP6 (provided by D. Poncet and A. Charpilienne, Institut de Biologie Integrative de la Cellule, Paris, France; Charpilienne et al., 2001) at a final concentration of 1 µg/ml. eGFP (Promega) was used as a negative control. All flow cytometry was performed on an LSR Fortessa, and FACS was performed on a FACSAriaII flow cytometer (both from BD). Data were analyzed using FlowJo 10 (Tree Star), and figures were assembled in Illustrator CS4 (Adobe).

Microscopy

Sections were cut from paraffin blocks in series at 4 µm, mounted on Superfrost Plus object glasses (Thermo Fisher

Scientific), and washed sequentially in xylene, ethanol, and PBS. Heat–induced epitope retrieval was performed by boiling sections for 20 min in Dako buffer and cooled to room temperature before staining. Sections were incubated with CEP X SpectrumOrange/Y SpectrumGreen DNA Probes (Abbott Molecular Inc.) for 12 h at 37°C before immunostaining according to standard protocol with anti-CD38 (clone SPC32; Novocastra), anti-CD45 (polyclonal; Abcam), and secondary antibodies targeting mouse IgG1 or rabbit IgG conjugated to Alexa Fluor 555 and 647, respectively. Stained sections were mounted with ProLong Diamond Antifade mountant (Molecular Probes). Sorted cells were attached to Superfrost Plus object glasses by centrifugation at 800 rpm for 3 min, stained with Hemacolor reagents (EMD Millipore), and mounted with Pertex mounting medium (Histolab Products AB). Light microscopy was conducted on a BX51 microscope (Olympus) using 10×/0.30 or 40×/0.75 UPlanFI objectives, and images were acquired with a Colorview IIIu camera (Olympus). Phase contrast micrographs of sorted cells cultured in vitro (Fig. S1 B, insets) were acquired on a microscope (DM IL; Leica Biosystems), with a 40×/0.50 Hi PLAN1 objective and a DCF290 camera (Leica Biosystems) using Cell^P software. Laser scanning confocal microscopy was performed on an Olympus FV1000 (BX61WI) system with 405-, 488-, 543-, and 633-nm laser lines using 20×/0.80 or 60×/1.35 UPlanSApo oil objectives (Olympus). Image z

stacks were acquired at 1-µm intervals and combined using the Z project max intensity function in Image J (National Institutes of Health). All microscopy images were assembled in Photoshop and Illustrator CS4 (Adobe).

Cell culture and ELISA

Cells were flow sorted as IgA$^+$ ($n = 5$) or IgM$^-$ ($n = 3$) and cultured for 40 h in RPMI medium with 10% heat-inactivated fetal calf serum, L-glutamine, and penicillin-streptomycin at a density of 2.5×10^5 cells/ml before cells were spun down at 500 rcf/7 min, and the supernatant was transferred in twofold dilution to 96-well plates precoated with rabbit anti–human IgA (A0262; Dako) and blocked with 1% BSA. Purified IgA monomer at known concentration was used as standard (courtesy of R. Iversen, Oslo University Hospital-Rikshospitalet and the University of Oslo, Oslo, Norway). Bound IgA was detected with goat anti–human IgA peroxidase conjugate (A0295; Sigma-Aldrich) and tetramethylbenzidine (Kirkegaard & Perry Laboratories).

High throughput sequencing of IGHV

10^4 IgA$^+$ cells of each subset from four donors were sorted into 25 µl of catch buffer (10 mM dithiothreitol and 2 U/µl RNAsin [Promega] in PBS) and snap frozen at −80°C. cDNA synthesis was performed using IGHJ reverse primers indexed to allow simultaneous sequencing of different samples, as well as six random nucleotides to generate unique molecular identifiers and a part of Illumina adapters (Snir et al., 2015). 3.5 µl of 10 µM indexed IGHJ primer was added together with 1.5% vol/vol NP-40 and 0.5 µl of 40 U/µl RNAsin (Promega) to 14 µl of lysate. Diethylpyrocarbonate-treated water was added to a final volume of 25 µl, and lysates together with primer mix were incubated at 65°C for 5 min. Next, 25 µl of reverse transcriptase mix (10 µl × 5 reverse transcriptase buffer, 3.5 µl of 100 mM dithiothreitol, 4.5 µl of 10 mM dNTP-Mix, 0.7 µl of 40 U/µl RNAsin [Promega], 0.9 µl Superscript III [Invitrogen], and diethylpyrocarbonate-treated water) was added. cDNA was synthesized at 42°C for 10 min, 25°C for 10 min, 50°C for 60 min, and 94°C for 5 min and stored at −20°C. Second-strand cDNA was synthesized using AmpliTaq Gold polymerase (Applied Biosystems) with forward IGHV1–6 framework region 2 (van Dongen et al., 2003), which was indexed and included six random nucleotides and a part of Illumina adapters. Second-strand synthesis was performed at 95°C for 7.5 min, 52°C for 2 min, and 72°C for 10 min. Double-stranded cDNA was further purified using an AMPure XP system (Beckman Coulter) at a 1:1 ratio according to the manufacturer's instructions. Next, the second part of the Illumina adapter was connected using R1 and R2 primers. PCR was performed using Multiplex PCR (QIA GEN) at 95°C for 15 min × 25 (95°C for 30 s, 60°C for 45 s, and 72°C for 90 s) and 72°C for 10 min. Final IGHV amplicon libraries were purified using the AMPure XP system and further run and extracted from agarose gel. Paired-end sequencing of 300 base pairs was performed using a MiSeq sequencer (Illumina) at the Norwegian Sequencing Centre in Oslo, Norway. Raw sequencing data were processed using pRES TO (Vander Heiden et al., 2014) as previously described (Snir et al., 2015). Unique sequences to which at least two copies were present were further aligned using the ImMunoGeneTics database (Lefranc et al., 2003), and their IGHV, IVHJ segments, and CDR3 were determined (Table S1). Clonally related sequences originating from a common ancestor were assigned within the PC subsets and between the different subsets using Change-O (Gupta et al., 2015), and the frequencies of clones that are shared between PCs subsets was further calculated. Presentation of clonal sharing between PC subsets was assembled in Circos (Krzywinski et al., 2009), where the size of each subset is determined based on the number of clones and duplicates within each subset. A threshold of 10 duplicates was applied for lines to be drawn between individual shared clones, and the width of connecting lines is proportional to the number of duplicates within single clones.

Bead–based PC sorting for carbon–14 dating

Single-cell suspensions from SI resections ($n = 6$; Whipple procedure; Table S2) were stained with biotinylated (DSB-X Biotin Protein kit; Molecular Probes) anti-CD38 antibody (clone HB7 from Absolut Antibody LTd). Bead-free CD38$^+$ cells were obtained after isolation with Flexicomp beads and subsequent incubation with releasing buffer, following the kit's instructions (11061D; Thermo Fisher Scientific). Rare contaminating CD38^{dim} T cells were depleted with anti-CD3 Dynabeads (11151D; Thermo Fisher Scientific) before release of CD38$^+$ PCs. Purity of sorted CD38$^+$ PCs was assessed by flow cytometry and was consistently >90%. CD19$^+$, CD45$^+$, and CD45$^-$ PC subsets were magnetic-activated cell sorted in two sequential steps: first applying CD19 microbeads and, then, sorting the resulting negative fraction with CD45 microbeads (both from Miltenyi Biotec).

DNA extraction for carbon–14 dating

A clean room (ISO8) was used to isolate the DNA. All glassware was baked for 4 h at 450°C before use. The cells were incubated at 65°C overnight with 1 ml of lysis buffer (100 mM Tris, pH 8.0, 200 mM NaCl, 1% SDS, and 5 mM EDTA) and 12 µl of 40 mg/ml proteinase K. 6 µl of RNase cocktail (Ambion) was added and incubated at 65°C for 1 h. Half a volume of 5 M NaCl was added to each sample. The tubes were vortexed for 30 s and then spun down at 13,000 rpm for 6 min. The supernatant was transferred to a glass vial containing absolute ethanol (three times the volume) and then gently agitated. The DNA was washed three times in washing buffer (70% ethanol [vol/vol] and 0.5 M NaCl) and dried at 65°C overnight. 500 µl of DNase/RNase free water (Gibco; Invitrogen) was used to resuspend the DNA. The purity and concentration were verified by UV spectroscopy (NanoDrop; Table S2).

Accelerator mass spectrometry and carbon–14 dating

A special sample preparation method has been developed for the microgram-sized DNA samples (Salehpour et al., 2013).

JEM

The purified DNA samples were received suspended in water. The samples were subsequently lyophilized to dryness under vacuum and centrifugation. Excess CuO was added to the dried samples in quartz tubes, which were then evacuated and sealed with a high temperature torch. The quartz tubes were placed in a furnace set at 900°C for 3.5 h to combust all carbon to CO_2. The evolved gas was cryogenically purified and trapped. The CO_2 gas was converted to graphite in individual submilliliter reactors at 550°C for 6 h in the presence of zinc powder as reducing agent and iron powder as catalyst. The graphite targets were measured at the Department of Physics and Astronomy, Ion Physics, Uppsala University using a 5-MV pelletron tandem accelerator (Salehpour et al., 2015). Stringent and thorough laboratory practice is necessary to minimize the introduction of stray carbon into the samples, including preheating of all glassware and chemicals before sample preparation. Large CO_2 samples (>100 µg) were split and $\delta^{13}C$ was measured by stable isotope ratio mass spectrometry, which established the $\delta^{13}C$ correction to $-24.1 \pm 1\%$ (2 SD) for leukocyte samples. Corrections and reduction of background contamination introduced during sample preparation were made as described by Hua et al. (2004) and Santos et al. (2007). The measurement error was determined for each sample and ranged between $\pm$ 8 and 24% (2 SD) $\Delta^{14}C$ for the large sample and small samples (10 µg C), respectively. All ^{14}C data are reported as decay corrected $\Delta^{14}C$ or Fraction Modern. All accelerator mass spectrometry analyses were performed blind to age and origin of the sample. Carbon-14 data are summarized in Table S2.

Statistical analysis

All statistical analysis was performed in Prism 6 (GraphPad Software). Statistical significance between subsets was calculated using Tukey's posthoc test for multiple comparisons. Paired Student's t test with two-tailed p-value (95% confidence interval) was used to compare ratios of PCs. Nonlinear fitting was applied using one-phase association. Correlation between age and subset abundance was calculated using Pearson correlation with two-tailed p-value (95% confidence interval). Morisita–Horn index for similarity between different subsets was calculated using the R spa package. Results are expressed as individual data points with median or mean values $\pm$ SD. P-values of <0.05 were considered significant. The tests used and magnitudes for p-values are indicated in each figure legend.

Online supplemental material

Fig. S1 presents gating strategy for flow cytometry and cell sorting. Table S1 provides additional IGHV sequencing data, and Table S2 presents detailed carbon-14 data.

REFERENCES

Barone, F., P. Patel, J.D. Sanderson, and J. Spencer. 2009. Gut-associated lymphoid tissue contains the molecular machinery to support T-cell-dependent and T-cell-independent class switch recombination. *Mucosal Immunol.* 2:495–503. http://dx.doi.org/10.1038/mi.2009.106

Bergmann, O., R.D. Bhardwaj, S. Bernard, S. Zdunek, F. Barnabé-Heider, S. Walsh, J. Zupicich, K. Alkass, B.A. Buchholz, H. Druid, et al. 2009. Evidence for cardiomyocyte renewal in humans. *Science*. 324:98–102. http://dx.doi.org/10.1126/science.1164680

Bhoj, V.G., D. Arhontoulis, G. Wertheim, J. Capobianchi, C.A. Callahan, C.T. Ellebrecht, A.E. Obstfeld, S.F. Lacey, J.J. Melenhorst, F. Nazimuddin, et al. 2016. Persistence of long-lived plasma cells and humoral immunity in individuals responding to CD19-directed CAR T-cell therapy. *Blood*. 128:360–370. http://dx.doi.org/10.1182/blood-2016-01-694356

Charpilienne, A., M. Nejmeddine, M. Berois, N. Parez, E. Neumann, E. Hewat, G. Trugnan, and J. Cohen. 2001. Individual rotavirus-like particles containing 120 molecules of fluorescent protein are visible in living cells. *J. Biol. Chem.* 276:29361–29367. http://dx.doi.org/10.1074/jbc.M101935200

Di Niro, R., L. Mesin, M. Raki, N.Y. Zheng, F. Lund-Johansen, K.E. Lundin, A. Charpilienne, D. Poncet, P.C. Wilson, and L.M. Sollid. 2010. Rapid generation of rotavirus-specific human monoclonal antibodies from small-intestinal mucosa. *J. Immunol.* 185:5377–5383. http://dx.doi.org/10.4049/jimmunol.1001587

El Kaissouni, J., M.C. Bene, S. Thionnois, P. Monin, M. Vidailhet, and G.C. Faure. 1998. Maturation of B cells in the lamina propria of human gut and bronchi in the first months of human life. *Dev. Immunol.* 5:153–159. http://dx.doi.org/10.1155/1998/42138

Farstad, I.N., H. Carlsen, H.C. Morton, and P. Brandtzaeg. 2000. Immunoglobulin A cell distribution in the human small intestine: phenotypic and functional characteristics. *Immunology.* 101:354–363. http://dx.doi.org/10.1046/j.1365-2567.2000.00118.x

Gupta, N.T., J.A. Vander Heiden, M. Uduman, D. Gadala-Maria, G. Yaari, and S.H. Kleinstein. 2015. Change-O: a toolkit for analyzing large-scale B cell immunoglobulin repertoire sequencing data. *Bioinformatics.* 31:3356–3358. http://dx.doi.org/10.1093/bioinformatics/btv359

Gustafson, C.E., D. Higbee, A.R. Yeckes, C.C. Wilson, E.F. De Zoeten, P. Jedlicka, and E.N. Janoff. 2014. Limited expression of APRIL and its receptors prior to intestinal IgA plasma cell development during human infancy. *Mucosal Immunol.* 7:467–477. http://dx.doi.org/10.1038/mi.2013.64

Halliley, J.L., C.M. Tipton, J. Liesveld, A.F. Rosenberg, J. Darce, I.V. Gregoretti, L. Popova, D. Kaminiski, C.F. Fucile, I. Albizua, et al. 2015. Long-lived plasma cells are contained within the CD19⁻CD38ʰⁱCD138⁺ subset in human bone marrow. *Immunity.* 43:132–145. http://dx.doi.org/10.1016/j.immuni.2015.06.016

Hapfelmeier, S., M.A. Lawson, E. Slack, J.K. Kirundi, M. Stoel, M. Heikenwalder, J. Cahenzli, Y. Velykoredko, M.L. Balmer, K. Endt, et al. 2010. Reversible microbial colonization of germ-free mice reveals the dynamics of IgA immune responses. *Science.* 328:1705–1709. http://dx.doi.org/10.1126/science.1188454

Horneland, R., V. Paulsen, J.P. Lindahl, K. Grzyb, T.J. Eide, K. Lundin, L. Aabakken, T. Jenssen, E.M. Aandahl, A. Foss, and O. Øyen. 2015. Pancreas transplantation with enteroanastomosis to native duodenum poses technical challenges—but offers improved endoscopic access for scheduled biopsies and therapeutic interventions. *Am. J. Transplant.* 15:242–250. http://dx.doi.org/10.1111/ajt.12953

Hua, Q., U. Zoppi, A. Williams, and A. Smith. 2004. Small-mass AMS radiocarbon analysis at ANTARES. *Nucl. Instrum. Methods Phys. Res. B.* 223–224:284–292. http://dx.doi.org/10.1016/j.nimb.2004.04.057

Krzywinski, M., J. Schein, I. Birol, J. Connors, R. Gascoyne, D. Horsman, S.J. Jones, and M.A. Marra. 2009. Circos: an information aesthetic for comparative genomics. *Genome Res.* 19:1639–1645. http://dx.doi.org/10.1101/gr.092759.109

Lefranc, M.P., C. Pommié, M. Ruiz, V. Giudicelli, E. Foulquier, L. Truong, V. Thouvenin-Contet, and G. Lefranc. 2003. IMGT unique numbering for immunoglobulin and T cell receptor variable domains and Ig superfamily V-like domains. *Dev. Comp. Immunol.* 27:55–77. http://dx.doi.org/10.1016/S0145-305X(02)00039-3

Lemke, A., M. Kraft, K. Roth, R. Riedel, D. Lammerding, and A.E. Hauser. 2016. Long-lived plasma cells are generated in mucosal immune responses and contribute to the bone marrow plasma cell pool in mice. *Mucosal Immunol.* 9:83–97. http://dx.doi.org/10.1038/mi.2015.38

Lindner, C., B. Wahl, L. Föhse, S. Suerbaum, A.J. Macpherson, I. Prinz, and O. Pabst. 2012. Age, microbiota, and T cells shape diverse individual IgA repertoires in the intestine. *J. Exp. Med.* 209:365–377. http://dx.doi.org/10.1084/jem.20111980

Mattioli, C.A., and T.B. Tomasi. 1973. The life span of IgA plasma cells from the mouse intestine. *J. Exp. Med.* 138:452–460. http://dx.doi.org/10.1084/jem.138.2.452

Mei, H.E., I. Wirries, D. Frölich, M. Brisslert, C. Giesecke, J.R. Grün, T. Alexander, S. Schmidt, K. Luda, A.A. Kühl, et al. 2015. A unique population of IgG-expressing plasma cells lacking CD19 is enriched in human bone marrow. *Blood.* 125:1739–1748. http://dx.doi.org/10.1182/blood-2014-02-555169

Mesin, L., R. Di Niro, K.M. Thompson, K.E. Lundin, and L.M. Sollid. 2011. Long-lived plasma cells from human small intestine biopsies secrete immunoglobulins for many weeks in vitro. *J. Immunol.* 187:2867–2874. http://dx.doi.org/10.4049/jimmunol.1003181

Nair, N., E.W. Newell, C. Vollmers, S.R. Quake, J.M. Morton, M.M. Davis, X.S. He, and H.B. Greenberg. 2016. High-dimensional immune profiling of total and rotavirus VP6-specific intestinal and circulating B cells by mass cytometry. *Mucosal Immunol.* 9:68–82. http://dx.doi.org/10.1038/mi.2015.36

O'Connor, B.P., V.S. Raman, L.D. Erickson, W.J. Cook, L.K. Weaver, C. Ahonen, L.L. Lin, G.T. Mantchev, R.J. Bram, and R.J. Noelle. 2004. BCMA is essential for the survival of long-lived bone marrow plasma cells. *J. Exp. Med.* 199:91–98. http://dx.doi.org/10.1084/jem.20031330

Pabst, O. 2012. New concepts in the generation and functions of IgA. *Nat. Rev. Immunol.* 12:821–832. http://dx.doi.org/10.1038/nri3322

Pellat-Deceunynck, C., and R. Bataille. 2004. Normal and malignant human plasma cells: proliferation, differentiation, and expansions in relation to CD45 expression. *Blood Cells Mol. Dis.* 32:293–301. http://dx.doi.org/10.1016/j.bcmd.2003.12.001

Peperzak, V., I. Vikström, J. Walker, S.P. Glaser, M. LePage, C.M. Coquery, L.D. Erickson, K. Fairfax, F. Mackay, A. Strasser, et al. 2013. Mcl-1 is essential for the survival of plasma cells. *Nat. Immunol.* 14:290–297. http://dx.doi.org/10.1038/ni.2527

Ruiz, P., H. Takahashi, V. Delacruz, E. Island, G. Selvaggi, S. Nishida, J. Moon, L. Smith, T. Asaoka, D. Levi, et al. 2010. International grading scheme for acute cellular rejection in small-bowel transplantation: single-center experience. *Transplant. Proc.* 42:47–53. http://dx.doi.org/10.1016/j.transproceed.2009.12.026

Salehpour, M., K. Håkansson, and G. Possnert. 2013. Accelerator mass spectrometry of ultra-small samples with applications in the biosciences. *Nucl. Instrum. Methods Phys. Res. B.* 294:97–103. http://dx.doi.org/10.1016/j.nimb.2012.08.054

Salehpour, M., K. Håkansson, and G. Possnert. 2015. Small sample accelerator mass spectrometry for biomedical applications. *Nucl. Instrum. Methods Phys. Res. B.* 361:43–47. http://dx.doi.org/10.1016/j.nimb.2015.04.047

Santos, G.M., J.R. Southon, S. Griffin, S. Beaupre, and E. Druffel. 2007. Ultra small-mass AMS 14C sample preparation and analyses at KCCAMS/UCI Facility. *Nucl. Instrum. Methods Phys. Res. B.* 259:293–302. http://dx.doi.org/10.1016/j.nimb.2007.01.172

Snir, O., L. Mesin, M. Gidoni, K.E. Lundin, G. Yaari, and L.M. Sollid. 2015. Analysis of celiac disease autoreactive gut plasma cells and their corresponding memory compartment in peripheral blood using high-throughput sequencing. *J. Immunol.* 194:5703–5712. http://dx.doi.org/10.4049/jimmunol.1402611

Vander Heiden, J.A., G. Yaari, M. Uduman, J.N. Stern, K.C. O'Connor, D.A. Hafler, F. Vigneault, and S.H. Kleinstein. 2014. pRESTO: a toolkit for processing high-throughput sequencing raw reads of lymphocyte receptor repertoires. *Bioinformatics.* 30:1930–1932. http://dx.doi.org/10.1093/bioinformatics/btu138

van Dongen, J.J., A.W. Langerak, M. Brüggemann, P.A. Evans, M. Hummel, F.L. Lavender, E. Delabesse, F. Davi, E. Schuuring, R. García-Sanz, et al. 2003. Design and standardization of PCR primers and protocols for detection of clonal immunoglobulin and T-cell receptor gene recombinations in suspect lymphoproliferations: report of the BIOMED-2 Concerted Action BMH4-CT98-3936. *Leukemia.* 17:2257–2317. http://dx.doi.org/10.1038/sj.leu.2403202
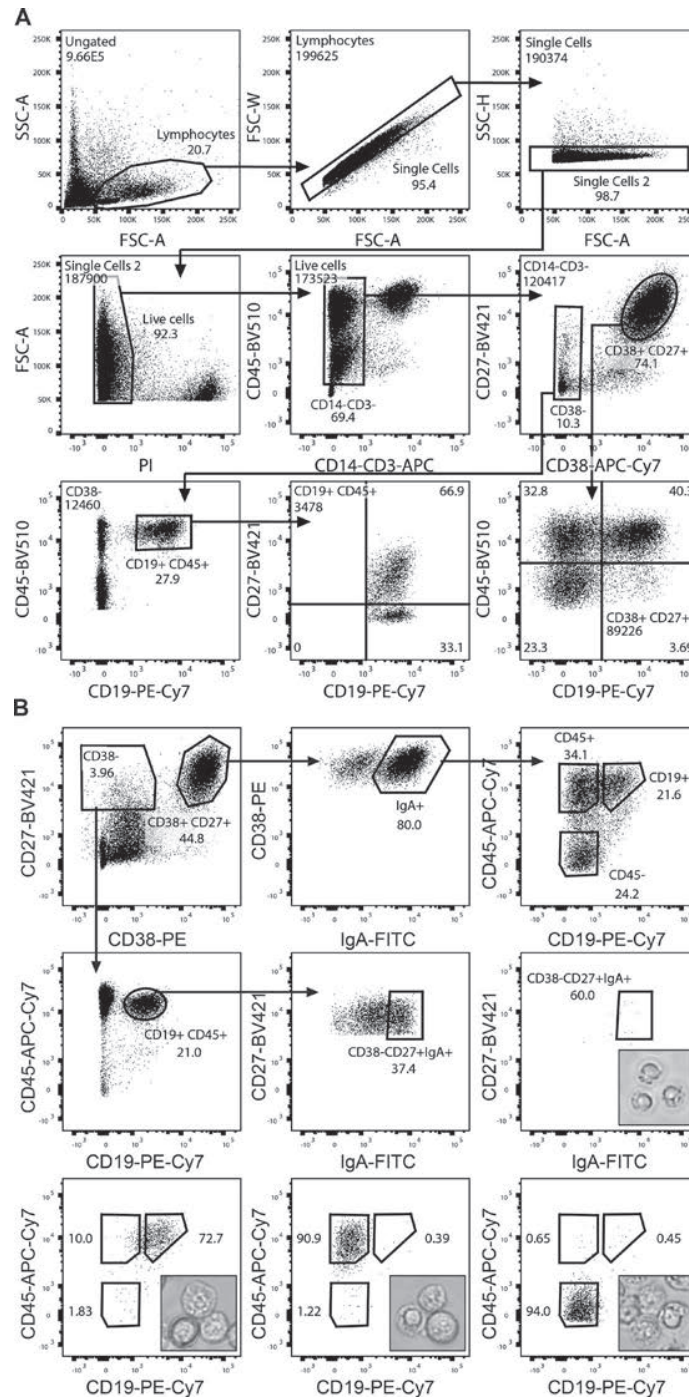
Figure S1. **Gating strategy for flow cytometry and cell sorting of B cells and PC subsets.** (A) Gating strategy for flow cytometric analysis of B cells and PCs in single-cell suspensions from human duodenal-jejunal resections and endoscopic biopsies. Arrows indicate sequential gating. Numbers indicate percentage of cells in gate or absolute number of cells in each plot. FSC, forward scatter; PI, propidium iodide; SSC, side scatter. (B) Gating strategy for cell sorting from SI resections with sorting purity check (middle right and bottom three dot plots). Cell debris, aggregates, and dead cells were gated out (as in A; top and middle left) before the CD27/CD38 gating (top left). Insets show phase contrast micrographs of sorted live cells from their respective gates after culture for 12 h in vitro.

Table S1. **Sequencing data**

	Donor 1 (male age 76)						Donor 2 (female age 77)						Donor 3 (male age 65)						Donor 4 (female age 61)					
	CD19+		CD45+		CD45−		CD19+		CD45+		CD45−		CD19+		CD45+		CD45−		CD19+		CD45+		CD45−	
VH1	648	13.9%	472	16.4%	1,047	14.3%	92	19.4%	127	19.8%	221	20.1%	253	9.4%	567	15.0%	859	14.9%	219	12.2%	82	24.6%	53	18.2%
VH2	200	4.3%	65	2.3%	156	2.1%	7	1.5%	9	1.4%	5	0.5%	42	1.6%	48	1.3%	87	1.5%	49	2.7%	2	0.6%	2	0.7%
VH3	2,289	49.3%	1,450	50.3%	3,622	49.3%	256	54.0%	355	55.5%	640	58.3%	1,852	68.5%	2,520	66.8%	3,387	58.9%	1,054	58.8%	149	44.6%	161	55.1%
VH4	1,216	26.2%	750	26.0%	2,217	30.2%	78	16.5%	85	13.3%	150	13.7%	387	14.3%	426	11.3%	1,079	18.8%	369	20.6%	75	22.5%	54	18.5%
VH5	207	4.5%	127	4.4%	259	3.5%	38	8.0%	58	9.1%	72	6.6%	139	5.1%	184	4.9%	312	5.4%	79	4.4%	16	4.8%	15	5.1%
VH6	86	1.9%	20	0.7%	46	0.6%	3	0.6%	6	0.9%	10	0.9%	29	1.1%	30	0.8%	27	0.5%	4	0.2%	2	0.6%	2	0.7%
VH7	0	0.0%	0	0.0%	0	0.0%	0	0.0%	0	0.0%	0	0.0%	0	0.0%	0	0.0%	0	0.0%	19	1.1%	8	2.4%	5	1.7%
No D	0	0.0%	5	0.2%	2	0.0%	0	0.0%	0	0.0%	2	0.2%	2	0.1%	2	0.1%	3	0.1%	4	0.2%	0	0.0%	1	0.3%
D1	459	9.9%	341	11.8%	605	8.2%	46	9.7%	57	8.9%	110	10.0%	240	8.9%	417	11.0%	460	8.0%	184	10.3%	39	11.7%	24	8.2%
D2	838	18.0%	527	18.3%	1,227	16.7%	93	19.6%	123	19.2%	224	20.4%	606	22.4%	900	23.8%	1,318	22.9%	405	22.6%	70	21.0%	64	21.9%
D3	1,858	40.0%	1,139	39.5%	3,364	45.8%	210	44.3%	238	37.2%	399	36.3%	941	34.8%	1,245	33.0%	2,124	36.9%	621	34.6%	129	38.6%	89	30.5%
D4	310	6.7%	182	6.3%	538	7.3%	21	4.4%	36	5.6%	60	5.5%	203	7.5%	267	7.1%	423	7.4%	118	6.6%	17	5.1%	22	7.5%
D5	436	9.4%	279	9.7%	617	8.4%	36	7.6%	59	9.2%	117	10.7%	274	10.1%	337	8.9%	543	9.4%	127	7.1%	20	6.0%	36	12.3%
D6	739	15.9%	404	14.0%	980	13.3%	64	13.5%	123	19.2%	179	16.3%	427	15.8%	597	15.8%	852	14.8%	325	18.1%	59	17.7%	54	18.5%
D7	6	0.1%	7	0.2%	14	0.2%	4	0.8%	4	0.6%	7	0.6%	9	0.3%	10	0.3%	28	0.5%	9	0.5%	0	0.0%	2	0.7%
JH1	80	1.7%	38	1.3%	59	0.8%	6	1.3%	10	1.6%	22	2.0%	60	2.2%	94	2.5%	128	2.2%	14	0.8%	1	0.3%	1	0.3%
JH2	63	1.4%	48	1.7%	118	1.6%	13	2.7%	19	3.0%	35	3.2%	106	3.9%	123	3.3%	215	3.7%	15	0.8%	7	2.1%	4	1.4%
JH3	700	15.1%	389	13.5%	799	10.9%	89	18.8%	59	9.2%	118	10.7%	307	11.4%	431	11.4%	655	11.4%	141	7.9%	18	5.4%	22	7.5%
JH4	2,037	43.8%	1,232	42.7%	3,338	45.4%	214	45.1%	279	43.6%	474	43.2%	1,330	49.2%	1,859	49.2%	2,590	45.0%	675	37.6%	142	42.5%	109	37.3%
JH5	700	15.1%	370	12.8%	876	11.9%	36	7.6%	90	14.1%	112	10.2%	325	12.0%	435	11.5%	659	11.5%	308	17.2%	41	12.3%	45	15.4%
JH6	1,066	22.9%	807	28.0%	2,157	29.4%	116	24.5%	183	28.6%	337	30.7%	574	21.2%	833	22.1%	1,504	26.2%	640	35.7%	125	37.4%	111	38.0%
Seq.	5,607		3,419		8,674		513		682		1,167		3,211		4,313		6,835		2,064		346		304	
Clones	1,661		1,397		1,890		353		456		715		1,288		1,761		1,927		994		269		233	

Table S2. **Carbon–14 data**

ID	Subject	Gender	Year of birth	Year isolated	Subset	Expected carbon (µg)	Measured carbon (µg)	F ^{14}C	Error, 2 s	Δ^{14}C	Error, 2 s	Nanodrop A260	Nanodrop A280	Nanodrop 260/280	Nanodrop 260/230	Estimated cell age
BM70	W89	male	1934	2016	CD19$^+$ PCs	17.38	13.31	1.0031	0.0194	−4.8	19	2.087	1.088	1.9	2.2	0
BM78	W92	male	1953	2016	CD19$^+$ PCs	12.33	11.19	1.0376	0.0230	29.4	23	1.481	0.770	1.9	2.1	0
BM64	W81	male	1956	2016	CD19$^+$ PCs	6.80	5.86	0.9822	0.0298	−25.6	30	0.815	0.428	1.9	2.1	0
BM74	W91	male	1961	2016	CD19$^+$ PCs	38.94	30.41	1.0110	0.0146	2.9	15	4.674	2.323	2.0	2.2	0
BM93	W110	male	1964	2016	CD19$^+$ PCs	24.60	21.02	1.0046	0.0150	−3.4	15	2.953	1.518	1.9	2.2	0
BM89	W103	female	1967	2016	CD19$^+$ PCs	13.55	10.42	1.0500	0.0199	41.7	20	1.626	0.823	2.0	2.2	5
BM71	W89	male	1934	2016	CD45$^+$ PCs	40.28	30.90	1.0615	0.0156	53.1	16	4.835	2.475	2.0	2.2	9
BM79	W92	male	1953	2016	CD45$^+$ PCs	11.95	10.02	1.0192	0.0250	11.1	25	1.434	0.742	1.9	2.1	0
BM63	W81	male	1956	2016	CD45$^+$ PCs	28.58	19.99	1.0677	0.0206	59.3	21	3.430	1.773	1.9	2.2	11
BM75	W91	male	1961	2016	CD45$^+$ PCs	39.13	34.38	1.0260	0.0166	17.8	17	4.695	2.400	2.0	2.2	0
BM94	W110	female	1967	2016	CD45$^+$ PCs	13.02	10.60	1.1012	0.0216	92.5	22	1.561	0.813	1.9	2.3	17
BM90	W103	female	1967	2016	CD45$^+$ PCs	54.57	43.67	1.0668	0.0117	58.3	12	6.548	3.275	2.0	2.2	11
BM80	W92	male	1953	2016	CD45$^-$ PCs	23.79	17.96	1.0787	0.0212	70.2	21	2.856	1.479	1.9	2.2	13
BM65	W81	male	1956	2016	CD45$^-$PCs	7.77	6.19	1.1348	0.0298	125.9	30	0.932	0.486	1.9	2.2	22
BM76	W91	male	1961	2016	CD45$^-$ PCs	29.11	21.61	1.0597	0.0180	51.3	18	3.493	1.784	2.0	2.2	9
BM95	W110	male	1964	2016	CD45$^-$ PCs	27.02	20.17	1.1365	0.0149	127.5	15	3.242	1.669	1.9	2.3	22
BM91	W103	female	1967	2016	CD45$^-$ PCs	10.08	8.22	1.1518	0.0243	142.6	24	1.210	0.604	2.0	2.2	24
BM73	W89	male	1934	2016	Epithelial cells	12.56	12.45	0.9994	0.0194	−8.5	19	1.507	0.774	1.9	2.2	0
BM81	W92	male	1953	2016	Epithelial cells	19.73	18.05	1.0174	0.0280	9.4	28	2.369	1.208	2.0	2.3	0
BM96	W110	male	1964	2016	Epithelial cells	46.65	46.28	1.0147	0.0105	6.6	11	5.598	2.822	2.0	2.3	0
BM92	W103	female	1967	2016	Epithelial cells	32.15	30.81	0.9790	0.0116	−13.2	12	3.859	1.931	2.0	2.2	0